Synthesis and Characterization of Multiblock Copolymer Proton Exchange Membranes for High Temperature Fuel Cell Applications

Hae-Seung Lee

Dissertation submitted to the faculty of Virginia Polytechnic Institute and State University in partial fulfillment of the requirements for the degree of

Doctor of Philosophy
In
Macromolecular Science and Engineering

Dr. James E. McGrath
Dr. Judy S. Riffle
Dr. John G. Dillard
Dr. Richey M. Davis
Dr. Alan R. Esker

April 24th 2009

Blacksburg, Virginia

Keywords: proton exchange membrane, fuel cell, disulfonated copolymer, multiblock copolymer, morphology, poly(arylene ether sulfone), polyimide, polybenzimidazole

Synthesis and Characterization of Multiblock Copolymer Proton Exchange Membranes for High Temperature Fuel Cell Applications

Hae-Seung Lee

ABSTRACT

The potential success of a proton exchange membrane (PEM) fuel cell as an alternative energy source depends highly upon the development of high performance PEMs. Typically, state-of-the-art PEMs have been perfluorinated sulfonated ionomer membranes such as Nafion® by DuPont. Although these membranes demonstrate good mechanical and electrochemical properties under moderate operating conditions (e.g., < 80 ºC), their performance at high temperature (e.g., > 80 ºC) and low relative humidity (RH) drastically deteriorates. To overcome these problems, PEM materials with enhanced properties are essential. Recently, the McGrath group has shown that PEM materials with hydrophilic-hydrophobic segments can significantly improve proton conductivity under low RH by forming enhanced hydrophilic domain connectivity.

In this dissultation, novel multiblock copolymers based on disulfonated hydrophilic-hydrophobic multiblocks were synthesized and investigated for their potential application as PEMs. The relationship between copolymer chemical composition and resulting properties was probed with a variety of hydrophilic and hydrophobic segments. Most multiblock copolymers in this research were developed with fully disulfonated poly(arylene ether sulfone) (BPS100) as the hydrophilic segment,

and various high performance polymers including polyimides, poly(arylene ether sulfone)s, and poly(arylene ether ketone)s as the hydrophobic segment. Ionic groups on the hydrophilic blocks act as proton conducting sites, while the non-ionic hydrophobic segments provide mechanical and dimensional stability. The correlation between the fuel cell performances and the hydrophilic-hydrophobic sequences was also evaluated. The morphological structures of the multiblock copolymers were investigated using tapping mode atomic force microscopy (TM-AFM), transmission electron microscopy (TEM), and dynamic mechanical analysis (DMA). The experiments demonstrated a well-defined nanophase separated morphology. Moreover, changes in block length had a pronounced effect on the development of phase separated morphology of the system. Proton conductivity measurements elucidated the transport process in the system, with the multiblock copolymers demonstrating higher conductivities compared to Nafion and random copolymer systems with similar ion exchange capacity (IEC) values. The new materials are strong candidates for use in PEM systems.

ACKNOWLEDGEMENTS

First and foremost, I extend my deepest gratitude to my research advisor, Dr. James E. McGrath. I can't find the proper words to express my appreciation for his guidance and encouragement. From the moment I joined his group, I could not stop thinking how lucky I was for the opportunity to work in such a rich academic and scientific environment. Not only did his avid knowledge of polymer science propel me into the world of research; Dr. McGrath as a human being—especially his patience and generosity—inspired my work and enabled me to finish my studies. I am very proud to have been a student of Dr. McGrath and will be forever grateful to him.

I would also like to thank the members of my advisory committee, Dr. Judy S. Riffle, Dr. John G. Dillard, Dr. Richey M Davis, and Dr. Alan Esker for their valuable suggestions and support. My work is better as a result of their input. Special thanks goes to Dr. Riffle for having given me the chance to be a Ph.D. student in one of the most prestigious polymer programs in the country. That association enabled me to learn so much and widened my horizons in polymer chemistry. In addition, her presentation and writing courses will be a precious asset for my career.

I would like to give a big thanks to our wonderful secretarial ladies, Mrs. Laurie Good, Mrs. Millie Ryan, and Mrs. Angie Flynn, for their kindness and tremendous assistance during my Ph.D. years. I can't imagine having graduated without their help. I particularly acknowledge Laurie and her high school-age son, Alec, who spent one summer as my research assistant. They made my life easier and helped to make the lab a more enjoyable place—especially you, Alec!

Many thanks go to my colleagues in our great research group for their selfless assistance and friendship: Dr. Brian Einsla, Dr. Melinda Einsla, Dr. Hang Wang, Dr. Yanxiang Li, Mrs. Juan Yang, Dr. Xiang Yu, Dr. Paul Mou, Dr. Natalie Arnett, Mrs. Rachael Van Houten, Dr Gwangsu Byun, Dr. Desmond VanHouten, Dr. Ruilan Guo, Mr. Yu Chen, and Dr. Chang-Hyun Lee. Special thanks go to Dr. Ahbishek Roy, Dr. Anand S. Badami, and Ms. Ozma Lane. Your tremendous efforts in the characterization of my materials contributed so much to my work and I deeply appreciate every suggestion, every helpful criticism, and every word of encouragement that you extended to me. I also deeply appreciate Dr. Yu Seung Kim at Los Alamos National Laboratory, who helped me a lot with the characterizations of my research and who also offered valuable advice on a variety of topics. I am truly grateful for his support.

I would also like to express my sincere thanks to my good friends, Simon Chang and Myoungbae Lee. Simon, who used to be my general chemistry lab student, is the person who helped me to be here now. Without his self-sacrificing support, I could not have smoothly settled down in this country. Now, I consider him as one of my family members and I would like to express my love to him. Myoungbae has been a great friend all throughout my Ph.D studies. He has been with me whatever the case, happy or sad, and I appreciate his friendship.

Finally, I would like to thank all my family members—especially my wife, Soo Hee Ahn, and my two princesses, Julie and Jade. From the time I decided to pursue my Ph. D. degree in the U.S, my wife has been a huge supporter. I sincerely thank her for her love, understanding, patience, and encouragement. I have no doubt that without her support I would not have succeeded thus far. Most importantly, I would like to thank my

dear daughters, Julie and Jade. You two have truly inspired me to do my best during these graduate student years. I promise that I will always be there for you.

ATTRIBUTION

Several colleagues and coworkers aided in the writing and research behind several of the chapters of this dissertation. A brief description of their contributions is included here.

Prof. James E. McGrath is the primary advisor and committee chair. Prof. McGrath gave the author tremendous help and guidance on this work.

Abhishek Roy aided in the discussion and measurements of proton exchange membrane properties in chapter 3, 4, 5, and 6.

Anand Badami helped with atomic force microscopy measurements in chapter 3.

Ozma Lane helped with the proton conductivity and atomic force microscopy measurements in chapter 4, 5, 6, and 7.

Stuart Dunn aided in the measurement of PEM properties in chapter 4.

TABLE OF CONTENTS

CHAPTER 4

CHAPTER 6

CHAPTER 7

TABLE OF FIGURES

TABLE OF TABLES

CHAPTER 1

Introduction

The fuel cell is an energy conversion device which directly transforms the chemical energy of fuels such as hydrogen and methanol into electrical energy.[1] The fuel cell has been receiving serious attention as a next-generation energy source owing to its advantages which include high efficiency, high energy density, quiet operation, and environmental friendliness relative to conventional energy generators such as internal combustion engines.[2] Among the various types of fuel cells, the proton exchange membrane fuel cell (PEMFC) is considered to be the most promising power source for portable and automotive applications.[3, 4] As its name implies, one of the core components of a PEMFC is the proton exchange membrane (PEM) also known as a polymer electrolyte membrane. Currently, the state-of-the-art PEMs are perfluorinated sulfonated ionomer membranes, such as Nafion® (DuPont), Aciplex® (Asahi Kasei), and Flemion® (Asahi Glass).[5] These membranes have good mechanical strength and high chemical stability along with high proton conductivity, especially under high relative humidities at moderate operation temperatures (e.g., < 80 °C).[6] However, at high operation temperatures (>80 °C), which are essential for many practical applications (e.g., high efficiency, fast kinetic etc.), mechanical and electrochemical properties of the perfluorinated membranes are severely deteriorated by the depressed hydrated α relaxations of the membranes.[7, 8] These disadvantages and others, such as cost, have limited the applicability of perfluorinated membranes and propelled the quest for alternative membranes.

Tremendous effort has been devoted in the study of aromatic polymers, including sulfonated poly(arylene ether sulfone)s, poly(ether ether ketone)s, and phosphoric acid doped polybenzimidazoles, to find cost-effective and high performance PEMs.[9, 10] Among them, 4, 4'-biphenol-based disulfonated poly(arylene ether sulfone) wholly aromatic random copolymers (BPSH) are strong candidates as alternative membranes and have been extensively investigated in higher temperature PEM applications.[9] These random copolymers were synthesized via direct step-growth polycondensation by using disulfonated and/or non-sulfonated dihalide diphenyl sulfone and biphenol type monomers.[11] Even though BPSH-type membranes demonstrated enhanced stability at high temperatures (e.g., > 80 °C) and performance comparable to Nafion®, their proton conductivities under low relative humidity were inadequate.[12]

Recently, PEMs based on multiblock copolymers have been considered as a solution to overcome the drawbacks of a random copolymer system.[13, 14] PEMs based on segmented multiblock copolymers consist of ion conducting hydrophilic blocks and mechanically robust hydrophobic blocks. Once they are cast into membranes, they can be designed to exhibit unique phase separated morphologies and each phase governs independent or distinct properties. The ionic groups of the hydrophilic blocks act as proton conducting sites while the nonionic hydrophobic component provides dimensional stability. In the case of direct methanol fuel cells (DMFCs), the hydrophobic component may also serve as a barrier against methanol transport.[15, 16] The proton conductivities, water uptake, and mechanical properties of multiblock copolymer based PEMs can be tailored by carefully adjusting the compositions and relative lengths of their hydrophilic and hydrophobic blocks and the research is ongoing.[17]

The research in this dissertation mainly focuses on the synthesis and characterization of novel multiblock copolymers based on hydrophilic and hydrophobic blocks for PEM applications. For the research, fully disulfonated poly(arylene ether sulfone) (BPSH100) will be used for proton conducting hydrophilic block and a variety of hydrophobic blocks will be explored to find potential candidates as PEMs. In addition, several parameters such as copolymer structure, block and total molecular weight, ion exchange capacity, and morphology will be examined to determine their impact on PEM performance.

CHAPTER 2

Literature Review

2.1. Fuel Cells

As fossil fuel resources are expected to enter their sunset years and pollution caused by their combustion becomes more severe, the need to find devices which can utilize alternative energy sources (e.g., H_2, CH_3OH) has become imperative. Among various energy conversion devices, the fuel cell is one of the most efficient energy converting devices which transforms chemical energy directly into electrical energy.[2] Also, its environmentally friendly nature has attracted much attention as a promising alternative to conventional energy sources. In this chapter, general fuel cell concepts will be outlined including historical aspects, core mechanisms, and applications.

2.1.1. Background of Fuel Cells

2.1.1.1. Historical Perspective of Fuel Cells

The first introduction of the fuel cell dates back to 1839 in England.[18, 19] Sir William Grove, who was a lawyer and scientist, demonstrated the first fuel cell based on a concept which was first proposed by Christian Friedrich Schonbein, a professor at the University of Basle. During the time, Sir William Grove was investigating the electrolysis of water, which is an electrochemical reaction generating hydrogen and oxygen utilizing an electric current to split water. Grove was also interested in the reverse reaction of the electrolysis of water (i.e., generating an electric current from the reaction between oxygen and hydrogen). To verify this reaction, he arranged two platinum electrodes in two separate sealed containers which were immersed in dilute sulfuric acid. The two sealed containers contained oxygen and hydrogen, respectively,

and to increase the voltage produced, he linked several of these devices in series. From this experiment, he proved that this device can generate electricity by the reverse reaction of electrolysis and named it a "gas battery": the first fuel cell. Figure 2.1 shows Grove's drawing of his experimental "gas battery".[20]

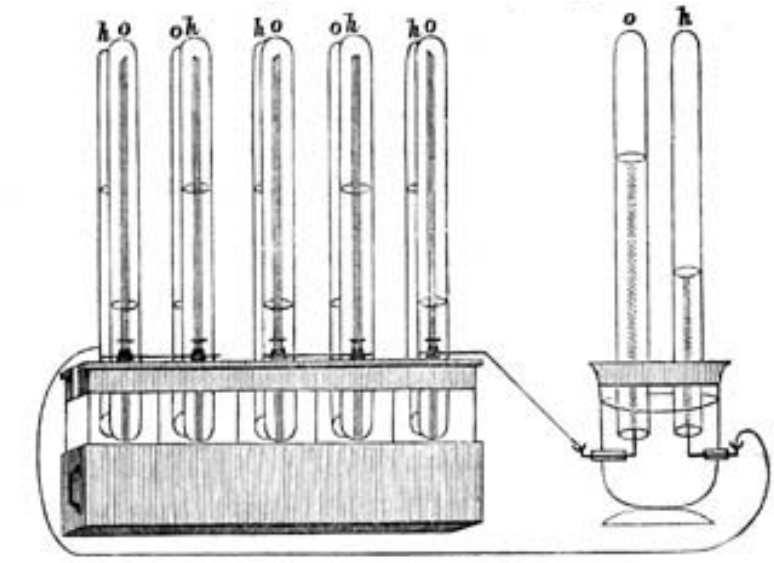

Figure 2. 1. First Fuel Cell Device Created by Sir Grove. Reprinted with permission from Journal of Power Sources. [20] Copyright 1990 Elsevier.

Few chemists attempted to build practical devices based upon Grove's instruments until the end of the 19th century. However, the introduction of the more practical internal combustion engine which could run on fossil fuels displaced fuel cells from mainstream scientific curiosity for a while.

It has only been in the last fifty years that the development of fuel cell technology has gained renewed attention. From the late 1950s to early 1960s, the National Aeronautics and Space Administration (NASA) devoted their efforts to find a power source for upcoming space flights. The candidates deemed suitable as power sources were battery, solar cell, nuclear power, and fuel cells. After careful consideration,

researchers concluded that the fuel cell would provide the best solution for selected space flight power sources. Accordingly, NASA then sponsored efforts to develop fuel cells that could be used during these space flights. These efforts led to the development of the first Proton Exchange Membrane Fuel Cell (PEMFC) which was used for the Gemini space program in the 1960s.[18]

2.1.1.2. Core Principles of Hydrogen Fuel Cells

A fuel cell is a device which is able to produce electrical energy via an electrochemical reaction. The core components of the fuel cell consist of an electrolyte and two electrodes (e.g., cathode and anode). When a fuel, such as hydrogen, is introduced at the negative anode, it is readily oxidized with a catalyst to produce protons and electrons.[21, 22] The protons then pass through the electrolyte from the anode to the cathode while the electrons travel through the external circuit. At the positive cathode, oxygen is reduced by reaction with the protons and electrons to generate water (Figure2.2).

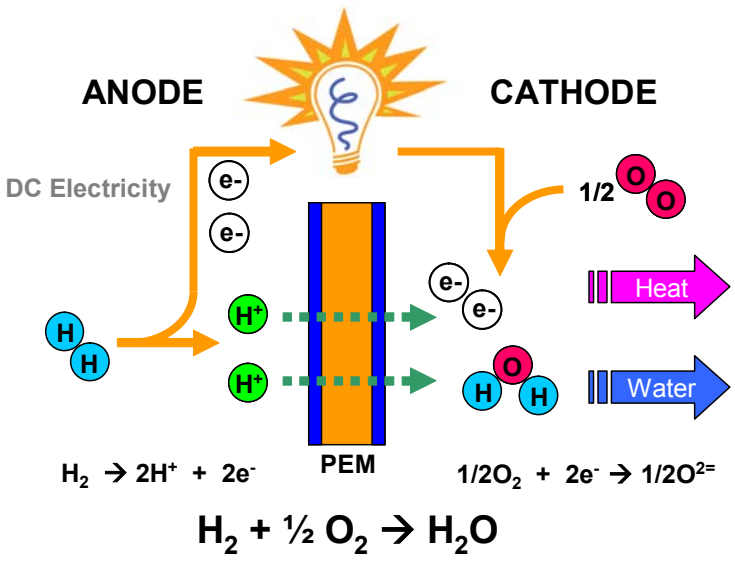

Figure 2. 2. Basic Principle of a Fuel Cell.

Clearly, the overall reaction is a reversal of the electrolysis of water. In the reaction, the type of electrolyte determines the operation temperature, catalyst, and the required purity of the fuel. Theoretical red-ox voltage of a fuel cell based on the hydrogen-oxygen reaction is 1.23V at 298K. However, the real voltage generated by the fuel cell under typical operating conditions ranges between 0.5 and 1 V. For practical applications, a fuel cell assembly is composed of multiple cells in a series of stacks to produce a higher voltage. Although numerous types of fuel cells have been developed in previous decades, they can be classified into six major types. Each type of fuel cell will be addressed in the following sections in detail.

2.1.2. Types of Fuel Cells

2.1.2.1. Alkaline Fuel Cell (AFC)

The alkaline fuel cell was the first fuel technology developed for practical applications. It was introduced in 1960s the Apollo space mission where it provided both a power and drinking water source for the astronauts. Alkaline fuel cells use an aqueous alkaline solution electrolyte (typically 30% potassium hydroxide solution) which is retained in a porous matrix.[23] The hydroxide ion in the electrolyte solution reacts with hydrogen at the anode to produce water and electrons. The water and electrons generated at the anode migrate to the cathode to regenerate hydroxide ions. A schematic operational scheme of alkaline fuel cell is depicted in Figure 2.3.

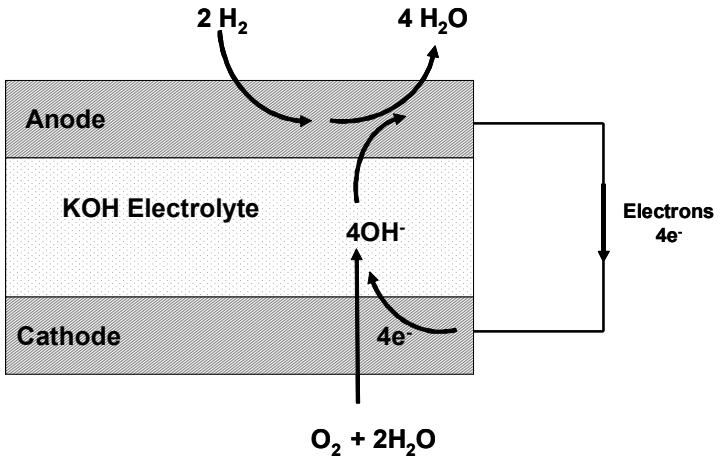

Figure 2. 3. Operating Principle of an Alkaline Fuel Cell.

Although their excellent power density and low operational temperature attracted a lot of attention in the early stages, alkaline fuel cell systems have a critical vulnerability which caused them to fall out of favor in the research community. Alkaline fuel cells are easily poisoned by carbon dioxide even at low concentrations.[24] For example, 50 ppm of carbon dioxide (much lower than the concentration in ambient air) results in a more than 30% decrease in performance with a non polymeric electrolyte. For this reason, the applications of alkaline fuel cells have been restricted to closed environments, such as space and undersea, and must be run on highly purified fuels and oxidants which do not contain carbon dioxide. However, there has been renewed interest developing because new copolymer systems showed some progress.[25] In the systems, ethanol can be used as fuel, and platinum catalysts are not required.[26, 27]

2.1.2.2. Proton Exchange Membrane Fuel Cell (PEMFC)

Proton exchange membrane fuel cells (PEMFC) are considered to be the fuel cell candidates that have the strongest potential to replace the conventional internal combustion engines in automobiles and batteries in electronic devices. Compared to other

types of fuel cells, PEMFCs have the highest energy density and this advantage may allow their use in compact and lightweight energy converting devices.[9, 28-31] Furthermore, their relatively low operational temperature (~100 ºC) is amenable to both quick start-up and rapid power response, which are core features for automobile power sources. Due to these outstanding features, PEMFCs have been the top candidate for most fuel cell applications since they were introduced to the world in the 1960s for the NASA Gemini space program.

PEMFCs have been developed for power systems ranging from 1W to 2kW. The electrolyte in PEMFC is a solid thin polymer membrane which contains ionic groups. The ionic groups are strong acid moieties such as sulfonic acid and phosphoric acid which can facilitate proton conduction in the membranes. The typical fuel for the PEMFC is hydrogen gas and it is oxidized into protons and electrons at the anode by a noble metal catalyst such as Pt. The generated protons and electrons are then transported to the cathode through the proton exchange membrane and external circuit, respectively. Upon arriving at the cathode, the protons and electrons react with the oxygen to generate water and heat. The operational principle of the PEMFC is depicted in Figure 2.4.

One challenge in developing PEMFCs for automobile power application is a management of water in the system. The proton conductivity is strongly dependent on the amount of water in the membrane.[7] Generally, the highest proton conductivities are obtained when the membranes are fully saturated with water. However, at the typical PEMFC working temperature of ~100 ºC, it is difficult to prevent evaporation of water from the membrane which results in a drop in conductivity.

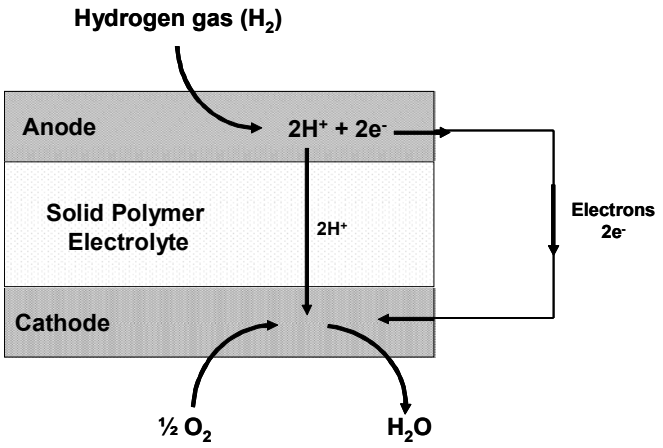

Figure 2. 4. Operating Principle of a PEM Fuel Cell.

2.1.1.3. Phosphoric Acid Fuel Cell (PAFC)

Although much effort has been devoted to commercialize PEMFCs, phosphoric acid fuel cells (PAFC) are already commercially produced and available in the market. Major PAFC developers include UTC Fuel Cells, Toshiba, and Fuji Electric. More than 500 PAFC power plants have been built and tested since the 1970s. The biggest fuel cell in fuel cell history is also a PAFC which was built by Tokyo Electric Power Co. (TEPCO) in Japan. It has an 11MW capacity and its stability and reliability has been proven by operating more than 230,000 hours since 1991. The typical efficiency of PAFC is over 35% and it can be increased to 85% when it is used in a Combined Heat and Power application (CHP). [32, 33]

The PAFCs use liquid phosphoric acid electrolyte which more recently has been imbibed in a basic polymer such as polybenzimidazole.[32] The basic sites on the polybenzimidazole can partially immobilize the phosphoric acid. In general, PAFCs operate at a relatively high temperature (e.g., 150-220 ºC) due to the low proton conductivity of phosphoric acid at ambient temperature.[34] By operating at the higher

temperature, PAFCs gain several advantages, including fast kinetics and an improved carbon monoxide tolerance. This high carbon monoxide tolerance can allow the PAFC to operate without complicated and expensive fuel reformers and may therefore result in a simplified fuel cell system. The energy generation mechanism of the PAFC is similar to the PEMFC. At the anode, hydrogen is introduced as a fuel and splits into protons and electrons by use of a catalyst. The generated hydrated protons are then transported to the cathode through the PEM while the electrons travel through the external circuit. At the cathode, the protons and electrons reunite when they combine with oxygen, usually from air to generate water and heat. The operating principle of a PAFC is depicted in Figure 2.5.

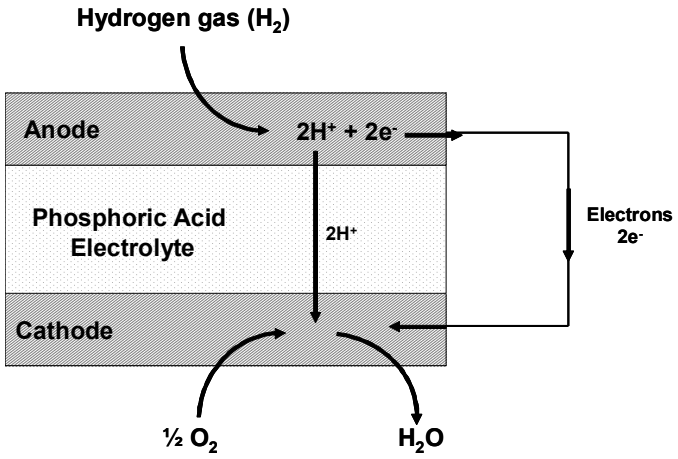

Figure 2. 5. Operating Principle of a Phosphoric Acid Fuel Cell.

Although the PAFC has some excellent technical advantages, it lost market attention due to several issues. One of the biggest technical problems is deterioration of the catalyst performance in the electrolyte. The relatively high cost of the system is another problem. A recent survey showed that the number of molten carbonate fuel cell and solid oxide fuel cell units built in 2003 already exceeded the number of PAFCs sold

in that year.[32] To regain interest for PAFCs, improvement of proton conductivities and reduction in cost should be addressed.

2.1.2.4. Molten Carbonate Fuel Cell (MCFC)

The molten carbonate fuel cell is one of the high temperature fuel cell classes. Its typical working temperature is 650 °C and the high operation temperature provides several advantages, including an increase in the reaction kinetics.[35, 36] For example, hydrocarbon fuel from natural gas can be directly used without the need for a fuel processor (reformer) because relatively impure fuel can be internally reformed at high temperature in the system. Also, by-product heat and steam from the system can be used for additional processes. However, the high operation temperatures also cause some problems. When the system starts up, it requires a significant amount of time to reach proper operation conditions and the system's response to changes in power demand is relatively slow. The requirements of molten carbonate fuel cell make it suitable for stationary power source applications only.

The typical electrolyte in the molten carbonate fuel cell is a mixture of lithium carbonate and potassium carbonate, or lithium carbonate and sodium carbonate. The mixture of different kinds of carbonates melts at high temperature and shows excellent ion mobility. The ion carrier in the system is the carbonate ion. The carbonate ions migrate from the cathode to the anode where they combine with hydrogen to produce water, carbon dioxide and electrons. Produced electrons travel through an external circuit back to the cathode and combine with oxygen and carbon dioxide to produce carbonate ion again. A schematic diagram of operation of molten carbonate fuel cell is depicted in Figure2.6.

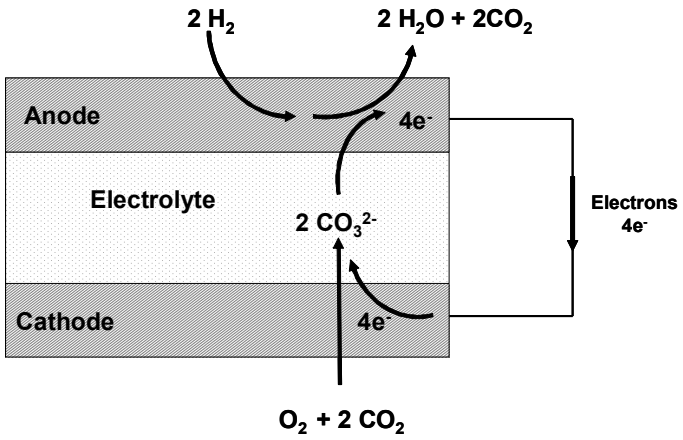

Figure 2. 6. Operating Principle of a Molten Carbonate Fuel Cell.

As described earlier, the high operation temperature is generally beneficial for the system but it is also the source of some problems. At high temperature, the carbonate ion electrolyte can cause electrode corrosion which may result in a decrease in the efficiency and performance. Furthermore, careful control of the carbon dioxide stream both at the anode side and the cathode side to achieve optimum performance is another challenge for molten carbonate fuel cells.

2.1.2.5. Solid Oxide Fuel Cell (SOFC)

As its name implies, solid oxide fuel cells utilize an inorganic metal oxide as the electrolyte. Their main application is for stationary power with an output from 1kW to 2 MW. The typical operation temperature range is from 700 to 1000 °C and nonporous Y_2O_3 stabilized ZrO_2 is used as the electrolyte material while $CoZrO_2$ and Sr doped $LaMnO_3$ are used in the anode and cathode, respectively.[37] The most remarkable difference between other types of fuel cells is its power generating mechanism. The electrolyte in SOFC transports oxygen ions instead of protons. At the cathode, oxygen is reduced to oxygen ions, which then pass thorough the electrolyte to the anode, where transported oxygen ions react with hydrogen and carbon monoxide which are generated

at the anode from the fuel. General fuel consists of natural gas and oxygen. By this process, the fuel cell produces electricity, heat, water and carbon dioxide. This process is shown schematically in Figure2.7.

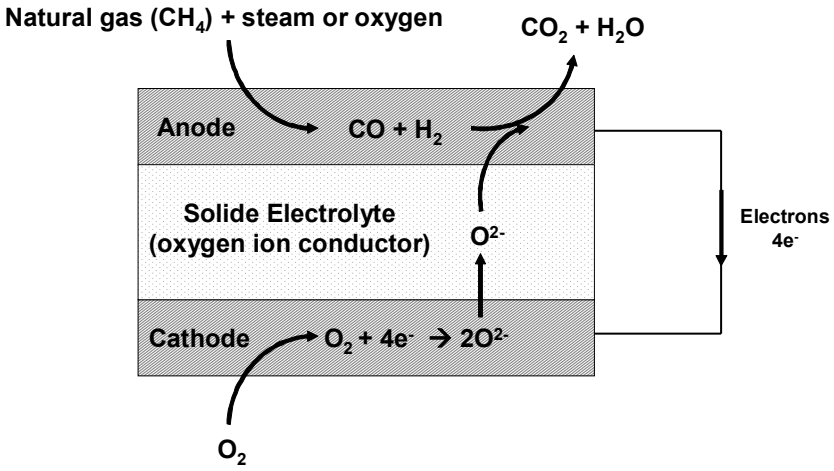

Figure 2. 7. Operating Principle of a Solid Oxide Fuel Cell.

Due to their high working temperature, solid oxide fuel cells can be a good solution for combined heat and power applications which provide both power and hot water from a single system. This hybrid system can improve solid oxide fuel cell's efficiency up to 70%. Moreover, the high operation temperature significantly increases the fuel cell's tolerance against sulfide containing compounds which can cause poisoning of the anode catalyst nickel. This improved tolerance can provide flexibility in the choice of fuel. For example, SOFC can be operated by utilizing impure fuels such as unreformed hydrogen from natural gas without the need of an expensive external fuel reformer. The impure hydrocarbon fuel is internally reformed to carbon monoxide and hydrogen by means of a catalyst at high operation temperature. Though significant improvement has been made in the fabrication and processing of inorganic materials, the

brittle nature of the cathode catalyst material (e.g., typically lanthanum strontium manganite) is still problematic.

2.1.3. Currently Used Proton Exchange Membranes

Among various types of PEMs, perfluorinated ionomer membranes have been considered as the most promising candidates for diverse applications including portable, automobile, and stationary power sources. Nafion®, a perfluorinated ionomer membrane manufactured by DuPont, is the benchmark of PEMs as it has been used in the US space and military programs for more than 35 years. The history of Nafion® goes back to the early 1960s when the Plastic Exploration Research Group in DuPont attempted to synthesize copolymers from tetrafluoroethylene (TFE) monomer. At a similar time, DuPont developed a sulfonic acid containing monomer perfluoro-3,6-dioxa-4-methyl-7-octene-sulfonyl fluoride (PSEPVE) (Figure 2.8).[5] By copolymerization of TFE and PSEPVE, DuPont could synthesize an unusual TFE-based copolymer containing branches with pendant sulfonyl fluoride groups via a free radical polymerization. The sulfonyl fluoride can be converted to sulfonic acid by subsequent hydrolysis, acidification, and washing processes. The resulting sulfonic acid containing copolymer is Nafion® and its chemical structure is depicted in Figure 2.9.

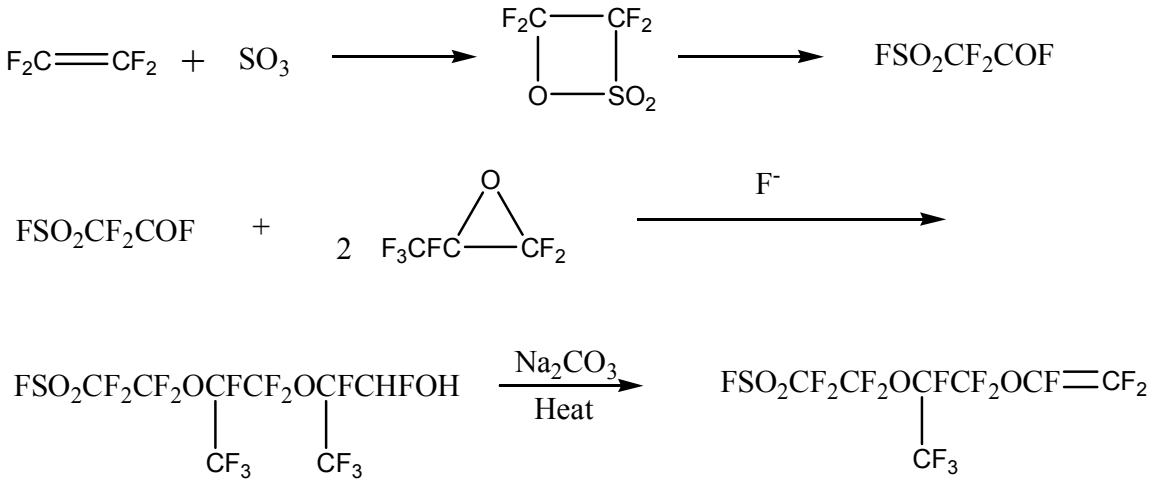

Figure 2. 8. Synthetic Scheme of Perfluoro-3,6-dioxa-4-methyl-7-octene-sulfonyl - fluoride (PSEPVE).

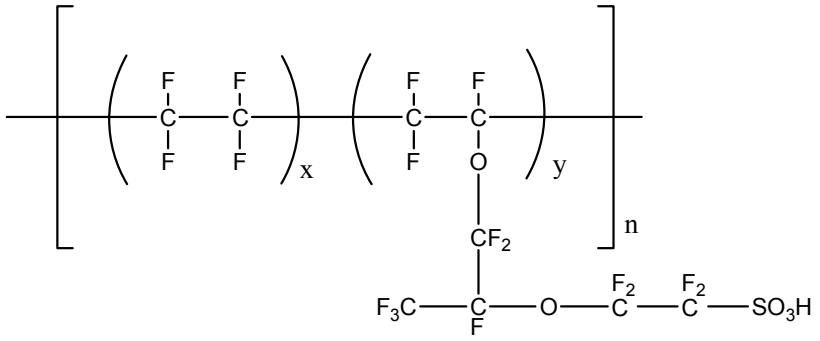

Figure 2. 9. Chemical Structure of Perfluorinated Ionomer Nafion®.

Although the synthesis of TEF based ionomer Nafion® was successful, its applications were not immediately clear. The initial and still major application of Nafion® was as a separator in a chlor-alkali process application due to its excellent separation properties and chemical stability. At this time, General Electric (GE) was developing sulfonic acid containing polystyrene PEMs for the NASA space program.

However, the poor chemical and oxidative stability of the polystyrene based PEMs were not sufficient to endure the harsh oxidative fuel cell operation conditions. Hence, GE was looking for a robust PEM which could replace polystyrene sulfonic acid membranes for the NASA space program. Nafion® met most of the requirements for the PEM including high proton conductivity and good oxidative stability and therefore was selected as the replacement PEM. This was the debut of Nafion membranes in fuel cell applications.

In today's PEM market, several perfluorinated sulfonic acid membranes, including Nafion®, are available from several different companies. Most of their chemical structures are similar to that of Nafion® as they are copolymers of tetrafluoroethylene (TFE) and perfluorovinyl ether with sulfonic acid groups on its side chains (typically 87 mole% of TFE and 13 mole% of the sulfonic monomer with EW of 1100). The main difference among those copolymers is the length of the side chain which contains the sulfonic acid group.[30] The structures of other commercially available perfluorinated sulfonic acid based PEMs are shown in Figure 2.10.

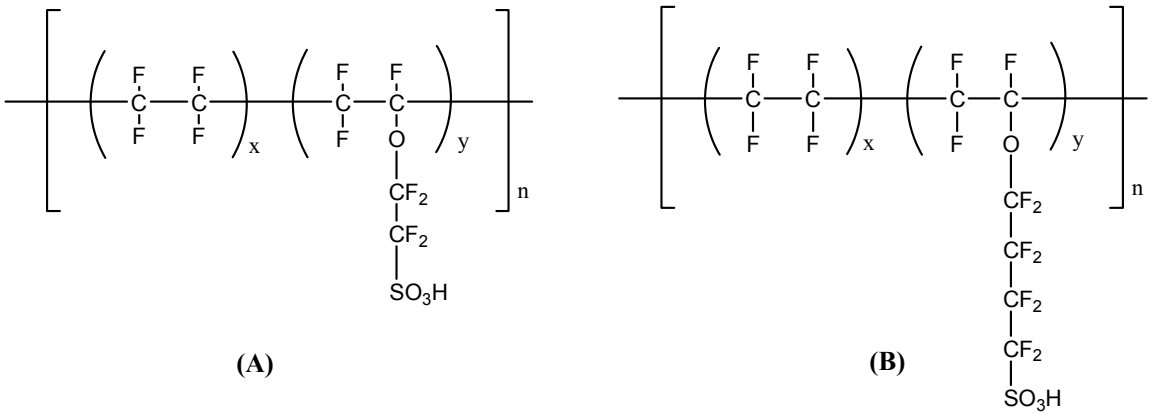

Figure 2. 10. Chemical Structures of a PEM by a) Dow Chemical and by b) 3M.

The Dow membrane was developed in the early 80s and was used in both chlorine production and fuel cell applications with excellent properties.[38] Although its performance as a PEM in fuel cell applications was comparable to that of Nafion®, Dow Chemical stopped its production a few years later. Now, the same polymer is being produced by Solvay Solexis with a different synthetic route under the trade name Hyflon Ion®.[39, 40] Detailed synthetic schemes by Dow Chemical and Solvay Solexis are depicted in Figure 2.11. While sulfonyl fluoride containing monomers by DuPont, Dow Chemical, and Solvay Solexis are synthesized by a reaction between TFE and SO_3, 3M developed a new synthetic route to synthesize a sulfonyl fluoride containing monomer by an electrochemical fluorination process (Fig.2.12).[41, 42]

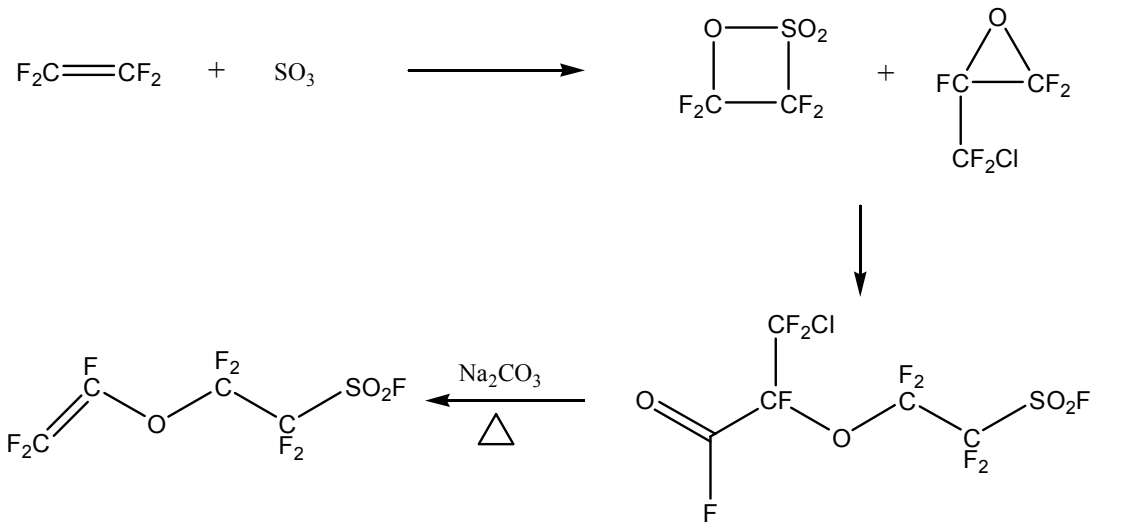

Synthetic Scheme by Dow Chemical

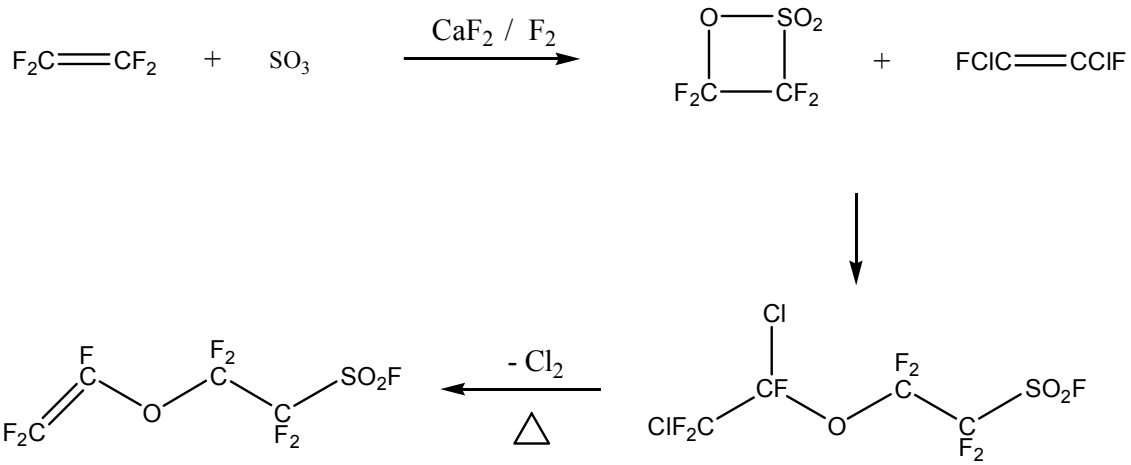

Synthetic Scheme by Solvay Solexis

Figure 2. 11. Different Synthetic Schemes for Short Side Chain Monomer by Dow and Solvay Solexis.

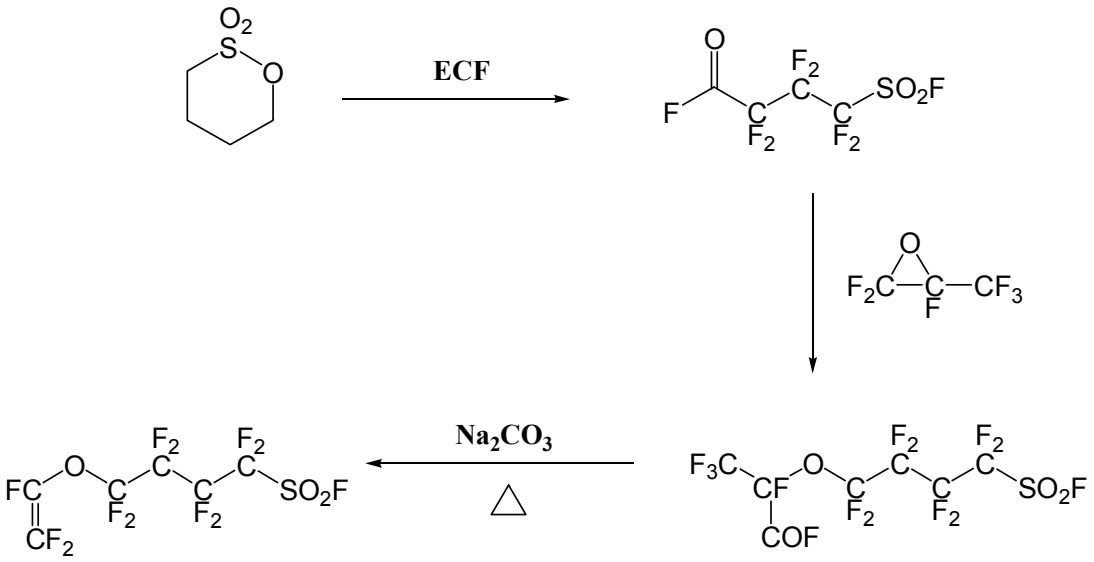

Figure 2. 12. Synthesis of Perfluorinated Monomer by 3M.

2.1.4. Nafion Type PEM Materials and Requirements for PEMs

The overall performance of a PEMFC is determined by the combined properties of its components including the PEM, catalyst electrode, gas diffusion layer and bipolar plate. Among them, the most crucial component which determines the performance of a fuel cell is the PEM. Several material requirements which high performance proton exchange membranes should possess include:[9]

• High proton conductivity (particularly at partially hydrated conditions for H_2/Air Fuel Cell)

• Low electronic conductivity (to prevent shorting between the anode and the cathode)

• Low permeability to fuel and oxidants (to minimize coulombic efficiency loss)

• Low water transport through diffusion and electro-osmosis

• Oxidative and hydrolytic stability (to survive under harsh operation conditions)

• Low swelling stresses (especially swelling-deswelling stability is imperative)

• Good mechanical properties both in the dry and hydrated state

• Affordable cost

• Capability of fabrication into membrane electrode assemblies (MEAs)

Commercially available Nafion® and similar perfluorinated sulfonic acid membranes have been extensively examined in terms of the above requirements.[5, 43] The perfluorinated sulfonic acid based membranes exhibited high proton conductivity (~0.10 S/cm) with moderate water uptake (15~21 H_2O molecules per sulfonic acid group) at room temperature under 100% relative humidity (RH). It has been understood that the proton conductivity of Nafion type membranes is strongly dependent on the amount of absorbed water around the sulfonic acid groups. The IEC of the Nafion type copolymers can be easily tailored by changing the feed ratio of the two monomers (e.g., TFE and sulfonated perfluorinated monomer) in the copolymerization step. Although higher IEC of a membrane generally increases its proton conductivity, it will also result in higher water uptake and swelling. For this reason, the IEC of a PEM should be carefully tailored to optimize several properties including proton conductivity, water uptake, and swelling. The chemical and hydrolytic stabilities of Nafion type membranes are excellent due to the inactivity of the Teflon-like backbone, and the existence of some crystallinity of the main backbone provides good mechanical properties. However Nafion type membranes have several demerits at high operation temperatures (e.g., > 100 ºC) which are essential for fast kinetics and high tolerance to CO poisoning. At the temperatures, the proton conductivity of Nafion® type membranes dramatically decreases due to the

loss of the absorbed water and the depressed hydrated α relaxation of the membranes.[7, 8] In addition, the low glass transition temperatures of Teflon type PEMs result in the deterioration of mechanical properties. The poor mechanical properties at high temperature were improved by fabrication of composite membranes utilizing Teflon fabric reinforcements by W.L. Gore and Asahi Chemical.[44] However, the high cost of Nafion-based membranes, along with high fuel permeability, has spurred the development of new PEM materials.

2.2. Proton Exchange Membranes (PEMs) Based on Poly(arylene ether sulfone)

2.2.1. General Properties of Poly(arylene ether sulfone)s

2.4.1.1. Introduction of Poly(arylene ether sulfone)s

Poly(arylene ether sulfone)s comprise a family of high-performance engineering thermoplastics which have been investigated by several chemical companies over the past forty years. Due to their outstanding properties such as high mechanical strength, high glass transition temperature (T_g), and good thermal and oxidative stability, poly(arylene ether sulfone)s have been chosen for a variety of applications.[45-48] Several amorphous commercial poly(arylene ether sulfone)s in the market are shown in Figure 2.13.

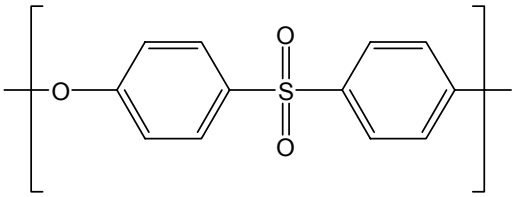

Victrex®

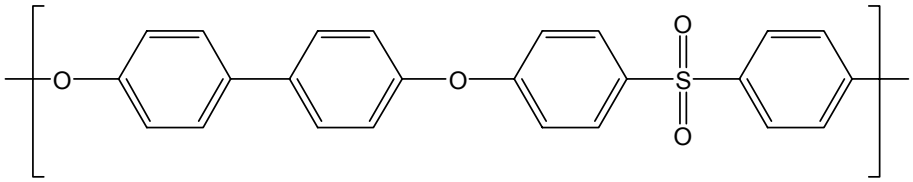

Radel®

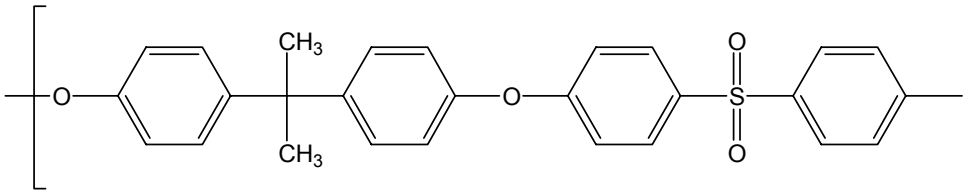

Udel®

Figure 2. 13. Commercial Poly(arylene ether sulfone)s.

Of the various excellent characteristics of poly (arylene ether sulfone)s, thermal and oxidative stabilities are the key features which make poly(arylene ether sulfone)s a melt processible engineering plastic.[49, 50] As a result of the high oxidation state of the sulfur atoms and the enhanced resonance structure of the sulfone group in the polymer structure, these polymers can be melt-fabricated at temperatures of up to 400 ºC without degradation.[51] The exceptional oxidative stability also allows poly(arylene ether sulfone)s for prolonged or continuous uses at the temperatures between 150 and 190 ºC. Typical poly(arylene ether sulfone)s display relatively high T_gs in the range of 180-250 ºC depending on the structure of the backbone. The high glass transition temperatures of poly(arylene ether sulfone)s can be explained by the strong dipole-dipole interactions between the rigid phenyl rings and sulfone groups in the backbones of neighboring polymer chains.[52, 53] On the other hand, the presence of flexible ether linkages can decrease strong inter-chain interactions by increasing conformational freedom. As a result, glass transition temperatures of poly(arylene ether sulfone)s are influenced both by the stiffness and flexibility of the polymer chemical structures. The glass transition temperatures of poly(arylene ether sulfone)s, which are synthesized by a step or polycondensation of the activated aromatic halide 4,4'-dichlorodiphenylsulfone (DCDPS) with different biphenols are summarized in Table 2.1. [45]

Table 2. 1. Glass Transition Temperatures of Poly(arylene ether sulfone)s Produced from the Reaction of 4,4'-Dichlorodiphenylsulfone(DCDPS) with Various Biphenols.[45]

Bisphenol	Chemical Structure	T_g (ºC)
4,4'-dihydroxyldiphenyl oxide	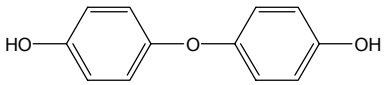	170
4,4'-dihydroxyldiphenyl sulfide	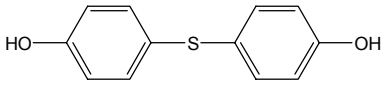	175
4,4'-dihydroxyldiphenyl methane	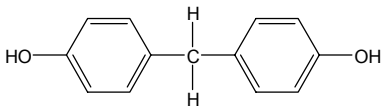	180
2,2'-bis(hydroxyphenyl)-propane	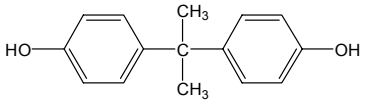	185
Hydroquinone		200
2,2'-bis(hydroxyphenyl) perfluoropropane	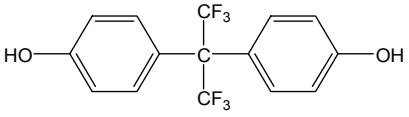	205
4,4'-dihydroxydiphenyl phenone	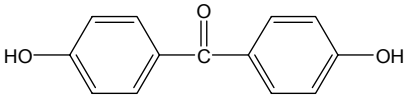	205
4,4'-dihydroxydiphenyl sulfone	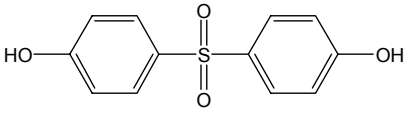	220
4,4'-dihydroxydiphenyl	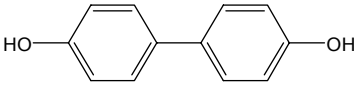	220
1,4-bis(4-hydroxyphenyl) benzene		250
4,4'-bis (4"-hydroxybenzenesulfonyl) diphenyl	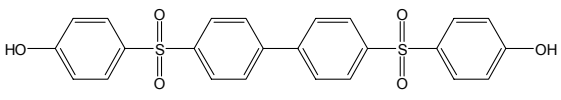	265

Poly(arylene ether sulfone)s are tough, rigid, and ductile materials with high impact strength and creep resistance.[45] Their stiffness and mechanical strength are much higher than those of unaltered aliphatic backbone amorphous plastics. It is understood that the toughness of poly(arylene ether sulfone)s is due to the existence of a strong second-order (β) transition at low temperature (e.g., -100ºC) which involves the segmental motion of the polymer.[52-54] This second order transition is believed to be due to a rotational motion of the aryl ether bond as well as a concerted motion of sulfone groups with water molecules bound to the sulfone groups.

Poly(arylene ether sulfone)s also show good solvent resistance to non-oxidizing acids, alkalis, salts, and aliphatic hydrocarbon solvents.[55-58] Moreover, poly(arylene ether sulfone)s exhibit exceptional hydrolytic stability compared to other engineering plastics such as polycarbonates, polyesters, and polyether imides. They showed no significant mechanical property degradation after hot steam tests which were carried out by 3 min exposure over 1000 times at 140ºC.[59] In spite of good mechanical properties and chemical resistance, poly(arylene ether sulfone)s were not initially considered a weather-resistant material because of the tendency of aromatic polymers to have a poor resistance to photooxidation. However, their weatherability has been significantly enhanced by incorporation of UV absorbers such as carbon black.

On account of outstanding properties including hydrolytic stability and mechanical properties, a wide range of applications has been developed for poly(arylene ether sulfone)s. They can be fabricated into injection molded parts, films, coatings, and composites which are served traditionally by metals, ceramics, glass and thermosetting resins. They are employed in medical and food service applications which require

prolonged exposure to hot, wet environments as well as repeated cleaning and sterilization. Bisphenol A based poly(arylene ether sulfone) is used in purification membrane applications such as reverse osmosis, ultrafiltration, and gas separation.[60-63] Recently, applications in the electronics field are expanding, particularly for injection-molded printed circuit boards and connectors.

2.2.2. Synthesis of Poly(arylene ether sulfone)s

Various synthetic methods for poly(arylene ether sulfone)s were developed independently in several laboratories: Union Carbide Corporation[46], 3M Corporation[64] in United States and ICI in the United Kingdom. In general, poly(arylene ether sulfone)s are synthesized via four different routes:

1. Polycondensation by means of an electrophilic substitution of aromatic compounds
2. Polycondensation by means of a nucleophilic substitution of a chloro, fluoro or nitroaromatics activated by a sulfonyl group in para-position
3. Chemical modification of precursor polymers
4. Ring-opening polymerization of cyclic oligo(ether sulfone)s

In the following chapters, each synthetic route will be discussed in detail.

2.2.2.1. Electrophilic Aromatic Substitution Route

The polycondensation route, which involves the electrophilic substitution of a phenyl ether group by an aromatic sulfonyl chloride group, is known as the oldest approach for the synthesis of poly(arylene ether sulfone).[65, 66] This approach is known as Friedel-Crafts sulfonylation and needs to be catalyzed by a strong Lewis acid such as $FeCl_3$, $AlCl_3$, or BF_3.[45, 67, 68] It is widely believed that the sulfonylation process involves a multi-

stage mechanism (Figure 2.14). In the first stage, the attacking reagent arylsulfonylium cation is formed by the reaction of the sulfonyl chloride with a strong Lewis acid. Then, the arylsulfonylium cation attacks the carbon on the aromatic nucleus to generate an intermediate, which subsequently converts to the final product by eliminating a proton.

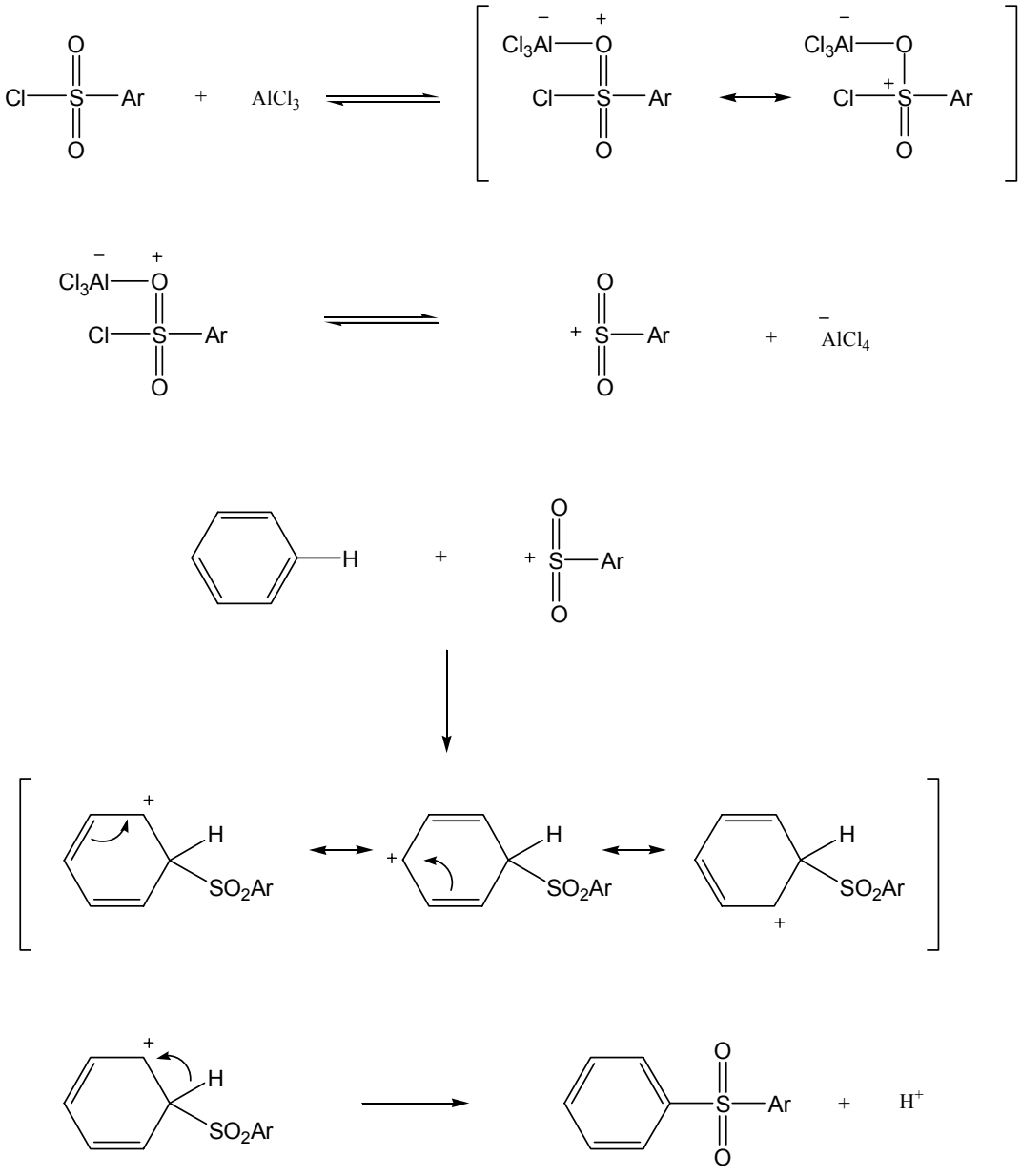

Figure 2. 14. Reaction Mechanism of Friedel-Crafts Sulfonylation.

The Friedel-Crafts sulfonation approach can be applicable for the preparation of poly(arylene ether sulfone)s by two different methods: the sulfonylation reaction of monomers containing both functional groups in one molecule (self-condensation of AB type monomer) or the sulfonylation reaction between nucleophilic monomers and electrophilic monomers (condensation of AA and BB monomers).[69-71] Two examples of these types of reactions are shown in Figure 2.15.

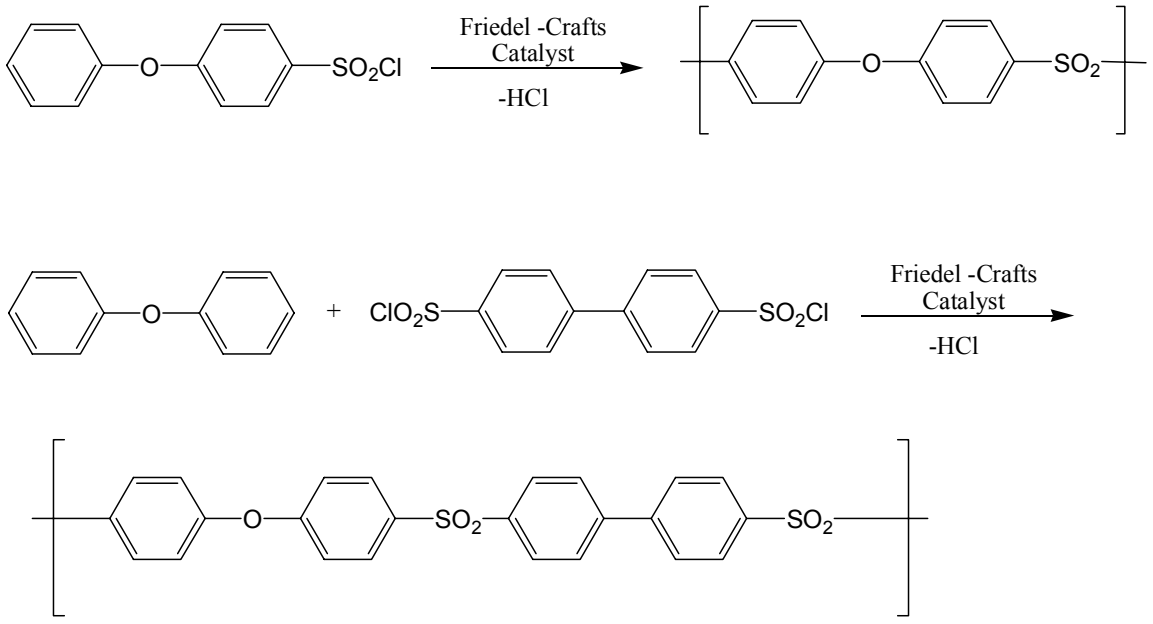

Figure 2. 15. Polycondensation of AA-BB and AB Types by Friedel-Crafts Sulfonylation.

The polysulfonation reaction can be performed either in the melt or in solution. Typical solvents for solution polymerization include nitrobenzene, dimethyl sulfone, and chlorinated biphenyls. Strong acids such as CF_3SO_3H and $MeSO_3H$-P_2O_5 mixture can be also used.[72]

2.2.2.2. Nucleophilic Aromatic Substitution Route

The nucleophilic aromatic substitution reaction (S_NAr) is the most widely used approach for the synthesis of poly(arylene ether sulfone)s in both academic research and commercial production. This synthetic method, developed at Union Carbide in the early 1960s, involves the reaction of equimolar amounts of an aromatic dichloro- or difluorosulfone and a bisphenol with either aqueous sodium hydroxide or dry K_2CO_3 (equimolar or slightly excess) in polar aprotic solvents such as N-methylpyrrolidone (NMP), dimethylacetamide (DMAc), dimethylsulfoxide (DMSO) or sulfolane.[47, 48, 59, 73] In this reaction, ether bonds are formed via the displacement of halogen by phenoxide anions with removal of the halide as an alkali metal halide. The generalized mechanism of the nucleophilic aromatic substitution (S_NAr) is depicted in Figure 2.16.[74, 75]

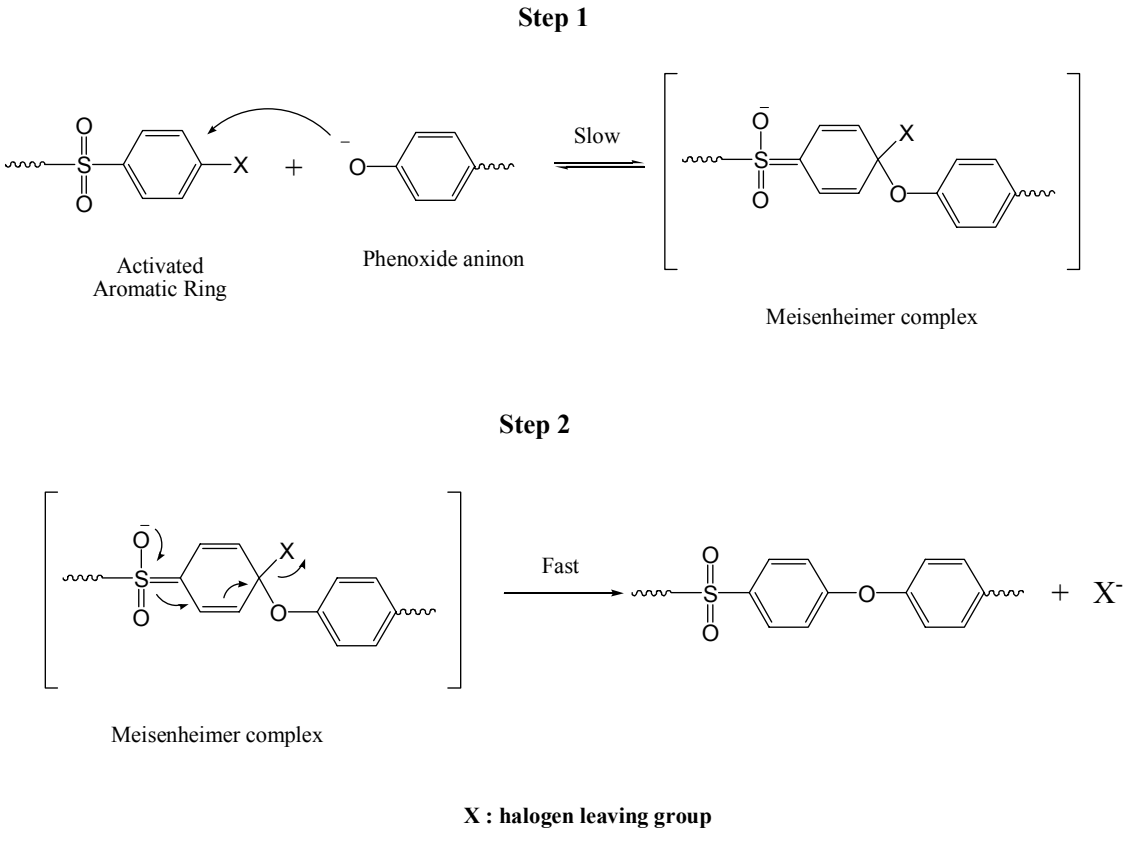

Figure 2. 16. Reaction Mechanism of Nucleophilic Aromatic Substitution.

In nucleophilic substitution polymerization, the reaction rates depend on the type of reaction medium, the basicity of the bisphenol salt, and the electron withdrawing capacity of the activating group in the dihalide monomer. Only processes in dipolar aprotic solvents can result in a good reaction rate.[76, 77] It is believed that dipolar aprotic solvents promote the reaction by enhancing the active concentration of the attacking nucleophile and stabilizing the bimolecular Meisenheimer intermediate. Strength and position of the activating groups are also key factors affecting the reaction rate. When major activating groups are positioned in the ortho and para positions of the halogen leaving groups, the nucleophilic substitution reaction can be accelerated since the electron withdrawing activating groups strongly stabilize the Meisenheimer intermediate. Another important consideration in reactivity is the electronegativity of the halogen leaving group in the dihalide monomer. In general, difluoride-based monomers show better reactivity and reaction rate than those of the dichloride-based monomers, but their higher cost limits their applications for commercial uses.[78] A typical polycondensation reaction of bisphenol A based polysulfone and the reaction developed by Union Carbide are shown in Figure 2.17.[48]

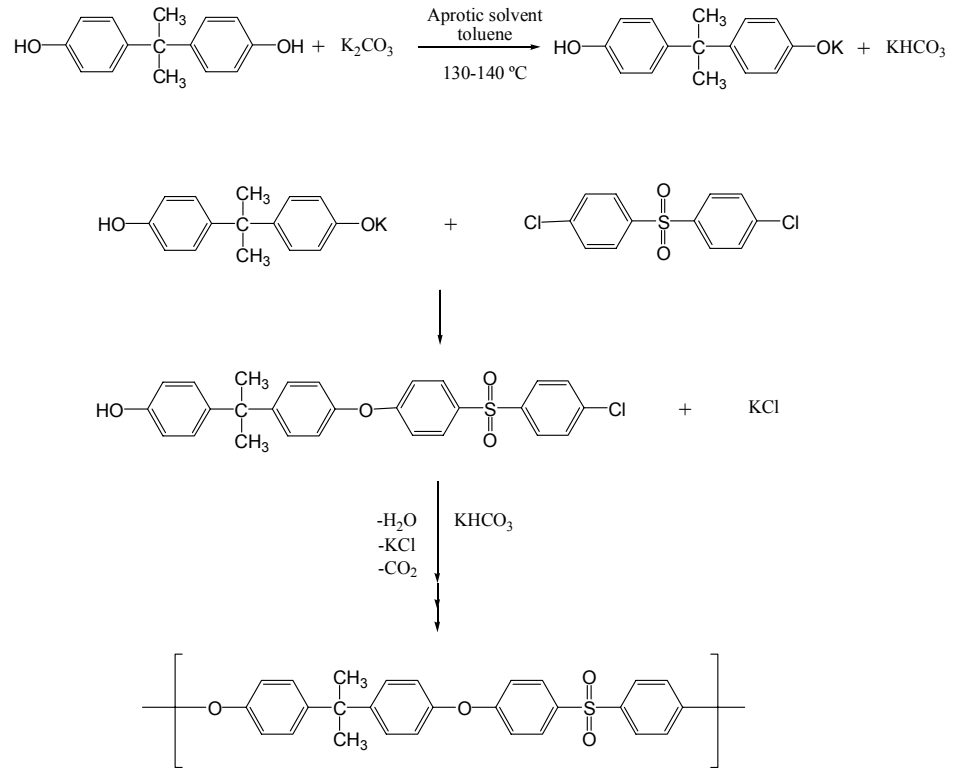

(A)

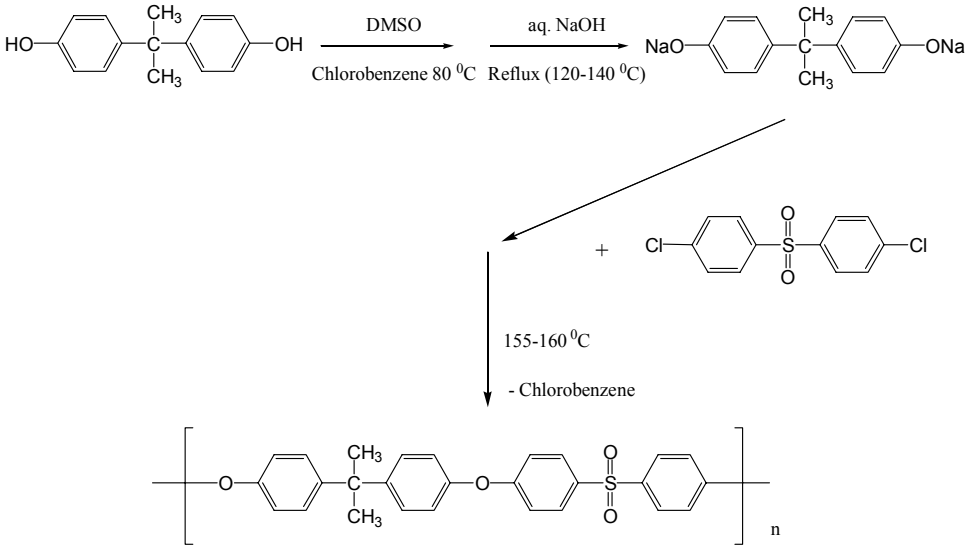

(B)

Figure 2. 17. A Typical Synthesis of Bisphenol A Based Poly(arylene ether sulfone) (A) and The Synthesis Developed by Union Carbide (B).[48]

2.2.2.3. Modification of Poly(arylene ether sulfone)s

Modification of a polymer enables the design of the polymer to fulfill the requirements for specific applications without sacrificing its intrinsic properties. Owing to its convenience and economic aspects, polymer modification has been an attractive synthetic method for generating new types of polymers. For poly(arylene ether sulfone)s, various modifications were explored, including the introduction of new functional groups and incorporation of cross-links in the system. For example, the solvent resistance of poly(arylene ether sulfone)s can be enhanced by an introduction of crystalline polymer blocks such as polyether ether ketone (PEEK). Another approach is the introduction of cross-links in linear poly(arylene ether sulfone)s by appropriate chain-end functionalization. [79-82]

For the past decades, various approaches of modification methods of poly(arylene ether sulfone)s have been reported.[83-86] For modifications, poly(arylene ether sulfone)s need to be activated either by controlled direct lithiation or by a dual process of bromination/lithiation. Both routes involve aromatic ring lithiated polymer intermediates which can react with a variety of electrophiles to give their respective products. It was reported that a maximum of two lithium atoms can be substituted per repeat unit. The substitution position of lithiation on the repeat unit by direct lithiation is mainly at the ortho-position to the sulfone, while ortho-position to the ether results from the bromination/lithiation method. Figure 2.18 shows the two distinct lithiation processes and their lithiation positions.

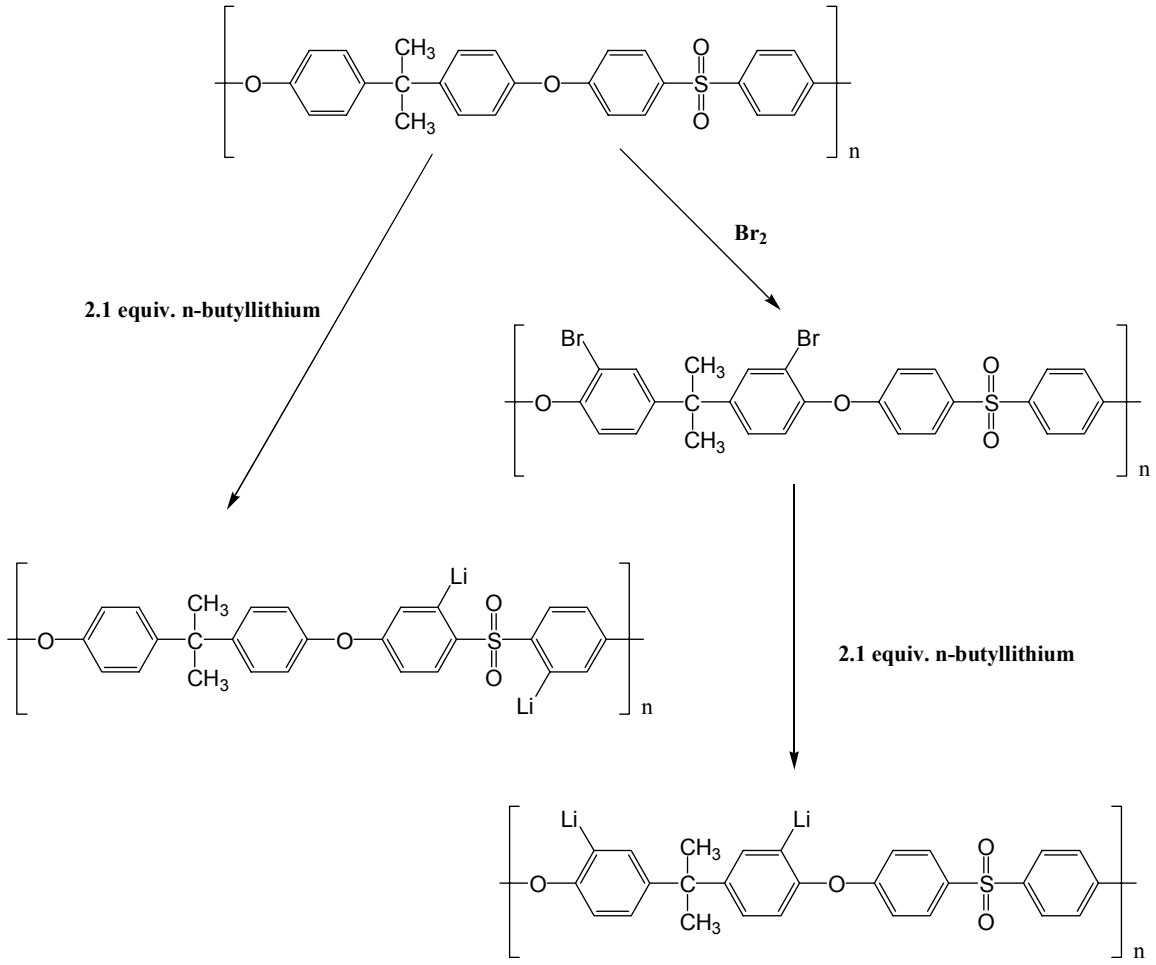

Figure 2. 18. Lithiation of Poly(arylene ether sulfone) by Direct Lithiation and Bromination/lithiation Two Step Method.

The lithiated intermediates can be further modified to azides by treatment with tosyl azides. Azides are thermally and photochemically labile groups capable of being transformed readily into a number of other useful derivatives such as amines. Various reactions of poly(arylene ether sulfone) bearing lithium or azide reactive groups are depicted in Figure 2.19.

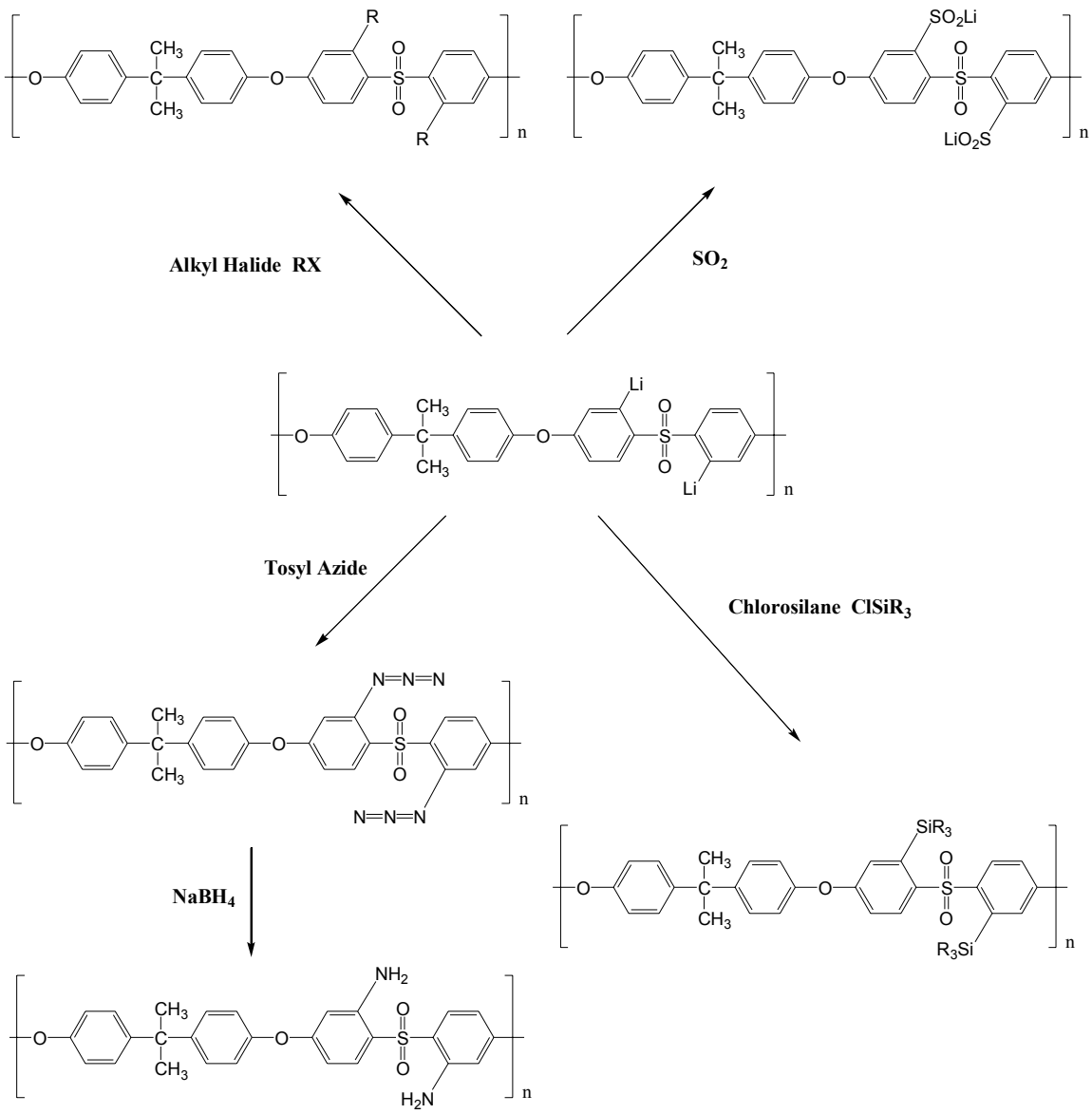

Figure 2. 19. Various Reactions with Lithiated Poly(arylene ether sulfone)s.

2.2.2.4. Synthesis of Poly(arylene ether sulfone)s by Ring-opening Polymerization

In recent years, a new but not yet important synthetic strategy of poly(arylene ether sulfone)s was developed based upon the ring-opening polymerization (ROP) of cylic oligo (ether sulfone)s, OESs.[87-89] Initially this synthetic method was applied for the synthesis of bisphenol-A-based polycarbonates by Brunelle et. al and triggered huge

interest for the synthesis of polycondensation type polymers such as polyesters, polyethers, and polythioether ketones. Compared to conventional step-growth polymerization, the ROP system has several advantages and disadvantages. The main drawback of this type of reaction is limited availability of the cyclic macromonomers. Only a few cyclic precursors are commercially available for poly(arylene ether sulfone) synthesis.

On the other hand, there are a number of advantages. First, the polymerization can be conducted in bulk as the low viscosity of the cyclic oligomer permits it to act as a reaction solvent. In addition, the reaction does not produce any byproducts. For these facts, the ROP approach is suitable for reaction-molding (RIM) applications. Also, a very high molecular weight (Mn > 10^5 Da) polymer can be easily obtained by using highly strained cyclic monomers. Third, various block copolymers can be synthesized by sequential copolymerization with other cyclic monomers. Several synthetic schemes of poly(arylene ether sulfone)s based on ROP are shown in Figure 2.20.

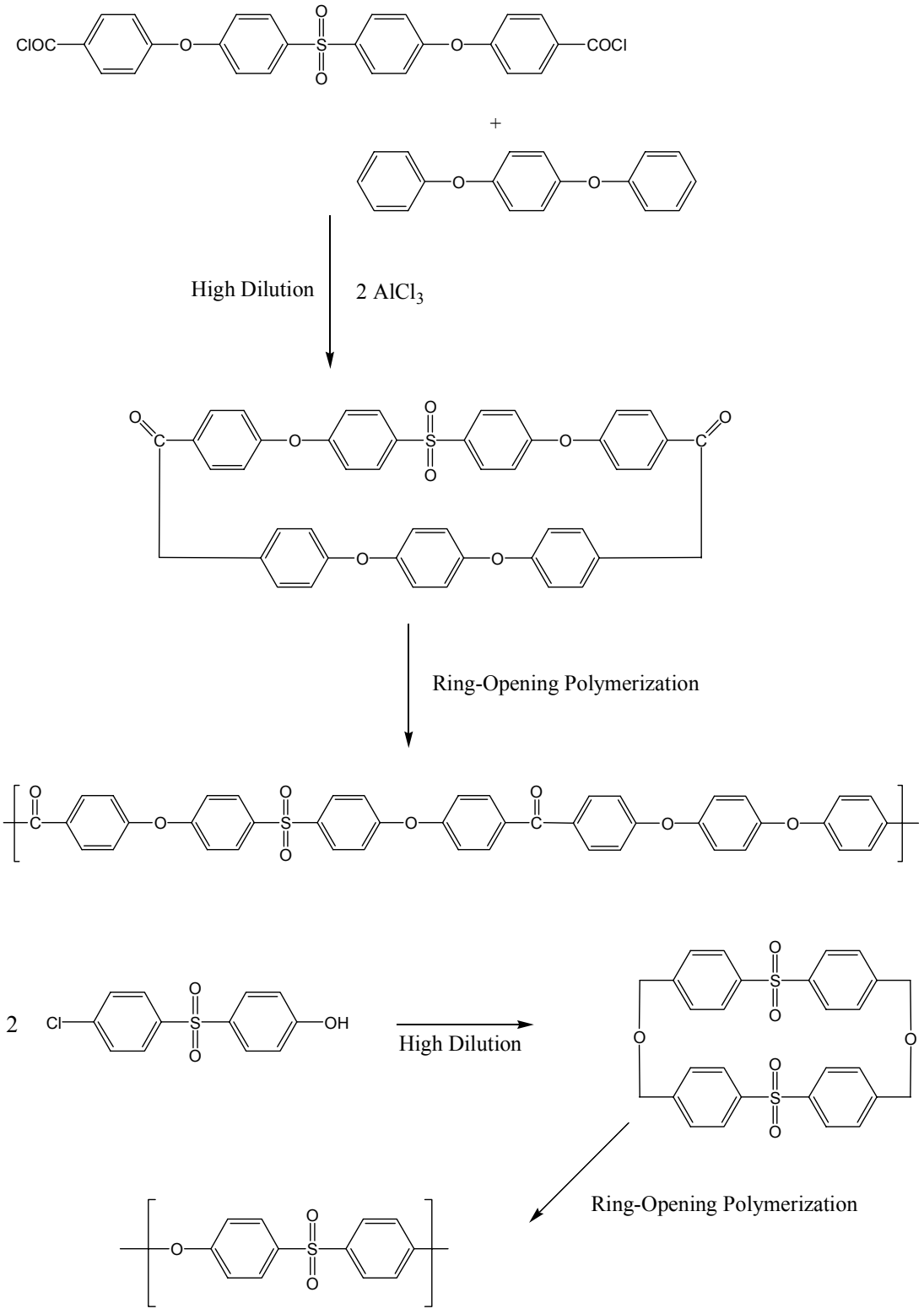

Figure 2. 20. Examples of Ring-opening Polymerization(ROP) of Poly(arylene ether sulfone).[88]

2.2.3. Poly(arylene ether sulfone)s for Proton Exchange Membrane Applications

As described in the earlier section, poly(arylene ether sulfone) is one of the engineering thermoplastics which possesses excellent thermal and oxidative stability, good mechanical properties, good processibility and exceptional hydrolytic stability. With these outstanding properties, poly(arylene ether sulfone)s are promising candidates for use in proton exchange membranes (PEMs) for fuel cell applications. Most PEM applications of poly(arylene ether sulfone) are based on incorporation of proton conductive sulfonic acid moieties on the polymer. There are two major methods to introduce sulfonic acid groups along polymers which will be described in the following chapters.

2.2.3.1. Post-sulfonation of Poly(arylene ether sulfone)s

Post-sulfonation of aromatic ring containing polymers is an electrophilic aromatic substitution reaction. Given that the reaction can easily produce sulfonated polymer by using commercially available polymers and sulfonation reagents, a lot of attention has been paid to this process since Quentin et. al[90] reported the first post-sulfonation of a bisphenol-A based poly(arylene ether sulfone) with chlorosulfonic acid for reverse osmosis membrane applications. Based on this pioneering research, various sulfonated poly(arylene ether sulfone)s have been successfully synthesized by post-sulfonation reactions using chlorosulfonic acid, sulfuric acid, sulfur trioxide, fuming sulfuric acid and acetyl sulfate.[91-95] The resulting sulfonic acid moieties attached to the polymer are capable of proton conduction.[96-98] Bishop et. al[99] adjusted the degree of sulfonation by varying the sulfonation reaction time and the acid concentration, yielding a degree of sulfonation of 30-100%. In general, proton conductivity and water uptake of the

sulfonated polymers increase along with the degree of sulfonation up to a certain point where the membranes lose their mechanical integrity because of an abrupt increase in swelling. Due to this trade-off between fuel cell performance and mechanical properties, the typical degree of sulfonation ranges between 60% and 80% of the repeat units. An example of a post-sulfonation reaction is depicted in Figure 2.21.

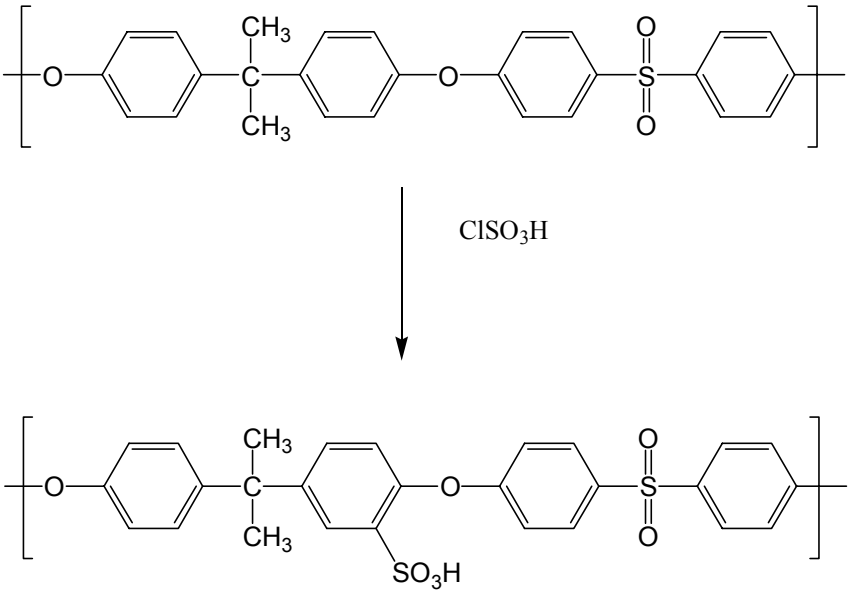

Figure 2. 21. Post-sulfonation of Poly(arylene ether sulfone)[91].

However, the harsh reaction conditions cause undesirable degradation and side reaction of polymers such as chain scission, branching, and crosslinking, especially in bisphenol A based poly(arylene ether sulfone) and when chlorosulfonic acid is used. To address these issues, Noshay and Robeson[94] introduced an alternative sulfonation method for commercially available poly(arylene ether sulfone).[94] For this approach, they used a 2:1 molar ratio complex of SO_3 and triethyl phosphate(TEP) as a sulfonating reagent at room temperature. This mild condition route could minimize possible side reactions but the

complexity of controlling the degree of sulfonation degree and difficulty of handling the chemicals limited further applications

As briefly introduced in the polymer modification section, the sulfonic acid moiety can also be incorporated via metallized polymer intermediates. This approach was initially proposed by Kerres et. al. and the procedure includes the lithiation of the Udel commercial poly(arylene ether sulfone) by n-butyllithium at low temperature, then conversion of lithiated polymer to sulfonated polymer by the reaction with sulfur dioxide (SO_2).[100] Figure 2.22 is the synthetic route to sulfonated poly(arylene ether sulfone) via metalation. Although proton exchange membranes synthesized via metalation showed promising results, this process is rather complicated and control of the reaction is still not easy.

Although the post-sulfonation process has a lot of advantages, including reaction convenience and low cost, several hurdles have limited its uses for PEM applications which require precisely controlled properties.[9] Specific disadvantages include 1) the control of the degree of sulfonation, 2) high degree of sulfonation is not feasible; only one sulfonic acid moiety per repeating unit can be incorporated because the first introduction of a sulfonated group to a repeating unit deactivates the aromatic ring which prohibits further sulfonation, 3) sulfonation on the polymer does not produce true a random copolymer because of the inhomogeneity of the reaction mixture and 4) the hydrolytic stability of the sulfonated polymer might be worse than that of the parent polymer.

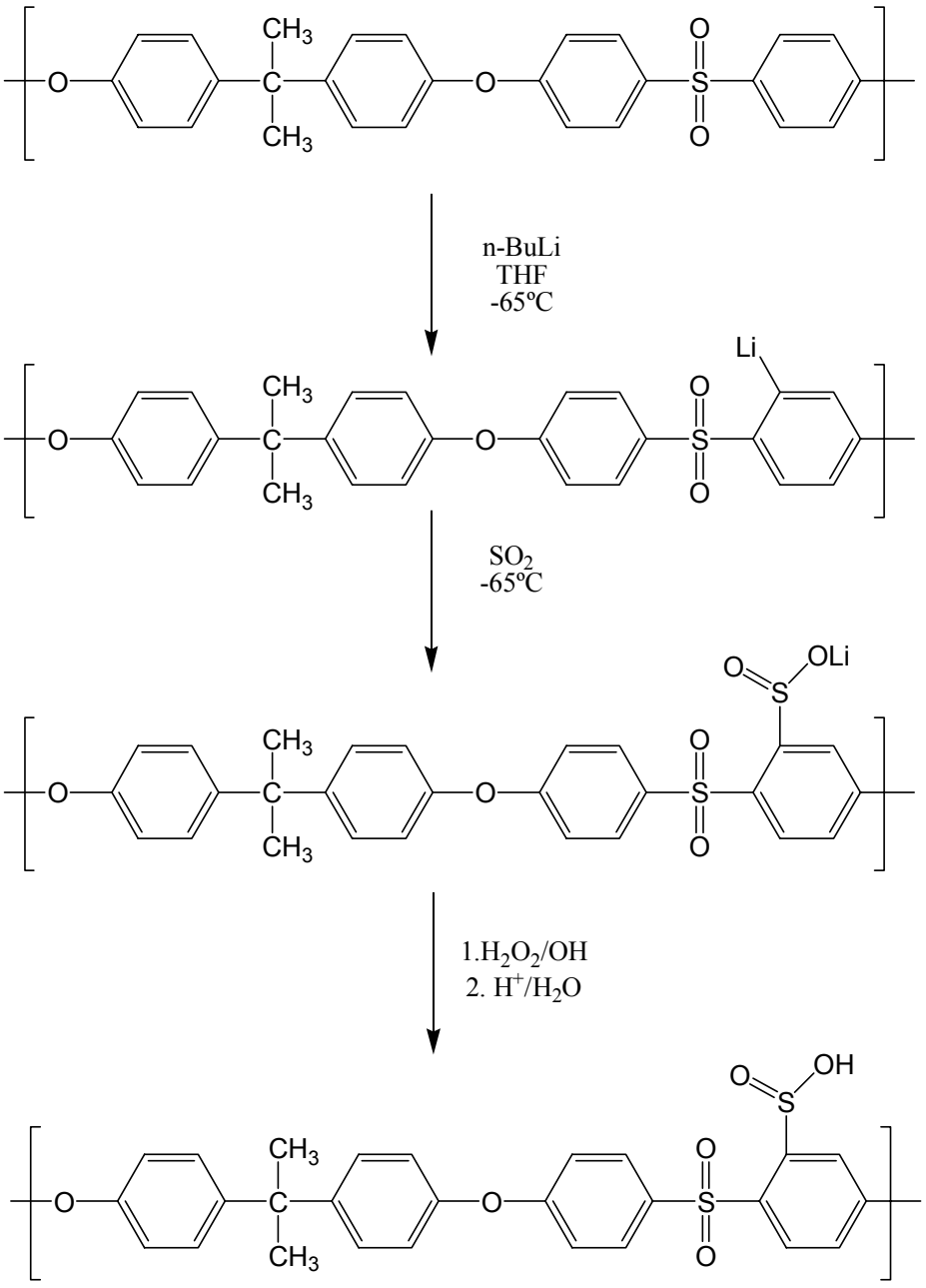

Figure 2. 22. Sulfonation of Poly(arylene ether sulfone) via the Metalation Route.[100]

2.2.3.2. Direct Statistical Copolymerization of Disulfonated Poly(arylene ether sulfone)s

Among the disadvantages of sulfonated poly(arylene ether sulfone) derived from the post-sulfonation route, its poor chemical stability has been become a critical issue for fuel cell applications. This instability of the polymer can be explained by the position of sulfonic acid moiety in poly(arylene ether sulfone). Generally, sulfonation via the post-sulfonation route occurs in the electron rich "activated" ring rather than electron deficient "deactivated" ring in the polymer, this sulfonation process decreases electron density of the ring and, as a result, makes the aromatic carbon-oxygen bond more labile to hydrolysis.[9] This hydrolytic instability has motivated researchers to develop sulfonated poly(arylene ether sulfone)s in which sulfonic acid groups are attached to the electron poor "deactivated" ring near the electron-withdrawing sulfone groups (Figure 2.23). The sulfonic acid groups on the deactivated ring might not only provide better hydrolytic stability but also higher acidity owing to the electron-withdrawing sulfone group. Sulfonation on the deactivated ring can be accomplished by two different methods: previously discussed metalation-sulfination-oxidation route developed by Kerres and coworkers in the chemical modification section[100], and the direct copolymerization of a modified monomer.[101, 102] However, the metalation-sulfination-oxidation route has unavoidable side reactions and is difficult to control, for these reasons the latter method is gaining more attraction for the synthesis of sulfonated poly(arylene ether sulfone)s.

Typical product by post-sulfonation

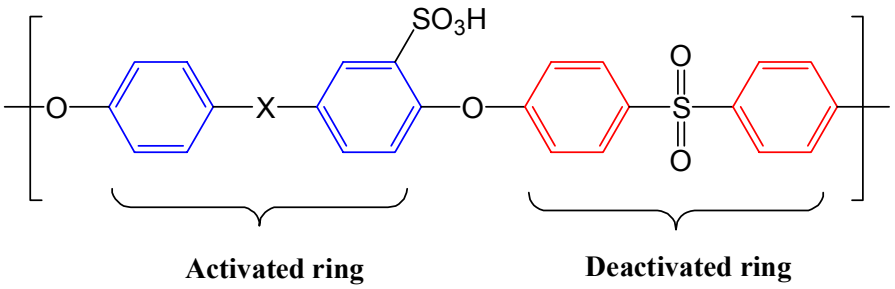

Typical product by direct copolymerization

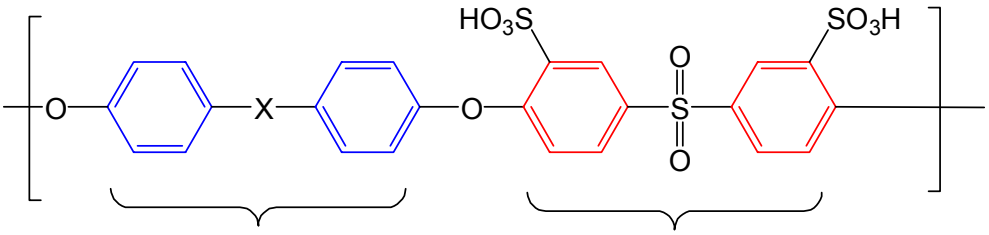

X : a bond or 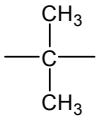

Figure 2. 23. Placement of Sulfonic Acid in Post-sulfonation and Direct Copolymerization Routes.

Direct copolymerization of a modified monomer affords better control of the sulfonation position and degree of sulfonation in the resulting copolymer. The first sulfonated poly(arylene ether sulfone) synthesized by the method was reported by Robeson and Matzner in 1983.[101] They showed sulfonation of 4,4'-dichlorodiphenyl sulfone (DCDPS) and synthesized a sulfonated poly(arylene ether sulfone) by using the sulfonated DCDPS as a monomer for the purpose of producing more fire-resistant material. Later, Ueda et al.[102] prepared 3,3'-disulfonated-4,4'-dichlorodiphenyl sulfone(SDCDPS) by reacting DCDPS with fuming sulfuric acid and reacted this

monomer with bisphenol A and unmodified DCDPS to synthesize a sulfonated poly(arylene ether sulfone) with a disulfonation degree of up to 30 mol %. The synthesis of the sulfonated monomer by the Ueda research group is shown in Figure 2.24.

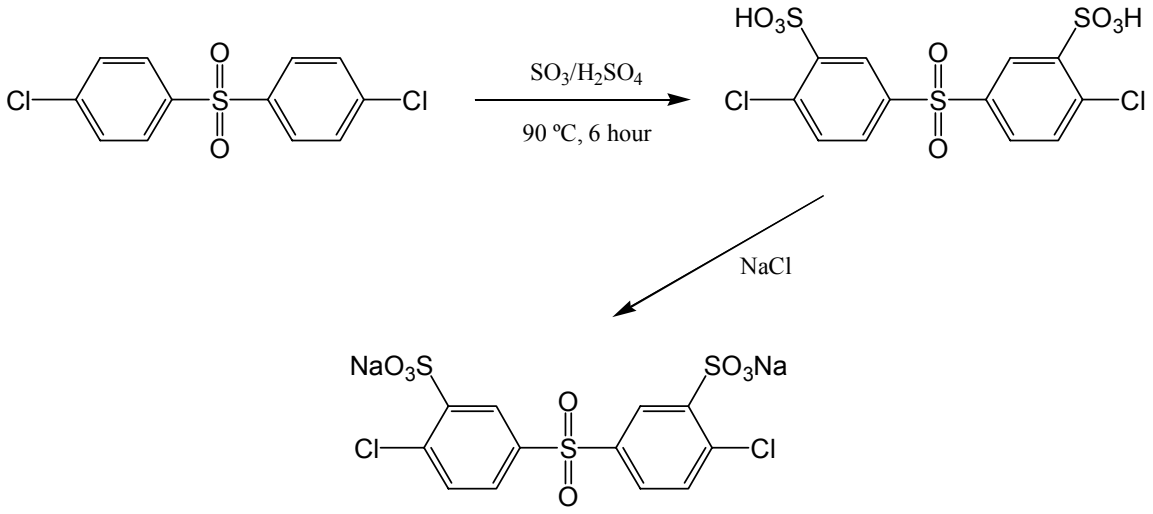

Figure 2. 24. Syntheiss of 3,3'-Disulfonated 4,4'-Dichlorodiphenyl Sulfone.[102]

Although pioneer researchers successfully synthesized sulfonated poly(arylene ether sulfone)s via monomer modification route, the new process did not immediately receive attention for other applications. However, more recently, McGrath et al. made considerable progress by preparing wholly aromatic sulfonated poly(arylene ether sulfone)s by direct copolymerization for fuel cell applications.[103-105] They also modified the synthetic route to increase the purity and yield of the sulfonated monomer and there is continuing interest in a one stage process that has the potential of reducing the yield loss upon recrystallization.[106, 107] Various copolymers were synthesized by the reaction of SDCDPS, DCDPS, and 4,4'-biphenol via a nucleophilic substitution route. The modified

monomer synthesis and direct copolymerization of wholly aromatic BPSH copolymers by the McGrath group are shown in Figures 2.25 and 2.26, respectively.

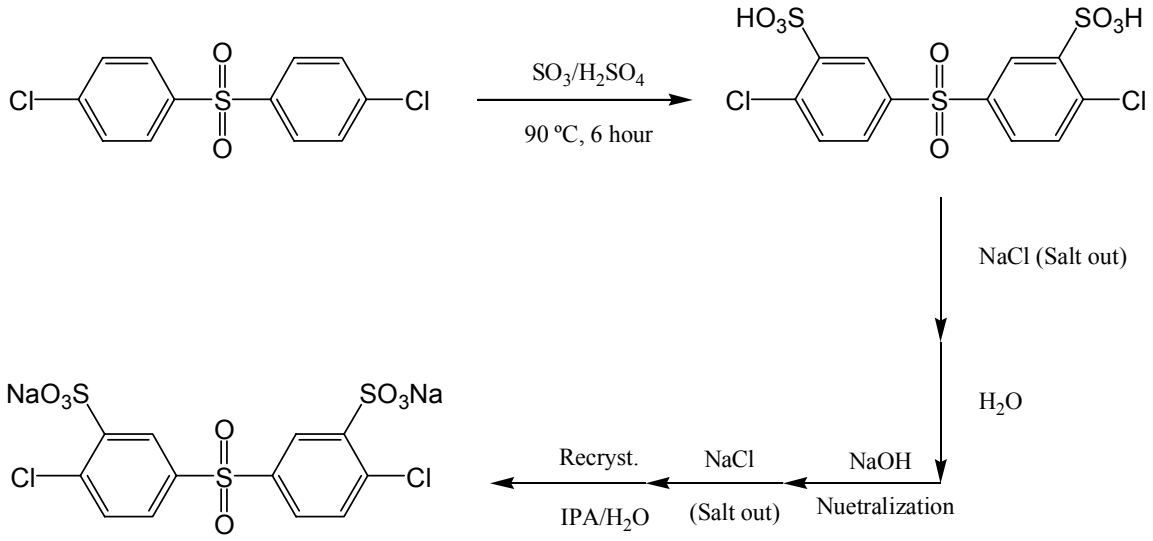

Figure 2. 25. Modified Synthetic Route of 3,3'-Disulfonated 4,4'-Dichlorodiphenyl Sulfone.

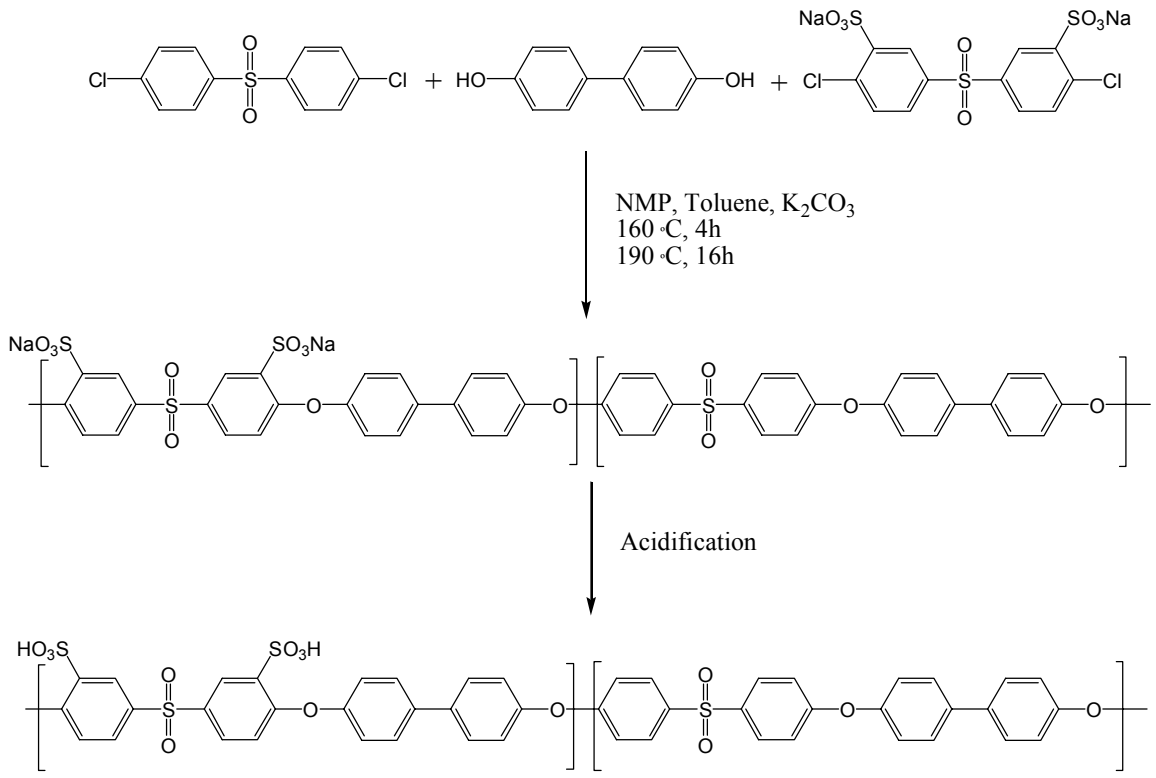

Figure 2. 26. Direct Copolymerization of Wholly Aromatic BPSH Copolymer.

The proton conductivity and water uptake of the resulting copolymer increased with the degree of disulfonation up to 60%. However, when the degree of disulfonation approaches 60%, its swelling dramatically increases and results in the deterioration of mechanical properties caused by semi-continuous hydrophilic domain morphology.[7, 12, 108] With a 35-40% disulfonation degree, this polymer showed very high proton conductivity which is comparable to that of Nafion. Furthermore, its lower cost and excellent stability made it attractive as a promising alternative to the perfluorinated Nafion-like materials for certain applications including direct methanol fuel cells (DMFCs) as portable power. Further research has been devoted to making various

copolymers by incorporation of functional groups onto the BPSH copolymer. Various moieties investigated in direct copolymerization by the same research group are summarized in Figure 2.27. [109]

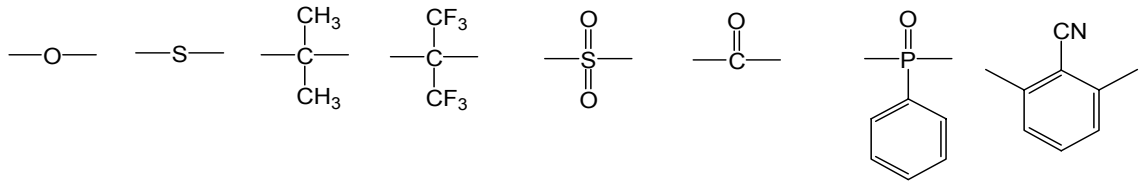

Figure 2. 27. Various Moieties Explored in Sulfonated Poly(arylene ether sulfone) Type Proton Exchange Membrane.[109]

2.3. Proton Exchange Membranes (PEMs) Based on Polyimides

2.3.1. General Properties of Polyimides

2.3.1.1. Introduction of Polyimides

Polyimides are polymers which have a heterocyclic imide moiety in the repeat unit. Most polyimides are synthesized from a condensation reaction between diamines and tetracarboxylic acid derivatives.[110, 111] The general structure of a polyimide is depicted in Figure 2.28.

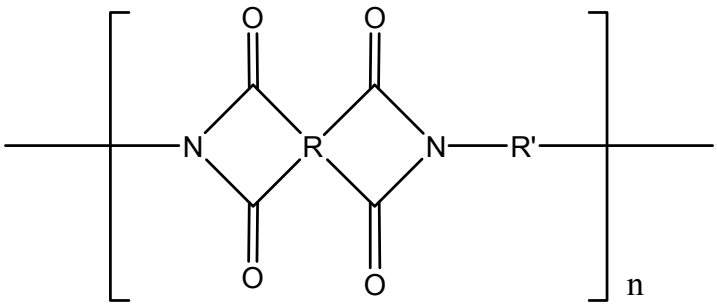

R : cycloaliphatic or cycloaromatic
R' : aliphatic or aromatic

Figure 2. 28. General Structure of a Polyimide.

The first report of aromatic polyimide synthesis goes back to 1908 by Bogert and Renshaw.[112] They found that the condensation reaction of 4-aminophthalic anhydride could afford a polymeric material. However, this research was not further developed until the 1950s, when DuPont's film department began to focus their research on the development of a "convertible polymer". The shape of a "convertible polymer" is easily changed when it is in its precursor state, but once treatments are applied it converts to a permanent configuration and is neither soluble nor fusible. Their early attempts to make

a “convertible polymer” were focused on an aliphatic polyimide system by the reaction between 4,4-dimethylheptamethylene diamine and pyromellitic dianhydride (PMDA). In 1955, the aliphatic monomer based polyimide was developed by the DuPont research group and named Polymer E.[113, 114] Although Polymer E gained some attention as a new material, its properties were not significantly superior to those of conventional polymers such as polyethylene terephthalate.

One of the approaches to enhance the properties of Polymer E by the film department was adopting aromatic diamine “m-phenylenediamine (m-PDA)” instead of aliphatic diamine for the synthesis. In 1956, Andy Endrey successfully synthesized an aromatic monomer based polyimide via poly(amic acid) precursor whose thermal, mechanical, and electrical properties exceed those of previous aliphatic polyimides.[115, 116] After further research, they found that polyimides synthesized from oxydianiline (ODA) monomer had better hydrolytic stability and processability than polyimides synthesized from m-PDA. Finally, the first commercial polyimide was introduced by DuPont with the trade name of Kapton® (Figure 2.29).

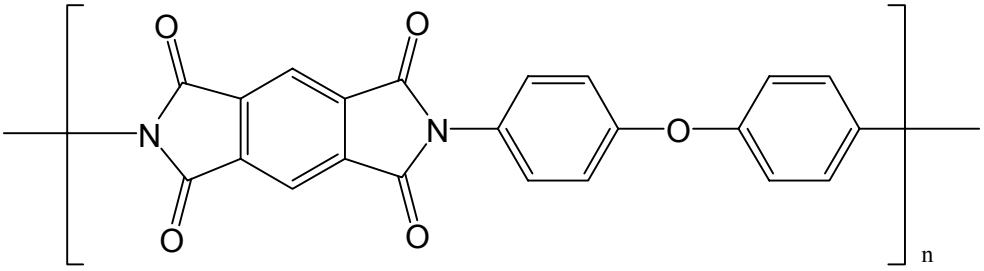

Figure 2. 29. Chemical Structure of Kapton® Polyimide.

2.3.1.2. General Applications of Polyimides

Polyimides have been widely used as engineering plastics due to their excellent thermal and chemical stabilities combined with mechanical toughness since DuPont commercialized Kapton®.[117, 118] In addition to thermal and mechanical properties, their excellent dielectric properties and the similar coefficient of thermal expansion (CTE) with a silicon substrate made polyimides one of the best microelectronic materials in the semiconductor industry.[119-123] Two major applications of polyimides as an electronics material are as a protective overcoating and an interlayer dielectric insulator.

In the final step of semiconductor production, fabricated microcircuits on silicon wafers need to be encapsulated by plastic molding. During the encapsulation process, the delicate circuits can be damaged by handling and induced stresses from the molding process. To protect the circuits from these possible damages, a 4-6 μm polyimide film is applied on the circuit using a solution spin coating process before the encapsulation. In this case, the polyimide film can protect the circuit as a protective overcoat and a stress buffer layer. The low dielectric constant of polyimides also made them useful as insulators.[124-127] Polyimides can be easily coated on copper or other electrical wire and act as an insulator. If this property is combined with photolithography, polyimides can be used as a more complex interlayer dielectric insulator layer in a semiconductor.

Polyimides are also important in aircraft and aerospace applications.[128-131] For aircraft and aerospace applications, their extreme environmental stresses have demanded not only high performance but also high reliability from candidate materials. Due to the excellent heat and chemical resistance as well as good mechanical properties, polyimides have been chosen as a leading candidate for aircraft and aerospace applications. The high flexural modulus and compressive strength results in excellent dimensional stability

which enabled polyimides to be used in structure components such as struts, brackets, and composites. Other applications in which polyimides can be implemented are coatings. Due to the ease of the coating process of the polyimide precursor for various shapes, DuPont's Kapton has been used for aerospace cables, wiring, and laminates.

2.3.2. Synthesis of Phthalic 5-Membered Ring Polyimides

It has been around 50 years since the first commercial polyimide was introduced to the market.[117] During this period, various synthetic methods have been developed by several research groups to facilitate more efficient and cost-beneficial methods of preparation. Even though there are several different synthetic routes for specific purposes, most reactions utilize the reaction of diamines with dianhydrides. In this chapter, discuss several synthetic methods in terms will be discussed of their mechanisms and reaction conditions.

2.3.2.1. Conventional Two-step Approach

Generally speaking, the direct one step synthesis of high molecular weight aromatic polyimide is not feasible. This is due to the insoluble and infusible nature of polyimides which tends to cause premature precipitation during the intermediate stages of polymerization. To overcome this problem, a two-step condensation strategy was first suggested by Edwards and successfully applied for the production of Kapton in 1965.

For the first stage of the two-step approach, diamine and dianhydride monomers are dissolved in a suitable polar aprotic solvent, such as dimethylaceteamide (DMAc), dimethylsulfoxide (DMSO), or N-methylpyrrolidinone (NMP). Then, the nucleophilic

amine moieties on diamine monomers attack the carbonyl carbons on the dianhydride monomers to produce a high molecular weight poly(amic acid).[131] Figure 2.30 shows the reaction mechanism between an anhydride and an amine.

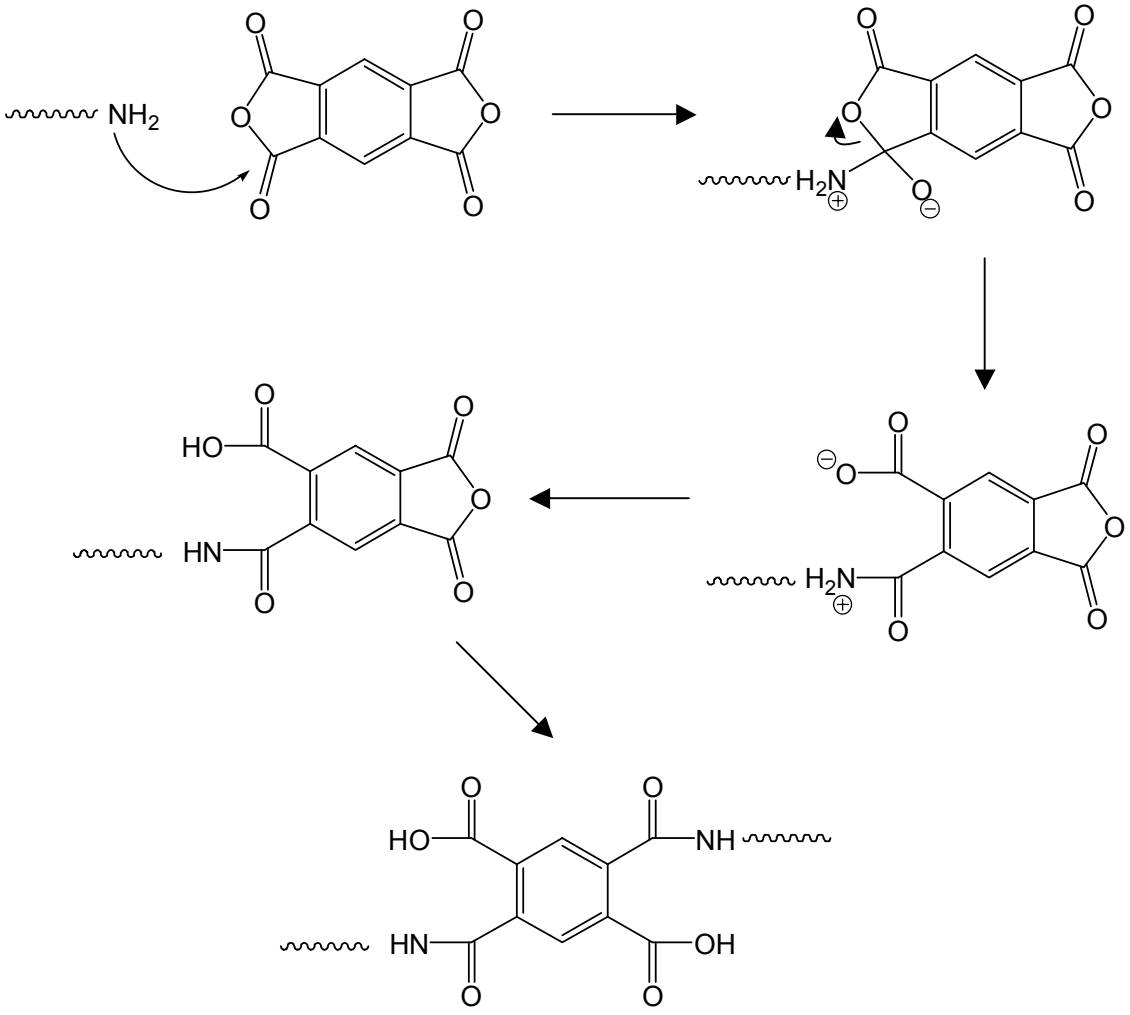

Figure 2. 30. Mechanism for Poly(amic acid) Formation via Nucleophilic Substitution Reaction.[110]

For the amidization reaction, several factors should be considered to produce a high molecular weight poly(amic acid). First, using more basic reaction solvents will push the reaction equilibrium towards producing poly(amic acid) since the reaction product poly(amic acid) is acidic, more basic solvents can stabilize the product by stronger hydrogen bonding.[132, 133] Second, a mild reaction temperature will shift the equilibrium to the product poly(amic acid). Due to the exothermic nature of the amidization reaction, a high reaction temperature will retard the reaction and as a result, low molecular weight poly(amic acid) will be obtained.[131, 134] For this reason, the first step of the synthesis is usually conducted below 30 ºC. Other factors which can affect the reaction rate and molecular weight of the poly(amic acid) are monomer reactivity and the presence of water during the reaction. Based on the fact that the amidization reaction is a nucleophilic substitution reaction, higher nucleophilicity of the amine and higher electrophilicity of the anhydride results in faster amidization reaction. In addition, the presence of water in the reaction mixture can decrease the molecular weight of poly(amic acid) which can react with dianhydride monomer to produce nonreactive diacid species.

The second step of the two-step reaction is the cyclodehydration reaction (imidization) of the poly(amic acid). It can be accomplished by several methods such as heat or chemicals (Figure 2.31). Detailed methods for the imidization reaction will be covered in the following chapters.

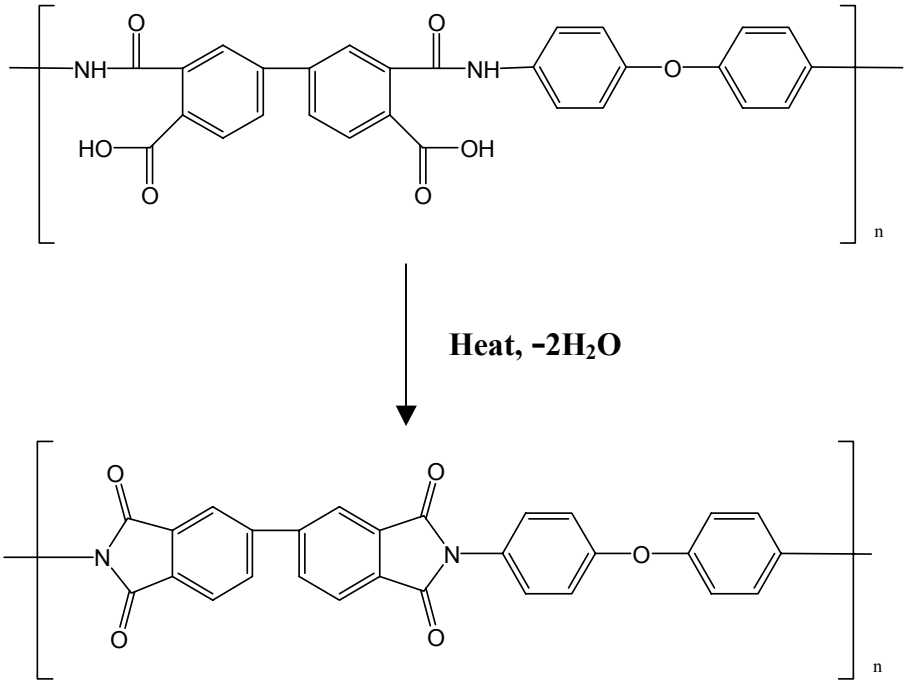

Figure 2. 31. Imidization Reaction of Poly(amic acid).

2.3.2.2. Bulk (Thermal) Imidization

The most frequently used method of imidizing poly(amic acid) is thermal imidization which is also known as bulk imidization.[135, 136] This method is especially useful for the preparation of film type insoluble polyimides. First, poly(amic acid) solution is cast onto a shaped substrate and heated to induce cyclization(imidization). The heating process is usually carried out under vacuum or in an inert atmosphere to promote the cyclization reaction by removing solvent and water, which is a byproduct of the cyclization reaction. The extent of imidization is governed by several parameters such as heating temperature, heating time, residual solvent, and the rigidity of the final polyimide. To obtain a high degree of imidization, the treatment temperature should be higher than the ultimate T_g of the system. As the solvents evaporate during the heat

treatment, the viscosity of the system drastically increases and at a certain point, further imidization is prohibited by a lack of mobility of the polymer chain. In this case, heat treatment above the system T_g can provide chain mobility to continue the reaction, resulting in a high degree of imidization. Residual solvent also can provide additional chain mobility of the system by plasticization of the polyimide.

2.3.2.3. Chemical Imidization

One of the drawbacks of thermal imidization is a possible hydrolytic degradation of the polymer by the water which is a byproduct of the imidization reaction. During the imidization reaction, water is continuously produced by the condensation reaction between acid and amide moieties and may cause degradation of unreacted poly(amic acid) (Figure 2.32).

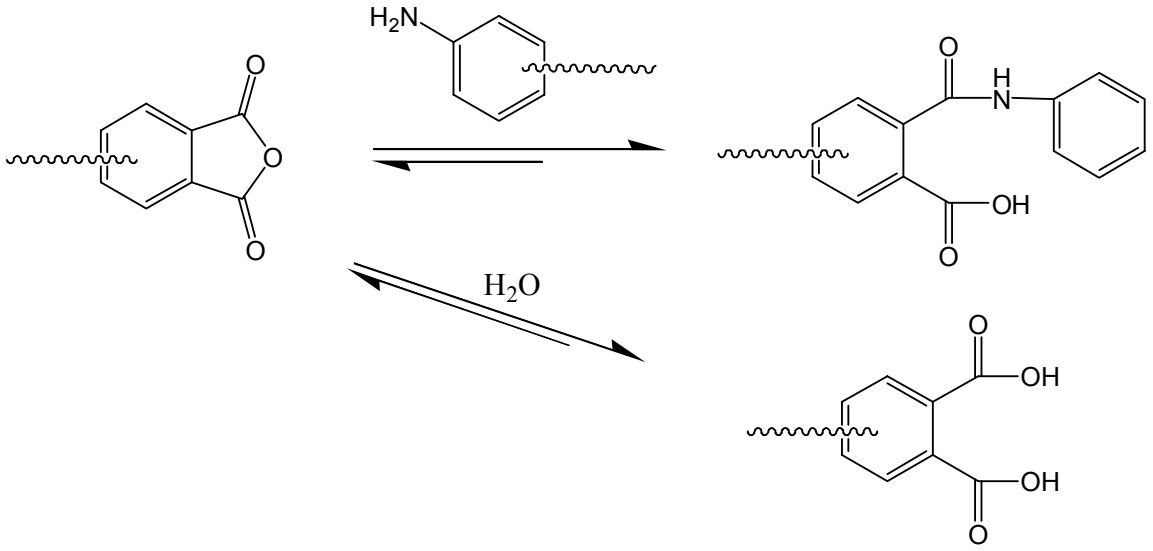

Figure 2. 32. A Mechanism of Hydrolytic Degradation of Poly(amic acid).[110]

The problem of hydrolytic degradation can be addressed by using a chemical imidization process whose reaction mechanism lacks a water production step. Typically, chemical imidization is carried out at room temperature with various combinations of anhydrides and amines as imidization catalysts.[137-139] A detailed mechanism of chemical imidization is shown in Figure 2.33.

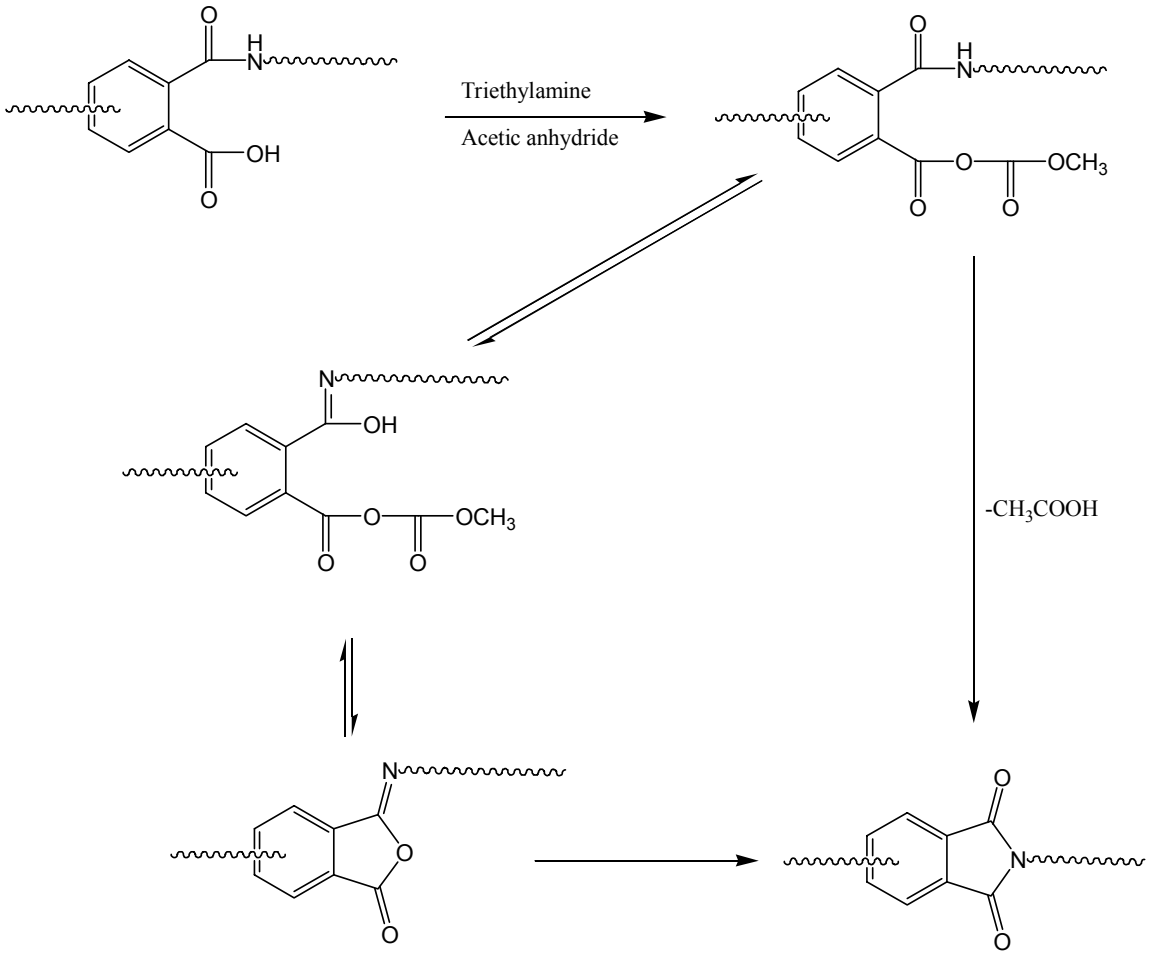

Figure 2. 33. Proposed Mechanism of Chemical Imidization.[110]

2.3.2.3. One-pot High-temperature Imidization

When polyimides are soluble in organic solvents, it is possible to synthesize them from their corresponding monomers by the so-called one-pot or one-step method.[140-144] In this method, dianhydride and diamines react to produce polyimide in a high boiling-temperature organic solvent typically higher than 160ºC. The most widely used solvents are m-cresol, NMP, nitrobenzene, and α-chloronaphthalene possibly with isoquinoline and benzoic acid as catalysts. The water generated by imidization during the reaction can be easily removed by using azeotroping agents such as N-cyclohexylpyrrolidone (CHP) or o-dichlorobenzene (DCB) at the high reaction temperatures. The one-pot method is especially useful for less reactive monomers whose structures are sterically hindered. Phenylated dianhydrides are typical monomers which have a sterically hindered structure and are not suitable for synthesizing high molecular weight poly(amic acid) by the conventional two-step method. However, these monomers can readily react with diamines to give high molecular weight polyimides using the one-step method. It is interesting to note that the polyimides synthesized via the one pot method may show a higher degree of crystallinity than those which can be obtained from the conventional two-step polymerization method. One possible explanation for this phenomenon is that the high degree of solvation of polyimides can be possible at the high reaction temperature which may allow it to obtain a more favorable conformation for packing.

It is also possible to design organic solvent soluble polyimides which can be synthesized in a one-pot reaction by structure modification.[110] The structure modification can reduce stiffness and interchange ordering of the polyimides and allow them to be soluble in organic solvents. Typical modification strategies are summarized below.[145]

1. incorporation of flexible structural units such as ether, SO_2, CF_3
2. utilizing "kinked" structures, such as meta- or orthocatenation between aromatic rings
3. incorporation of bulky pendant groups along the chain.
4. limiting molecular weight by monofunctional end capping agents

In spite of extensive research, there is still an incomplete understanding of the mechanism of one-pot polyimide synthesis. It is highly likely that the formation of polyimide proceeds via a poly(amic acid) route but the observed lifetimes of the amic acid moieties on poly(amic acid) were extremely short. This suggested mechanism has been supported by kinetic studies which have shown that the rate-determining step in imide formation is the second-order reaction between the anhydride and the amine.[146] Thus imidization occurs either simultaneously with propagation, or very quickly thereafter. The typical degree of amidization by one-pot reaction is almost 100%. A widely known example of a commercial polyimide by one-pot high temperature reaction is General Electric's Ultem^{TM}, The reaction scheme is shown in Figure 2.34.

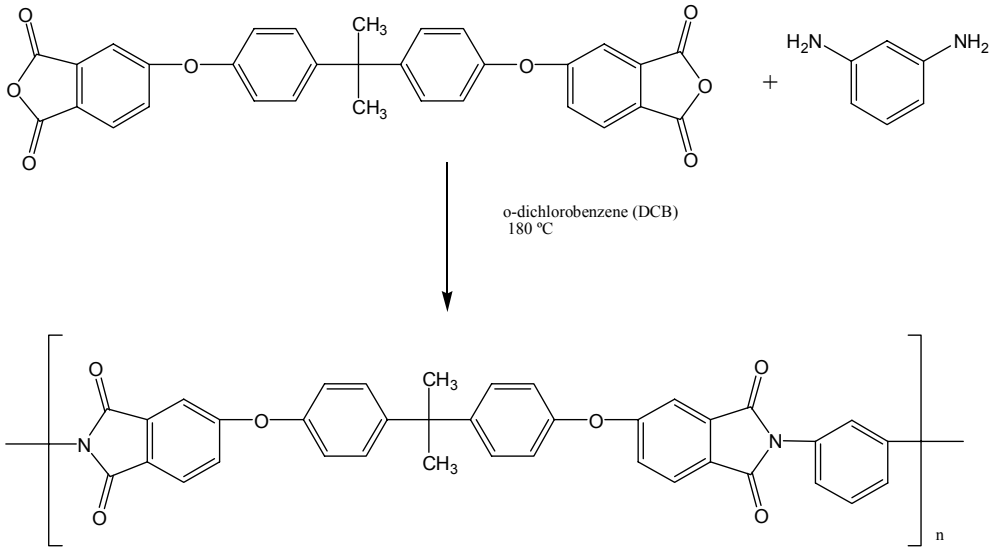

Figure 2. 34. Reaction Scheme of Ultem^{TM} Polyimide by One-pot Polymerization.

2.3.3. Six-membered Ring Polyimides

In the past decades, most of polyimide research has been focused on five-membered ring polyimides. On account of these intense efforts, extensive information about five-membered ring polyimides has been well established such as the reaction mechanism, structure-property relationships, and synthetic methods. Recently, more attention has been paid to six-membered ring polyimides because of their superior thermal, chemical, and hydrolytic stabilities over conventional five-membered ring polyimides.[147, 148] These enhanced properties are attributed to the relatively less strained six-membered imide ring structure which is more stable toward nucleophilic attack. However, a high molecular weight six-membered ring aromatic polyimide cannot be made by the conventional two-step method because of the low reactivity of six-membered ring anhydrides towards aromatic amines at low reaction temperature. To overcome this low reactivity of six-membered ring anhydrides, a higher reaction temperature is necessary to carry out the reaction. Typically, the reactions are carried out in m-cresol as a reaction solvent at temperatures higher than 140 ºC using catalysts.[149-152]

2.3.3.1. Dianhydrides for Six-membered Ring Polyimides

All dianhydride derivatives which can form six-membered ring polyimides are based upon naphthalene. The two most widely used commercial dianhydrides are naphthalene-1,4,5,8-tetracarboxylic dianhyride (NDA) and perylene-3,4,9,10-tetracarboxylic dianhydride (PDA) (Figure 2.35).[153-155]

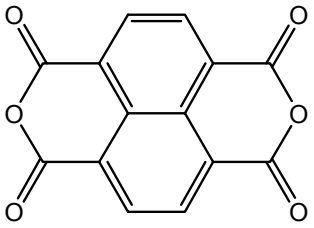

naphthalene-1,4,5,8-tetracarboxylic dianhyride (NDA)

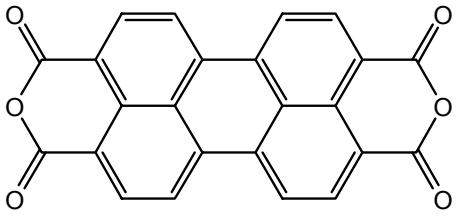

perylene-3,4,9,10-tetracarboxylic dianhydride (PDA)

Figure 2. 35. Chemical Structures of NDA and PDA.

As described in the earlier section, the poor solubility and melt processibility of many five-membered ring polyimides can be overcome by using a two-step polymerization method which involves the formation of soluble poly(amic acid) and followed by the imidization process. On the other hand, due to the impossibility of utilizing the two-step synthetic method for six-membered ring polyimide, the chemical structures of diamine monomers which give organic soluble polyimides are very important. Generally, the incorporation of flexible bridging units such as ether, CH_2, C=O, $C(CF_3)_2$, and SO_2 into the diamine structure is considered.

2.3.3.2. Reaction Conditions for Six-membered Ring Imide Formation.

While six-membered ring polyimides show improved thermal and hydrolytic stabilities due to the less strained and stable six-membered imide ring in their structure, the lower reactivity of six-membered ring dianhydride monomers toward diamine monomers needs special reaction conditions to obtain high molecular weight polyimides. General approaches in order to overcome the low reactivity between six-membered ring dianhydrides and diamines include reaction temperature, catalyst, and reaction solvent.

Among them, intense research has explored catalysts such as benzoic acid, isoquinoline, imidazole, quinoline, pyridine, triphenylphospine, and triphenyl phosphine oxide.[149-152] In addition to the types of catalyst, the concentration of catalyst, auxiliary catalyst, and addition time of each catalyst has also been studied. Based on a model synthesis, most viscous six-membered ring polyimides were synthesized when the reaction was carried out in m-cresol reaction solvent with benzoic acid and isoquinoline as catalysts.[156] Furthermore, the addition order of the catalysts and the mole ratio of the catalyst and dianhydrides were also evaluated. The most effective catalyst system was a 2:1 molar ratio of benzoic acid and isoquinoline to a dianhydride monomer while benzoic acid should be added at the beginning of the reaction, with isoquinoline added after nine hours. As a result of these observations, most contemporary research groups who are synthesizing six-membered ring polyimides utilize these reaction conditions.[157, 158]

2.3.3.3. Reaction Mechanism for Six-membered Ring Imide Formation.

In order to determine the catalytic effect on the reaction mechanism of one-step high temperature polycondensation of six-membered ring polyimides, a series of model compounds was synthesized from 4-benzoyl-1.8-naphthalenene anhydride with various aromatic diamines by Schab-Balcerzak et al.[159] At first, they tried to determine whether the mechanism of one-step high temperature polycondensation of six-membered ring polyimides involves the formation of poly(amic acid) similar to those of conventional one-step high temperature imidization. If the mechanism has poly(amic acid) as an intermediate, the formation of poly(amic acid) should be promoted by acid catalyst. However, the results showed a reverse trend, as higher acidity of the catalyst resulted in a

lower yield of the final product. Based on this observation, they concluded that the poly(amic acid) is not an intermediate in a high temperature condensation reaction of a six-membered ring polyimde.

Then, to understand the role of acid catalysts, especially benzoic acid, in six-membered ring imidization, various analysis techniques were conducted for model compounds which were synthesized from 4-benzoyl-1,8-naphthalene anhydride and several amines (ODA, 4-biphenylamine, 4-phenyloxyaniline). From ^{15}N-NMR analysis, it was discovered that the nitrogen atoms in the model compounds have sp^2 hybridization which is not consistent with an imide structure. In addition, ^{13}C-NMR showed that the chemical shifts of the model compounds are consistent with those of isoimides. Further analyses, such as ultraviolet-visible spectroscopy (UV-VIS), mass spectroscopy, and differential scanning calorimetry (DSC) confirmed that the intermediate in the one-step high temperature imidization is the isoimide structure.

For isoimide compounds, two stereoisomers (cis and trans) may exist. In order to determine the effect of the acid catalyst (i.e., benzoic acid) on the chemical structure of the model compounds, two series of model compounds were synthesized.[160, 161] One was synthesized with acid catalyst and the other was synthesized without acid catalysis. Based on the UV-VIS spectral analysis along with DSC analysis, the result suggests that the model compounds which were synthesized in the absence of acid catalyst were completely cis-isoimide while the model compounds prepared with acid catalyst were a mixture of cis and trans-isoimide. Furthermore, they discovered that only the trans-isoimide can be converted to the consequent imide structure with base catalyst i.e.,

isoquinoline under high temperature conditions. A summary of the proposed reaction mechanism is shown in Figure 2.36.

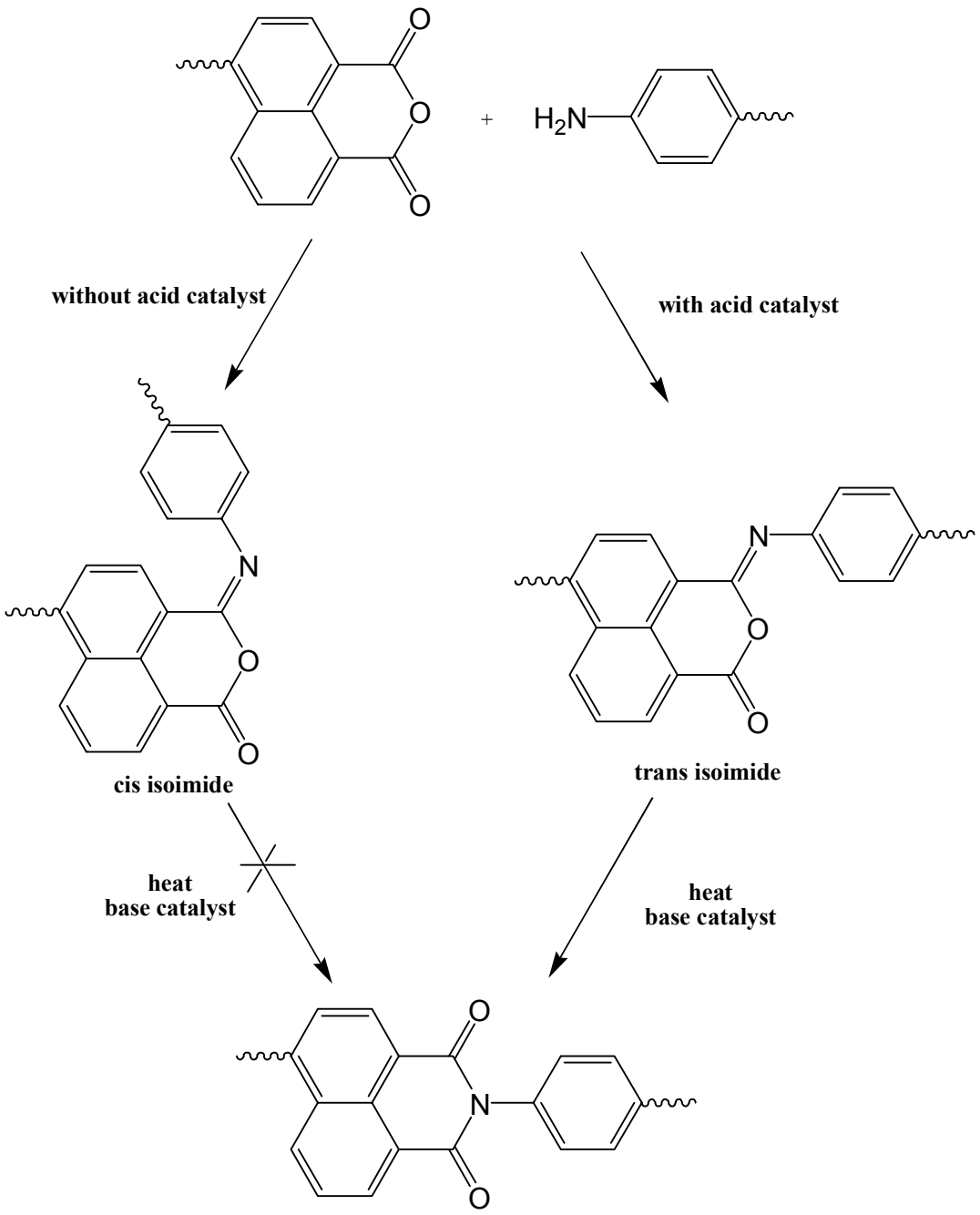

Figure 2. 36. Summary of the Reaction of 1,8-Naphthalene Type Anhydride with Aromatic Amine.

2.3.4. PEMs Based on Polyimides

Most of polyimides' properties, including excellent thermal stability, high mechanical strength, good film forming ability, and good chemical resistance meet the requirements for being an ideal PEM. For this reason, sulfonated polyimides have been studied for many years as a PEM material. Initial approaches utilized conventional five-membered ring polyimides based on phthalic anhydride. However, due to the ease of hydrolysis of the imido rings under acidic fuel cell environments, sulfonated phthalic polyimides for PEM applications were not successful. Hydrolysis of the imido rings causes chain scissions and reduces the polymers' original molecular weight.[162, 163] Several scientists have shown that this problem can be addressed by using six-membered ring polyimides, which are more hydrolytically stable under acidic conditions than five-membered ring polyimide due to the reduced ring strain in the structures. Genies et al. conducted a systematic hydrolytic stability study with sulfonic acid containing polyimides based both on five-membered(phtahlic imide) and six-membered ring(naphthalenic imide) as model compounds.[163] Those model compounds were placed in 80 ºC water and their chemical structure changes were monitored. For the sulfonic acid containing phthalic imide, an NMR study revealed that it started to degrade after 1 h and was completely modified in 10 h. On the other hand, sulfonic acid containing naphthalenic imide started to change its structure after 120 h which confirmed the superior hydrolytic stability of the six-membered ring polyimide over the five-membered ring polyimide.

For the last decade, various sulfonated polyimides based on naphthalenic imide have been synthesized and characterized.[157, 162, 164-167] Most researchers utilize commercially available naphthalenetetracarboxylic dianhydride (NTDA) and

sulfonated/nonsulfonated diamines for the polyimides synthesis. These copolymers can be classified into two groups based on the used sulfonated diamine structure.[168, 169] "Type I" sulfonated diamines have sulfonic acid and amine moieties on the same aromatic rings such as 2,2'-benzidinedisulfonic acid (BDSA), 4,4-diamino-diphenyl-ether-2,2'-disulfonic acid (ODADS), and 4,4'-bis(4-amino-2-sulfophenoxy)biphenyl (*i*BAPBDS). In contrast, amine moieties and sulfonic acids are located on different aromatic rings for "Type II" sulfonated diamines such as 4,4'-bis(4-aminophenoxy)biphenyl-3.3'-disulfonic acid (*p*BAPBDS), 4,4'-bis(3-aminophenoxy)biphenyl-3,3'-disulfonic acid (BAPFDS), and bis[4-(4-aminophenoxy)-phenyl]sulfone-3,3'-disulfonic acid (*p*BAPPSDS) (Figure 2.37).

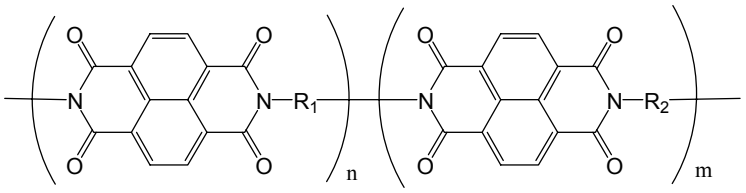

Copolymer Structure

R_1 Sulfonate Diamines

Type I

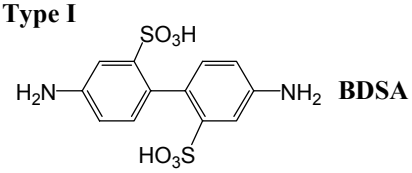

BDSA

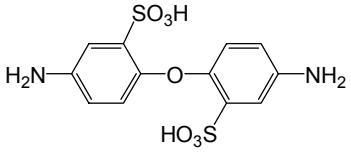

ODADS

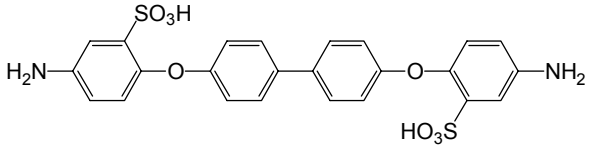

***i*BAPBDS**

Type II

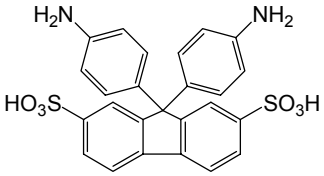

BAPFDS

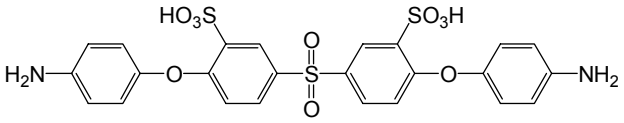

***p*BAPPSDS**

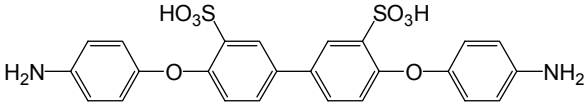

***p*BAPBDS**

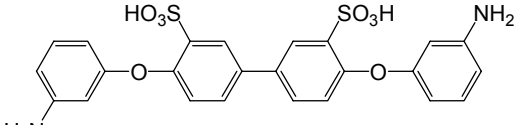

***m*BAPBDS**

R_2 Nonsulfonate Diamines

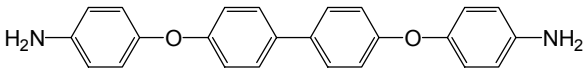

BAPB

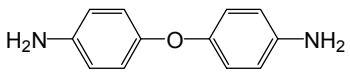

ODA

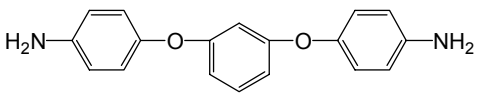

BAPBz

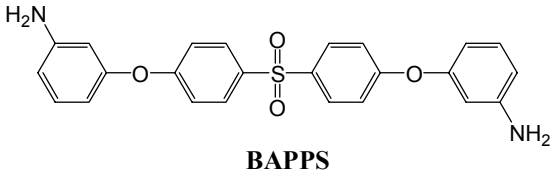

BAPPS

Figure 2. 37. Two Types of Monomers for Sulfonated Polyimide Random Copolymers.

It has been believed that sulfonated polyimides from "Type I" and "Type II" monomers have different hydrolytic stabilities. Since high electron withdrawing sulfonic acid groups and nitrogen atoms are on the same aromatic rings for "Type I" monomer based polyimides, the nitrogen atoms and the next carbon atoms are electron deficient and open to attack by water molecules. In contrast, for "Type II" monomer based polyimides, the nitrogen atoms and electron withdrawing sulfonic acid groups are attached on different aromatic rings. This structure difference makes the nitrogen atoms and the next carbon atoms on "Type II" monomer based polyimides less positive and results in enhanced hydrolytic stability (Figure 2.38).

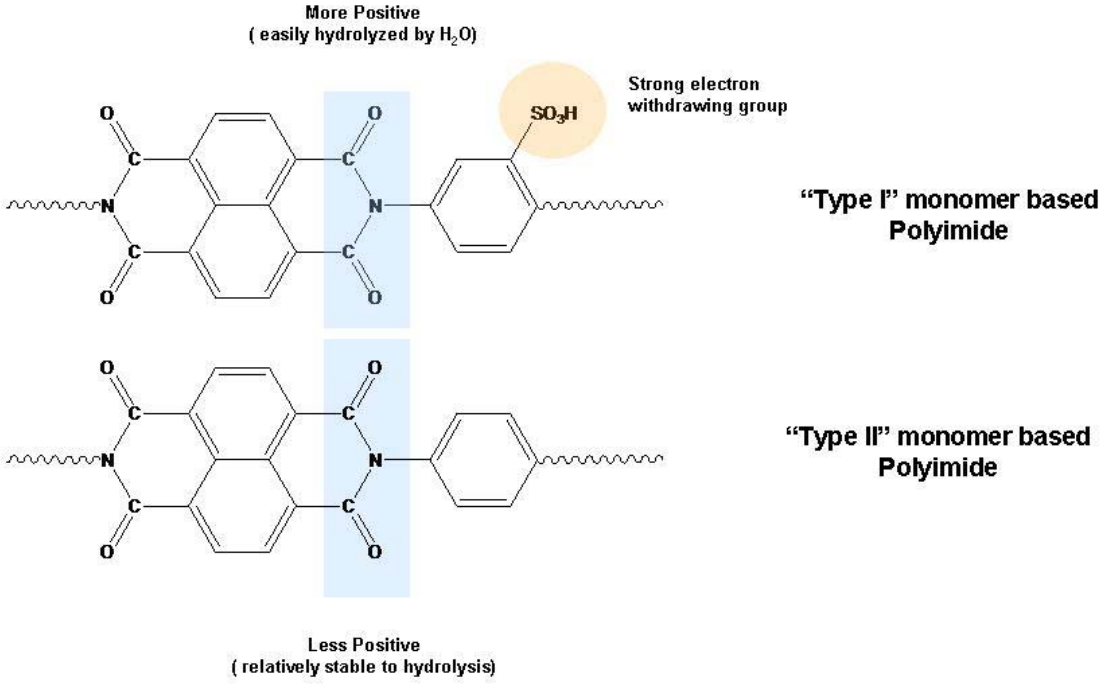

Figure 2. 38. Hydrolytic Stability of Polyimides Derived from Different Monomer Types.

Recently, Watanabe et. al prepared polyimides with pendant, bulky unsulfonated hydrophobic groups to make inter-chain spacing in the polymers.[170-172] By introducing bulky pendant groups in polyimides, the authors tried to make a more open structure by preventing typical close packing of the polyimide backbones. The open structure of PEMs may hold more water and consequently higher conductivity is expected. Figure 2.39 shows the polyimide structures which have bulky pendant groups. Although the polyimides with bulky pendant groups showed very high conductivities at high RH which were about one order of magnitude higher than Nafion 112, the conductivities at low RH rapidly decreased and were below the Nafion control.

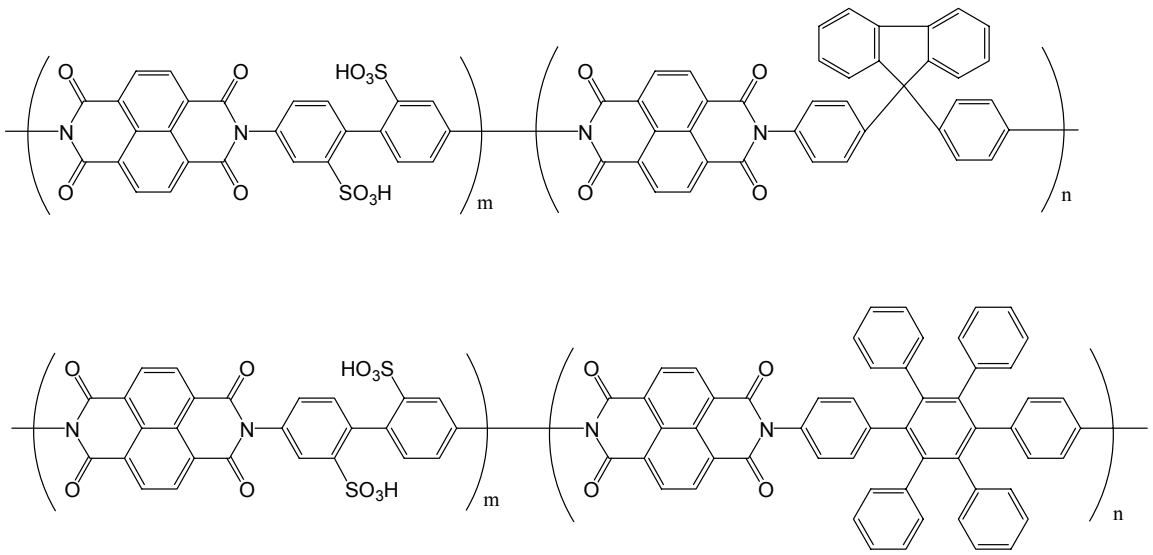

Figure 2. 39. Naphthalenic Polyimides with Bulky Pendant Groups.

Another approach to improve hydrolytic stability of sulfonated naphthalenic polyimide based PEM was made by Einsla et al.[157, 158] They synthesized two types of naphthalenic polyimides with novel sulfonated diamine monomer 3,3'-disulfonic acid-bis[4-(3-aminophenoxy)phenyl]sulfone which contained flexible sulfone and ether linkages (Figure 2.3.12). These polyimides showed good proton conductivities, low

methanol permeation as well as low electro-osmotic drag coefficients. However, their hydrolytic stability remained limited.

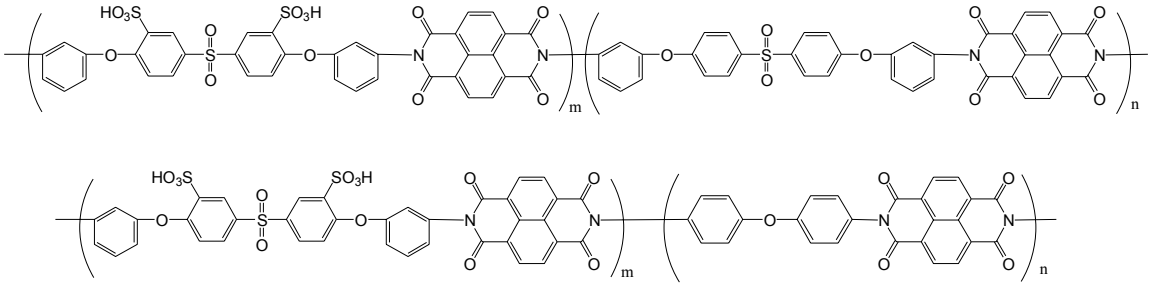

Figure 2. 40. Naphthalenic Polyimides with Flexible Sulfone and Ether Linkages.

2.4. Proton Exchange Membranes (PEMs) Based on Block Copolymers

2.4.1. Morphology of Ionomer Membranes

For past decades, various morphological explanations have been proposed to explain the ion transport mechanism of Nafion® type membranes. In the late 1970s, the morphology of Nafion was initially characterized by means of small-angle X-ray scattering(SAXS) and wide-angle X-ray diffraction(WAXD). The results revealed that the sulfonic acid groups in dry Nafion membranes tend to aggregate to form ion clusters while TFE main backbone forms crystallites. Based on these observations, Gierke proposed a cluster-network model to explain the ion transport phenomenon in the water swollen ionomer membranes.[173, 174] When the Nafion membrane is swollen with water, the ionic clusters swell and are connected by narrow channels which can form a continuous pathway for ion transport.(Fig.2.41).

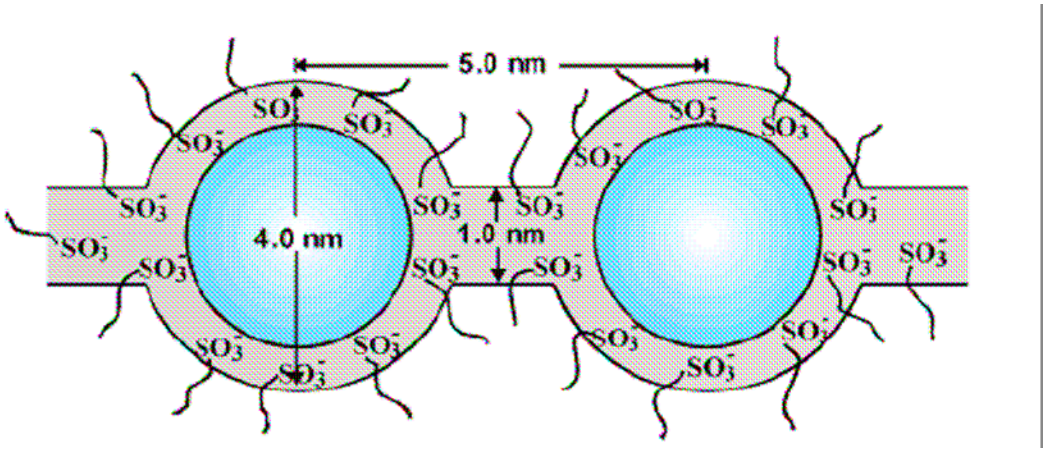

Figure 2. 41. Cluster-network Model for the Morphology of Hydrated Nafion®. Reprinted with permission from Journal of Membrane Science.[175] Copyright 1983 Elsevier.

Other research groups proposed different models to explain ion transport in Nafion type membranes, including the lamellar-structure model, the modified hard-

sphere model, and the depleted-zone core-shell model.[176-179] Although the true morphology of Nafion is still a subject of debate, the cluster-network model has been the most widely accepted in the ionomer membrane related literature and provides a fundamental foundation for structure-property relationship of ionomer membranes. It is believed that the ion transport phenomenon in ionomer membranes is closely related to their nano-scale phase separated morphologies.

The morphology and microstructure of Nafion becomes more important if Nafion is used for PEM applications. For higher proton conductivity, the ionic clusters in Nafion should be well connected by ionic channels to provide an easy pathway for proton conduction. It is believed that the arrangement of the ionic and crystalline regimes in Nafion can be altered by the processing history.[6] For example, when extruded Nafion is transformed into fine dispersions in an alcohol/water mixture and cast into a membrane (often called "recast" Nafion), its mechanical properties and proton conductivities are significantly different from those of the extruded film. Moore et al discovered that recast Nafion was "mud-cracked", brittle, and could form a fine dispersion at room temperature in several polar organic solvents which are not observed for an extruded Nafion membrane.[6] Further WAXD and SAXS studies revealed that a recast membrane was virtually amorphous while extruded Nafion was semicrystalline.

2.4.2. Self Assembly Properties of Block Copolymers

Knowing that the morphologies of ionomer membranes play a crucial role in ion transport phenomenon, intense efforts have been made to enhance proton conductivity and other properties of PEMs by tailoring their morphologies. The main research goal to

obtain high performance PEMs has been focused on an establishment of nano-phase separated morphology of hydrophilic and hydrophobic domains in PEMs by using block copolymers.

Block copolymers can be defined as polymers which consist of two or more segments of homopolymers (blocks) joined by covalent bonds.[180, 181] In general, block copolymers can be classified in three main categories: diblock copolymer, triblock copolymers, multiblock copolymers. They are sometimes referred to as AB, ABA, and $(AB)_n$ type copolymers, respectively. In addition to these conventional block copolymers, there are special types of block copolymers including ABC type block copolymers and star block copolymers (Figure 2.42).

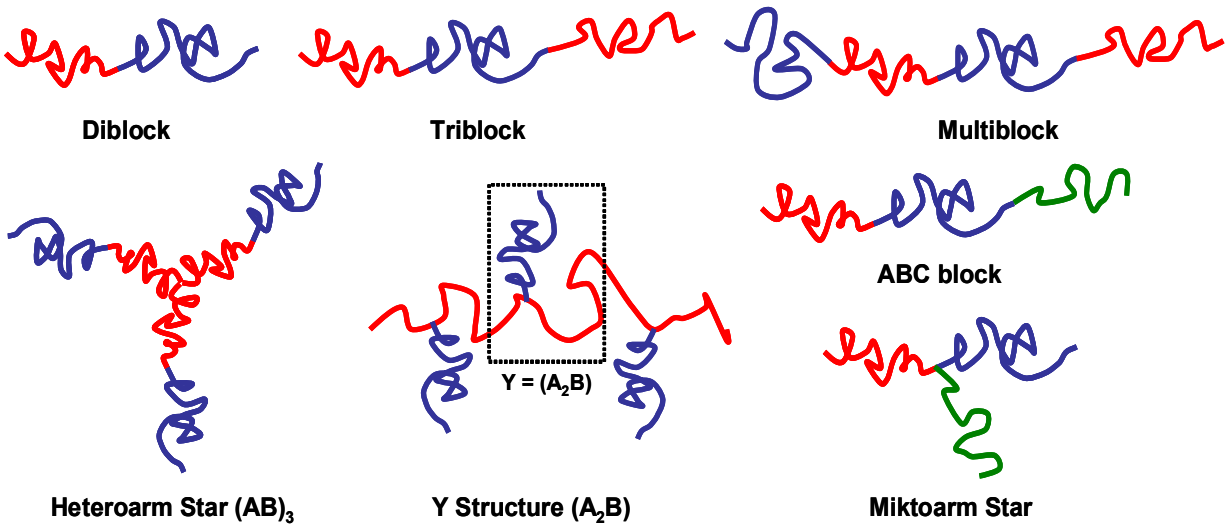

Figure 2. 42. Schematic Representation of Different Types of Block Copolymers.

One of the interesting features of block and graft copolymers is their ability to self assemble to afford various types of microphase separated morphologies.[181-183] For

symmetric diblock copolymers (AB), it is known that several different equilibrium symmetries are possible: lamellae, hexagonal-packed cylinders, bicontinuous gyroid, and body-centered cubic arrays (Figure 2.43). If there are more than three different components in block copolymers, numerous phases can be generated and more than 30 morphologies have been identified for ABC type block copolymers.

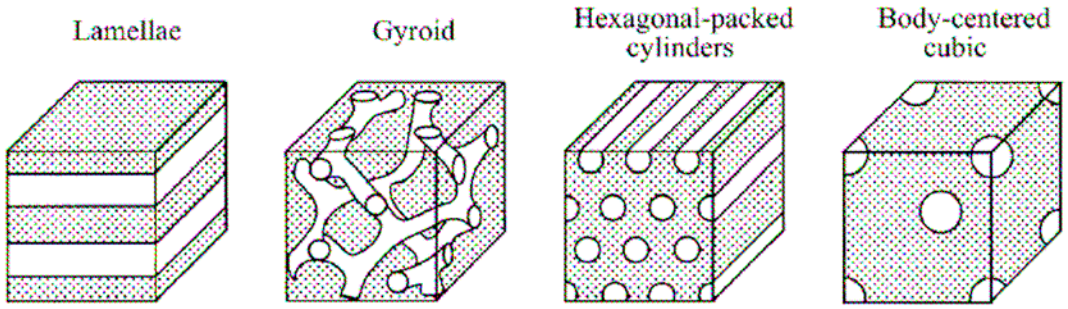

Figure 2. 43. Equilibrium Morphologies for Symmetric Diblock Copolymers as a Function of Compositions. Reprinted with Permission from Current Opinion in Solid State & Materials Science.[184] Copyright 2005 Elsevier.

The phase behavior of block copolymers can be illustrated by a morphology diagram in terms of volume fraction of one component(*f*) (Figure 2.44) where χN represents the enthalphic-entropic balance (χ is the Flory-Huggins interaction parameter, N is the degree of polymerization). When the χN value exceeds its order-disorder transition value [$(\chi N)_{ODT}$], the block copolymer initiates its microphase separation into a periodically ordered structure. It is believed that the extent of microphase separation of block copolymer is dictated by three factors of the segments: 1) compositional incompatibility 2) molecular weight of each segment, and 3) ability to form crystallites by segments.

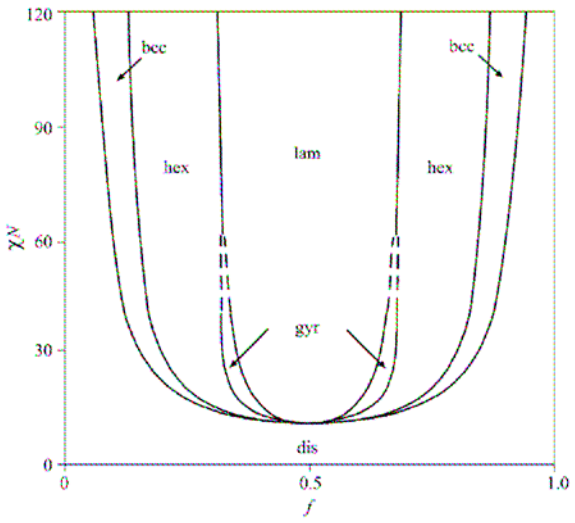

Figure 2. 44. Phase Diagram for a Symmetric Diblock Copolymers. In the Phase Diagram, Regions of Stability of Disordered (dis), Lamellar (lam), Gyroid (gyr), Hexagonal (hex) and Body-centered Cubic (bcc) Phases are Indicated. Reprinted with Permission from Current Opinion in Solid State & Materials Science.[184] Copyright 2005 Elsevier.

This spontaneous formation of well defined phase-separated morphology of block copolymers attracted many scientists for their possible PEM applications. Figure 2.45 shows co-continuous phase-separated morphology in the styrene-butadiene diblock copolymer system.[185] They hypothesized that if well defined co-continuous lamellar structures can be developed in PEMs with hydrophobic-hydrophilic block copolymers similar to a styrene-butadiene system, continuous hydrophilic channels will provide easy pathways for proton conduction especially under low relative humidity conditions.

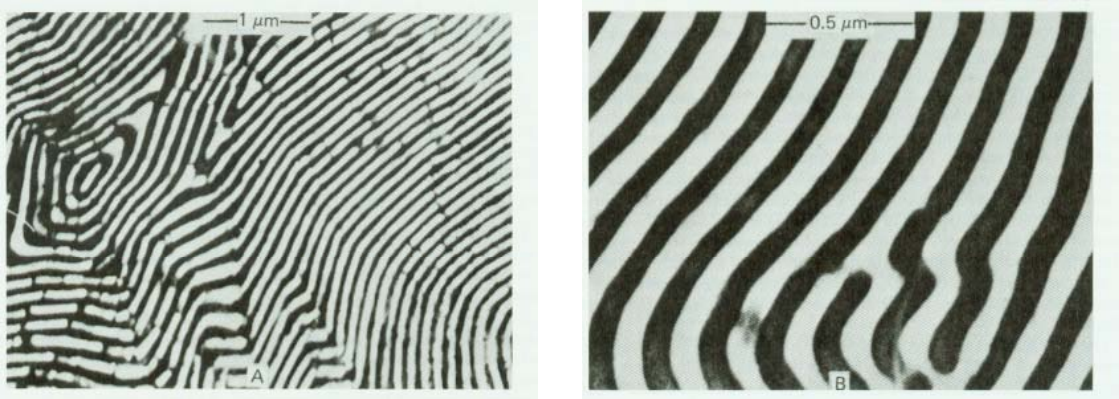

A. Noshay and J.E. McGrath, "Block Copolymers: Overview and Critical Survey," 520 pages, Academic Press, New York, January 1977, p.91.

Figure 2. 45. Co-continuous Phase-separated Morphology in Styrene-butadiene Diblock Copolymer.

2.4.3. Recent Research Trends on Block Copolymers as PEMs

To utilize the self-assembly ability of block copolymers for PEM applications, a variety of block copolymers based on hydrophilic-hydrophobic segments has been explored. Among numerous types of block copolymers, the most extensively studied block copolymers are disulfonated poly(arylene ether sulfone) based multiblock copolymers. As described earlier, disulfonated poly(arylene ether sulfone) based random copolymers (BPSH) show excellent proton conductivity under fully hydrated conditions as well as exceptional mechanical and chemical stabilities. The major drawback of BPSH type PEMs is low conductivity under low humidity conditions. McGrath et. al have tried to overcome this weakness of BPSH type PEM by adopting multiblock architectures.[13, 14, 186-189] The researchers prepared fully disulfonated poly(arylene ether sulfone)s as hydrophilic blocks and conducted coupling reactions with different types of hydrophobic blocks to produce multiblock copolymers (Figure 2.46).

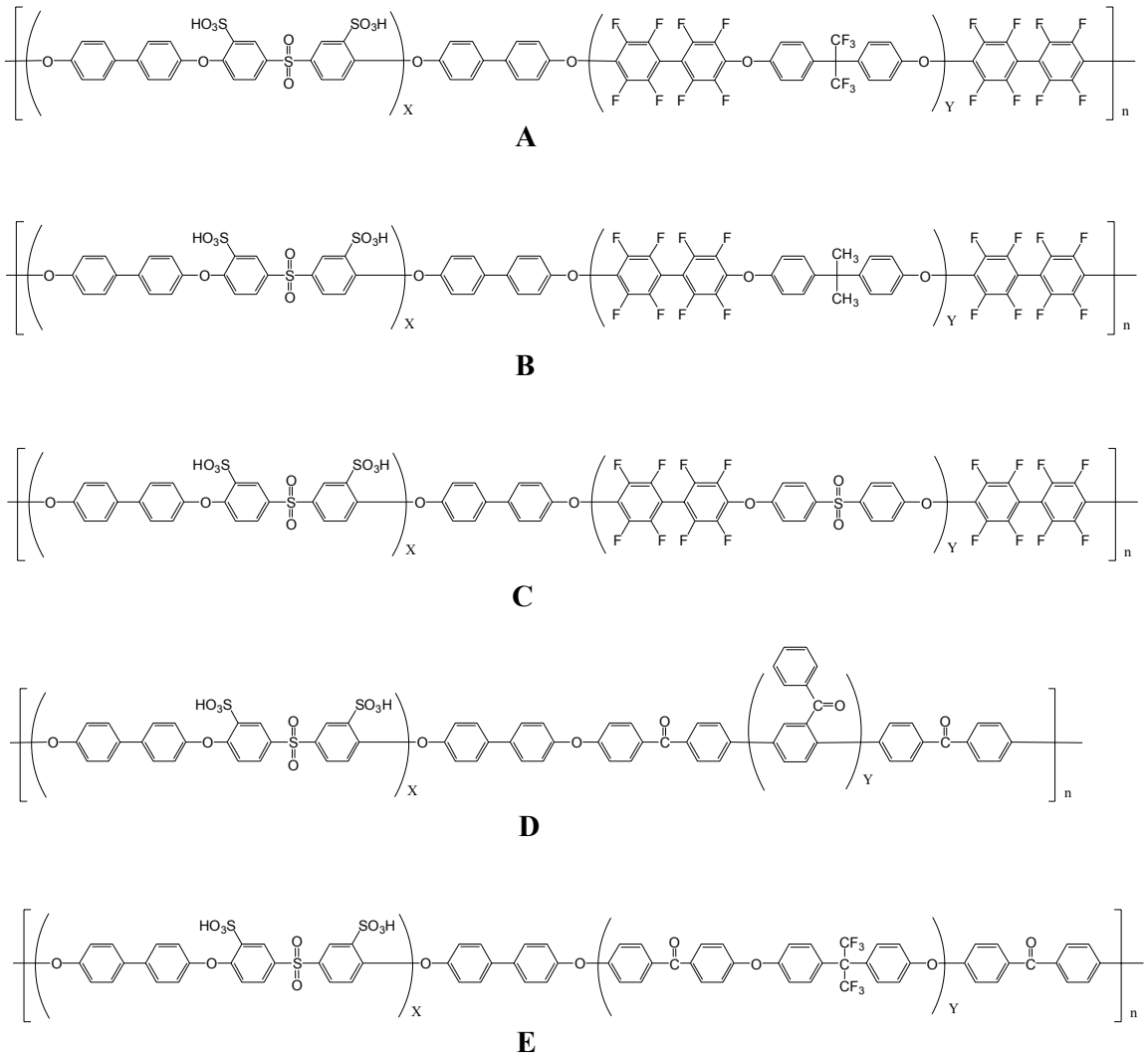

Figure 2. 46. Disulfonated Poly(arylene ether sulfone) Hydrophilic Segments Based Multiblock Copolymers.

Multiblock copolymers A,[188] B,[190] and C[186] utilize fluorine containing decafluorobiphenyl monomers to produce hydrophobic segments for enhanced phase separation. A hexafluoroisopropylidene unit, an isopropylidene unit, and a sulfone unit containing comonomers are used for hydrophobic block synthesis respectively to differentiate their chemical structures. The study of structure-property correlation by proton conductivity and self-diffusion coefficient of water revealed that the length of

hydrophilic and hydrophobic blocks plays a critical role in the transport properties. The self-diffusion coefficient of water, which cannot only explain transport properties but also reflects the extent of morphological barrier of water increases with increasing block lengths. In addition, the proton conductivities showed a similar increasing trend as the block length increases and the enhancement of proton conductivity was more significant under partially hydrated conditions.[186] (Figure 2. 47)

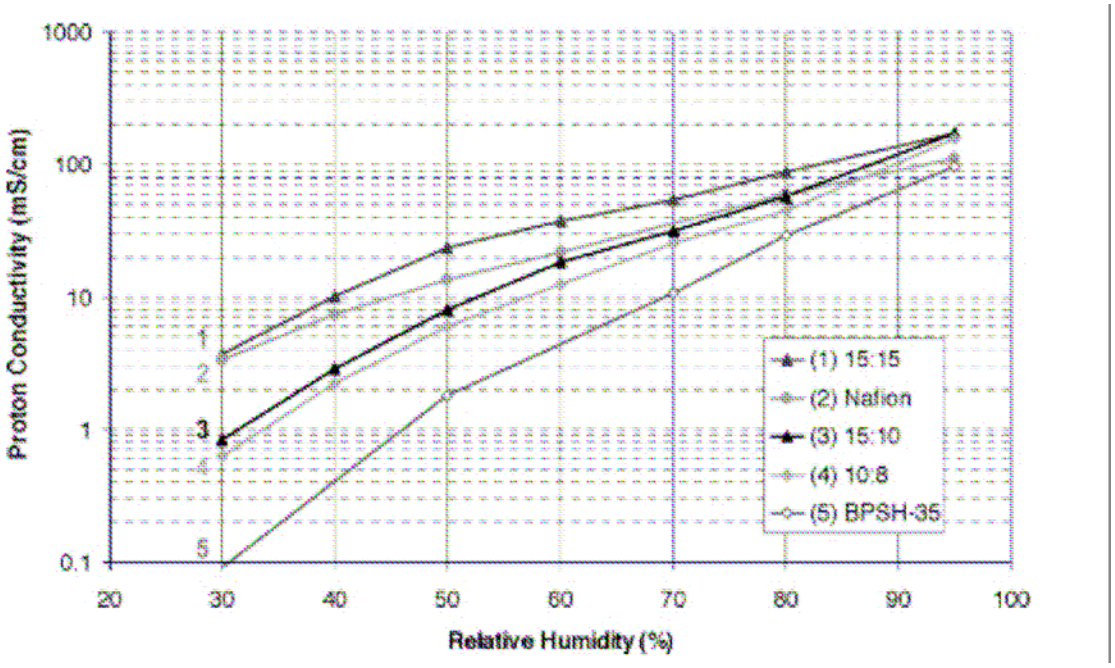

Figure 2. 47. Proton Conductivity of BisSF-BPSH (Structure C in Figure 2.4.6 under Partially Hydrated Conditions). Reprinted with Permission from Journal of Membrane Science.[191] Copyright 2009 Elsevier.

Similar trends were observed for other multiblock copolymers and the authors concluded that block lengths of the multiblock copolymers dictate the morphologies of the copolymer membranes and the morphologies can be tailored by altering block lengths to maximize the performances as PEMs.

A different approach to preparing block copolymers by utilizing poly(arylene ether sulfone) was explored by Holdcroft.et.al.[192-195] The researchers synthesized phenoxide terminated poly(arylene ether sulfone) by a step-growth polymerization of bisphenol-A monomer. The resulting poly(arylene ether sulfone) oligomers were reacted with bromine terminated polyvinylidene fluoride(PVDF) oligomers to produce multiblock copolymers. Sulfonic acid groups which facilitate proton conduction were introduced by post-sulfonation with trimethylsilyl chlorosulfonate. The reaction scheme of polysulfone and poly(vinylidene fluoride) based multiblock copolymers(SPSF-*b*-PVDF) are shown in Figure 2.48.

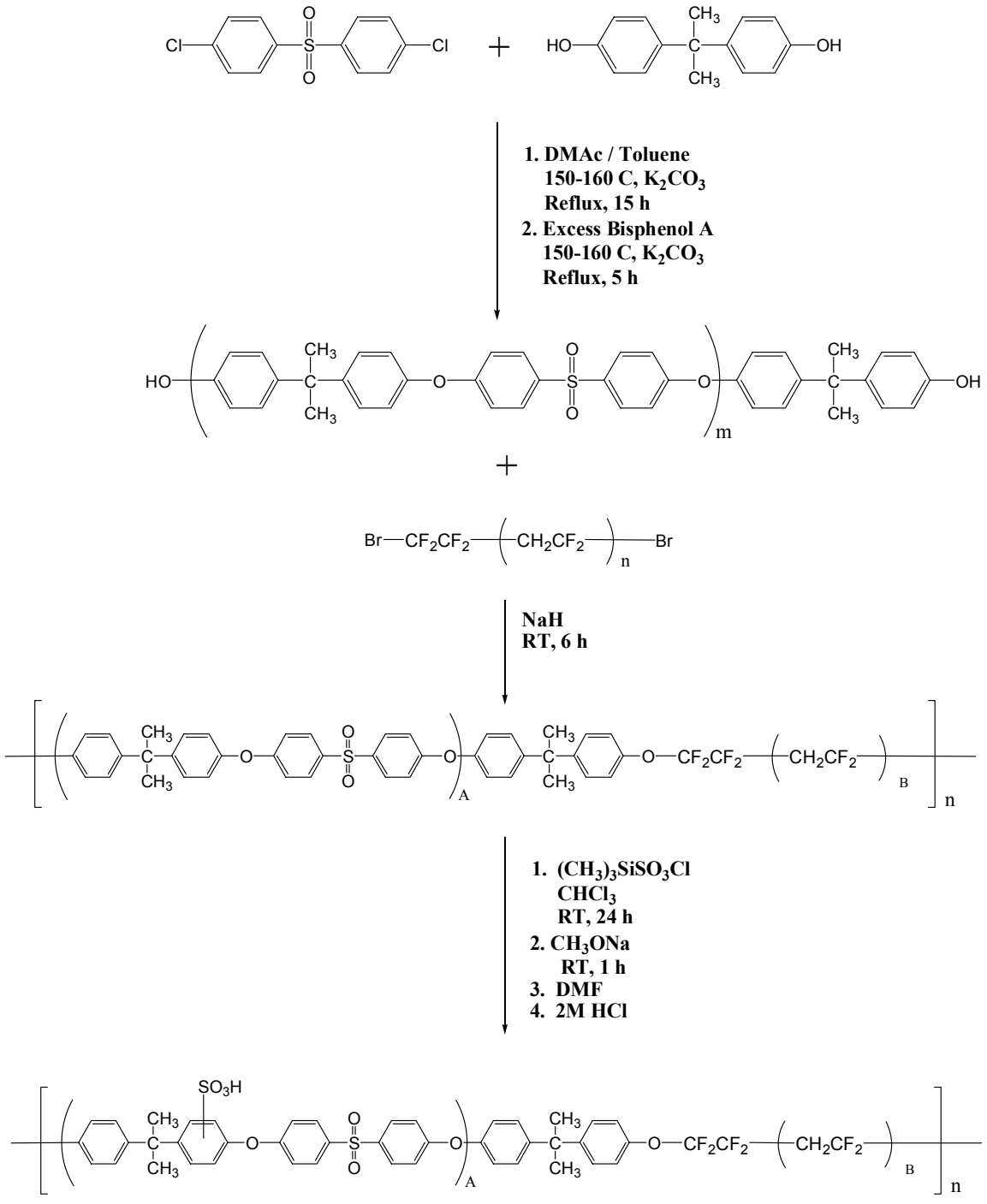

Figure 2. 48. Synthesis of SPSF-*b*-PVDF Block Copolymer.[194]

To evaluate the effects of the fluorine containing hydrophobic blocks in the system, the multiblock copolymers were examined in terms of proton conductivity and morphology. Then, the data were compared with a statistically copolymerized sulfonated bisphenol A based poly(arylene ether sulfone) (SPSF). The proton conductivity comparison between SPSF and SPSF-*b*-PVDF revealed that SPSF-*b*-PVDF have four orders greater proton conductivities than those of SPSF random copolymers in the low IEC region (e.g., lower than 1.0 mequi/g). However, as the IEC increases, the conductivity difference became smaller and diminishes entirely when IEC is higher than 1.5 mequi/g. (Figure 2.49) They explained the high conductivity of the block copolymers at lower IEC is due to the assistance of the fluorocopolymer the development of ionic aggregates and an ionic network. In addition, the disappearance of conductivity enhancement in high IEC regime was explained by higher acid concentrations in the membrane which can easily form ionic networks.

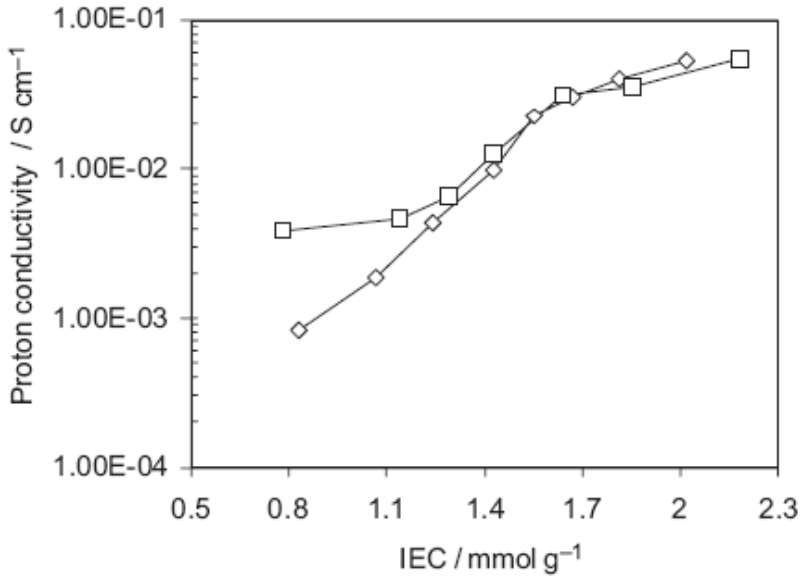

Figure 2. 49. Proton Conductivity vs. IEC of Multiblock Copolymer (SPSF-*b*-PVDF(Square) and Random SPSF (Diamond).[194]

Except sulfonated poly(arylene ether sulfone) based block copolymers, sulfonated polyimide may be the most intensively and systematically explored PEM material among other block copolymer systems. Genies et al. investigated series of sequenced sulfonated naphthalenic polyimides with different chemical components.[163] Figure 2.50 shows the synthetic strategy to produce segmented sulfonated polyimide copolymers.

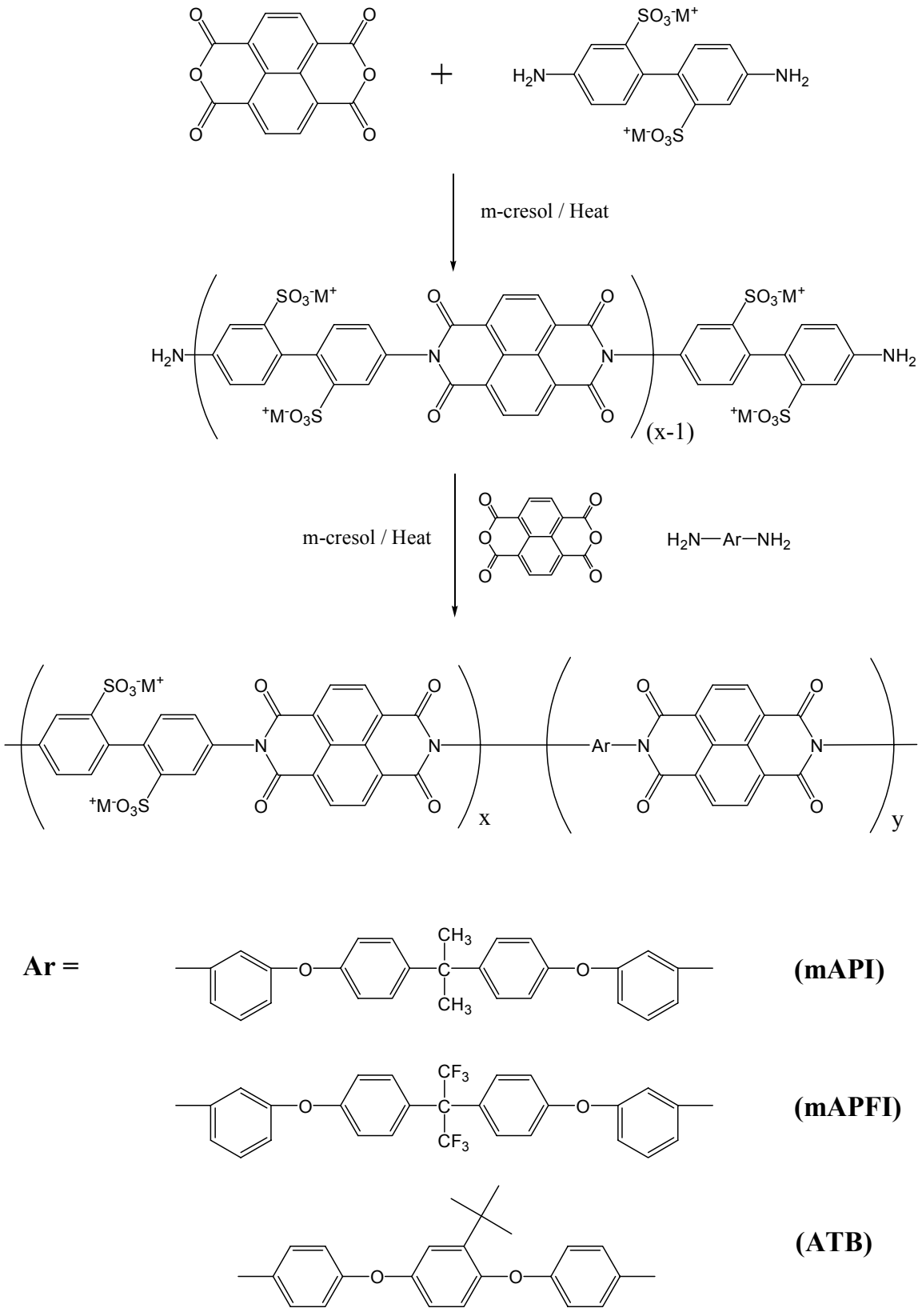

Figure 2. 50. Synthetic Scheme for Segmented Sulfonated Polyimides.[163]

In the first polymerization step, oligomeric sulfonated polyimide is synthesized via step growth polymerization with 4,4'-diamino-2,2'-biphenyl disulfonic acid (BDA) and 1,4,5,8-tetracarboxylic dianhydride (NDA). The diamine telechelic functionality and molecular weight of the resulting sulfonated polyimide were adjusted by varying feed ratios of two monomers. In the second polymerization step, pre-made sulfonated polyimide blocks were coupled with NDA and various non-sulfonated diamine monomers. The control of the IEC value of the copolymers was adjusted by the molar ratio of BDA and the unsulfonated diamines.

The principal characteristics such as proton conductivity and water uptake were determined for the sulfonated naphthalenic block copolymers in terms of sulfonated block length. The water uptake values ranged from 14 to 47% for IEC values varying from 0.5 to 1.9 meq/g. As the hydrophilic block length increases, a linear increase in water uptake and λ ($[H_2O]/[SO_3H]$) was observed. However, proton conductivity which can be typically related to the water uptake and λ did not show the same trend. The proton conductivity decreased for longer ionic block length. They demonstrated that the decreased conductivity of high IEC is due to the ionic domain percolation. For low IEC samples, there are not enough ionic groups to establish continuous ionic domains and the proton conductivities will be directly proportional to the IEC values. However, once the IEC values reach the percolation threshold, the proton conductivity is no longer dictated by the IEC while the water uptake still increases along with increasing IEC.

In this dissultation, novel multiblock copolymers with hydrophilic-hydrophobic sequences are reported including their syntheses and investigation for their potential application as PEMs. The hydrophilic-hydrophobic sequences in the systems are

expected to form nanophase separated morophologies which can improve proton conductivity especially under partially hydrated conditions. The relationship between copolymer chemical composition and resulting properties will be probed with a variety of hydrophilic and hydrophobic segments. The correlation between the fuel cell performances and the hydrophilic-hydrophobic sequences will be also evaluated.

2.5 References

1. Lashway, Robert W. Fuel cells: The next evolution. *MRS Bulletin* **2005,** 30, (8), 581-583.
2. de Bruijn, Frank. The current status of fuel cell technology for mobile and stationary applications. *Green Chemistry* **2005,** 7, (3), 132-150.
3. Kreuer, K. D. On the development of proton conducting polymer membranes for hydrogen and methanol fuel cells. *Journal of Membrane Science* **2001,** 185, (1), 29-39.
4. Steele, Brian C. H.; Heinzel, Angelika. Materials for fuel-cell technologies. *Nature (London, United Kingdom)* **2001,** 414, (6861), 345-352.
5. Banerjee, Shoibal; Curtin, Dennis E. Nafion perfluorinated membranes in fuel cells. *Journal of Fluorine Chemistry* **2004,** 125, (8), 1211-1216.
6. Mauritz, Kenneth A.; Moore, Robert B. State of understanding of Nafion. *Chemical Reviews (Washington, DC, United States)* **2004,** 104, (10), 4535-4585.
7. Kim, Yu Seung; Dong, Limin; Hickner, Michael A.; Glass, Thomas E.; Webb, Vernon; McGrath, James E. State of Water in Disulfonated Poly(arylene ether sulfone) Copolymers and a Perfluorosulfonic Acid Copolymer (Nafion) and Its Effect on Physical and Electrochemical Properties. *Macromolecules* **2003,** 36, (17), 6281-6285.
8. Savadogo, O. Emerging membranes for electrochemical systems Part II. High temperature composite membranes for polymer electrolyte fuel cell (PEFC) applications. *Journal of Power Sources* **2004,** 127, (1-2), 135-161.
9. Hickner, Michael A.; Ghassemi, Hossein; Kim, Yu Seung; Einsla, Brian R.; McGrath, James E. Alternative Polymer Systems for Proton Exchange Membranes (PEMs). *Chemical Reviews (Washington, DC, United States)* **2004,** 104, (10), 4587-4611.
10. Smitha, B.; Sridhar, S.; Khan, A. A. Solid polymer electrolyte membranes for fuel cell applications - a review. *Journal of Membrane Science* **2005,** 259, (1-2), 10-26.
11. Wang, Feng; Hickner, Michael; Kim, Yu Seung; Zawodzinski, Thomas A.; McGrath, James E. Direct polymerization of sulfonated poly(arylene ether sulfone) random (statistical) copolymers: candidates for new proton exchange membranes. *Journal of Membrane Science* **2002,** 197, (1-2), 231-242.
12. Kim, Yu Seung; Wang, Feng; Hickner, Michael; McCartney, Stephan; Hong, Young Taik; Harrison, William; Zawodzinski, Thomas A.; McGrath, James E. Effect of acidification treatment and morphological stability of sulfonated poly(arylene ether sulfone) copolymer proton-exchange membranes for fuel-cell use above 100 Deg. *Journal of Polymer Science, Part B: Polymer Physics* **2003,** 41, (22), 2816-2828.
13. Ghassemi, Hossein; Ndip, Grace; McGrath, James E. New multiblock copolymers of sulfonated poly(4'-phenyl-2,5-benzophenone) and poly(arylene ether sulfone) for proton exchange membranes. II. *Polymer* **2004,** 45, (17), 5855-5862.
14. Wang, Hang; Badami, Anand S.; Roy, Abhishek; McGrath, James E. Multiblock copolymers of poly(2,5-benzophenone) and disulfonated poly(arylene ether sulfone) for proton-exchange membranes. I. Synthesis and characterization. *Journal of Polymer Science, Part A: Polymer Chemistry* **2006,** 45, (2), 284-294.

15. Okamoto, Ken-ichi. Sulfonated polyimides for polymer electrolyte membrane fuel cell. *Journal of Photopolymer Science and Technology* **2003,** 16, (2), 247-254.
16. Okamoto, Ken-ichi; Yin, Yan; Yamada, Otoo; Islam, Md Nurul; Honda, Tatsuaki; Mishima, Takashi; Suto, Yoshiki; Tanaka, Kazuhiro; Kita, Hidetoshi. Methanol permeability and proton conductivity of sulfonated co-polyimide membranes. *Journal of Membrane Science* **2005,** 258, (1-2), 115-122.
17. Roy, Abhishek; Hickner, Michael A.; Yu, Xiang; Li, Yanxiang; Glass, Thomas E.; McGrath, James E. Influence of chemical composition and sequence length on the transport properties of proton exchange membranes. *Journal of Polymer Science, Part B: Polymer Physics* **2006,** 44, (16), 2226-2239.
18. Perry, M. L.; Fuller, T. F. A historical perspective of fuel cell technology in the 20th century. *Journal of the Electrochemical Society* **2002,** 149, (7), S59-S67.
19. Ellis, Peter. Sir William Grove (1811-1896). 1996.
20. Appleby, A. J. From Sir William Grove to today: fuel cells and the future. *Journal of Power Sources* **1990,** 29, (1-2), 3-11.
21. Winter, Martin; Brodd Ralph, J. What are batteries, fuel cells, and supercapacitors? *Chemical reviews* **2004,** 104, (10), 4245-4269.
22. Ni, Meng. Current status of fuel cell technologies. *Energy Exploration & Exploitation* **2005,** 23, (3), 207-214.
23. McLean, G. F.; Niet, T.; Prince-Richard, S.; Djilali, N. An assessment of alkaline fuel cell technology. *International Journal of Hydrogen Energy* **2002,** 27, (5), 507-526.
24. Van den Broeck, Hugo. Research, development, and demonstration of alkaline fuel cell systems. *Fuel Cell Syst.* **1993**, 245-269.
25. Bauer, Bernd; Strathmann, Heiner; Effenberger, Franz. Anion-exchange membranes with improved alkaline stability. *Desalination* **1990,** 79, (2-3), 125-144.
26. Bauer, B. The quality of combined energy conversion: part II. Numerical examples. *Brennstoff-Waerme-Kraft (1949-1999)* **1990,** 42, (12), 724-729.
27. Bauer, B. The quality of combined energy transformation: Part I. Fundamentals. *Brennstoff-Waerme-Kraft (1949-1999)* **1990,** 42, (11), 664-669.
28. Scott, K.; Stamatin, I. Polymer electrolyte fuel cells, advances in research and development. *Journal of Optoelectronics and Advanced Materials* **2007,** 9, (6), 1597-1605.
29. Scott, K.; Shukla, A. K. Polymer electrolyte membrane fuel cells: Principles and advances. *Reviews in Environmental Science and Bio/Technology* **2004,** 3, (3), 273-280.
30. Hamrock, Steven J.; Yandrasits, Michael A. Proton exchange membranes for fuel cell applications. *Polymer Reviews (Philadelphia, PA, United States)* **2006,** 46, (3), 219-244.
31. Roziere, Jacques; Jones, Deborah J. Non-fluorinated polymer materials for proton exchange membrane fuel cells. *Annual Review of Materials Research* **2003,** 33, 503-555.
32. Sammes, Nigel; Bove, Roberto; Stahl, Knut. Phosphoric acid fuel cells: fundamentals and applications. *Current Opinion in Solid State & Materials Science* **2005,** 8, (5), 372-378.

33. Steininger, H.; Schuster, M.; Kreuer, K. D.; Kaltbeitzel, A.; Bingoel, B.; Meyer, W. H.; Schauff, S.; Brunklaus, G.; Maier, J.; Spiess, H. W. Intermediate temperature proton conductors for PEM fuel cells based on phosphonic acid as protogenic group: A progress report. *Physical Chemistry Chemical Physics* **2007,** 9, (15), 1764-1773.
34. Li, Q.; He, R.; Jensen, J. O.; Bjerrum, N. J. PBI-based polymer membranes for high temperature fuel cells - preparation, characterization and fuel cell demonstration. *Fuel Cells (Weinheim, Germany)* **2004,** 4, (3), 147-159.
35. Dicks, Andrew L. Molten carbonate fuel cells. *Current Opinion in Solid State & Materials Science* **2005,** 8, (5), 379-383.
36. Bischoff, Manfred. Molten carbonate fuel cells: A high temperature fuel cell on the edge to commercialization. *Journal of Power Sources* **2006,** 160, (2), 842-845.
37. Lashtabeg, Anna; Skinner, Stephen J. Solid oxide fuel cells - a challenge for materials chemists? *Journal of Materials Chemistry* **2006,** 16, (31), 3161-3170.
38. Ezzell, Bobby Ray; Carl, William Paul; Mod, William August Improved sulfonic acid electrolytic cell membranes,(Dow Chemical Co., USA), EP81-104463 41733. 81-104463, 41733, 19810610., 1981.
39. Arcella, Vincenzo; Troglia, Claudio; Ghielmi, Alessandro. Hyflon ion membranes. *Industrial & Engineering Chemistry Research* **2005,** 44, (20), 7646-7651.
40. Ghielmi, Alessandro; Meunier, Vincent; Merlo, Luca; Arcella, Vincenzo. Short-side-chain perfluorinated proton exchange membranes for PEMFC's. *Preprints of Symposia - American Chemical Society, Division of Fuel Chemistry* **2005,** 50, (2), 521-522.
41. Hamrock, Steven J.; Rivard, Linda M.; Yandrasits, Michael A.; Pierpont, Daniel M. Method of fabrication of polymer electrolyte membrane for fuel cells,(3M Innovative Properties Company, USA), US2003-697831, 2005095487. 2003-697831, 2005095487, 20031030., 2005.
42. Hamrock, Steven Joseph; Rivard, Linda Mae; Innes Moore, George Gower; Freemyer, Harold Todd Polymer electrolyte membrane for electrochemical cell, (3M Innovative Properties Company, USA), US2002-325278, 2004121210. 2002-325278, 2004121210, 20021219., 2004.
43. Curtin, Dennis E.; Lousenberg, Robert D.; Henry, Timothy J.; Tangeman, Paul C.; Tisack, Monica E. Advanced materials for improved PEMFC performance and life. *Journal of Power Sources* **2004,** 131, (1-2), 41-48.
44. Heitner-Wirguin, Carla. Recent advances in perfluorinated ionomer membranes: structure, properties and applications. *Journal of Membrane Science* **1996,** 120, (1), 1-33.
45. Rose, J. B. Preparation and properties of poly(arylene ether sulfones). *Polymer* **1974,** 15, (7), 456-465.
46. Hale, Warren F.; Farnham, Alford G.; Johnson, Robert Norman; Clendinning, Robert A. Thermal stability of poly(aryl ethers) prepared by aromatic nucleophilic substitution. *Polymer Preprints (American Chemical Society, Division of Polymer Chemistry)* **1966,** 7, (2), 503-512.
47. Hale, Warren F.; Farnham, Alford G.; Johnson, Robert Norman; Clendinning, Robert A. Poly(aryl ethers) by nucleophilic aromatic substitution. II. Thermal

stability. *Journal of Polymer Science, Polymer Chemistry Edition* **1967,** 5, (9), 2399-2414.

48. Johnson, Robert Norman; Farnham, Alford G.; Clendinning, Robert A.; Hale, Warren F.; Merriam, Charles N. Poly(aryl ethers) by nucleophilic aromatic substitution. I. Synthesis and properties. *Journal of Polymer Science, Polymer Chemistry Edition* **1967,** 5, (9), 2375-2398.
49. Wang, Sheng; McGrath, J. E. Synthesis of poly(arylene ether)s *Synthetic Methods in Step-Growth Polymers (edited by Martin E.Rogers and Timothy E. Long)* **2003**, 327-374.
50. Rao, V. Lakshmana. Polyether sulfones. *Journal of Macromolecular Science, Reviews in Macromolecular Chemistry and Physics* **1999,** C39, (4), 655-711.
51. Wu, Zhongwen; Zheng, Yubin; Yan, Hongmao; Nakamura, Tomoki; Nozawa, Takafumi; Yosomiya, Ryutoku. Molecular aggregation of PEEK with PES [polyethersulfone] blends and the block copolymers composed of PEEK and PES components. *Angewandte Makromolekulare Chemie* **1989,** 173, 163-181.
52. Dumais, J. J.; Cholli, A. L.; Jelinski, L. W.; Hedrick, J. L.; McGrath, J. E. Molecular basis of the b-transition in poly(arylene ether sulfones). *Macromolecules* **1986,** 19, (7), 1884-1889.
53. Robeson, L. M.; Farnham, A. G.; McGrath, J. E. Synthesis and dynamic mechanical characteristics of poly(aryl ethers). *Applied Polymer Symposia* **1975,** 26, (Polym. Polycondensat), 373-385.
54. Robeson, L. M.; Farnham, A. G.; McGrath, J. E. Dynamic mechanical characteristics of polysulfone and other poly(arylethers). *Midland Macromolecular Monographs* **1978,** 4, (Mol. Basis Transitions Relaxations), 405-425.
55. Robeson, L. M.; Crisafulli, S. T. Microcavity formation in engineering polymers exposed to hot water. *Journal of Applied Polymer Science* **1983,** 28, (9), 2925-2936.
56. Kambour, R. P.; Romagosa, E. E.; Gruner, C. L. Swelling, crazing, and cracking of an aromatic copolyether-sulfone in organic media. *Macromolecules* **1972,** 5, (4), 335-340.
57. Leslie, Victor J. Polysulfone solutions, (Imperial Chemical Industries Ltd., UK), GB73-4126, 1405052, 73-4126, 1405052, 19731211., 1975.
58. Attwood, T. E.; King, T.; Leslie, V. J.; Rose, J. B. Poly(arylene ether sulfones) by polyetherification. 4. Physical properties in relation to molecular structure. *Polymer* **1977,** 18, (4), 369-374.
59. Johnson, Robert Norman; Farnham, Alford G. Poly(aryl ethers) by nucleophilic aromatic substitution. III. Hydrolytic side reactions. *Journal of Polymer Science, Polymer Chemistry Edition* **1967,** 5, (9), 2515-2527.
60. Ghosal, K.; Chern, R. T.; Freeman, B. D. Gas permeability of Radel A polysulfone. *Journal of Polymer Science, Part B: Polymer Physics* **1993,** 31, (7), 891-893.
61. McHattie, J. S.; Koros, W. J.; Paul, D. R. Gas transport properties of polysulfones. 2. Effect of bisphenol connector groups. *Polymer* **1991,** 32, (14), 2618-2625.
62. Mohr, J. M.; Paul, D. R.; Tullos, G. L.; Cassidy, P. E. Gas transport properties of a series of poly(ether ketone) polymers. *Polymer* **1991,** 32, (13), 2387-2394.

63. McHattie, J. S.; Koros, W. J.; Paul, D. R. Gas transport properties of polysulfones. 1. Role of symmetry of methyl group placement on bisphenol. *Polymer* **1991,** 32, (5), 840-850.
64. Vogel, Herward A. Polysulfones and process for their preparation (Minnesota Mining and Manufacturing Co.). 64-397295, 3406149, 19640917., 1968.
65. Olah, George A., *Interscience Monographs on Organic Chemistry: Friedel-Crafts Chemistry*. 1973; p 581 pp.
66. Olah, George A.; Kobayashi, Shiro; Nishimura, Jun. Aromatic substitution. XXXI. Friedel-Crafts sulfonylation of benzene and toluene with alkyl- and arylsulfonyl halides and anhydrides. *Journal of the American Chemical Society* **1973,** 95, (2), 564-569.
67. Jones, Michael Edward Benet Polysulfones and method of preparation, (Imperial Chemical Industries Ltd., UK), US63-320508, 4008203. 63-320508, 4008203, 19631031., 1977.
68. Jones, Michael Edward B. Article comprising an adherend with a thermoplastic polymer including - ArSO2- repeating units adhering thereto, (Imperial Chemical Industries Ltd., UK), US72-315904, 3983300. 72-315904, 3983300, 19721218., 1976.
69. Jennings, Brian E.; Jones, Michael E. B.; Rose, John Brewster. Synthesis of poly(arylene sulfones) and poly(arylene ketones) by reactions involving substitution at aromatic nuclei. *Journal of Polymer Science, Polymer Symposia* **1967,** 16, (Pt. 2), 715-724.
70. Cudby, M. E. A.; Feasey, R. G.; Gaskin, S.; Jones, Michael Edward Benet; Rose, John B. Polycondensation of arenesulfonyl chlorides under Friedel-Crafts conditions in nitrobenzene solution. *Journal of Polymer Science, Polymer Symposia* **1967,** 22, (Pt. 2), 747-760.
71. Cudby, M. E. A.; Feasey, R. G.; Gaskin, S.; Kendall, Mrs V.; Rose, J. B. Structures of the poly(diphenylene ether sulfones) obtained by polysulfonylation. *Polymer* **1968,** 9, (5), 265-281.
72. Rose, John Brewster Aromatic polysulfones, (Imperial Chemical Industries PLC, UK), European Patent Application. 81-304211, 49070, 19810915., 1982.
73. Farnham, Alford G.; Johnson, Robert Norman Polyarylene polyethers, (Union Carbide Corp.), US3332909. 3332909, 19650715., 1967.
74. Miller, Joseph, *Aromatic Nucleophilic Substitution (Reaction Mechanisms in Organic Chemistry, Monograph 8)*. 1968; p 408 pp.
75. Meisenheimer, Jakob. Reactions of aromatic nitro structures. *Justus Liebigs Annalen der Chemie* **1902,** 323, 205-226.
76. Alexander, R.; Ko, E. C. F.; Parker, A. J.; Broxton, T. J. Solvation of ions. XIV. Protic-dipolar aprotic solvent effects on rates of bimolecular reactions. Solvent activity coefficients of reactants and transition states at 25.deg. *Journal of the American Chemical Society* **1968,** 90, (19), 5049-5069.
77. Fuchs, Richard; Cole, Larry L. Transition state enthalpies of transfer in the reaction of nucleophiles with n-hexyl tosylate. *Journal of the American Chemical Society* **1973,** 95, (10), 3194-3197.
78. Bunnett, Joseph F.; Zahler, Roland E. Aromatic nucleophilic substitution reactions. *Chemical Reviews (Washington, DC, United States)* **1951,** 49, 273-412.

79. Garcia, Dana. Styrene-terminated polysulfone reactive oligomers: cure and properties. *Journal of Polymer Science, Part B: Polymer Physics* **1987,** 25, (8), 1581-1594.
80. Lucotte, Georges; Cormier, Laurent; Delfort, Bruno. Ethynyl-terminated polyethers from new end-capping agents. II. End-chain functionalization through nitro displacement. *Journal of Polymer Science, Part A: Polymer Chemistry* **1991,** 29, (6), 897-903.
81. Lyle, G. D.; Jurek, M. J.; Mohanty, D. K.; Wu, S. D.; Hedrick, J. C.; McGrath, J. E. Solvent-resistant maleimide-modified poly(arylene ether) thermoplastics and thermosets. *Polymer Preprints (American Chemical Society, Division of Polymer Chemistry)* **1987,** 28, (1), 77-79.
82. Lyle, G. D.; Senger, J. S.; Chen, D. H.; Kilic, S.; Wu, S. D.; Mohanty, D. K.; McGrath, J. E. Synthesis, curing and physical behavior of maleimide-terminated poly(ether ketones). *Polymer* **1989,** 30, (6), 978-985.
83. Guiver, Michael D.; Black, Paul; Tam, Chung M.; Deslandes, Yves. Functionalized polysulfone membranes by heterogeneous lithiation. *Journal of Applied Polymer Science* **1993,** 48, (9), 1597-1606.
84. Guiver, Michael D.; Kutowy, Oleh Aromatic polysulfones bearing functional groups,(National Research Council of Canada, Can.), US88-281042 4999415. 88-281042, 4999415, 1988, 1207., 1991.
85. Guiver, Michael D.; Kutowy, O.; ApSimon, John W. Functional group polysulfones by bromination-metalation. *Polymer* **1989,** 30, (6), 1137-1142.
86. Guiver, Michael D.; Apsimon, John W.; Kutowy, O. The modification of polysulfone by metalation. *Journal of Polymer Science, Part C: Polymer Letters* **1988,** 26, (2), 123-127.
87. Ben-Haida, Abderrazak; Hodge, Philip; Nisar, Mohammed; Helliwell, Madeleine. Synthesis of 2,2'-biphenol- and 1,1'bi(2-naphthol)-based poly(ether sulfones) and copolymers by classical step-growth polymerization and by entropically-driven ring-opening polymerization of macrocyclic oligomers. *Polymers for Advanced Technologies* **2006,** 17, (9-10), 682-690.
88. Colquhoun, Howard M.; Lewis, David F.; Ben-Haida, Abderrazak; Hodge, Philip. Ring-Chain Interconversion in High-Performance Polymer Systems. 2. Ring-Opening Polymerization-Copolyetherification in the Synthesis of Aromatic Poly(ether sulfones). *Macromolecules* **2003,** 36, (10), 3775-3778.
89. Xie, Donghang; Ji, Qing; Gibson, Harry W. Synthesis and Ring-Opening Polymerization of Single-Sized Aromatic Macrocycles for Poly(arylene ether)s. *Macromolecules* **1997,** 30, (17), 4814-4827.
90. Quentin, Jean P. Polysulfones, (Rhone-Poulenc S. A.), DE70-2021383, 2021383. 70-2021383, 2021383, 19700430., 1970.
91. Genova-Dimitrova, P.; Baradie, B.; Foscallo, D.; Poinsignon, C.; Sanchez, J. Y. Ionomeric membranes for proton exchange membrane fuel cell (PEMFC): sulfonated polysulfone associated with phosphatoantimonic acid. *Journal of Membrane Science* **2001,** 185, (1), 59-71.
92. Bailly, Christian; Williams, David J.; Karasz, Frank E.; MacKnight, William J. The sodium salts of sulfonated poly(aryl-ether-ether-ketone) (PEEK): preparation and characterization. *Polymer* **1987,** 28, (6), 1009-1016.

93. Johnson, B. C.; Yilgor, I.; Tran, C.; Iqbal, M.; Wightman, J. P.; Lloyd, D. R.; McGrath, J. E. Synthesis and characterization of sulfonated poly(arylene ether sulfones). *Journal of Polymer Science, Polymer Chemistry Edition* **1984,** 22, (3), 721-737.
94. Noshay, A.; Robeson, L. M. Sulfonated polysulfone. *Journal of Applied Polymer Science* **1976,** 20, (7), 1885-1903.
95. Litter, Marta I.; Marvel, C. S. Polyaromatic ether-ketones and polyaromatic ether-ketone sulfonamides from 4-phenoxybenzoyl chloride and from 4,4'-dichloroformyldiphenyl ether. *Journal of Polymer Science, Polymer Chemistry Edition* **1985,** 23, (8), 2205-2223.
96. Tian, S. H.; Shu, D.; Wang, S. J.; Xiao, M.; Meng, Y. Z. Poly(arylene ether)s with sulfonic acid groups on the backbone and pendant for proton exchange membranes used in PEMFC applications. *Fuel Cells (Weinheim, Germany)* **2007,** 7, (3), 232-237.
97. Liu, Baijun; Robertson, Gilles P.; Kim, Dae-Sik; Guiver, Michael D.; Hu, Wei; Jiang, Zhenhua. Aromatic Poly(ether ketone)s with Pendant Sulfonic Acid Phenyl Groups Prepared by a Mild Sulfonation Method for Proton Exchange Membranes. *Macromolecules (Washington, DC, United States)* **2007,** 40, (6), 1934-1944.
98. Le Ninivin, C.; Balland-Longeau, A.; Demattei, D.; Palmas, P.; Saillard, J.; Coutanceau, C.; Lamy, C.; Leger, J. M. Determination of the physicochemical characteristics and electrical performance of post-sulfonated and grafted sulfonated derivatives of poly(para-phenylene) as new proton-conducting membranes for direct methanol fuel cell. *Journal of Applied Polymer Science* **2006,** 101, (2), 944-952.
99. Bishop, Matthew T.; Karasz, Frank E.; Russo, Paul S.; Langley, Kenneth H. Solubility and properties of a poly(aryl ether ketone) in strong acids. *Macromolecules* **1985,** 18, (1), 86-93.
100. Kerres, J.; Cui, W.; Reichle, S. New sulfonated engineering polymers via the metalation route. I. Sulfonated poly(ether sulfone) PSU Udel via metalation-sulfination-oxidation. *Journal of Polymer Science, Part A: Polymer Chemistry* **1996,** 34, (12), 2421-2438.
101. Robeson, Lloyd Mahlon; Matzner, Markus Flame retardant polyarylate compositions, (Union Carbide Corp., USA), EP82-101026, 58403. 82-101026, 58403, 19820211., 1982.
102. Ueda, Mitsuru; Toyota, Hidetsugu; Ouchi, Takao; Sugiyama, Junichi; Yonetake, Koichiro; Masuko, Toru; Teramoto, Takero. Synthesis and characterization of aromatic poly(ether sulfone)s containing pendent sodium sulfonate groups. *Journal of Polymer Science, Part A: Polymer Chemistry* **1993,** 31, (4), 853-858.
103. Wang, Feng; Kim, Yuseung; Hickner, Michael; Zawodzinski, Tom A.; McGrath, James E. Synthesis of polyarylene ether block copolymers containing sulfonate groups. *Polymeric Materials Science and Engineering* **2001,** 85, 517-518.
104. Wang, Feng; Mecham, J.; Harrison, W.; Hickner, Michael; Kim, Y.; McGrath, J. E. Synthesis of sulfonated poly(arylene ether phosphine oxide sulfone)s via direct polymerization. *Abstracts of Papers, 221st ACS National Meeting, San Diego, CA, United States, April 1-5, 2001* **2001**, PMSE-508.

105. Wang, Feng; Ji, Qing; Harrison, William; Mecham, Jeff; McGrath, James E.; Formato, R.; Kovar, R. Synthesis of sulfonated poly(arylene ether sulfone)s via direct polymerization. *Book of Abstracts, 219th ACS National Meeting, San Francisco, CA, March 26-30, 2000* **2000**, POLY-151.
106. Sankir, M.; Bhanu, V. A.; Harrison, W. L.; Ghassemi, H.; Wiles, K. B.; Glass, T. E.; Brink, A. E.; Brink, M. H.; McGrath, J. E. Synthesis and characterization of 3,3'-disulfonated-4,4'-dichlorodiphenyl sulfone (SDCDPS) monomer for proton exchange membranes (PEM) in fuel cell applications. *Journal of Applied Polymer Science* **2006,** 100, (6), 4595-4602.
107. Li, Yanxiang. The Influence of Aromatic Disulfonated Random and Block Copolymers' Molecular Weight, Composition,and Microstructure on the Properties of Proton Exchange Membranes for Fuel Cells. *Virginia Polytechnic Institute and State University, Dissertation* **2007**.
108. Kim, Yu Seung; Hickner, Michael A.; Dong, Limin; Pivovar, Bryan S.; McGrath, James E. Sulfonated poly(arylene ether sulfone) copolymer proton exchange membranes: composition and morphology effects on the methanol permeability. *Journal of Membrane Science* **2004,** 243, (1-2), 317-326.
109. Harrison, W. L.; Hickner, M. A.; Kim, Y. S.; McGrath, J. E. Poly(arylene ether sulfone) copolymers and related systems from disulfonated monomer building blocks: synthesis, characterization, and performance - a topical review. *Fuel Cells (Weinheim, Germany)* **2005,** 5, (2), 201-212.
110. Bower, G. M.; Frost, L. W. Aromatic polyimides. *Journal of Polymer Science* **1963,** 1, (Pt. A;10), 3135-3150.
111. Kreuz, John A.; Endrey, A. L.; Gay, F. P.; Sroog, C. E. Studies of thermal cyclizations of polyamic acids and tertiary amine salts. *Journal of Polymer Science, Polymer Chemistry Edition* **1966,** 4, (10), 2607-2616.
112. Bogert, M. T.; Renshaw, R. R. 4-Amino-o-Phthalic Acid and Some of its Derivatives. *Journal of the American Chemical Society* **1908,** 30, 1135-1144.
113. Edwards, Walter M.; Robinson, Ivan M. Polyimides of pyromellitic acid (E. I. du Pont de Nemours & Co.), US2710853, . 2710853, 1955.
114. Edwards, Walter M.; Robinson, Ivan M.; Squire, Edward N. High-molecular-weight polypyromellitimides,(E. I. du Pont de Nemours & Co.), US2867609. 2867609, 1959.
115. Endrey, Andrew L. Aromatic polyimide particles from polycyclic diamines,(E. I. du Pont de Nemours & Co.), US3179631. 3179631, 19590401., 1965.
116. Polyimides (E. I. du Pont de Nemours & Co.), US982914. 982914, 1965.
117. Ghosh, Malay K.; Mittal, K. L.; Editors, *Polyimides: Fundamentals and Applications. [In: Plast. Eng. (N. Y.), 1996; 36]*. 1996; p 891 pp.
118. Feger, Claudius; Khojasteh, Mahmoud M.; McGrath, James E., *Polyimides: Materials Chemistry and Characterization. Proceedings of the 3rd International Conference on Polyimides, Ellenville, N.Y., November 2-4, 1988*. 1989; p 787 pp.
119. Volozhin, A. I.; Krut'ko, E. T.; Savich, I. G.; Yurina, O. D. Investigation of photoresistive polyimide composition. *Polyimides Other High-Temp. Polym., Proc. Eur. Tech. Symp., 2nd* **1991**, 493-496.

120. Boiteux, G.; Oraison, J. M.; Seytre, G.; Rabilloud, G.; Sillion, B. Soluble polyimides with specific dielectric behavior. *Polyimides Other High-Temp. Polym., Proc. Eur. Tech. Symp., 2nd* **1991**, 437-446.
121. Blyumenfel'd, A. B.; Vdovina, A. L. Thermal behavior and heat stabilization of polyimides and related polymers. *Polyimides Other High-Temp. Polym., Proc. Eur. Tech. Symp., 2nd* **1991**, 183-188.
122. Dubois, J. C.; Bureau, J. M. Photosensitive polyimides. *Polyimides Other High-Temp. Polym., Proc. Eur. Tech. Symp., 2nd* **1991**, 461-470.
123. Sillion, B.; Verdet, L. Heat-resistant polymers for electronics applications. *Polyimides Other High-Temp. Polym., Proc. Eur. Tech. Symp., 2nd* **1991**, 363-386.
124. Yamanaka, Kazuhiro; Romeo, Michael; Maeda, Kazuhiko; Henderson, Clifford L. Novel low-dielectric constant photodefinable polyimides for low-temperature polymer processing. *ECS Transactions* **2006,** 3, (11, Science and Technology of Dielectrics for Active and Passive Photonic Devices), 107-115.
125. Zhao, Gufan; Ishizaka, Takayuki; Kasai, Hitoshi; Oikawa, Hidetoshi; Nakanishi, Hachiro. Preparation of multilayered film of polyimide nanoparticles for low-k applications. *Molecular Crystals and Liquid Crystals* **2007,** 464, 613-620.
126. Carter, K. R. Recent advances in low k polymeric materials. *Materials Research Society Symposium Proceedings* **1997,** 476, (Low-Dielectric Constant Materials III), 87-97.
127. Oota, Naoto; Matsura, Shuichi; Myadera, Yasuo Polyimide-based films with low dielectric constant (Hitachi Chemical Co Ltd, Japan).Application: JP. 93-129066, 06340808, 19930531., 1994.
128. Lee, Y. J.; Gungor, A.; Yoon, T. H.; McGrath, J. E. Adhesive and thermomechanical behavior of phosphorus-containing thermoplastic polyimides. *Journal of Adhesion* **1995,** 55, (1-2), 165-177.
129. Tan, B.; Vasudevan, V.; Lee, Y. J.; Gardner, S.; Davis, R. M.; Bullions, T.; Loos, A. C.; Parvatareddy, H.; Dillard, D. A.; McGrath, E.; Cella, J. Design and characterization of thermosetting polyimide structural adhesive and composite matrix systems. *Journal of Polymer Science, Part A: Polymer Chemistry* **1997,** 35, (14), 2943-2954.
130. Meyer, G. W.; Tan, B.; McGrath, J. E. Solvent-resistant polyether imide network systems via (phenylethynyl)phthalic anhydride endcapping. *High Performance Polymers* **1994,** 6, (4), 423-435.
131. Harris, Frank W. Synthesis of aromatic polyimides from dianhydrides and diamines. *Polyimides, Editor(s): Wilson, Doug; Stenzenberger, Horst D.; Hergenrother, Paul M.* **1990**, 1-37.
132. Solomin, V. A.; Kardash, I. E.; Snagovskii, Yu S.; Messerle, P. E.; Zhubanov, B. A.; Pravednikov, A. N. Kinetics of the acylation of amines by aromatic and alicyclic carboxylic acid anhydrides. *Doklady Akademii Nauk SSSR* **1977,** 236, (1), 139-142 [Chem].
133. Solomin, V. A.; Messerle, P. E.; Zhubanov, B. A. Reversible nature of the reaction of alicyclic tetracarboxylic acid dianhydrides with aromatic diamines. *Doklady Akademii Nauk SSSR* **1977,** 234, (2), 397-398 [Phys Chem].

134. Sroog, C. E.; Endrey, A. L.; Abramo, S. V.; Berr, C. E.; Edwards, W. M.; Olivier, K. L. Aromatic polypyromellitimides from aromatic polyamic acids. *Journal of Polymer Science, Part A: General Papers* **1965,** 3, (4), 1373-1390.
135. Snyder, Randy W.; Painter, Paul C. Dynamic Fourier transform-IR analysis of cure reactions and kinetics of polyimides. *ACS Symposium Series* **1989,** 407, (Polym. Mater. Electron. Packag. Interconnect.), 49-56.
136. Snyder, R. W.; Thomson, B.; Bartges, B.; Czerniawski, D.; Painter, P. C. FTIR studies of polyimides: thermal curing. *Macromolecules* **1989,** 22, (11), 4166-4172.
137. Roderick, William R. The isomerism of N-substituted maleimides. *Journal of the American Chemical Society* **1957,** 79, 1710-1712.
138. Meyer, G. W.; Heidbrink, J. L.; Franchina, J. G.; Davis, R. M.; Gardner, S.; Vasudevan, V.; Glass, T. E.; McGrath, J. E. Phenylmaleimide endcapped arylene ether imide oligomers. *Polymer* **1996,** 37, (22), 5077-5088.
139. Endrey, Andrew L. Ammonium salts of aromatic polyamide acids and polyimides therefrom,(E. I. du Pont de Nemours & Co.), US3242136. 3242136, 19620309., 1966.
140. Waldbauer, R. O.; Rogers, M. E.; Arnold, C. A.; York, G. A.; McGrath, J. E. Synthesis of soluble, melt-processible polyimides of controlled structure. *International SAMPE Symposium and Exhibition* **1990,** 35, (1, Adv. Mater.: Challenge Next Decade), 97-107.
141. McGrath, J. E.; Rogers, M. E.; Arnold, C. A.; Kim, Y. J.; Hedrick, J. C. Synthesis and blend behavior of high-performance homo- and segmented thermoplastic polyimides. *Makromolekulare Chemie, Macromolecular Symposia* **1991,** 51, (Int. Symp. Spec. Polymn. 1990), 103-125.
142. Yagci, Havva; Ostrowski, Cher; Mathias, Lon J. Synthesis and characterization of novel aromatic polyimides from 4,4-bis(p-aminophenoxymethyl)-1-cyclohexene. *Journal of Polymer Science, Part A: Polymer Chemistry* **1999,** 37, (8), 1189-1197.
143. Ayala, David; Lozano, Angel E.; De Abajo, Javier; De La Campa, Jose G. Novel polyimides with p-nitrophenyl pendant groups. Synthesis and characterization. *Journal of Polymer Science, Part A: Polymer Chemistry* **1999,** 37, (16), 3377-3384.
144. Ayala, David; Lozano, Angel E.; De Abajo, Javier; De La Campa, Jose G. Synthesis and characterization of novel polyimides with bulky pendant groups. *Journal of Polymer Science, Part A: Polymer Chemistry* **1999,** 37, (6), 805-814.
145. Huang, Samuel J.; Hoyt, Andrea E. The synthesis of soluble polyimides. *Trends in Polymer Science (Cambridge, United Kingdom)* **1995,** 3, (8), 262-271.
146. Kim, Y. J.; Glass, T. E.; Lyle, G. D.; McGrath, J. E. Kinetic and mechanistic investigations of the formation of polyimides under homogeneous conditions. *Macromolecules* **1993,** 26, (6), 1344-1358.
147. Rusanov, Alexandr L. Novel bis(naphthalic anhydrides) and their polyheteroarylenes with improved processability. *Advances in Polymer Science* **1994,** 111, (Polymer Synthesis), 115-175.
148. Korshak, V. V.; Bulycheva, E. G.; Shifrina, Z. B.; Berlin, A. M.; Shalikiani, M. O.; Butskhrikidze, B. A.; Rusanov, A. L.; Mironov, G. S.; Moskvichev, Yu A.; et al. Novel bis(naphthalic anhydrides) and polyheteroarylenes on their basis. *Acta Polymerica* **1988,** 39, (8), 460-464.

149. Sek, Danuta; Jedlinski, Zbigniew; Pijet, Pawel; Wanic, Andrzej Manufacture of soluble aromatic polyimides, (Centrum Chemii Polimerow PAN, Pol.), PL90-287953, 163253. 90-287953, 163253, 19901127., 1994.
150. Sek, Danuta; Wanic, Andrzej; Schab-Balcerzak, Ewa. Development of investigations on polyimides. *Wiadomosci Chemiczne* **1994,** 48, (5-6), 381-405.
151. Sek, Danuta; Wanic, Andrzej; Schab-Balcerzak, Ewa. Novel approach to the mechanism of the high-temperature formation of naphthalimides. *Polymer* **1993,** 34, (11), 2440-2442.
152. Sek, Danuta; Pijet, Pawel; Wanic, Andrzej. Investigation of polyimides containing naphthalene units: 1. Monomer structure and reaction conditions. *Polymer* **1992,** 33, (1), 190-193.
153. Choi, Dong-Sook; Chong, Yong S.; Whitehead, Daniel; Shimizu, Ken D. Molecules with Shape Memory Based on Restricted Rotation. *Organic Letters* **2001,** 3, (23), 3757-3760.
154. Hodgkin, J. H. Polyimide model compounds. *Journal of Applied Polymer Science* **1976,** 20, (9), 2339-2346.
155. Hodgkin, J. H. Reactivity changes during polyimide formation. *Journal of Polymer Science, Polymer Chemistry Edition* **1976,** 14, (2), 409-431.
156. Piroux, Fabienne; Mercier, Regis; Picq, Dominique; Espuche, Eliane. On the polynaphthalimide synthesis-influence of reaction conditions. *Polymer* **2004,** 45, (19), 6445-6452.
157. Einsla, Brian R.; Hong, Young-Taik; Kim, Yu Seung; Wang, Feng; Gunduz, Nazan; McGrath, James E. Sulfonated naphthalene dianhydride based polyimide copolymers for proton-exchange-membrane fuel cells. I. Monomer and copolymer synthesis. *Journal of Polymer Science, Part A: Polymer Chemistry* **2004,** 42, (4), 862-874.
158. Einsla, Brian R.; Kim, Yu Seung; Hickner, Michael A.; Hong, Young-Taik; Hill, Melinda L.; Pivovar, Bryan S.; McGrath, James E. Sulfonated naphthalene dianhydride based polyimide copolymers for proton-exchange-membrane fuel cells. II. Membrane properties and fuel cell performance. *Journal of Membrane Science* **2005,** 255, (1-2), 141-148.
159. Schab-Balcerzak, Ewa; Sek, Danuta. New soluble polyimides containing hydroxylic groups: I. Synthesis and characterization. *High Performance Polymers* **2001,** 13, (1), 45-53.
160. Sek, D.; Wanic, A. High-temperature polycondensation of six membered dianhydrides with o-substituted aromatic diamines 1. Model compounds investigations. *Polymer* **1999,** 41, (7), 2367-2372.
161. Sek, Danuta; Wanic, Andrzej; Janeczek, Henryk; Abadie, Marc J. M. Investigation of polyimides containing naphthalene units. IV. Mechanism of naphthalisoimide formation and isomerization to naphthalimides. *Journal of Polymer Science, Part A: Polymer Chemistry* **1999,** 37, (17), 3523-3529.
162. Faure, Sylvain; Cornet, Nathalie; Gebel, Gerard; Mercier, Regis; Pineri, Michel; Sillion, Bernard. Sulfonated polyimides as novel proton exchange membranes for H2/O2 fuel cells. *New Materials for Fuel Cell and Modern Battery Systems II, Proceedings of the International Symposium on New Materials for Fuel Cell and Modern Battery Systems, 2nd, Montreal, July 6-10, 1997* **1997**, 818-827.

163. Genies, C.; Mercier, R.; Sillion, B.; Petiaud, R.; Cornet, N.; Gebel, G.; Pineri, M. Stability study of sulfonated phthalic and naphthalenic polyimide structures in aqueous medium. *Polymer* **2001,** 42, (12), 5097-5105.
164. Lee, Young-moo; Park, Ho-Bum; Lee, Chang-Hyun Crosslinked sulfonated polyimide films, their preparation and membranes, (Hanyang Hak Won Co., Ltd., S. Korea), WO2002-KR1583, 2003018669. 2002-KR1583, 2003018669, 20020821., 2003.
165. Besse, S.; Capron, P.; Diat, O.; Gebel, G.; Jousse, F.; Marsacq, D.; Pineri, M.; Marestin, C.; Mercier, R. Sulfonated polyimides for fuel cell electrode membrane assemblies (EMA). *Journal of New Materials for Electrochemical Systems* **2002,** 5, (2), 109-112.
166. Gunduz, Nazan; Inan, Tulay Yilmaz; Yildiz, Emel; McGrath, James E. Sulfonated six-membered ring polyimides as proton exchange membranes: Synthesis and characterization. *Abstracts of Papers, 221st ACS National Meeting, San Diego, CA, United States, April 1-5, 2001* **2001**, PMSE-507.
167. Genies, C.; Mercier, R.; Sillion, B.; Cornet, N.; Gebel, G.; Pineri, M. Soluble sulfonated naphthalenic polyimides as materials for proton exchange membranes. *Polymer* **2000,** 42, (2), 359-373.
168. Yin, Yan; Chen, Shouwen; Guo, Xiaoxia; Fang, Jianhua; Tanaka, Kazuhiro; Kita, Hidetoshi; Okamoto, Ken-Ichi. Structure-property relationship of polyimides derived from sulfonated diamine isomers. *High Performance Polymers* **2006,** 18, (5), 617-635.
169. Yin, Yan; Yamada, Otoo; Tanaka, Kazuhiro; Okamoto, Ken-Ichi. On the development of naphthalene-based sulfonated polyimide membranes for fuel cell applications. *Polymer Journal (Tokyo, Japan)* **2006,** 38, (3), 197-219.
170. Asano, Naoki; Miyatake, Kenji; Watanabe, Masahiro. Sulfonated block polyimide copolymers as a proton-conductive membrane. *Journal of Polymer Science, Part A: Polymer Chemistry* **2006,** 44, (8), 2744-2748.
171. Asano, Naoki; Miyatake, Kenji; Watanabe, Masahiro. Hydrolytically Stable Polyimide Ionomer for Fuel Cell Applications. *Chemistry of Materials* **2004,** 16, (15), 2841-2843.
172. Asano, Naoki; Aoki, Makoto; Suzuki, Shinsuke; Miyatake, Kenji; Uchida, Hiroyuki; Watanabe, Masahiro. Aliphatic/aromatic polyimide ionomers as a proton conductive membrane for fuel cell applications. *Journal of the American Chemical Society* **2006,** 128, (5), 1762-1769.
173. Gierke, T. D.; Hsu, W. Y. The cluster-network model of ion clustering in perfluorosulfonated membranes. *ACS Symposium Series* **1982,** 180, (Perfluorinated Ionomer Membr.), 283-307.
174. Gierke, T. D.; Munn, G. E.; Wilson, F. C. Morphology of perfluorosulfonated membrane products. Wide-angle and small-angle x-ray studies. *ACS Symposium Series* **1982,** 180, (Perfluorinated Ionomer Membr.), 195-216.
175. Hsu, William Y.; Gierke, Timothy D. Ion transport and clustering in Nafion perfluorinated membranes. *Journal of Membrane Science* **1983,** 13, (3), 307-326.
176. Litt, Morton H. A reevaluation of Nafion morphology. *Polymer Preprints (American Chemical Society, Division of Polymer Chemistry)* **1997,** 38, (1), 80-81.

177. Litt, Morton. A reevaluation of Nafion morphology. *Book of Abstracts, 213th ACS National Meeting, San Francisco, April 13-17* **1997**, POLY-033.
178. Rubatat, L.; Gebel, G.; Diat, O. Fibrillar Structure of Nafion: Matching Fourier and Real Space Studies of Corresponding Films and Solutions. *Macromolecules* **2004,** 37, (20), 7772-7783.
179. Van der Heijden, P. C.; Rubatat, L.; Diat, O. Orientation of Drawn Nafion at Molecular and Mesoscopic Scales. *Macromolecules* **2004,** 37, (14), 5327-5336.
180. Lodge, Timothy P. Block copolymers: past successes and future challenges. *Macromolecular Chemistry and Physics* **2003,** 204, (2), 265-273.
181. Hamley, I. W. Introduction to block copolymers. *Developments in Block Copolymer Science and Technology* **2004**, 1-29.
182. Krausch, Georg; Magerle, Robert. Nanostructured thin films via self-assembly of block copolymers. *Advanced Materials (Weinheim, Germany)* **2002,** 14, (21), 1579-1583.
183. Park, Cheolmin; Yoon, Jongseung; Thomas, Edwin L. Enabling nanotechnology with self assembled block copolymer patterns. *Polymer* **2003,** 44, (22), 6725-6760.
184. Castelletto, V.; Hamley, I. W. Morphologies of block copolymer melts. *Current Opinion in Solid State & Materials Science* **2005,** 8, (6), 426-438.
185. Noshay, Allen; McGrath, James E., *Block Copolymers: Overview and Critical Survey*. 1977; p 516 pp.
186. Yu, Xiang; Roy, Abhishek; Dunn, Stuart; Yang, Juan; McGrath, James E. Synthesis and characterization of sulfonated-fluorinated, hydrophilic-hydrophobic multiblock copolymers for proton exchange membranes. *Macromolecular Symposia* **2006,** 245/246, (World Polymer Congress--MACRO 2006), 439-449.
187. Li, Yanxiang; Roy, Abhishek; Badami, Anand S.; Yang, Juan; Zhang, Zhongbiao; McGrath, James E. Synthesis and characterization of partially fluorinated poly(arylene ether ketone)- poly(arylene ether sulfone) (6FK- BPSH) multiblock copolymers containing sulfonate groups for proton exchange membrane. *Abstracts of Papers, 232nd ACS National Meeting, San Francisco, CA, United States, Sept. 10-14, 2006* **2006**, FUEL-183.
188. Ghassemi, Hossein; McGrath, James E.; Zawodzinski, Thomas A. Multiblock sulfonated-fluorinated poly(arylene ether)s for a proton exchange membrane fuel cell. *Polymer* **2006,** 47, (11), 4132-4139.
189. Li, Yanxiang; Roy, Abhishek; Badami, Anand S.; Hill, Melinda; Yang, Juan; Dunn, Stuart; McGrath, James E. Synthesis and characterization of partially fluorinated hydrophobic-hydrophilic multiblock copolymers containing sulfonate groups for proton exchange membrane. *Journal of Power Sources* **2007,** 172, (1), 30-38.
190. Yu, Xiang; Roy, Abhishek; McGrath, James E. Synthesis and characterization of multiblock copolymers for proton exchange membranes. *Preprints of Symposia - American Chemical Society, Division of Fuel Chemistry* **2005,** 50, (2), 577-578.
191. Roy, Abhishek; Yu, Xiang; Dunn, Stuart; McGrath, James E. Influence of microstructure and chemical composition on proton exchange membrane properties of sulfonated-fluorinated, hydrophilic-hydrophobic multiblock copolymers. *Journal of Membrane Science* **2009,** 327, (1+2), 118-124.

192. Shi, Zhiqing; Holdcroft, Steven. Synthesis of Block Copolymers Possessing Fluoropolymer and Non-Fluoropolymer Segments by Radical Polymerization. *Macromolecules* **2004,** 37, (6), 2084-2089.
193. Yang, Yunsong; Shi, Zhiqing; Holdcroft, Steven. Synthesis of poly[arylene ether sulfone-b-vinylidene fluoride] block copolymers. *European Polymer Journal* **2004,** 40, (3), 531-541.
194. Yang, Yunsong; Shi, Zhiqing; Holdcroft, Steven. Synthesis of Sulfonated Polysulfone-block-PVDF Copolymers: Enhancement of Proton Conductivity in Low Ion Exchange Capacity Membranes. *Macromolecules* **2004,** 37, (5), 1678-1681.
195. Ding, Jianfu; Tang, Qinying; Holdcroft, Steven. Morphologically controlled proton-conducting membranes using graft polymers possessing block copolymer graft chains. *Australian Journal of Chemistry* **2002,** 55, (6 & 7), 461-466.

CHAPTER 3

Segmented Sulfonated Poly(arylene ether sulfone)-*b*-polyimide Copolymers for Proton Exchange Membrane Fuel Cells. I. Copolymer Synthesis and Fundamental Properties

Hae-Seung Lee, Anand S. Badami, Abhishek Roy and James E. McGrath*

Macromolecules and Interfaces Institute,
Virginia Polytechnic Institute and State University, Blacksburg, Virginia 24061

*Correspondence to: James E. McGrath (Email: jmcgrath@vt.edu)

Taken from *Journal of Polymer Science: Part A: Polymer Chemistry,* Vol 45, 4879-4890 (2007)

3.1. Abstract

Segmented disulfonated poly(arylene ether sulfone)-*b*-polyimide copolymers based on hydrophilic and hydrophobic oligomers were synthesized and evaluated for use as proton exchange membranes (PEMs). Amine terminated sulfonated poly(arylene ether sulfone) hydrophilic oligomers and anhydride terminated naphthalene based polyimide hydrophobic oligomers were synthesized via step growth polymerization including high temperature one-pot imidization. Synthesis of the multiblock copolymers was achieved by an imidization coupling reaction of hydrophilic and hydrophobic oligomers in a m-cresol/NMP mixed solvent system, producing high molecular weight tough and ductile membranes. Proton conductivities and water uptake increased with increasing ion exchange capacities (IECs) of the copolymers as expected. The morphologies of the multiblock copolymers were investigated by tapping mode atomic force microscopy (TM-AFM) and their measurements revealed that the multiblock copolymers had well-defined nano-phase separated morphologies which were clearly a function of block lengths. Hydrolytic stability testing at 80 ºC in water for 1000 hr showed that multiblock copolymer membranes retained intrinsic viscosities of about 80% of their original values and maintained flexibility which was much improved over polyimide random copolymers. The synthesis and fundamental properties of the multiblock copolymers are reported here and the systematic fuel cell properties will be provided in a separate article.

Keywords: multiblock copolymer; sulfonated poly(arylene ether sulfone); polyimide; phase separated morphology; proton exchange membrane

3.2. Introduction

The fuel cell is an energy conversion device which directly transforms the chemical energy of fuels such as hydrogen and methanol into electrical energy.[1] The fuel cell has been gaining serious attention as a next-generation energy device owing to its advantages including high efficiency, high energy density, quiet operation, and environmental friendliness relative to conventional energy generators such as internal combustion engines.[2] Among the various types of fuel cells, the proton exchange membrane fuel cell (PEMFC) is considered to be the most promising power source for portable and automotive applications.[3, 4] As its name implies, one of the core components of a PEMFC is the proton exchange membrane (PEM). Currently, the state-of-the-art PEMs are perfluorinated sulfonated ionomer membranes, such as Nafion® (DuPont), Aciplex® (Asahi Kasei), and Flemion® (Asahi Glass).[5] These membranes have good mechanical strength and high chemical stability along with high proton conductivity, especially under high relative humidities at moderate operation temperatures.[6] However, at high operation temperatures (>80°C), which are essential for practical applications, mechanical and electrochemical properties of the perfluorinated membranes are severely deteriorated by the depressed hydrated α relaxations of the membranes.[7, 8] These disadvantages and others, such as cost, have limited perfluorinated membranes' applicability and triggered the quest for alternative membranes.

Much effort has been devoted in the study of aromatic polymers, including sulfonated poly(arylene ether sulfone)s, poly(ether ether ketone)s, and polybenzimidazoles, in order to find cost-effective and high performance PEMs.[9, 10] Among them, 4, 4'-biphenol-based disulfonated poly(arylene ether sulfone) random copolymers (BPSH) are strong candidates as alternative membranes and have been extensively investigated in high

temperature PEM applications. These random copolymers were synthesized via direct step-growth polycondensation by using disulfonated and/or non-sulfonated dihalide diphenyl sulfone and biphenol type monomers.[11] Even though BPSH-type membranes demonstrated enhanced stability at high temperatures and performance comparable to Nafion®, their proton conductivities under low relative humidity were inadequate.[12] To increase the proton conductivity under partially hydrated conditions, the degree of disulfonation was increased. However, once the degree of disulfonation reaches 60 mol%, a percolated hydrophilic phase appears and results in excessive water swelling, forming a hydrogel that is impractical as a PEM.[13, 14]

Recently, PEMs based on multiblock copolymers have been considered as a solution to overcome the drawbacks of a random copolymer system.[15, 16] PEMs based on segmented multiblock copolymers consist of ion conducting hydrophilic blocks and mechanically robust hydrophobic blocks. Once they are cast into membranes, they exhibit unique phase separated morphologies and each phase governs independent or distinct properties. The ionic groups of the hydrophilic blocks act as proton conducting sites while the nonionic hydrophobic component provides dimensional stability. In the case of direct methanol fuel cells (DMFCs), the hydrophobic component may serve as a barrier against methanol transport.[17, 18] The proton conductivities, water uptake, and mechanical properties of multiblock copolymer based PEMs can be tailored by carefully adjusting the relative lengths of their hydrophilic and hydrophobic blocks.[19]

One strong candidate for the hydrophobic blocks in multiblock copolymer-based PEMs may be polyimides due to their high performance properties.[20, 21] These properties include excellent thermal stability, high mechanical strength, good film-forming ability,

low gas permeability, and superior chemical resistance. Not all polyimides are ideal for PEM applications. For example, conventional five-membered ring polyimides based on phthalic anhydride are easily degraded under acidic conditions due to the ease of hydrolysis of imido rings.[22-25] Several scientists have shown that this problem can be partially addressed by using six-membered ring polyimides, which are found to be more hydrolytically stable under acidic conditions than five-membered ring polyimides, yet slow hydrolysis can still be problematic.[26-31]

In this paper, the synthesis of a full series of multiblock copolymers produced by a coupling reaction between hydrophilic BPSH oligomers and hydrophobic polyimide oligomers as an extension of our earlier research is reported.[32] The BPSH oligomers were capped with primary amine groups and prepared with different block lengths ranging from 5 kg/mol to 20 kg/mol. These functionalized BPSH telechelic oligomers were then combined with controlled molecular weight anhydride terminated naphthalene based polyimide oligomers of the same molecular weight range to produce high molecular weight multiblock copolymers. By the described synthetic route, a series of multiblock copolymers with different block lengths was synthesized and fundamental properties were characterized. This paper also evaluates the effect of block lengths in terms of the morphologies and membrane properties, including atomic force microscopy (AFM), impedance spectroscopy, and hydrolytic stability.

3.3. Experimental

3.3.1. Materials

N,N-Dimethylacetamide (DMAc), N-methyl-2-pyrrolidinone (NMP), 3-methylphenol (*m*-cresol), and toluene were purchased from Aldrich and distilled from calcium hydride before use. Monomer grade 4,4'-dichlorodiphenyl sulfone (DCDPS) and 4,4'-biphenol (BP) were provided by Solvay Advanced Polymers and Eastman Chemical Company, respectively, and vacuum dried at 110 °C prior to use. 1,4,5,8-Naphthalenetetracarboxylic dianhydride (NDA) and fuming sulfuric acid (SO_3 content ~30%), were used as received from Aldrich. Bis[4-(3-aminophenoxy)phenyl]sulfone (m-BAPS) was purchased from TCI and purified by recrystallization from ethanol. 3-Aminophenol (m-AP) was purchased from Aldrich and sublimed *in vacuo* before use. Potassium carbonate, benzoic acid, ethanol, 2-propanol (IPA), and isoquinoline were purchased from Aldrich and used without further purification.

3.3.2. Synthesis of 3,3'-Disulfonated-4,4'-dichlorodiphenylsulfone

3,3'-Disulfonated-4,4'-dichlorodiphenylsulfone (SDCDPS) was prepared by the reaction of DCDPS and fuming sulfuric acid. The detailed synthesis of and purification of SDCDPS has been described in the literature.[33]

3.3.3. Synthesis of Controlled Molecular Weight Disulfonated Poly(arylene ether sulfone)s with Telechelic Amine Functionality

Disulfonated poly(arylene ether sulfone) hydrophilic blocks (BPSH) with molecular weights ranging from 5 to 20 kg/mol were synthesized via nucleophilic aromatic substitution. Molecular weight control and telechelic amine functionality of BPSH hydrophilic blocks were achieved by using stoichiometrically adjusted amounts of monomers (BP, SDCDPS) and end-capping reagent (m-AP). A typical coupling reaction was performed as follows: 7.54 g (40.5 mmol) of BP, 21.61 g (44.0 mmol) of SDCDPS, 0.77 g (7.1 mmol) of m-AP and 7.05 g (51 mmol) of potassium carbonate were added to a three-necked 250-mL flask equipped with a condenser, a Dean Stark trap, a nitrogen inlet/outlet, and a mechanical stirrer. Distilled DMAc (70 mL) and toluene (35 mL) were added to the flask. The solution was allowed to reflux at 150 °C while the toluene azeotropically removed the water in the system. After 4 h, the toluene was completely removed from the flask by slowly increasing the temperature to 180 ºC. The reaction was allowed to proceed for another 96 h. The resulting viscous solution was cooled to room temperature and diluted with DMAc to facilitate filtration. After filtration, the polymer solution was coagulated in IPA. The polymer was dried at 120 °C *in vacuo* for at least 24 h.

3.3.4. Synthesis of Controlled Molecular Weight Anhydride-terminated Polyimides

Naphthalene dianhydride-based polyimide hydrophobic blocks with molecular weights ranging from 5 to 20 kg/mol were synthesized via a one-pot high temperature imidization process. Molecular weight control and end group functionality were achieved by

stoichiometrically adjusted amounts of the monomers. A typical coupling reaction was performed as follows: 4.96 g (18.5 mmol) of NDA, 7.05 g (16.3 mmol) of m-BAPS, and 2.26 g (18.5 mmol) of benzoic acid were dissolved in 108 mL of *m*-cresol in a three-necked 250-mL flask equipped with a condenser, a Dean Stark trap, a nitrogen inlet/outlet and a mechanical stirrer. The reaction mixture was heated at 80 ºC for 4 h and then at 180 ºC for 12 h. Then 2.39 g (18.5 mmol) of isoquinoline was added and the reaction was conducted at 180 ºC for another 12 h. The resulting dark red polymer solution was precipitated in IPA. The polymer was filtered and purified in a Soxhlet extractor with methanol overnight. The polymer was dried at 120 °C *in vacuo* for at least 24 h.

3.3.5. Synthesis of Hydrophilic-hydrophobic Multiblock Copolymers

A series of multiblock copolymers was synthesized via a modified one-pot high temperature imidization. The series consisted of 16 different copolymers with a systematic combination of hydrophilic and hydrophobic block lengths. A typical coupling reaction was performed as follows: 3.0 g (0.6 mmol) of hydrophilic oligomer ($\overline{M_n}$ = 5 kg/mol), 3.0 g (0.6 mmol) of hydrophobic oligomer ($\overline{M_n}$ = 5 kg/mol), 0.73g (6 mmol) of benzoic acid, and 30 mL of NMP were added to a three-necked 100-mL flask equipped with a mechanical stirrer, and a nitrogen inlet/outlet. The reaction mixture was heated at 80 ºC for 4 h to obtain a homogeneous solution. Approximately 15 mL of m-cresol was slowly added until the mixture became inhomogeneous. The solution homogeneity was recovered by adding additional NMP (approximately 15 mL) to achieve a final solution concentration of approximately 10% (w/v) solid. A coupling

reaction was conducted at 180 ºC for 12 h and then 0.78 g (6 mmol) of isoquinoline was added. The reaction was allowed to proceed for another 12 h at 180 ºC. The resulting dark red viscous polymer solution was precipitated in IPA. The polymer was filtered and purified in a Soxhlet extractor with methanol overnight. The polymer was dried at 120 °C *in vacuo* for at least 24 h.

3.3.6. Characterization

^{1}H NMR analyses were conducted on a Varian INOVA 400 MHz spectrometer with DMSO-d_6 to confirm the chemical structures of oligomers and copolymers. ^{1}H NMR spectroscopy was also used to determine copolymer compositions and molecular weights of the oligomers via end-group analyses. Intrinsic viscosities were determined in NMP containing 0.05 M LiBr at 25 ºC using an Ubbelohde viscometer. Thermooxidative behavior of both the salt- and acid-form copolymers was measured on a TA Instruments TGA Q500. The samples were evaluated over the range of 80-800 °C at a heating rate of 10 °C/min in air. The ion exchange capacity (IEC) values of the acid-form copolymers were determined by titration with 0.01 M NaOH.

3.3.7. Film Casting and Membrane Acidification

Copolymer membranes in the potassium sulfonate salt form were prepared by solution casting. The copolymers were dissolved in NMP (10% w/v), filtered through 0.45 μm Teflon® syringe filters, and cast onto clean glass substrates. The solvent was evaporated under an infrared lamp for 48 h, resulting in transparent, tough, and flexible films. The films were further dried *in vacuo* at 120 °C for 24 h to remove residual solvent. The salt

form films were acidified by boiling in 0.5 M sulfuric acid for 2 h, followed by boiling in deionized water for 2 h.

3.3.8. Determination of Proton Conductivity and Water Uptake

Proton conductivities were measured in liquid water at 30 °C. All conductivity measurements were made using a Solartron (1252A +1287) impedance/gain-phase analyzer over the frequency range of 10 Hz - 1 MHz. The conductivity of the membrane was determined from the geometry of the cell and resistance of the film which was taken at the frequency that produced the minimum imaginary response. To obtain water uptake values, membranes were dried *in vacuo* for 24 h at 100 °C, weighed, and then immersed in deionized water at room temperature for 24 h. The wet membranes were blotted dry and immediately re-weighed. The water uptake of the membranes was calculated from the ratio of the increase in membrane weight divided by the dry membrane weight and expressed as a weight percent.

3.3.9. Atomic Force Microscopy (AFM) Characterization

AFM images were obtained with a Digital Instruments MultiMode scanning probe microscope with a NanoScope IVa controller (Veeco Instruments, Santa Barbara, CA) in tapping mode. A silicon probe (Veeco) with an end radius of less than 10 nm and a force constant of 5 N/m was used to image samples. The ratio of amplitudes used in the feedback control was adjusted to 0.90-0.98 of the free-air amplitude. The samples were dried *in vacuo* at 60 °C for 3 h and then equilibrated at 30% relative humidity for at least

12 h before being imaged immediately at room temperature and a relative humidity of approximately 15-20% .

3.4. Results and Discussion

3.4.1. Synthesis of Hydrophilic and Hydrophobic Oligomers

Amine-terminated sulfonated poly(arylene ether sulfone) hydrophilic oligomers (BPSH) were synthesized via polycondensation of SDCDPS, BP, and *m*-AP (Fig. 3.1). The *m*-AP was used as an end-capping agent to produce amine telechelic functionality of the oligomers. The target number-average molecular weights of the BPSH oligomers were 5, 10, 15, and 20 kg/mol. Control of molecular weight was achieved by stoichiometric imbalance of monomers and end-capping agent. The number-average molecular weights of the BPSH oligomers were determined by ^{1}H NMR spectra end group analysis. The peaks at 6.15 and 8.25 ppm were assigned to the protons on the *m*-AP moieties, which are located at the end of the oligomers, and the protons on the phenyl ring next to the sulfonated groups, respectively (Fig. 3.2). The integrals of both peaks were compared to calculate the number-average molecular weights of the hydrophilic oligomers (Table 3.1). These match well with the target molecular weights.

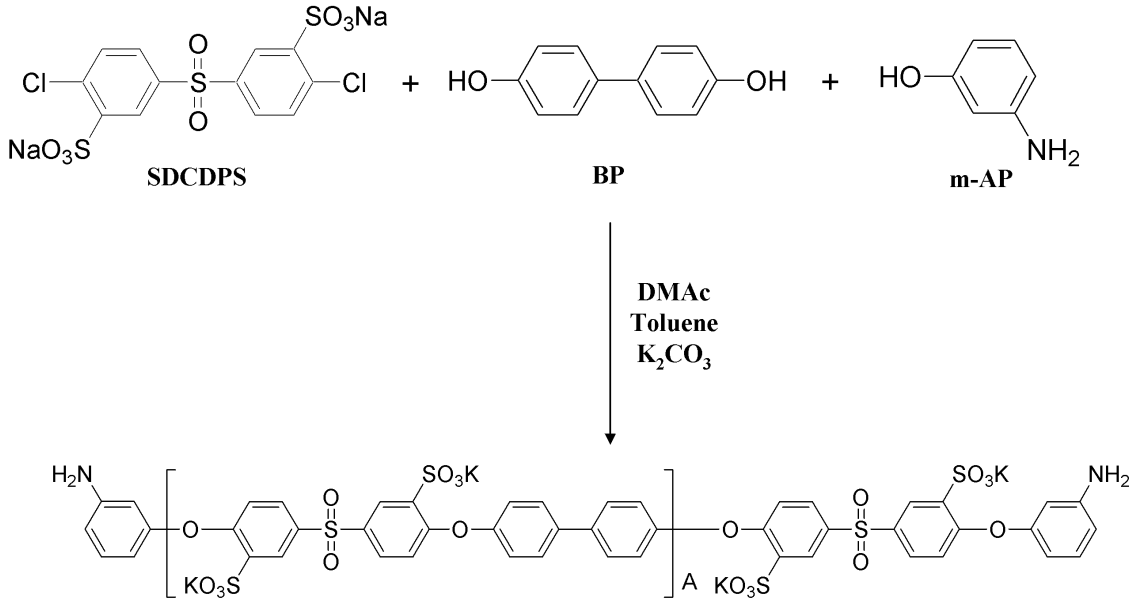

Figure 3. 1. Synthesis of an Amine-terminated Disulfonated Hydrophilic Oligomer.

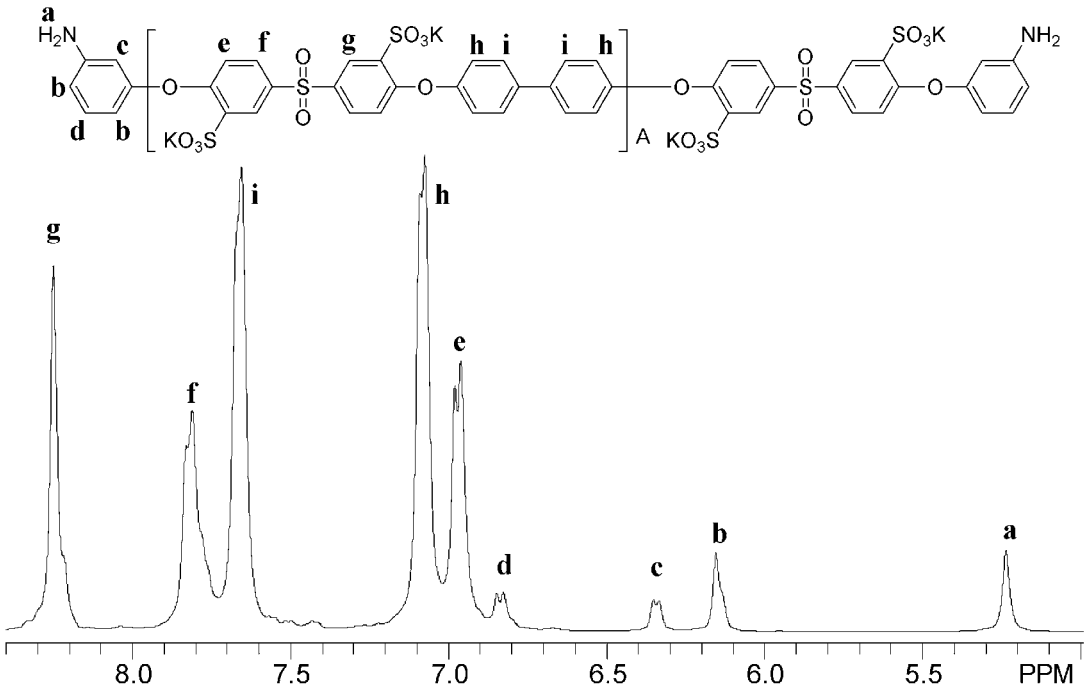

Figure 3. 2. [1]H NMR Spectrum of an Amine-terminated Disulfonated Hydrophilic Oligomer.

Table 3. 1. Characterization of Hydrophilic and Hydrophobic Telechelic Oligomers.

Target M_n (g mol^{-1})	Hydrophilic Blocks		Hydrophobic Blocks	
	M_n (g mol^{-1})[a]	IV (dL g^{-1})[b]	M_n (g mol^{-1})[a]	IV (dL g^{-1})[b]
5,000	5,500	0.18	5,600	0.16
10,000	9,800	0.28	10,200	0.22
15,000	14,500	0.30	17,200	0.34
20,000	20,100	0.47	23,800	0.41

[a] Determined by ^{1}H NMR.
[b] In NMP with 0.05 M LiBr at 25 ºC.

Naphthalene dianhydride-based polyimide hydrophobic oligomers (PI) were synthesized via a one-pot high-temperature imidization of NDA and *m*-BAPS (Fig. 3.3). NDA is a six-membered ring anhydride, and due to lower strain in the structure, is less reactive with amines than five-membered ring anhydrides. To overcome the low reactivity of NDA, benzoic acid and isoquinoline were used as catalysts.[26, 34] In addition, the imidization was carried out in *m*-cresol, which has been reported as the sole successful solvent for the synthesis of six-membered ring polyimides.[26-31] The molecular weight control and anhydride end group functionality of the oligomers were achieved by offsetting monomer stoichiometry. The number-average molecular weights of the PI oligomers were determined by ^{1}H NMR spectra. The peaks ranging from 8.5 to 8.7 ppm and from 7.8 to 8.0 were assigned to the protons on the naphthalene moieties and the protons on the *m*-BAPS phenyl ring, respectively (Fig. 3.4). By comparing the integrals, number-average molecular weights were determined and are summarized in Table 3.1. A log-log plot between intrinsic viscosity and number-average molecular weight showed a linear relationship, confirming successful control of molecular weight for each hydrophilic and hydrophobic block series (Fig. 3.5, 3.6).

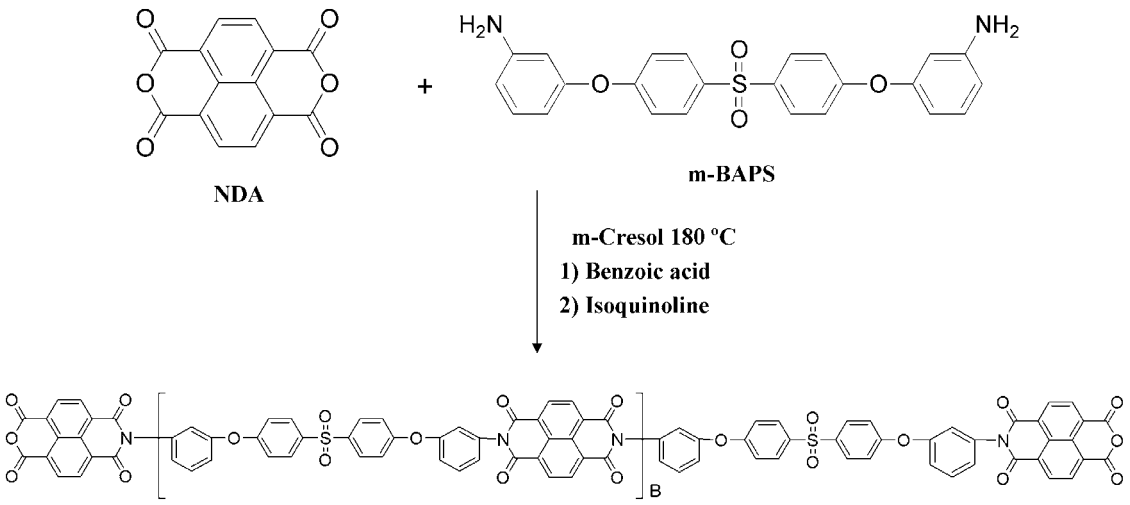

Figure 3. 3. Synthesis of an Anhydride-terminated Polyimide Hydrophobic Oligomer.

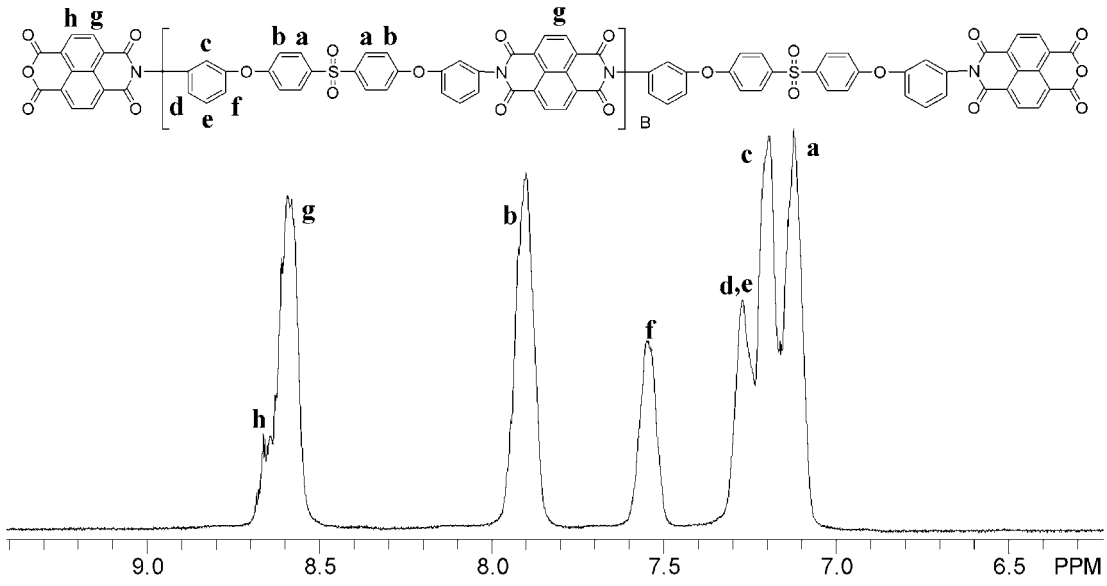

Figure 3. 4. ^{1}H NMR Spectrum of an Anhydride-terminated Polyimide Hydrophobic Oligomer.

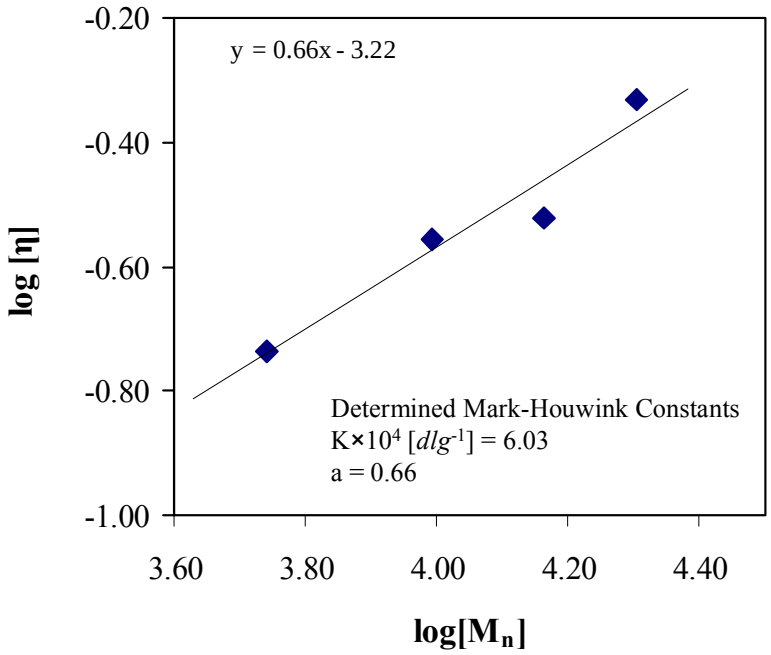

Figure 3. 5. Double Logarithmic Plot of [η] versus M_n of Disulfonated Poly(arylene ether sulfone) Hydrophilic Oligomers. Intrinsic Viscosity was Measured in NMP with 0.05 M LiBr at 25 ºC.

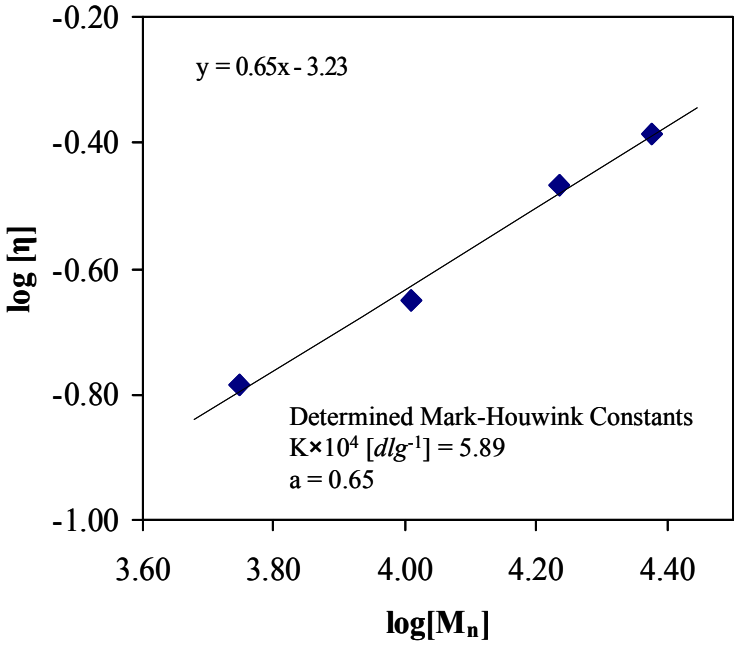

Figure 3. 6. Double Logarithmic Plot of [η] versus M_n of Polyimide Hydrophobic Oligomers. Intrinsic Viscosity was Measured in NMP with 0.05 M LiBr at 25 ºC.

3.4.2. Synthesis of BPSH-PI Multiblock Copolymers

A series of multiblock copolymers was synthesized by an imidization coupling reaction between amine moieties on the BPSH oligomers and anhydride moieties on the PI oligomers (Fig. 3.7). As described in the section on PI synthesis, a successful imidization of six-membered ring anhydrides needs to be conducted in *m*-cresol with catalysts. However, the coupling reaction between BPSH and PI oligomers in *m*-cresol was unsuccessful due to the insolubility of BPSH oligomers in *m*-cresol. Although many sulfonated compounds can be dissolved in *m*-cresol by converting the sulfonic acid groups into triethylammonium salts,[26-31] this modification did not improve the solubility of the BPSH oligomers. For this reason, early attempts of the coupling reaction were performed in NMP, which dissolved both BPSH and PI oligomers. Unfortunately, the coupling reaction in the absence of *m*-cresol resulted in relatively low molecular weight multiblock copolymers. Their intrinsic viscosities ranged from 0.3 to 0.45 dL g^{-1} and the copolymers did not produce tough ductile membranes (Table 3.2).

This low degree of coupling reaction was addressed by utilizing a mixed solvent system which consisted of *m*-cresol and NMP. By using a mixed solvent system, NMP provided good solubility of both oligomers, and this afforded homogeneous solutions wherein *m*-cresol facilitated the imidization coupling reaction. On the NMR spectrum of BPSH5-PI5 copolymer, the disappearance of the end group peaks of the BPSH oligomer confirmed that the coupling reaction was successful (Fig. 3.8). The BPSH-PI multiblock copolymers which were synthesized from the mixed solvent system showed higher intrinsic viscosities and produced tough, ductile membranes. A comparison of the membrane properties synthesized in different solvents is summarized in Table 3.2.

Table 3. 2. Comparison of Membrane Properties of BPSHx –PIy [a] Copolymers Synthesized in Different Reaction Solvents.

Copolymers	NMP			Mixed Solvent (NMP + m-Cresol)		
	IV ($dL\ g^{-1}$)[b]	Water Uptake (%)	Conductivity ($S\ cm^{-1}$)[c]	IV ($dL\ g^{-1}$)[b]	Water Uptake (%)	Conductivity ($S\ cm^{-1}$)[c]
BPSH5 – PI5	0.30	58	0.054	0.50	55	0.090
BPSH10 – PI10	0.35	100	0.060	0.63	70	0.100
BPSH15 – PI15	0.40	-[d]	-[d]	0.68	85	0.110
BPSH20 – PI20	0.44	-[d]	-[d]	1.20	56	0.100

[a] Acronym for copolymers (BPSHx – PIy) :
x = molecular weight of the hydrophilic block (BPSH) in units of kg/mol
y = molecular weight of the hydrophobic block (polyimide) in units of kg/mol
[b] In NMP with 0.05 M LiBr at 25 ºC
[c] Measured in deionized water at 30 ºC
[d] Not available due to poor mechanical strength of hydrated film

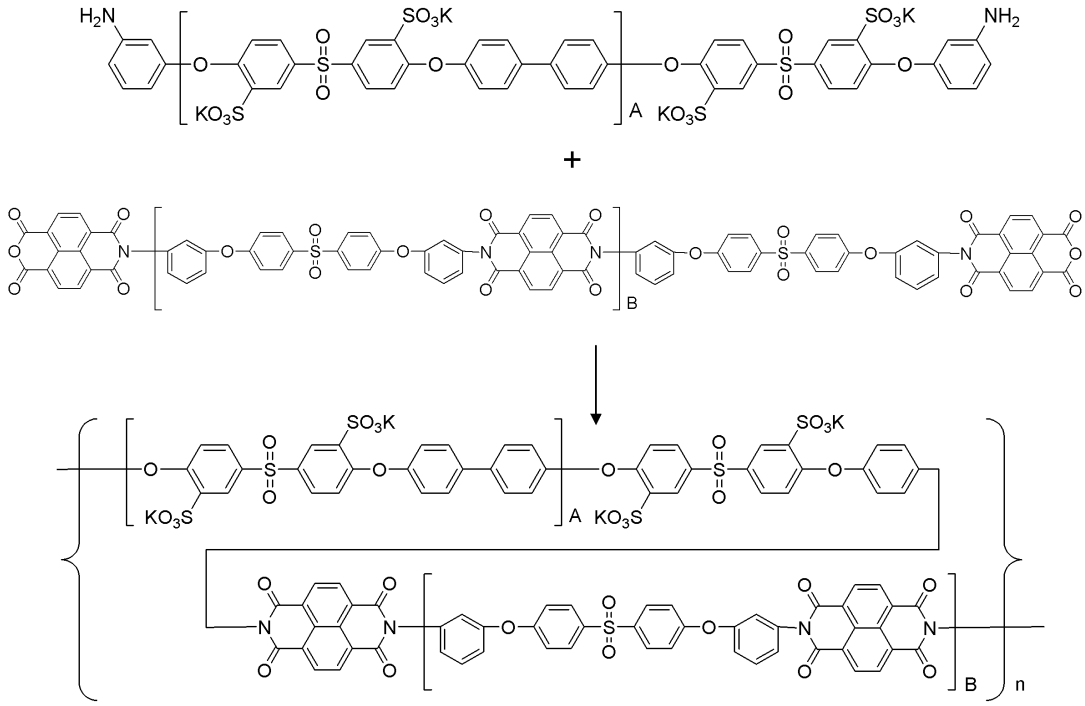

Figure 3. 7. Synthesis of a Segmented Sulfonated Poly(arylene ether sulfone)-*b*-polyimide Copolymer.

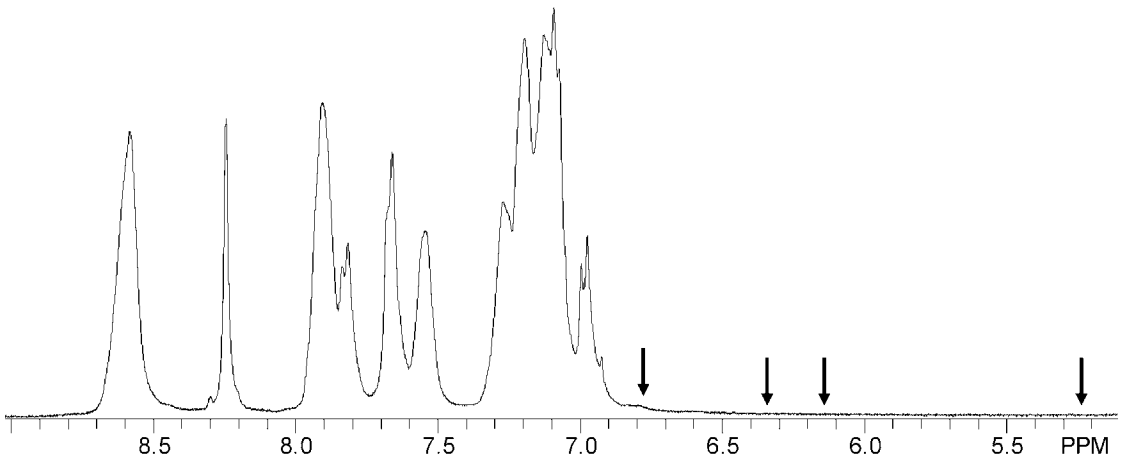

Figure 3. 8. ^{1}H NMR Spectrum of a Poly(arylene ether sulfone)-*b*-polyimide Copolymer. Black Arrows Represent the Disappearance of the Amine End Groups on the Hydrophilic Blocks after the Coupling Reaction with Anhydride-terminated Hydrophobic Blocks.

3.4.3. Characterization of Membrane Properties of BPSH-PI Multiblock Copolymers

The IEC values of the copolymers were determined by titrating the acid form membranes in aqueous sodium sulfate solution with standard sodium hydroxide solution (0.01 N). In all cases, the IEC values agreed with the theoretical values (Table 3.3). The proton conductivities of the multiblock copolymers were measured under fully hydrated conditions in water at room temperature. The proton conductivities showed linear correlation with the IECs and increased up to 1.6 S cm^{-1} at an IEC of 1.9 meq g^{-1}. Conductivities of the samples with IECs higher than 1.9 meq g^{-1} could not be determined due to the poor mechanical strength of the hydrated membranes. The water uptake of the multiblock copolymers was investigated as a function of IEC (Fig. 3.9). It also exhibited a linear relationship with IEC values up to 1.8 meq g^{-1}. However, once the IEC reached 1.8 meq g^{-1}, a drastic increase in water uptake was observed and the membranes became highly swollen hydrogels. This phenomenon can be explained by the development of a percolated morphology in the hydrophilic phase.[10] A systematic explanation of the relationship between IECs, water uptake and proton conductivity will be provided in a separate article.

Thermal and oxidative stabilities of the copolymers in their acid form were investigated by TGA. The copolymer samples were pre-heated at 200 ºC for 10 min in the TGA furnace to remove the moisture. The TGA was conducted from 100 to 800 ºC at a heating rate of 10 ºC min^{-1} under air (Fig. 3.10). All films displayed a two-step degradation profile. The initial weight loss was observed from 300 ºC and was assigned to the decomposition of sulfonic acid groups on the BPSH block. The second decomposition, which ranged from 550 to 650 ºC, was assigned to main-chain polymer

degradation. As the hydrophilic component of the copolymer increased, the weight loss between 300 and 400 ºC increased due to the increase of sulfonic acid content in the copolymer.

Table 3. 3. Properties of BPSH–PI Multiblock Copolymers in the Sulfonic Acid Form.

Copolymers	Calculated IEC (meq g^{-1})	Experimental IEC (meq g^{-1})[a]	Intrinsic Viscosity (dL g^{-1})[b]	Water Uptake (%)	Conductivity (S cm^{-1})[c]	Temp. at 5% Weight Loss (ºC)[d]
BPSH5 – PI5	1.63	1.65	0.50	55	0.090	367
BPSH5 – PI10	1.13	1.09	0.74	22	0.018	448
BPSH5 – PI15	0.80	0.78	0.71	15	0.010	484
BPSH5 – PI20	0.62	0.53	0.71	12	0.006	493
BPSH10 – PI5	2.10	1.98	0.61	-[e]	-[e]	340
BPSH10 – PI10	1.59	1.57	0.63	70	0.100	346
BPSH10 – PI15	1.20	1.17	0.72	40	0.073	351
BPSH10 – PI20	0.96	0.86	0.92	24	0.030	507
BPSH15 – PI5	2.38	2.12	0.77	-[e]	-[e]	347
BPSH15 – PI10	1.91	1.83	0.71	156	0.161	369
BPSH15 – PI15	1.51	1.55	0.68	85	0.110	373
BPSH15 – PI20	1.25	1.12	0.89	38	0.055	510
BPSH20 – PI5	2.58	2.20	0.75	-[e]	-[e]	317
BPSH20 – PI10	2.17	2.02	0.92	-[e]	-[e]	333
BPSH20 – PI15	1.78	1.71	0.83	97	0.092	345
BPSH20 – PI20	1.51	1.20	1.20	56	0.100	365

[a] Determined by titration with NaOH.
[b] In NMP with 0.05 M LiBr at 25 ºC.
[c] Measured in deionized water at 30 ºC.
[d] Conducted under air.
[e] Not available due to poor mechanical strength of the hydrated film.

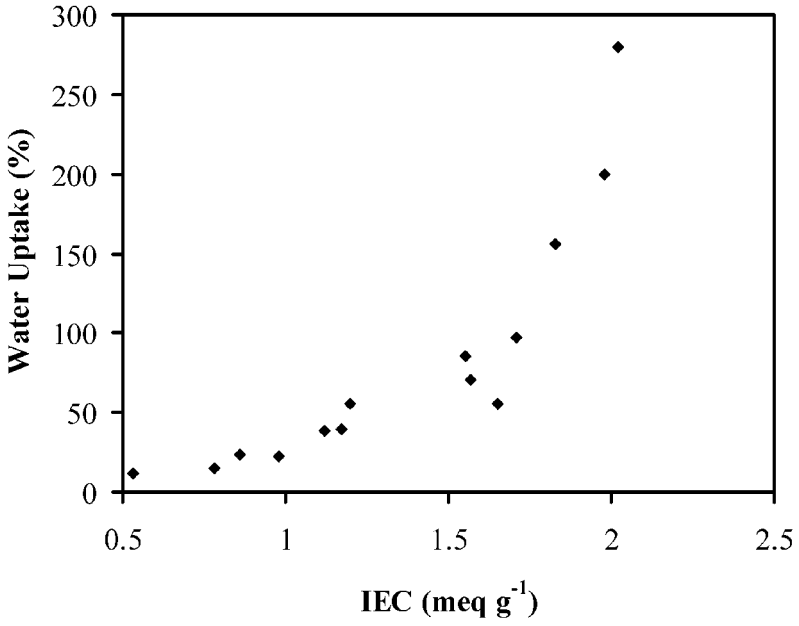

Figure 3. 9. Influence of IEC on Water Uptake of BPSH-PI Multiblock Copolymers.

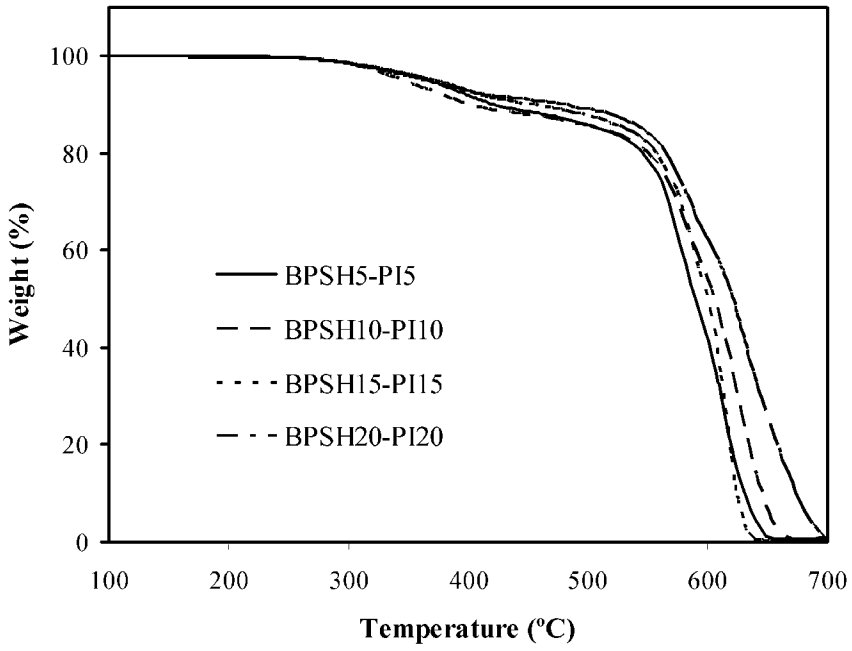

Figure 3. 10. TGA Thermograms of BPSH-PI Multiblock Copolymers with Different Hydrophilic and Hydrophobic Block Lengths.

3.4.4. Morphological Characterization of the Multiblock Copolymers

Phase separated morphologies of the cast film surfaces were characterized by tapping mode atomic force microscopy (TM-AFM). It has been shown that water adsorbed on the surface of a sample increases adhesive forces between the tip and sample.[35] This causes energy dissipation which results in a phase lag between the cantilever's oscillation and the initial oscillation imparted by the piezoelectric actuator. In these BPSH-PI films, the ionic groups on the BPSH adsorb water, resulting in an increased phase lag. Consequently, the ionic domains of the films appear darker in the TM-AFM phase images while the non-ionic domains appear brighter. Contrast in the TM-AFM height images is based on height; lower features appear darker and higher features appear brighter.

TM-AFM images were obtained for the BPSH-PI copolymers. While phase separated morphologies were observed for multiblock copolymers with unequal block lengths, the sharpest and most uniform phase separated morphologies were observed for the copolymers with equal block lengths (Fig. 3.11). The brighter non-ionic domains increased in size from small round domains (Fig. 3.11a) to co-continuous lamellar structures (Fig. 3.11c) as block length increases. The darker ionic domains also formed longer channels with increasing block length. These morphologies were not limited to isolated regions within each membrane, but existed over longer scales across each membrane surface as evidenced by the uniform, long-range order displayed in the height and phase micrographs of BPSH15-PI15 (Fig. 3.11d and 3.11e).

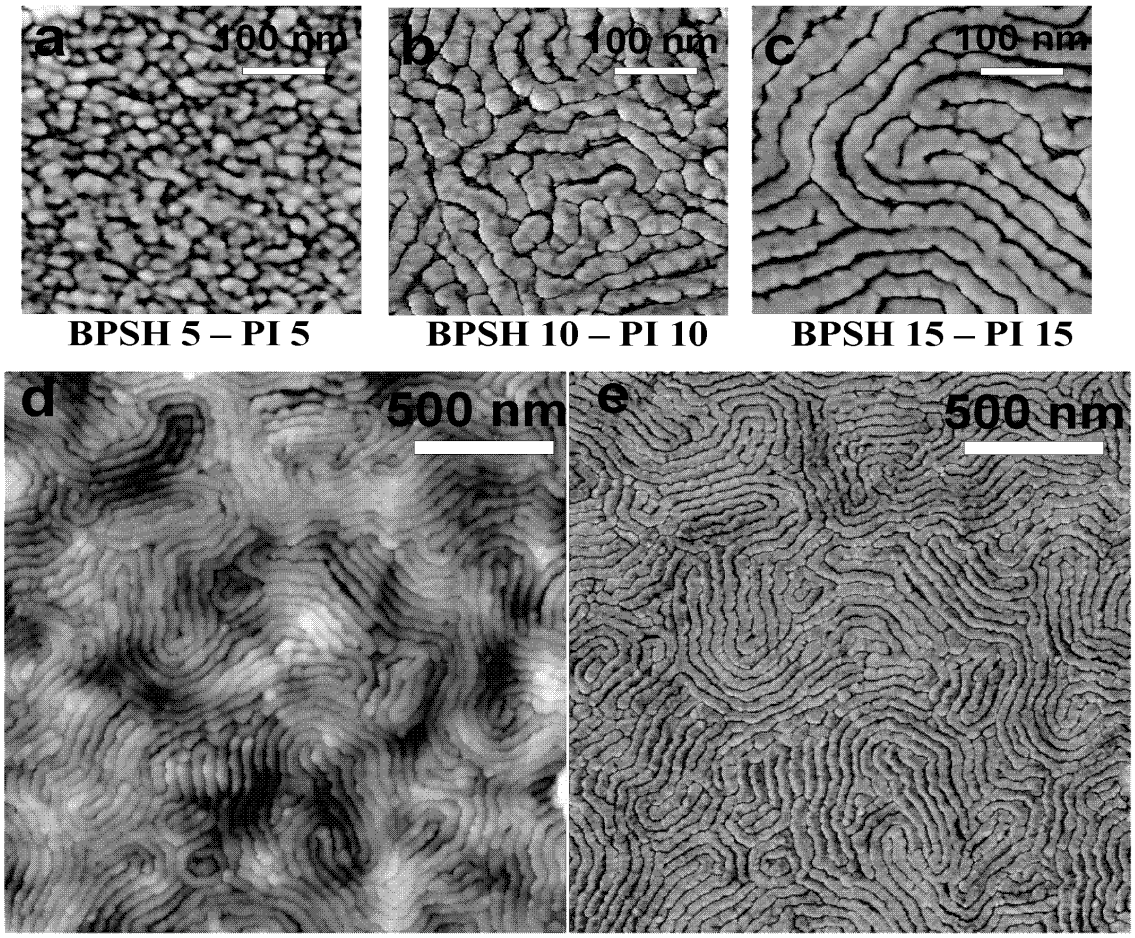

Figure 3. 11. (a)-(c) Tapping Mode AFM Phase Images of BPSH-PI Multiblock Copolymers with Different Block Lengths, (d) Height Image and (e) Phase Image of BPSH15-PI15 Demonstrating Long-range Order.

3.4.5. Hydrolytic Stability Test

Hydrolytic stability of a PEM is a crucial property for long-term fuel cell operation. Intense research on sulfonated polyimides revealed that five-membered ring polyimides were not suitable for PEM applications due to hydrolysis of the imido ring under acidic conditions.[22-25] Although this poor hydrolytic stability has been improved by using a six-membered ring polyimide,[26-31] their long-term stability under a harsh fuel cell environment is still suspect. The hydrolytic stabilities of two series of sulfonated naphthalene dianhydride-based random copolymers were previously reported by our laboratory.[26, 27] Those membranes became brittle in less than 100 hours of submersion in 80 ºC water. The intrinsic viscosities of the samples after the test were reduced to 10-20% of the original values, which is attributed to hydrolysis of the imide moieties within the polymer.

Hydrolytic stabilities of the BPSH-PI copolymers were determined by monitoring changes in intrinsic viscosity and mechanical flexibility. The acid-form membranes were placed in 80 ºC water and tested for 1000 hours. The flexibilities of the membranes were evaluated by manually bending the hydrated membranes 90º.[27] After the 1000-hour test, all samples still maintained flexibility, and their intrinsic viscosities were 76-85% of the original values (Table 3.4). In addition, ^{1}H NMR revealed that the IECs were 84-95% of the original values. The morphologies of the multiblock copolymers may explain their enhanced hydrolytic stabilites relative to the random copolymers. It is tempting to speculate that in the phase-separated morphology, the hydrolytically unstable polyimide hydrophobic regime was somewhat isolated from the acidic, moisture-rich hydrophilic regime.

Table 3. 4. Hydrolytic Stabilities of BPSH–PI Multiblock Copolymers at 80 ºC for 1000 Hours.

Copolymers	Before Hydrolytic Stability Test		After Hydrolytic Stability Test	
	IV (dL g^{-1})[a]	IEC (meq g^{-1})[b]	IV (dL g^{-1})[a]	IEC (meq g^{-1})[b]
BPSH 5 – PI 5	0.49	1.69	0.40	1.60
BPSH 10 – PI 10	0.71	1.57	0.60	1.39
BPSH 15 – PI 15	0.67	1.55	0.51	1.30

[a] In NMP with 0.05 M LiBr at 25 ºC
[b] Determined by titration with NaOH

3.5. Conclusions

Novel multiblock copolymers based on hydrophilic and hydrophobic blocks were developed and characterized. The multiblock copolymers were synthesized from amine terminated sulfonated poly(arylene ether sulfone) as hydrophilic block and anhydride terminated polyimide as hydrophobic block by imidization coupling reaction. In the coupling reaction, *m*-cresol and catalysts were required to produce high molecular weight multiblock copolymers. Transparent and ductile membranes were prepared from NMP by solvent casting. Their proton conductivities and water uptake values were influenced by IEC values. Morphological characterization by tapping-mode AFM showed clear nano-phase separation of hydrophilic and hydrophobic domains. Changes in block length affected the morphologies of the multiblock copolymers and the BPSH15-PI15 membrane showed long-range co-continuous morphology of the hydrophilic and hydrophobic regimes. Hydrolytic stability testing of the multiblock copolymers in 80 ºC water revealed that they maintained flexibility after 1000 hour, which is much improved over earlier random copolymer systems.

The authors thank the Department of Energy (DE-FG36-06G016038) for its support of this research.

3.6. References

1. Lashway, Robert W. Fuel cells: The next evolution. *MRS Bulletin* **2005,** 30, (8), 581-583.
2. de Bruijn, Frank. The current status of fuel cell technology for mobile and stationary applications. *Green Chemistry* **2005,** 7, (3), 132-150.
3. Kreuer, K. D. On the development of proton conducting polymer membranes for hydrogen and methanol fuel cells. *Journal of Membrane Science* **2001,** 185, (1), 29-39.
4. Steele, Brian C. H.; Heinzel, Angelika. Materials for fuel-cell technologies. *Nature (London, United Kingdom)* **2001,** 414, (6861), 345-352.
5. Banerjee, Shoibal; Curtin, Dennis E. Nafion perfluorinated membranes in fuel cells. *Journal of Fluorine Chemistry* **2004,** 125, (8), 1211-1216.
6. Mauritz, Kenneth A.; Moore, Robert B. State of understanding of Nafion. *Chemical Reviews (Washington, DC, United States)* **2004,** 104, (10), 4535-4585.
7. Kim, Yu Seung; Dong, Limin; Hickner, Michael A.; Glass, Thomas E.; Webb, Vernon; McGrath, James E. State of Water in Disulfonated Poly(arylene ether sulfone) Copolymers and a Perfluorosulfonic Acid Copolymer (Nafion) and Its Effect on Physical and Electrochemical Properties. *Macromolecules* **2003,** 36, (17), 6281-6285.
8. Savadogo, O. Emerging membranes for electrochemical systems Part II. High temperature composite membranes for polymer electrolyte fuel cell (PEFC) applications. *Journal of Power Sources* **2004,** 127, (1-2), 135-161.
9. Smitha, B.; Sridhar, S.; Khan, A. A. Solid polymer electrolyte membranes for fuel cell applications - a review. *Journal of Membrane Science* **2005,** 259, (1-2), 10-26.
10. Hickner, Michael A.; Ghassemi, Hossein; Kim, Yu Seung; Einsla, Brian R.; McGrath, James E. Alternative Polymer Systems for Proton Exchange Membranes (PEMs). *Chemical Reviews (Washington, DC, United States)* **2004,** 104, (10), 4587-4611.
11. Wang, Feng; Hickner, Michael; Kim, Yu Seung; Zawodzinski, Thomas A.; McGrath, James E. Direct polymerization of sulfonated poly(arylene ether sulfone) random (statistical) copolymers: candidates for new proton exchange membranes. *Journal of Membrane Science* **2002,** 197, (1-2), 231-242.
12. Kim, Yu Seung; Wang, Feng; Hickner, Michael; McCartney, Stephan; Hong, Young Taik; Harrison, William; Zawodzinski, Thomas A.; McGrath, James E. Effect of acidification treatment and morphological stability of sulfonated poly(arylene ether sulfone) copolymer proton-exchange membranes for fuel-cell use above 100 Deg. *Journal of Polymer Science, Part B: Polymer Physics* **2003,** 41, (22), 2816-2828.
13. Kim, Yu Seung; Hickner, Michael A.; Dong, Limin; Pivovar, Bryan S.; McGrath, James E. Sulfonated poly(arylene ether sulfone) copolymer proton exchange membranes: composition and morphology effects on the methanol permeability. *Journal of Membrane Science* **2004,** 243, (1-2), 317-326.
14. Harrison, W. L.; Hickner, M. A.; Kim, Y. S.; McGrath, J. E. Poly(arylene ether sulfone) copolymers and related systems from disulfonated monomer building

blocks: synthesis, characterization, and performance - a topical review. *Fuel Cells (Weinheim, Germany)* **2005,** 5, (2), 201-212.
15. Ghassemi, Hossein; Ndip, Grace; McGrath, James E. New multiblock copolymers of sulfonated poly(4'-phenyl-2,5-benzophenone) and poly(arylene ether sulfone) for proton exchange membranes. II. *Polymer* **2004,** 45, (17), 5855-5862.
16. Wang, Hang; Badami, Anand S.; Roy, Abhishek; McGrath, James E. Multiblock copolymers of poly(2,5-benzophenone) and disulfonated poly(arylene ether sulfone) for proton-exchange membranes. I. Synthesis and characterization. *Journal of Polymer Science, Part A: Polymer Chemistry* **2006,** 45, (2), 284-294.
17. Okamoto, Ken-ichi. Sulfonated polyimides for polymer electrolyte membrane fuel cell. *Journal of Photopolymer Science and Technology* **2003,** 16, (2), 247-254.
18. Okamoto, Ken-ichi; Yin, Yan; Yamada, Otoo; Islam, Md Nurul; Honda, Tatsuaki; Mishima, Takashi; Suto, Yoshiki; Tanaka, Kazuhiro; Kita, Hidetoshi. Methanol permeability and proton conductivity of sulfonated co-polyimide membranes. *Journal of Membrane Science* **2005,** 258, (1-2), 115-122.
19. Roy, Abhishek; Hickner, Michael A.; Yu, Xiang; Li, Yanxiang; Glass, Thomas E.; McGrath, James E. Influence of chemical composition and sequence length on the transport properties of proton exchange membranes. *Journal of Polymer Science, Part B: Polymer Physics* **2006,** 44, (16), 2226-2239.
20. Devadoss, E. High-performance polyimide coatings for electronic and space applications. *Journal of Scientific & Industrial Research* **1989,** 48, (1), 22-30.
21. Senzenberger, Horst D. Preparation and properties of high performance polyimide composites. *Applied Polymer Symposia* **1973,** No. 22, 77-88.
22. Genies, C.; Mercier, R.; Sillion, B.; Petiaud, R.; Cornet, N.; Gebel, G.; Pineri, M. Stability study of sulfonated phthalic and naphthalenic polyimide structures in aqueous medium. *Polymer* **2001,** 42, (12), 5097-5105.
23. Meyer, Gilles; Gebel, Gerard; Gonon, Laurent; Capron, Philipe; Marscaq, Didier; Marestin, Catherine; Mercier, Regis. Degradation of sulfonated polyimide membranes in fuel cell conditions. *Journal of Power Sources* **2006,** 157, (1), 293-301.
24. Meyer, Gilles; Perrot, Carine; Gebel, Gerard; Gonon, Laurent; Morlat, Sandrine; Gardette, Jean-Luc. Ex situ hydrolytic degradation of sulfonated polyimide membranes for fuel cells. *Polymer* **2006,** 47, (14), 5003-5011.
25. Perrot, C.; Meyer, G.; Gonon, L.; Gebel, G. Aging mechanisms of proton exchange membrane used in fuel cell applications. *Fuel Cells (Weinheim, Germany)* **2006,** 6, (1), 10-15.
26. Einsla, Brian R.; Hong, Young-Taik; Kim, Yu Seung; Wang, Feng; Gunduz, Nazan; McGrath, James E. Sulfonated naphthalene dianhydride based polyimide copolymers for proton-exchange-membrane fuel cells. I. Monomer and copolymer synthesis. *Journal of Polymer Science, Part A: Polymer Chemistry* **2004,** 42, (4), 862-874.
27. Einsla, Brian R.; Kim, Yu Seung; Hickner, Michael A.; Hong, Young-Taik; Hill, Melinda L.; Pivovar, Bryan S.; McGrath, James E. Sulfonated naphthalene dianhydride based polyimide copolymers for proton-exchange-membrane fuel cells. II. Membrane properties and fuel cell performance. *Journal of Membrane Science* **2005,** 255, (1-2), 141-148.

28. Genies, C.; Mercier, R.; Sillion, B.; Cornet, N.; Gebel, G.; Pineri, M. Soluble sulfonated naphthalenic polyimides as materials for proton exchange membranes. *Polymer* **2000,** 42, (2), 359-373.
29. Guo, Xiaoxia; Fang, Jianhua; Watari, Tatsuya; Tanaka, Kazuhiro; Kita, Hidetoshi; Okamoto, Kenichi. Novel Sulfonated Polyimides as Polyelectrolytes for Fuel Cell Application. 2. Synthesis and Proton Conductivity of Polyimides from 9,9-Bis(4-aminophenyl)fluorene-2,7-disulfonic Acid. *Macromolecules* **2002,** 35, (17), 6707-6713.
30. Hu, Zhaoxia; Yin, Yan; Chen, Shouwen; Yamada, Otoo; Tanaka, Kazuhiro; Kita, Hidetoshi; Okamoto, Ken-Ichi. Synthesis and properties of novel sulfonated (co)polyimides bearing sulfonated aromatic pendant groups for PEFC applications. *Journal of Polymer Science, Part A: Polymer Chemistry* **2006,** 44, (9), 2862-2872.
31. Miyatake, Kenji; Asano, Naoki; Watanabe, Masahiro. Synthesis and properties of novel sulfonated polyimides containing 1,5-naphthylene moieties. *Journal of Polymer Science, Part A: Polymer Chemistry* **2003,** 41, (24), 3901-3907.
32. Lee, Hae-Seung; Roy, Abhishek; Badami, Anand S.; McGrath, James E. Synthesis and characterization of sulfonated poly(arylene ether) polyimide multiblock copolymers for proton exchange membranes. *Macromolecular Research* **2007,** 15, (2), 160-166.
33. Sankir, M.; Bhanu, V. A.; Harrison, W. L.; Ghassemi, H.; Wiles, K. B.; Glass, T. E.; Brink, A. E.; Brink, M. H.; McGrath, J. E. Synthesis and characterization of 3,3'-disulfonated-4,4'-dichlorodiphenyl sulfone (SDCDPS) monomer for proton exchange membranes (PEM) in fuel cell applications. *Journal of Applied Polymer Science* **2006,** 100, (6), 4595-4602.
34. Sek, Danuta; Pijet, Pawel; Wanic, Andrzej. Investigation of polyimides containing naphthalene units: 1. Monomer structure and reaction conditions. *Polymer* **1992,** 33, (1), 190-193.
35. James, P. J.; Antognozzi, M.; Tamayo, J.; McMaster, T. J.; Newton, J. M.; Miles, M. J. Interpretation of Contrast in Tapping Mode AFM and Shear Force Microscopy. A Study of Nafion. *Langmuir* **2001,** 17, (2), 349-360.

CHAPTER 4

Hydrophilic-Hydrophobic Multiblock Copolymers Based on Poly(arylene ether sulfone) via Low Temperature Coupling Reactions for Proton Exchange Membrane Fuel Cells

Hae-Seung Lee[1], Abhishek Roy[1], Ozma Lane[1], Stuart Dunn[1,2] and James E. McGrath[1,*]

[1]Macromolecules and Interfaces Institute,

Virginia Polytechnic Institute and State University, Blacksburg, VA 24061

[2] Department of Chemistry, University of North Carolina, Chapel Hill, NC 27599

*Correspondence to: James E. McGrath

(Email: jmcgrath@vt.edu, Phone: 540-231-5976, Fax: 540-231-8517)

Taken from *Polymer*, 49 (2008), 715-723

4.1. Abstract

Two series of multiblock copolymers based on poly(arylene ether sulfone)s were developed and evaluated for use as proton exchange membranes (PEMs). The multiblock copolymers were synthesized by a coupling reaction between phenoxide terminated fully disulfonated poly(arylene ether sulfone) (BPSH100) and decafluorobiphenyl (DFBP) or hexafluorobenzene (HFB) end-capped unsulfonated poly(arylene ether sulfone) (BPS0) as hydrophilic and hydrophobic blocks, respectively. The highly reactive nature of DFBP and HFB allowed the coupling reactions to be accomplished under mild reaction conditions (e.g., < 105 °C). The low coupling temperatures prevented possible ether-ether exchange reactions which can cause a loss of order due to randomization of the hydrophilic-hydrophobic sequences. The multiblock copolymers produced tough and ductile membranes and their fundamental properties as PEMs were explored. They showed enhanced conductivities under fully hydrated conditions when compared with a random BPSH copolymer with a similar IEC. These copolymers also showed anisotropic swelling behavior, whereas the random copolymers were isotropic. The synthesis and fundamental properties of the multiblock copolymers are reported here and the systematic fuel cell properties and more detailed morphology characterization will be provided elsewhere.

Keywords: Hydrophilic-hydrophobic multiblock copolymers; Sulfonated poly(arylene ether sulfone); fluoroaromatic endlinking

4.2. Introduction

Fossil fuel resources are limited, expensive and combustion engines can contribute to environmental degradation; the need to find alternative energy sources has thus becomes imperative.[1] Polymer electrolyte membrane fuel cells (PEMFC) are potentially one of the best candidates to replace conventional internal combustion engines in automobiles, stationary power and batteries in portable electronic devices because of their high energy efficiency and environmental friendliness.[2]

Nafion® is a perfluorosulfonic acid (PFSA) ionomer manufactured by DuPont which has been fabricated into membranes by both extrusion of a precursor and dispersion casting. It has been the benchmark membrane as a result of its outstanding properties, such as high proton conductivity, stability in the fuel cell environment, mechanical toughness and moderate water uptake.[3] Furthermore, the nature of the poly(tetrafluoroethylene)-like backbone (~ 87 mole %) and the existence of partial-crystallinity in the main backbone provides excellent chemical and hydrolytic stabilities, as well as good mechanical properties.[4] However, Nafion-type membranes have several disadvantages at higher operation temperatures (e.g., > 100 ºC) which are desirable for several reasons, including faster electrode kinetics and higher tolerance to CO poisoning. Absorbed water also depresses the glass transition temperature (Tg) and α relaxation of the membranes, resulting in the deterioration of mechanical properties as well as fuel cell performance.[5, 6] Although the poor mechanical properties at high temperature may be improved by fabrication of composite membranes with Teflon fabric reinforcements,[7] the high cost along with high fuel permeability have spurred the development of new PEM materials.

As an alternative to Nafion, sulfonated poly(arylene ether) copolymers have been proposed as one of the most attractive new PEM materials due to their excellent thermal and oxidative stability, good mechanical properties, good processability and exceptional hydrolytic stability.[8, 9] The direct copolymerization of partially disulfonated poly(arylene ether sulfone) random copolymers (BPSH) was largely developed in our research group, [10] and we have intensively explored their performance and properties for PEM applications.[11, 12] Although the excellent stability and proton conductivity under fully hydrated conditions makes BPSH system a promising and likely lower cost alternative to Nafion, the proton conductivities under low humidity were significantly lower.[13]

Rencent efforts to address this drawback has been pursued using hydrophilic-hydrophobic multiblock copolymer systems that can have much higher water diffusion coefficients than either the random copolymers or the perfluorosulfonic acid (PFSA) ionomers, which is important for conductivity at lower humidities. Several series of multiblock copolymers were synthesized via coupling reactions of fully disulfonated poly(arylene ether sulfone) hydrophilic blocks (BPSH100) and various types of hydrophobic blocks.[14-19] The multiblock copolymer membranes exhibited unique phase separated morphologies and permitted significantly enhanced proton conductivities under partially hydrated conditions by forming well connected hydrophilic domains.[19, 20] Most recent research activities was to prepare hydrophilic-hydrophobic multiblock copolymers whose chemical components are similar to that of BPSH random copolymer. By adopting ordered hydrophilic-hydrophobic sequences in the multiblock copolymers, the proton conductivities can be significantly improved with the same chemical components of BPSH random copolymers.

Unfortunately, conventional approaches to prepare multiblock copolymers (e.g., coupling reactions between two different telechelic oligomers via nucleophilic aromatic substitution) are highly limited since their high reaction temperatures can randomize hydrophilic-hydrophobic sequences by well-known ether-ether exchanges which can take place under nucleophilic step copolymerization conditions. Of the different approaches to preventing the ether-ether exchange reactions, lowering the reaction temperature should be the simplest methodology. For this reason, utilizing perfluorinated small molecules such as decafluorobiphenyl (DFBP) and hexafluorobenzene (HFB) as the linkage groups between the hydrophilic and hydrophobic oligomers is appealing. Their highly reactive nature in nucleophilic aromatic substitution reactions can permit a significantly lower coupling reaction temperature which should minimize side-reactions, including the ether-ether exchange reaction.

In this chapter the synthesis and characterization of segmented sulfonated multiblock copolymers based on poly(arylene ether sulfone) by utilizing DFBP and HFB as linkage groups are described. The multi-block copolymers were produced by coupling reactions between hydrophilic BPSH100 and DFBP or HFB end-capped hydrophobic BPS0 blocks, respectively. The highly reactive perfluorinated end groups on the hydrophobic blocks allowed the coupling reaction to proceed below 105 °C and prevented potential ether-ether exchange reactions. By the described synthetic routes, two series of multiblock copolymers with different linkage groups were synthesized and characterized. This paper also evaluates the effect of block length on proton conductivity, water uptake and other membrane properties.

4.3. Experimental

4.3.1. Materials

Monomer grade 4,4'-dichlorodiphenyl sulfone (DCDPS) and 4,4'-biphenol (BP) were provided by Solvay Advanced Polymers and Eastman Chemical Company, respectively, and dried *in vacuo* at 110 °C prior to use. The enabling comonomer ,3,3'-Disulfonated-4,4'-dichlorodiphenylsulfone (SDCDPS) was synthesized from DCDPS and purified according to a procedure reported elsewhere.[21] Decafluorobiphenyl (DFBP) and hexafluorobenzene (HFB) were used as received from Lancaster and Aldrich, respectively. N-methyl-2-pyrrolidinone (NMP), N,N-dimethylaceteamide (DMAc), cyclohexane, and toluene were purchased from Aldrich and distilled from calcium hydride before use. Potassium carbonate, chloroform, acetone, and 2-propanol (IPA) were purchased from Aldrich and used without further purification.

4.3.2. Synthesis of Phenoxide Terminated Fully Disulfonated Hydrophilic Oligomer (BPSH100)

A series of fully disulfonated poly(arylene ether sulfone) hydrophilic oligomers (BPSH100) was synthesized with different molecular weights. A sample synthesis of 5,000 g/mol BPSH100 is as follows: 8.9720 g (48.2 mmol) of BP, 21.0280 g (42.8 mmol) of SDCDPS and 7.9911 g (57.8 mmol) of potassium carbonate were charged to a three-necked 250-mL flask equipped with a condenser, a Dean Stark trap, a nitrogen inlet, and a mechanical stirrer. Then distilled DMAc (120 mL) and toluene (60 mL) were added to the flask and the reaction was heated at 145 °C with stirring. The solution was allowed to reflux at 145 °C while the toluene azeotropically removed the water in the system. After

4 h, the toluene was removed from the reaction by slowly increasing the temperature to 180 ºC. The reaction was allowed to proceed for another 96 h. The resulting viscous solution was cooled to room temperature and diluted with DMAc to facilitate filtration. After filtration, the solution was coagulated in IPA. The oligomer was dried at 120 °C *in vacuo* for at least 24 h.

4.3.3. Synthesis of Phenoxide Terminated Unsulfonated Hydrophobic Oligomers (BPS0)

A series of unsulfonated poly(arylene ether sulfone) hydrophobic oligomers (BPS0) was synthesized with different molecular weights.. A sample synthesis of 5,000 g/mol BPS0 oligomer is as follows: 13.0210 g (66.5 mmol) of BP, 12.0210 g (61.4 mmol) of DCDPS and 11.0245 g (79.8 mmol) of potassium carbonate were charged to a three-necked 250-mL flask equipped with a condenser, a Dean Stark trap, a nitrogen inlet, and a mechanical stirrer. Distilled DMAc (120 mL) and toluene (60 mL) were added to the flask and the solution was heated at 145 °C with stirring. The solution was allowed to reflux at 145 °C while the toluene azeotropically removed the water in the system. After 4 h, the toluene was removed from the flask by slowly increasing the temperature to 180 ºC. The reaction was allowed to proceed for another 48 h. The same isolation and purification process of BPSH100 oligomer was applied for BPS0 oligomers.

4.3.4. End-capping of Phenoxide Terminated Hydrophobic Oligomers with DFBP and HFB

Phenoxide terminated BPS0 oligomers were end-capped with DFBP or HFB via a nucleophilic aromatic substitution reaction. A typical end-capping reaction of 5,000 g/mol BPS0 oligomer is as follows: 5.0000 g (1.0 mmol) of BPS0 oligomer, 0.5528 g (4.0 mmol) of potassium carbonate were charged to a three-necked 100-mL flask equipped with a condenser, a Dean Stark trap, a nitrogen inlet, and a mechanical stirrer. Distilled DMAc (50 mL) and cyclohexane (15 mL) were added to the flask. The solution was allowed to reflux at 100 °C to azeotropically remove the water in the system. After 4 h, the cyclohexane was removed from the system. The reaction temperature was set to 105 °C (DFBP) or 80 °C (HFB). When HFB was used, the nitrogen purge was stopped at this point because of its lower boiling point. Then 2.0047 g (6.0 mmol) of DFBP or 1.1163 g (6.0 mmol) of HFB was added and the reaction was allowed to proceed for 12 h. The solution was then cooled to room temperature and filtered. The filtered solution was coagulated in methanol. The polymer was dried at 110 °C *in vacuo* for 24 h.

4.3.5. Synthesis of Hydrophilic-hydrophobic Multiblock Copolymers

Two series of multiblock copolymers with different linkage groups were synthesized via a coupling reaction between phenoxide terminated BPSH100 oligomers and DFBP or HFB end-capped BPS0 oligomers. A typical coupling reaction was performed as follows: 5.0000 g (1.0 mmol) of BPSH100 ($\overline{M_n}$ = 5,000 g/mol), 0.5528 g (4.0 mmol) of potassium carbonate, 100 mL of DMAc, and 30 mL of cyclohexane were added to a three-necked 250 mL flask equipped with a condenser, a Dean Stark trap, a nitrogen inlet,

and a mechanical stirrer. The reaction mixture was heated at 100 ºC for 4 h to dehydrate the system with refluxing cyclohexane. After removing the cyclohexane, 5.0000 g (1.0 mmol) of DFBP or HFB end-capped BPS0 ($\overline{M_n}$ = 5,000 g/mol) was added. The coupling reaction was conducted at 105 ºC for 24 h. The resulting yellowish polymer solution was filtered and precipitated in IPA. The copolymer was purified in a Soxhlet extractor with methanol for 24 h and with chloroform for another 24 h. The copolymer was dried at 120 °C *in vacuo* for 24 h.

4.3.6. Characterization

^{1}H and ^{13}C NMR analyses were conducted on a Varian INOVA 400 MHz spectrometer with DMSO-d_6 to confirm the chemical structures of the oligomers and copolymers. ^{1}H NMR spectroscopy was also used to determine number-average molecular weights of the oligomers via end-group analysis. Intrinsic viscosities were determined in NMP containing 0.05 M LiBr at 25 ºC using an Ubbelohde viscometer. The thermooxidative stabilities of the acid-form membranes were determined by using a TA Instruments TGA Q500. Prior to TGA characterization, the membranes were placed in the TGA furnace at 150 °C in a nitrogen atmosphere for 30 min to remove residual solvent and moisture. The samples were then evaluated over the range of 80-800 °C at a heating rate of 10 °C/min under nitrogen atmosphere. The ion exchange capacity (IEC) values of the acid-form copolymers were determined by titration with 0.01 M NaOH solution.

4.3.7. Film Casting and Membrane Acidification

The copolymers in salt form were dissolved in NMP (7% w/v) and filtered through 0.45 μm Teflon® syringe filters. The solutions were then cast onto clean glass substrates. The films were dried for 2 days with an infrared lamp at 45-55 °C for 48 h. The residual solvent was removed by drying in a vacuum oven at 110 °C for 24 h. The membranes in the salt form were converted to acid form by boiling in 0.5 M sulfuric acid for 2 h, followed by boiling in deionized water for 2 h.

4.3.8. Determination of Proton Conductivity and Water Uptake

Proton conductivities under fully hydrated conditions were evaluated in liquid water. The conductivity of the membrane was determined from the geometry of the cell and resistance of the film which was taken at the frequency that produced the minimum imaginary response. A Solartron (1252A +1287) impedance/gain-phase analyzer over the frequency range of 10 Hz - 1 MHz was used for the measurements. The membrane water uptake was determined by the weight difference between dry and wet membranes. The vacuum dried membranes were weighed (W_{dry}), and then immersed in deionized water at room temperature for 24 h. The wet membrane was blotted dry and immediately weighed again (W_{wet}). The water uptake of the membranes was calculated according to the following equation.

$$Water\,Uptake\ (\%) = \frac{W_{wet} - W_{dry}}{W_{dry}} \times 100$$

The hydration number (λ) which can be defined as the number of water molecules absorbed per sulfonic acid unit, was determined from the water uptake and the ion content of the dry membrane according to the following equation.

$$\lambda = \frac{(W_{wet} - W_{dry}) / MW_{H_2O}}{IEC \times W_{dry}} \times 1000$$

where MW_{H2O} is the molecular weight of water (18.01 g/mol).

4.3.9. Determination of Swelling Ratio

The volume swelling ratios of all of the membranes were determined from the dimensional changes from wet to dry state in both in-plane and through-plane. Initially, samples were equilibrated in water and wet dimensions were measured. The dried dimensions were obtained by drying the wet membrane at 80 ^{o}C in convection oven for 2 h.

4.4. Results and Discussion

4.4.1. Synthesis of Hydrophilic and Hydrophobic Oligomers

Fully disulfonated poly(arylene ether sulfone) hydrophilic oligomers (BPSH100) and unsulfonated poly(arylene ether sulfone) hydrophobic oligomers (BPS0) with phenoxide telechelic functionality were synthesized via step growth polymerization (Fig. 4.1, 4.2). The control of the molecular weight and end group functionality was achieved by off-setting the molar ratios of monomers for the synthesis. In all cases, the molar feed ratios of BP over SDCDPS or DCDPS were greater than 1 to produce phenoxide telechelic functionality. The target number-average molecular weights of the oligomers ranged from 3 to 20 kg/mol. The number-average molecular weights of the oligomers were determined by ^{1}H NMR end group analysis. On the ^{1}H NMR spectra of both BPSH100 and BPS0, four small peaks at 6.80 , 7.40, 7.05 and 6.80 ppm were assigned to the protons on the BP moieties which are located at the end of the oligomers. Meanwhile, the peaks at 7.1, 7.65 and 7.1, 7.9 were assigned to the protons on the BP moieties in the middle of the main chain of BPSH 100 and BPS0, respectively (Fig. 4.3, 4.4). By comparing the integrations of the end group BP and the main chain BP, the number-average molecular weights of oligomers were determined. The determined molecular weights and measured intrinsic viscosities of the oligomers are summarized in Table 4.1. When a log-log plot between the intrinsic viscosities and the number-average molecular weights was made, it showed a linear relationship, confirming successful control of molecular weight for both hydrophilic and hydrophobic block series (Fig. 4.5).

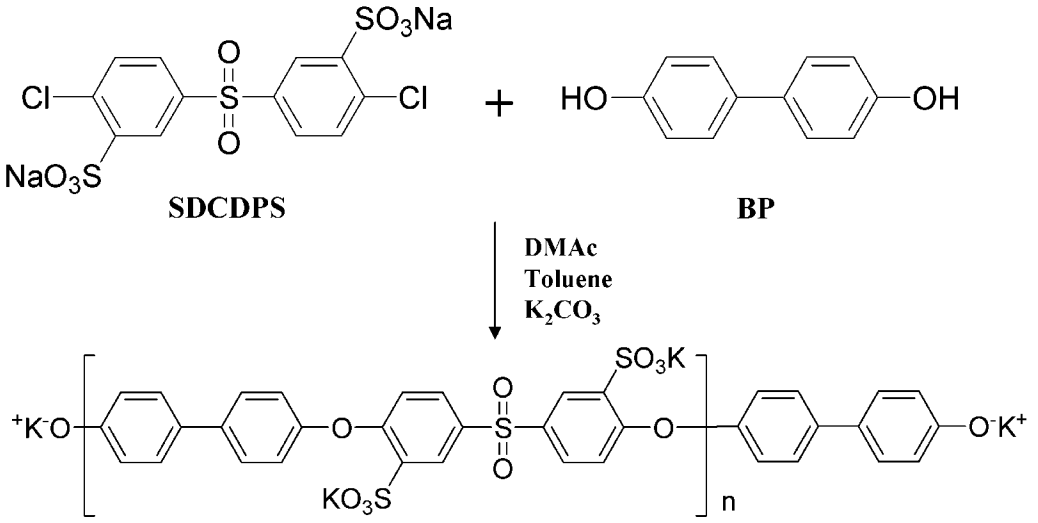

Figure 4. 1. Synthesis of a Fully Disulfonated Hydrophilic Oligomer with Phenoxide Telechelic Functionality.

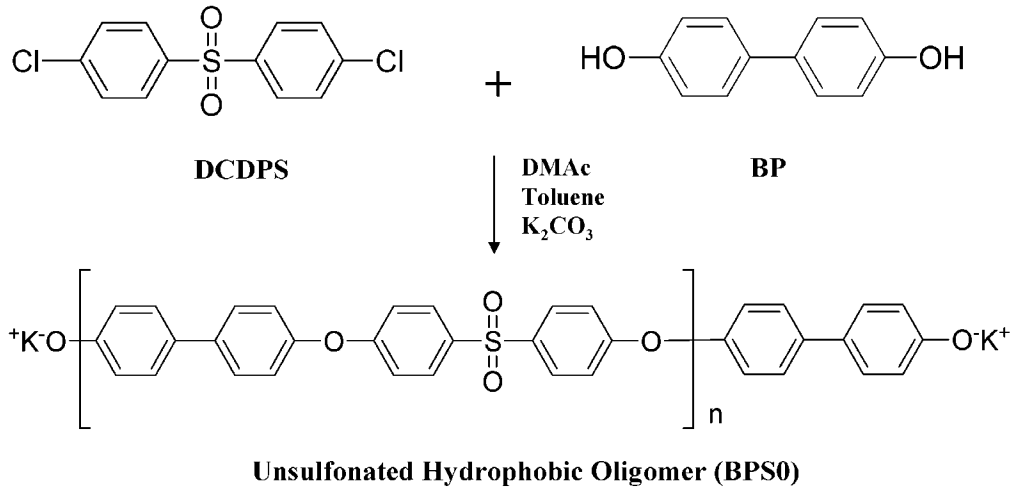

Figure 4. 2. Synthesis of an Unsulfonated Hydrophobic Oligomer with Phenoxide Telechelic Functionality.

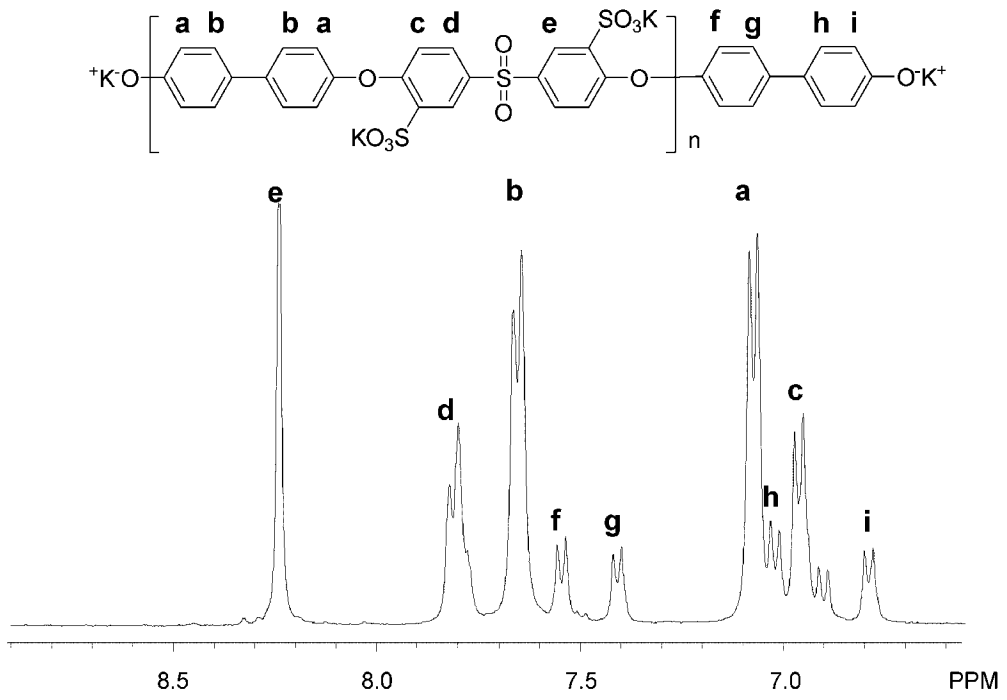

Figure 4. 3. ^{1}H NMR Spectrum of Phenoxide Terminated BPSH100 Hydrophilic Oligomer.

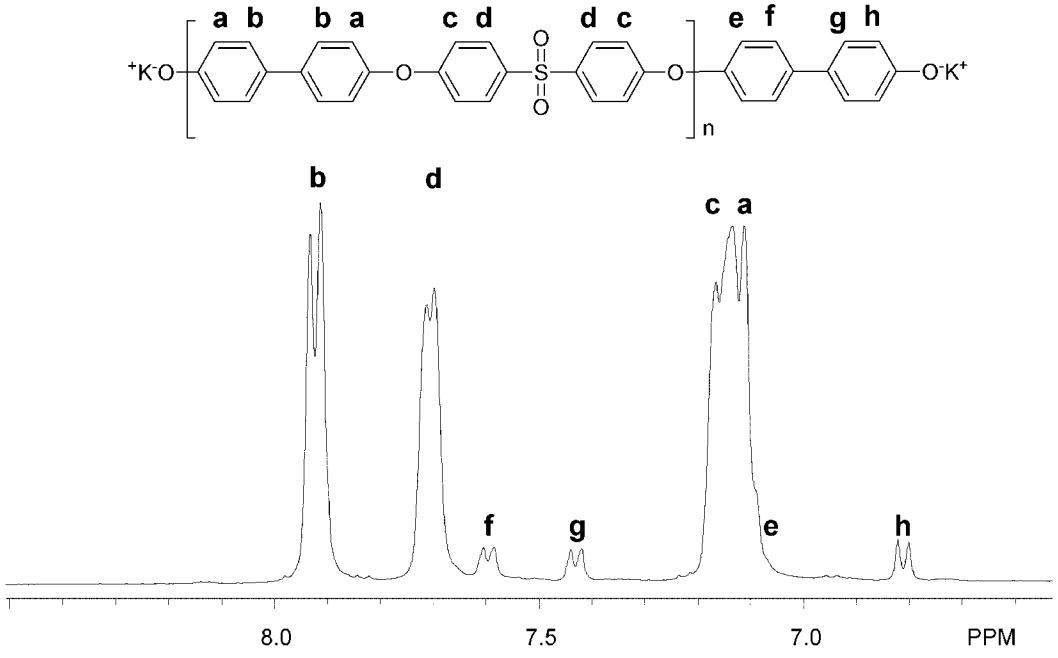

Figure 4. 4. ^{1}H NMR Spectrum of Phenoxide Terminated BPS0 Hydrophobic Oligomer.

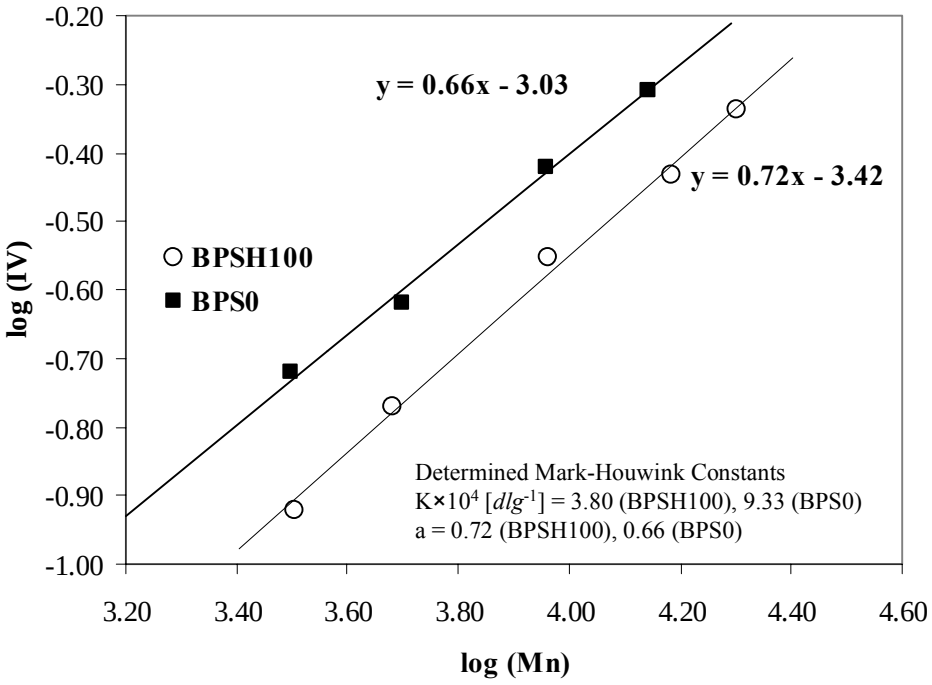

Figure 4. 5. Double Logarithmic Plot of [η] versus M_n of Hydrophilic (BPSH100) and Hydrophobic (BPS0) Oligomers. Intrinsic Viscosity was Measured in NMP with 0.05M LiBr at 25 ºC.

Table 4. 1. Characterization of Hydrophilic and Hydrophobic Telechelic Oligomers.

Target M_n (g mol^{-1})	Hydrophilic Blocks		Hydrophobic Blocks	
	M_n (g mol^{-1})[a]	IV (dL g^{-1})[b]	M_n (g mol^{-1})[a]	IV (dL g^{-1})[b]
3,000	3,190	0.12	3,160	0.19
5,000	4,790	0.17	5,020	0.24
10,000	9,180	0.28	9,130	0.38
15,000	15,290	0.37	13,900	0.49
20,000	20,000	0.46	-	-

[a] Determined by ^{1}H NMR.
[b] In NMP with 0.05 M LiBr at 25 ºC.

4.4.2. End-capping of the Hydrophobic Oligomers

Since both the BPSH100 and BPS0 oligomers have the same telechelic functionality (e.g., phenoxide end group), a modification of one of the oligomers is necessary to facilitate a coupling reaction for producing multiblock copolymers. In the research, BPS0 hydrophobic blocks were end-capped with HFB or DFBP to produce fluorine terminated end group functionality (Fig.4.6). The amounts of the end-capping reagents used in the reaction were a 200% molar excess. Due to the high reactivity of DFBP and HFB, the end-capping reactions were completed in 12 h under mild conditions. The end-capping reaction temperatures were 105 and 80 °C for DFBP and HFB, respectively. To prevent a loss of low-temperature boiling HFB (e.g., 80 °C) during the reaction, the temperature was chosen not to exceed its boiling temperature without a nitrogen purge. On the ^{1}H NMR spectra of the end-capped oligomers, the disappearance of the phenoxide bearing BP peaks at 6.80 , 7.40, and 7.60 ppm confirmed that all of the phenoxide groups reacted with the end-capping reagents (Fig. 4.7). Although the disappearance of the end group peaks on the NMR spectra is an evidence of the end-capping reaction, there is still possibility of inter-oligomer coupling between the BPS0 oligomers since DFBP and HFB are multifunctional. If there was a significant degree of the inter-oligomer coupling, the intrinsic viscosities after end-capping should be much higher than the initial values. This possibility was excluded by comparing the intrinsic viscosities of BPS0 oligomers before and after the end-capping reaction. Table 4.2 shows the intrinsic viscosity change before and after the end-capping reaction. Slight increases in the intrinsic viscosity were observed for the end-capped BPS0. However, these increases are not due to the inter-oligomer coupling reaction but the chain length extension by the end-capping reagents. This conclusion was also confirmed by

conducting the end-capping reaction with various amounts of end-capping reagents (Fig 4.8). Even with a 400% molar excess of the end-capping agents, slight increases in intrinsic viscosity were observed, but no further increases were observed until 200% molar excess was used. Then, the increases were significantly enlarged at a molar excess of less than 100% due to the inter-oligomer coupling reactions. Therefore, a molar excess of 200% is sufficient for preventing inter-oligomer coupling.

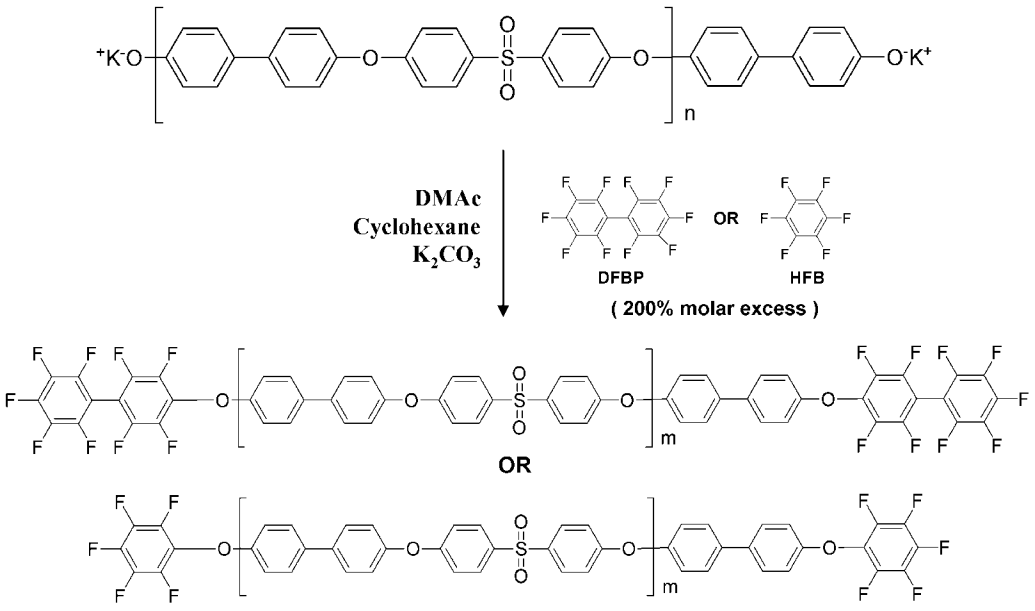

Figure 4. 6. End-capping of BPS0 Hydrophobic Oligomer with DFBP or HFB.

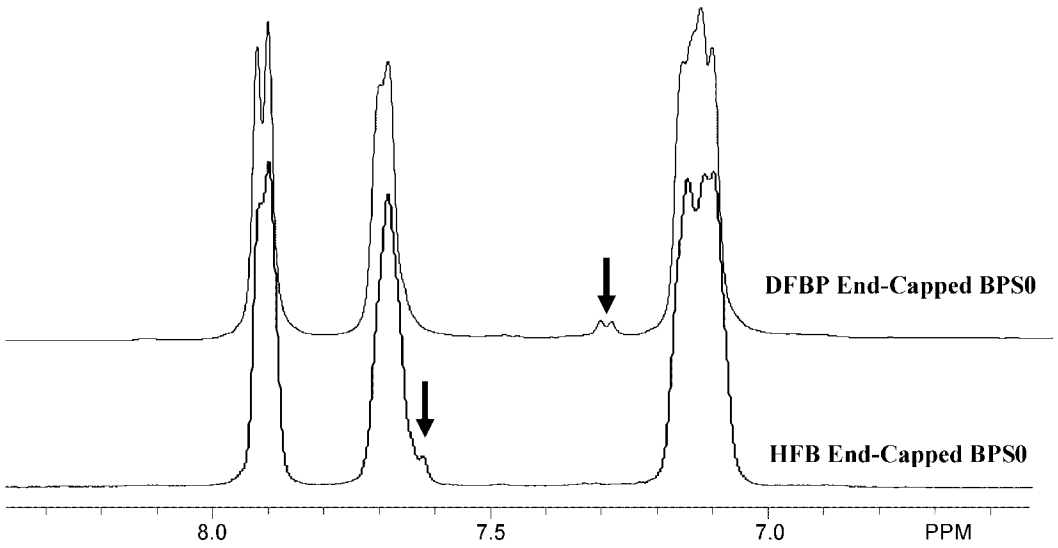

Figure 4. 7. ^{1}H NMR Spectra of BPSH and HFB End-capped BPS0 Hydrophobic Oligomers. Black Arrows Indicate the Peaks from the End-capped BP Moieties.

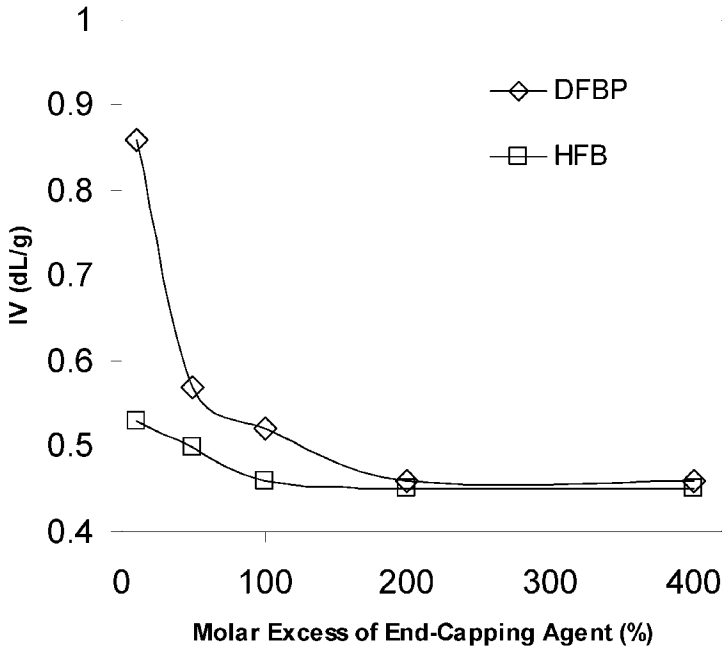

Figure 4. 8. Changes in Intrinsic Viscosity of the End-capped BPS0 Hydrophobic Oligomer as a Function of the Molar Excess of End-capping Reagent. The Initial Intrinsic Viscosity of the Oligomer was 0.41 dL/g.

Table 4. 2. Intrinsic Viscosities of BPS0 Hydrophilic Blocks Before and After End-capping.

M_n[a] (g mol^{-1})	Initial IV (dL g^{-1})[b]	IV after end-capping (dL g^{-1})[b]	
		DFBP	HFB
3,160	0.19	0.23	0.22
5,020	0.24	0.29	0.26
9,130	0.38	0.44	0.39
13,900	0.49	0.56	0.50

[a] Determined by ^{1}H NMR.

[b] In NMP with 0.05 M LiBr at 25 ºC.

4.4.3. Synthesis of BPSH-BPS Multiblock Copolymers

Two series of multiblock copolymers were synthesized by a coupling reaction between phenoxide terminated BPSH100 oligomers and DFBP or HFB end-capped BPS0 oligomers (Fig. 4.9). Hereafter, an acronym of the multiblock copolymer BPSHx-BPSy will be used where the BPSH and BPS imply the used BPSH100 and BPS0, while x and y denote the molecular weight of the reacted oligomers, respectively. The coupling reactions were conducted between the fluorine on the hydrophobic oligomers and the phenoxide end groups on the hydrophilic oligomers. The disappearance of the phenoxide end group peaks from the hydrophilic oligomer confirmed that the coupling reaction was successful (Fig. 4.10). As we hypothesized earlier, the low temperature of the coupling reaction minimized the ether-ether chain exchange reaction as confirmed by the ^{13}C NMR spectra. Figure 4.11 is a comparison of the ^{13}C NMR of the BPSH35 random copolymer and BPSH10-BPS10 multiblock copolymer. As can be seen, each peak from the random copolymer shows multiplet, suggesting a random sequence of sulfonated moieties on the

main chain. On the other hand, the multiblock copolymer showed sharp narrow peaks, explaining the ordered sequences in the copolymer and confirming the prevention of randomization during the reaction.

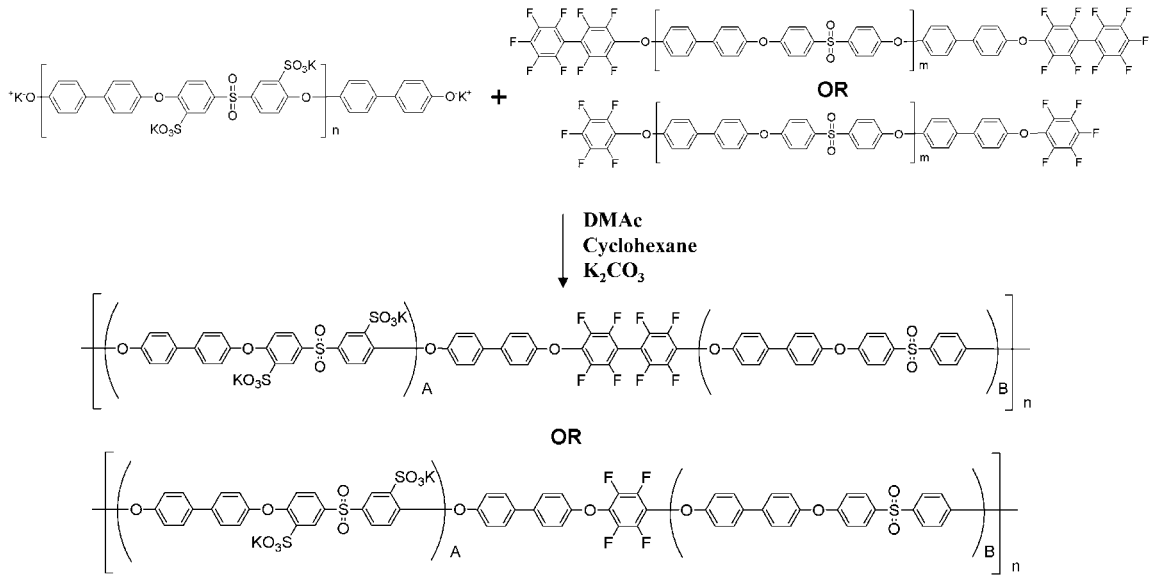

Figure 4. 9. Synthesis of Segmented Sulfonated Multiblock Copolymers (BPSH-BPS) with Different Linkage Groups.

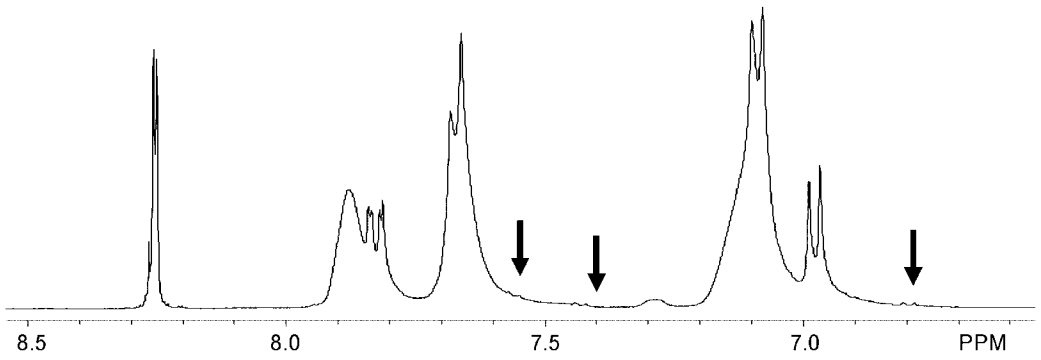

Figure 4. 10. ^{1}H NMR Spectrum of BPSH5-BPS5 with DFBP Linkage. Black Arrows Indicate the Disappearance of the End Groups on the Hydrophilic Blocks after the Coupling Reaction with Fluorine-terminated Hydrophobic Blocks.

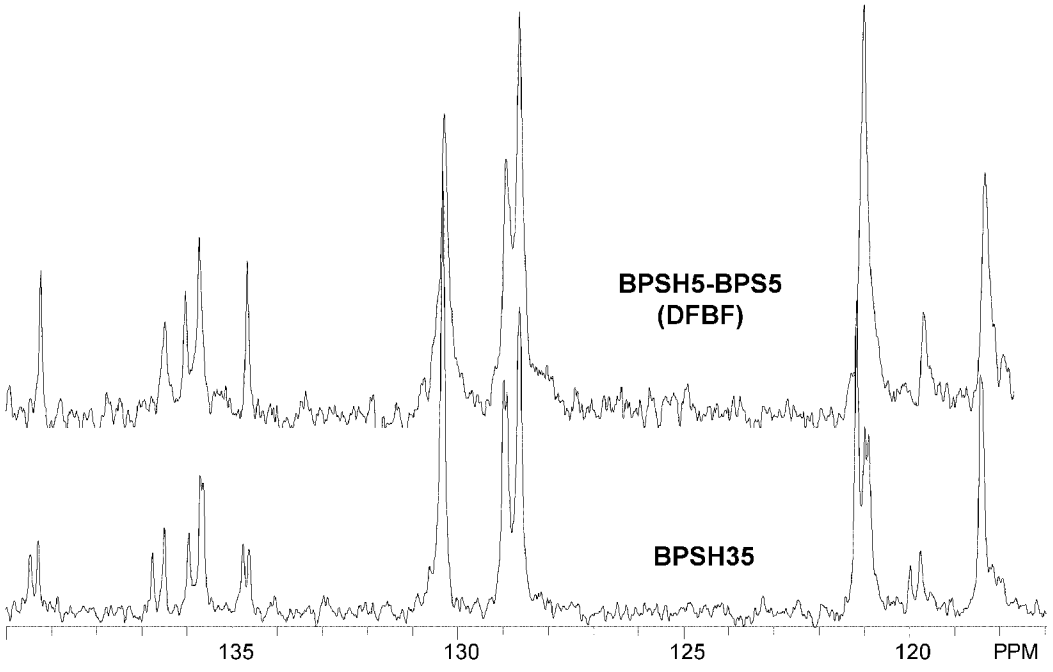

Figure 4. 11. ^{13}C NMR Spectra of BPSH35 Random Copolymer and BPSH5-BPS5 Multiblock Copolymer with DFBP Linkage.

4.4.4. Characterization of Membrane Properties of BPSH-BPS Multiblock Copolymers

One of the primary objectives in the preparation of this copolymer series was to keep the IEC fixed by varying hydrophilic and hydrophobic block lengths. To synthesize the fixed IEC copolymers, equal block lengths of hydrophilic hydrophobic blocks were used with 1:1 stoicheometry (e.g., BPSH3-BPS3, BPSH5-BPS5 etc.). The other objective was to make higher IEC copolymers by using longer hydrophilic blocks than hydrophobic blocks with 1:1 stoichiometry (e.g., BPSH10-BPS5, BPSH15-BPS10 etc.). The developed copolymers and their fundamental properties are summarized in Table 4.3. BPSH 35 random copolymer was put in the table as a control. The determined IEC values by titration were close to the theoretical values. For the equal block length copolymers, the IEC values ranged from 1.28 to 1.40 meq/g and were slightly lower than BPSH35 random copolymer value of 1.50 meq/g. However, even with lower IECs, the proton conductivity values of the BPSH-BPS copolymers ranged from 0.065 to 0.120 S/cm, which are comparable or even higher than that of BPSH35. It is interesting to observe the effect of block length on the proton conductivity and water uptake. Multiblock copolymers based on hydrophilic and hydrophobic blocks are known to have an ability to form phase separated morphologies.[14, 19, 20, 22] It has been also reported that the degree of phase separation increases with increasing block lengths and that the developed phase separated morphologies enhances proton conductivity by forming a well connected hydrophilic domain. This trend was confirmed in BPSH-BPS copolymers with equal block lengths. For example, with DFBP linkage group, as the block length increases from 3 to 15k, the proton conductivities also increase from 0.065 to 0.120 S/cm. The water uptake of the multiblock copolymers revealed the similar trend of the proton

conductivities and increased with increasing block lengths with the equal block lengths. For higher IEC copolymers with unequal block lengths, their proton conductivities were exceptionally high and reached up to 0.160 S/cm with an IEC of 1.83 meq/g. Except for the higher water uptake and hydration number values which were observed in the HFB linked copolymers, no significant differences were noticed between DFBP and HFB linked systems. A systematic explanation of the relationship between IECs, water uptake and proton conductivity will be provided in a separate article.

Figure 4.12 shows the swelling ratios of BPSH-BPS with the DFBP linkage group. The x,y represent the in-plane swelling and z represents the through-plane swelling. All multiblock copolymers showed anisotropic swelling behaviors in comparison to BPSH 35 and Nafion (NRE211). Although all the multiblock copolymers showed similar in-plane swelling, the through-plane swelling increased along with block length. The increase in water uptake and through-plane swelling with increasing block length may suggest the formation of ordered hydrophilic domains within the copolymer. Also the in plane swelling measurements for the higher block length materials were lower than NRE211. In-plane swelling is considered to be an important property for addressing durability under low relative humidity cycling operation.

Thermal and oxidative stabilities of the copolymers in their acid form were investigated by TGA (Fig. 4.13). All films displayed a two-step degradation profile. The initial weight loss was observed at 270 ºC and was assigned to the decomposition of the sulfonic acid groups on the BPSH100 block. The second decomposition, which started at 500 ºC, was attributed to main-chain polymer degradation. For BPSH3-BPS3 and BPSH5-BPS5 which have relatively short block lengths, their initial 5% weight loss

temperatures ranged from 300 to 313 °C and were similar to the 5% weight loss temperature 313 °C of the BPSH 35 random copolymer. However, BPSH10-BPS10 and BPSH15-BPS15 showed much higher temperatures ranged from 357 to 367 °C. This might be another block length effect on the thermal stability of the copolymers.

In this study, the various properties of BPSH-BPS copolymers using both DFBP and HFB linkage groups have been characterized. Assuming that two copolymers, which feature the same hydrophilic and hydrophobic blocks but with different linkage groups, do not have significantly different properties, HFB is the preferred linkage group due to its commercial availability and cost. According to the Chemical Abstracts Service (CAS) database, only HFB is available in a kilogram-scale quantity at a tenth of the cost of DFBP. When we consider that the molecular weight of DFBP is almost twice that of HFB, the molar cost of HFB is far more affordable.

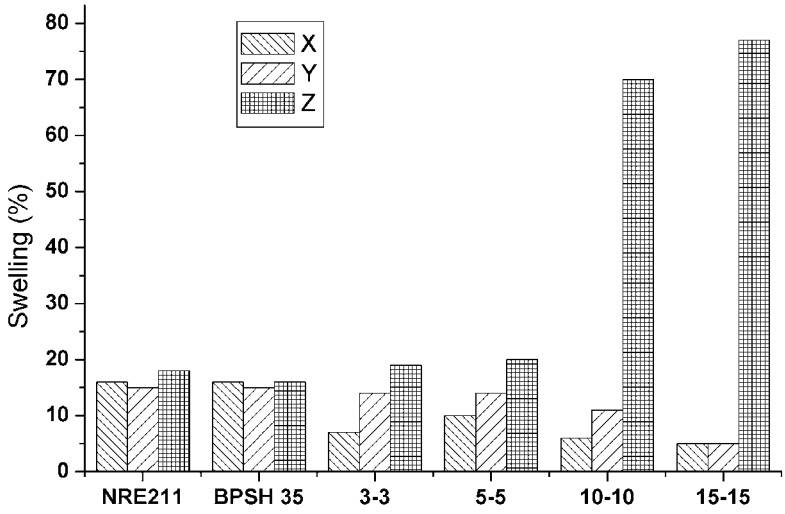

Figure 4. 12. Comparison of Swelling Ratios of Random Copolymer and BPSH-BPS Multiblock Copolymers with DFBP Linkage.

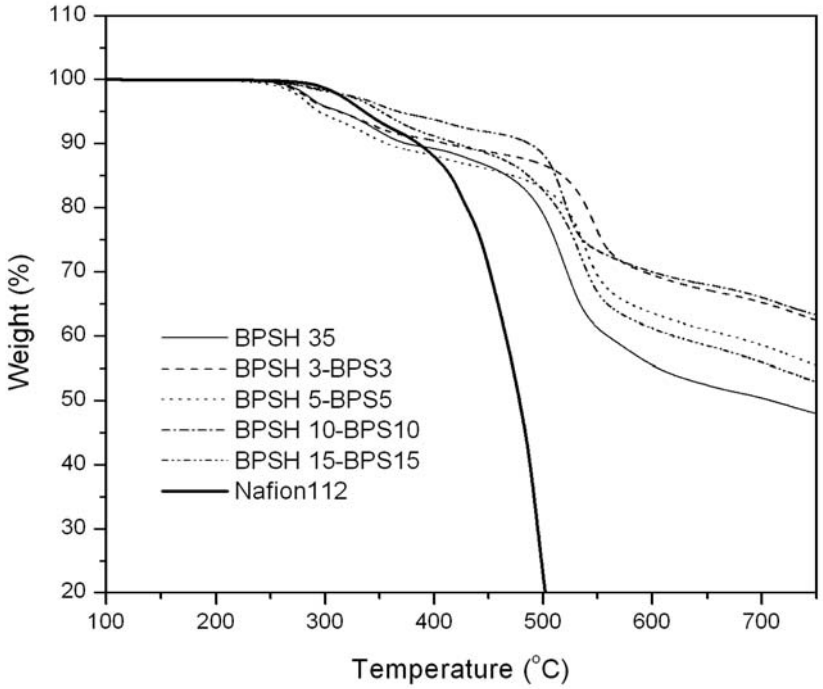

Figure 4. 13. TGA Thermograms of BPSH35, Nafion112 and BPSH-BPS Multiblock Copolymers with Different Block Lengths.

Table 4. 3. Properties of BPSH–BPS Multiblock Copolymers in the Sulfonic Acid Form.

Copolymers	Linkage	Calculated IEC (meq g^{-1})	Experimental IEC (meq g^{-1})[a]	Intrinsic Viscosity (dL g^{-1})[b]	Water Uptake (%)	Conductivity (S cm^{-1})[c]	Hydration Number (λ)
Nafion 112	-	-	0.90	-	25	0.090	15.0
BPSH 35	-	1.53	1.50	0.70	36	0.070	13.3
BPSH3 – BPS3	DFBP	1.42	1.33	0.78	30	0.065	12.5
BPSH5 – BPS5	DFBP	1.46	1.39	1.01	33	0.088	13.2
BPSH10 – BPS10	DFBP	1.57	1.28	0.68	60	0.095	25.6
BPSH15 – BPS15	DFBP	1.67	1.33	0.94	74	0.120	30.9
BPSH10 – BPS5	DFBP	1.97	1.83	0.94	100	0.160	30.3
BPSH15 – BPS10	DFBP	1.86	1.71	0.97	90	0.140	29.2
BPSH20 – BPS15	DFBP	1.79	1.71	1.12	70	0.120	22.7
BPSH5 – BPS5	HFB	1.55	1.30	0.62	52	0.090	22.2
BPSH10 – BPS10	HFB	1.57	1.38	0.76	79	0.100	31.8
BPSH15 – BPS15	HFB	1.66	1.40	0.94	79	0.090	31.3
BPSH10 – BPS5	HFB	2.08	2.06	1.01	158	0.120	43.1
BPSH15 – BPS10	HFB	1.98	1.83	0.85	139	0.120	42.2
BPSH20 – BPS15	HFB	1.88	1.91	0.85	107	0.140	31.1

[a] Determined by titration with NaOH.
[b] In NMP with 0.05 M LiBr at 25 ºC.
[c] Measured in deionized water at 30 ºC.

4.5. Conclusions

Hydrophilic-hydrophobic multiblock copolymers based on poly(arylene ether sulfone) were developed and characterized. The multiblock copolymers were synthesized utilizing highly reactive DFBP and HFB as the linkage groups to lower the coupling reaction temperatures. The mild reaction conditions prevented possible ether-ether exchange reactions which can randomize the hydrophilic-hydrophobic sequences. The multiblock copolymers showed ordered sequences which were confirmed by ^{13}C NMR. Transparent and ductile membranes were prepared from NMP by solvent casting. Their proton conductivities and water uptake values were influenced by block lengths at similar IEC values. As the block length increased, the proton conductivity and water uptake increased. The proton conductivities of the multiblock copolymers were comparable or even higher than those of BPSH random copolymers with similar IECs which supports the existence of well connected hydrophilic domains in the system.

Acknowledgments:

The authors thank the Department of Energy (DE-FG36-06G016038) and the Nissan Motor Co. for its support of this research.

4.6. References

1. de Bruijn, Frank. The current status of fuel cell technology for mobile and stationary applications. *Green Chemistry* **2005,** 7, (3), 132-150.
2. Hickner, Michael A.; Ghassemi, Hossein; Kim, Yu Seung; Einsla, Brian R.; McGrath, James E. Alternative Polymer Systems for Proton Exchange Membranes (PEMs). *Chemical Reviews (Washington, DC, United States)* **2004,** 104, (10), 4587-4611.
3. Banerjee, Shoibal; Curtin, Dennis E. Nafion perfluorinated membranes in fuel cells. *Journal of Fluorine Chemistry* **2004,** 125, (8), 1211-1216.
4. Mauritz, Kenneth A.; Moore, Robert B. State of understanding of Nafion. *Chemical Reviews (Washington, DC, United States)* **2004,** 104, (10), 4535-4585.
5. Kim, Yu Seung; Dong, Limin; Hickner, Michael A.; Glass, Thomas E.; Webb, Vernon; McGrath, James E. State of Water in Disulfonated Poly(arylene ether sulfone) Copolymers and a Perfluorosulfonic Acid Copolymer (Nafion) and Its Effect on Physical and Electrochemical Properties. *Macromolecules* **2003,** 36, (17), 6281-6285.
6. Savadogo, O. Emerging membranes for electrochemical systems Part II. High temperature composite membranes for polymer electrolyte fuel cell (PEFC) applications. *Journal of Power Sources* **2004,** 127, (1-2), 135-161.
7. Bahar, B.; Cavalca, C.; Cleghorn, S.; Kolde, J.; Lane, D.; Murthy, M.; Rusch, G. Effective selection and use of advanced membrane electrode power assemblies. *Journal of New Materials for Electrochemical Systems* **1999,** 2, (3), 179-182.
8. Wang, Sheng; McGrath, J. E. Synthesis of poly(arylene ether)s. *Synthetic Methods in Step-Growth Polymers* **2003**, 327-374.
9. Rose, J. B. Preparation and properties of poly(arylene ether sulfones). *Polymer* **1974,** 15, (7), 456-465.
10. Wang, Feng; Hickner, Michael; Ji, Qing; Harrison, William; Mecham, Jeffrey; Zawodzinski, Thomas A.; McGrath, James E. Synthesis of highly sulfonated poly(arylene ether sulfone) random (statistical) copolymers via direct polymerization. *Macromolecular Symposia* **2001,** 175, (Polymerization Processes and Polymer Materials II), 387-395.
11. Kim, Yu Seung; Hickner, Michael A.; Dong, Limin; Pivovar, Bryan S.; McGrath, James E. Sulfonated poly(arylene ether sulfone) copolymer proton exchange membranes: composition and morphology effects on the methanol permeability. *Journal of Membrane Science* **2004,** 243, (1-2), 317-326.
12. Harrison, W. L.; Hickner, M. A.; Kim, Y. S.; McGrath, J. E. Poly(arylene ether sulfone) copolymers and related systems from disulfonated monomer building blocks: synthesis, characterization, and performance - a topical review. *Fuel Cells (Weinheim, Germany)* **2005,** 5, (2), 201-212.
13. Kim, Yu Seung; Wang, Feng; Hickner, Michael; McCartney, Stephan; Hong, Young Taik; Harrison, William; Zawodzinski, Thomas A.; McGrath, James E. Effect of acidification treatment and morphological stability of sulfonated poly(arylene ether sulfone) copolymer proton-exchange membranes for fuel-cell

use above 100 Deg. *Journal of Polymer Science, Part B: Polymer Physics* **2003,** 41, (22), 2816-2828.

14. Wang, Hang; Badami, Anand S.; Roy, Abhishek; McGrath, James E. Multiblock copolymers of poly(2,5-benzophenone) and disulfonated poly(arylene ether sulfone) for proton-exchange membranes. I. Synthesis and characterization. *Journal of Polymer Science, Part A: Polymer Chemistry* **2006,** 45, (2), 284-294.
15. Ghassemi, Hossein; Ndip, Grace; McGrath, James E. New multiblock copolymers of sulfonated poly(4'-phenyl-2,5-benzophenone) and poly(arylene ether sulfone) for proton exchange membranes. II. *Polymer* **2004,** 45, (17), 5855-5862.
16. Yu, Xiang; Roy, Abhishek; Dunn, Stuart; Yang, Juan; McGrath, James E. Synthesis and characterization of sulfonated-fluorinated, hydrophilic-hydrophobic multiblock copolymers for proton exchange membranes. *Macromolecular Symposia* **2006,** 245/246, (World Polymer Congress--MACRO 2006), 439-449.
17. Lee, Hae-Seung; Roy, Abhishek; Badami, Anand S.; McGrath, James E. Synthesis and characterization of sulfonated poly(arylene ether) polyimide multiblock copolymers for proton exchange membranes. *Macromolecular Research* **2007,** 15, (2), 160-166.
18. Li, Yanxiang; Roy, Abhishek; Badami, Anand S.; Hill, Melinda; Yang, Juan; Dunn, Stuart; McGrath, James E. Synthesis and characterization of partially fluorinated hydrophobic-hydrophilic multiblock copolymers containing sulfonate groups for proton exchange membrane. *Journal of Power Sources* **2007,** 172, (1), 30-38.
19. Lee, Hae-Seung; Badami, Anand S.; Roy, Abhishek; McGrath, James E. Segmented Sulfonated Poly(arylene ether sulfone)-b-Polyimide Copolymers for Proton Exchange Membrane Fuel Cells. I. Copolymer Synthesis and Fundamental Properties. *Journal of Polymer Science, Part A: Polymer Chemistry* **2007,** 45, (21), 4879-4890.
20. Roy, Abhishek; Hickner, Michael A.; Yu, Xiang; Li, Yanxiang; Glass, Thomas E.; McGrath, James E. Influence of chemical composition and sequence length on the transport properties of proton exchange membranes. *Journal of Polymer Science, Part B: Polymer Physics* **2006,** 44, (16), 2226-2239.
21. Sankir, M.; Bhanu, V. A.; Harrison, W. L.; Ghassemi, H.; Wiles, K. B.; Glass, T. E.; Brink, A. E.; Brink, M. H.; McGrath, J. E. Synthesis and characterization of 3,3'-disulfonated-4,4'-dichlorodiphenyl sulfone (SDCDPS) monomer for proton exchange membranes (PEM) in fuel cell applications. *Journal of Applied Polymer Science* **2006,** 100, (6), 4595-4602.
22. Kim, Yu Seung; Einsla, Melinda L. ; Hawley, Marilyn; Pivovar, Bryan S.; Lee, Hae-Seung; Roy, Abhishek; McGrath, James E. Multiblock Copolymers for Low Relative Humidity Fuel Cell Operations *ECS Transactions* **2007,** 11, (1), 49.

CHAPTER 5

Synthesis and Characterization of Poly(arylene ether sulfone)-*b*-polybenzimidazole Copolymers for High Temperature Low Humidity Proton Exchange Membrane Fuel Cells

Hae-Seung Lee, Abhishek Roy, Ozma Lane and James E. McGrath*

Chemistry Department, Macromolecules and Interfaces Institute (MII), and Institute for Critical Technology and Applied Sciences (ICTAS)
Virginia Polytechnic Institute and State University, Blacksburg, Virginia 24061

*Correspondence to: James E. McGrath
(Email: jmcgrath@vt.edu, Phone: 540-231-5976, Fax: 540-231-8517)

Taken from *Polymer*, 49 (2008), 5387-5396

5.1. Abstract

Multiblock copolymers based on poly(arylene ether sulfone) and polybenzimidazole (PBI) with different block lengths were synthesized by coupling carboxyl functional aromatic poly(arylene ethers) with ortho diamino functional PBI oligomers in NMP, selectively doped with phosphoric acid, and evaluated as a high temperature proton exchange membrane (PEM). Transparent and ductile membranes were produced by solvent casting from DMAc. From dynamic mechanical analysis (DMA), the neat copolymer membranes showed two distinct glass transition temperatures which implies the existence of a nanostructured morphology in the membranes. These two nanophases became more distinct with increasing block length. The membranes were immersed in various concentrations of phosphoric acid solution to produce the proton conductivity. The doping level increased with increasing concentration of the acid solution and a maximum doping level of 12 was achieved when 14.6 M phosphoric acid solution was used. The acid doped membranes showed significantly reduced swelling behavior compared to a control conventional phosphoric acid doped PBI homopolymer system which appears to be related to the selective sorption into the PBI phase. The ionic conductivity of the doped samples at 200 °C afforded up to 47 mS/cm without external humidification. The protonic conductivity was found to increase with block length at a given doping level, reflecting the sharpness of the nanophase separation and the effect was even more prominent at a low doping level of 6-7. It is suggested that the phosphoric acid doped multiblock copolymer system would be a strong candidate for high temperature and low relative humidity PEM applications such as those required for stationary power.

Keywords: multiblock copolymer; poly(arylene ether sulfone); polybenzimidazole; proton exchange membrane

5.2. Introduction

The fuel cell is well known to be an energy conversion device which transforms chemical energy directly into electrical energy.[1] Its high energy efficiency and environmentally friendly nature have attracted much attention, making the fuel cell an alternative to conventional energy conversion devices such as internal engines. Among several types of fuel cells, polymer electrolyte membrane fuel cells (PEMFCs) have been most intensively explored for the past two decades due to their promise for mobile, automotive, and stationary applications.[2] The state-of-the-art PEMs are perfluorinated sulfonic acid containing ionomers (PFSAs) which have demonstrated excellent performance including high proton conductivity and excellent chemical stability.[3, 4] However, their mechanical and electrochemical properties deteriorate [5] at higher operating temperatures and low relative humidity (RH) conditions since the proton transport of sulfonic acid based PEMs strongly depends on water in the membranes. It has been proposed that the proton conduction of the sulfonic acid containing PEMs is governed by a vehicle mechanism, where water acts as the vehicle for proton transport.[6] Hence at high temperature and at very low RH, the proton transport is restricted due to insufficient water. Consequently, various approaches have been made to develop PEMs which are suitable for high temperature applications under low RH conditions.

One of the successful high temperature, low RH PEMs is well recognized to be an inorganic acid doped polymer membrane system.[7-10] The inorganic acids act as ion conducting materials while polymers, which typically possess basic moieties which can immobilize the acid. Among various inorganic acids, phosphoric acid (H_3PO_4) has been widely studied due to its excellent thermal stability, low vapor pressure, and high ionic conductivity even under anhydrous conditions.[11-15] For the matrix polymer, the

polybenzimidazole (PBI) family, especially poly 2,2'-*m*-(phenylene)-5,5'-bibenzimidazole, has been intensively studied due to the ease of synthesis and commercial availability.[16, 17] Phosphoric acid doped PBI membranes can be easily fabricated by immersing solvent cast PBI membranes in phosphoric acid solution. The doping level which can be defined as the number of moles of phosphoric acid per one repeat unit of PBI is controlled by using different concentrations of the doping solution.[18] More recently, Benicewicz *et al*. have elegantly shown one can directly polymerize and cast from polyphosphoric acid (PPA). The controlled hydrolysis of the PPA in the film affords very large doping levels and excellent performance.[19]

In contrast to sulfonic acid based PEMs, the ion transport in phosphoric acid doped systems under anhydrous conditions is thought to follow a proton hopping or Grotthus mechanism.[20, 21] The mechanism is reported to depend strongly on acid doping level, water content and temperature. At low doping levels, the proton transport has been suggested to take place between the N-H sites of the polymer and phosphate anion. At higher doping levels, the presence of "free" acid facilitates the enhanced transport from the more rapid diffusion of additional phosphate anions.[22] In the presence of water, ions such as H_3O^+ also can be involved as an additional proton carrier. At high temperatures in the condensed phosphoric acid state, ion transport involving protonic diffusion via the vehicle mechanism is also proposed.[23]

Generally, the ionic conductivity of phosphoric acid doped PBI homopolymers increases along with doping level and temperature. However, doping levels higher than 5 may not be desirable in current commercial PBI due to high swelling and deterioration of mechanical properties.[24] Although several approaches have been attempted to address

this problem, such as crosslinking of the matrix polymer,[25, 26] and introducing inorganic fillers to reinforce the membrane,[27] highly doped membranes still suffer from mechanical property deterioration and a perceived and perhaps actual problem with electrode performance.

Similar trade-offs between proton conductivity and dimensional stability have been observed in sulfonic acid containing PEM systems. Although an increased degree of sulfonation in the system enhances proton conductivity, beyond a certain concentration a percolated hydrophilic phase develops resulting in excessive water swelling, and a hydrogel which is impractical as a PEM.[28, 29] Recently, these problems have been successfully addressed by utilizing multiblock copolymers based on ion conducting hydrophilic blocks and mechanically robust hydrophobic blocks.[30-34] Once the block copolymers are cast into membranes, they can exhibit unique phase separated morphologies and each phase governs independent properties. The ionic groups of the hydrophilic blocks act as proton conducting sites while the nonionic hydrophobic component provides dimensional stability.

In this chapter, a series of multiblock copolymers was produced by a homogeneous coupling reaction in DMAc between highly reactive o-diamino functional PBI oligomers and carboxylic acid terminated poly(arylene ether sulfone) oligomers.[35] The latter was prepared by using m-hydroxybenzoic acid as an efficient end-capper during the nucleophilic step polymerization. The carboxylate formed is unreactive but the phenoxy anion is quite reactive with the activated aromatic halide. The PBI segments in the system facilitate ionic conduction by providing a selective site for absorption of H_3PO_4 while poly(arylene ether sulfone) segments are unaffected and maintain the

dimensional and mechanical stability. Ionic transport measurements on the copolymers have been investigated in the absence and presence of water as a function of doping level, temperature and morphology.

5.3. Experimental

5.3.1. Materials

N,N-Dimethylacetamide (DMAc), N-methyl-2-pyrrolidinone (NMP), and toluene were purchased from Aldrich and distilled from calcium hydride before use. Monomer grade 4,4'-dichlorodiphenyl sulfone (DCDPS) and 4,4'-biphenol (BP) were provided by Solvay Advanced Polymers and Eastman Chemical Company, respectively, and vacuum dried at 110 °C prior to use. Potassium carbonate, 3-hydroxybenzoic acid (99%) (3-HBA), isophthalic acid (99%), 3,3'-diaminobenzidine (99%) (DAB), phosphoric acid (85%) and polyphosphoric acid (115%) were purchased from Aldrich and used without further purification.

5.3.2. Synthesis of Controlled Molecular Weight Poly(arylene ether sulfone)s with Telechelic Benzoic Acid Functionality

Benzoic acid terminated poly(arylene ether sulfone) oligomers (BPS) with molecular weights of 5, 10, and 15 kg/mol were synthesized. An example of the synthesis of 5 kg/mol BPS is as follows: 10.6730 g (57.3 mmol) of BP, 17.9209 g (62.4 mmol) of DCDPS, 1.4061 g (10.2 mmol) of 3-HBA and 11.1900 g (81.0 mmol) of potassium carbonate were added to a three-necked 250-mL flask equipped with a condenser, a Dean Stark trap, a nitrogen inlet/outlet, and a mechanical stirrer. Distilled DMAc (120 mL) and toluene (60 mL) were added to the flask. The solution was allowed to reflux at 155 °C while the toluene azeotropically removed the water from the system. After 4 h, the toluene was completely removed from the system and the reaction temperature was increased to 180 ºC. The reaction was allowed to proceed for another 48 h. The resulting

viscous solution was filtered to remove the salts and coagulated in methanol. The telechelic benzoic acid functionality of the oligomer was recovered from its potassium salt form by stirring the coagulated polymer in 0.1 M aqueous sulfuric acid solution for 24 h. The polymer was dried at 110 °C *in vacuo* for at least 24 h.

5.3.3. Synthesis of Controlled Molecular Weight Diamine-terminated Polybenzimidazole

Diamine terminated polybenzimidazole blocks with molecular weight 5, 10, and 15 kg/mol were synthesized. A typical coupling reaction was performed as follows: 5.8977 g (35.5 mmol) of isophthalic acid and 8.0995 g (37.8 mmol) of DAB were mixed with 126 g of polyphosphoric acid in a three-necked 250-mL flask equipped with a nitrogen inlet/outlet and a mechanical stirrer. The mixture was heated at 200 ºC for 24 h. The resulting dark brown polymer solution was coagulated in deionized water and stirred for 24h. The telechelic oligomer was filtered and washed with deionized water several times. The residual acid in the polymer was neutralized with 1M NaOH solution. It was dried at 120 °C *in vacuo* for at least 24 h.

5.3.4. Synthesis of Poly(arylene ether sulfone)-*b*-Polybenzimidazole Multiblock Copolymers.

Multiblock copolymers were synthesized via a coupling reaction between the benzoic acid and o-diamino end groups on the poly(arylene ether sulfone) and polybenzimidazole oligomers, respectively. A typical coupling reaction was performed as follows: 3.0000 g (0.6 mmol) of poly(arylene ether sulfone) oligomer ($\overline{M_n}$ = 5 kg/mol), 3.0000 g (0.6

mmol) of highly reactive polybenzimidazole oligomer ($\overline{M_n}$ = 5 kg/mol) and 60 mL of NMP were added to a three-necked 100-mL flask equipped with a mechanical stirrer, and a nitrogen inlet/outlet. The reaction mixture was heated at 200 ºC and allowed to proceed for 48 h. The resulting dark brown viscous copolymer solution was precipitated in methanol and filtered. The polymer was dried at 120 °C *in vacuo* for at least 24 h.

5.3.5. Characterization of Copolymers

^{1}H NMR analyses were conducted on a Varian INOVA 400 MHz spectrometer with DMSO-d_6 or DMAc-d_9 to confirm the chemical structures of oligomers and copolymers. ^{1}H NMR spectroscopy was also used to determine copolymer compositions and number-average molecular weights of the oligomers via end-group analyses. Intrinsic viscosities were determined using NMP at 25 ºC using an Ubbelohde viscometer. Dynamic mechanical analysis was performed on a TA DMA 2980 using a thin film tension clamp in order to characterize the thermal properties of the multiblock copolymers. After heating to 220 °C to evaporate any remaining trace amounts of solvent, the samples were then equilibrated for 10 minutes at 0 °C under nitrogen and heated at a rate of 3 °C/min to 450 °C, using an oscillation of 1 Hz.

5.3.6. Film Casting and H_3PO_4 Doping

Multiblock copolymer membranes were prepared by solution casting from DMAc. The copolymers were dissolved in DMAc (10% w/v), filtered through 0.45 μm Teflon® syringe filters, and cast onto clean glass substrates. The solvent was evaporated under an infrared lamp for 48 h at 50-70 °C, resulting in transparent, tough, and flexible films.

The films were further dried *in vacuo* at 110 °C for 24 h to remove residual solvent. The H_3PO_4 doped membranes were prepared by immersing the cast membranes in a various concentrations (3-14.6M) of aqueous H_3PO_4 solution for 72 h at room temperature.

5.3.7. Determination of Doping Level, Water Uptake, and Swelling Ratio

The doping level and water uptake of the H_3PO_4 doped membranes were determined by weight comparisons between undoped, doped, and vacuum dried doped membranes. First, the DMAc cast membranes were dried at 150 °C *in vacuo* for 24 h and their weights (W_{dry}) were recorded. The dried membranes were then immersed in H_3PO_4 solutions. After 72 h, the membranes were taken out, wiped dry, and weighed (W_{wet}). Finally, the membranes were dried in a vacuum oven at 110 °C for 24 h and weighed (W_{acid}).

$$Weight\ Increase\ (\%) = \frac{W_{wet} - W_{dry}}{W_{dry}} \times 100$$

$$Water\ Uptake\ (\%) = \frac{W_{wet} - W_{acid}}{W_{dry}} \times 100$$

$$Doping\ Level = \frac{(W_{acid} - W_{dry})/MW_{PA}}{(W_{dry} \times F_{PBI})/MW_{PBI}} \times 100$$

where MW_{PA} and MW_{PBI} represent the molecular weight of phosphoric acid and repeat unit of PBI repeat unit, respectively. F_{PBI} is the fraction of PBI portion in the multiblock copolymer (e.g., % PBI composition divided by 100).

The swelling ratios of copolymers were determined as follows

$$Swelling\ Ratio\ (\%) = \frac{(l_{wet} - l_{dry})}{l_{dry}} \times 100$$

where l_{dry} and l_{wet} represents the length or thickness of dry and wet films, respectively.

5.3.8. Tensile Testing

Uniaxial load tests were performed using an Instron 5500R universal testing machine equipped with a 200 lb load cell at room temperature and 44-54% relative humidity (RH). Crosshead displacement speed was 5 mm/min and gauge lengths were set to 25 mm. A dogbone die was used to punch specimens 50 mm long with a minimum width of 4 mm. Prior to testing, specimens were dried under vacuum at 100 °C for at least 12 h and then equilibrated at 40% RH and 30 °C. All specimens were mounted in manually tightened grips. At least five replicates were tested for each membrane. Modulus values for each specimen were calculated based on the stress and elongation values for the specimen at the first data point at or above 2% elongation.

5.3.9. Determination of Ionic Conductivity

All conductivity measurements were made using a Solartron (1252A +1287) impedance/gain-phase analyzer over the frequency range of 10 Hz - 1 MHz. The conductivity of the membrane was determined from the geometry of the cell and resistance of the film which was taken at the frequency that produced the minimum imaginary response. For the temperature sweep experiments, the conductivity cells with the membranes were equilibrated at 100 ^{0} C for 4-5 h before the start of the experiment. This was done to remove the excess water from the membranes. In situ measurements

were taken as a function of increasing temperature with the cells equilibrated in a convection oven. Equilibration time at each temperature was kept fixed at 3 hours.

5.4. Results and Discussion

5.4.1. Synthesis of Poly(arylene ether sulfone) and Polybenzimidazole Oligomers

Carboxylic acid-terminated poly(arylene ether sulfone) oligomers (BPS) whose molecular weights range from 5 to 15 kg/mol were synthesized via step-growth polymerization of DCDPS, BP, and 3-HBA (Fig. 5.1). Telechelic benzoic acid functionality of the oligomers was achieved by utilizing 3-HBA as an end-capping agent as reported earlier.[35] Molecular weights of the oligomers were controlled by using stoichiometrically adjusted amounts of monomers and end-capping reagent. The number-average molecular weights of the BPS oligomers were determined by end group analysis of the ^{1}H NMR spectra. The peak at 7.61 ppm was assigned to one of the protons on the benzoic acid end group while the peak at 7.71 ppm was assigned to the protons on the phenyl ring next to the sulfone groups (Fig. 5.2). By comparing the integrations of both peaks, the number-average molecular weights of the BPS oligomers were determined (Table 5.1).

Table 5. 1. Characterization of BPS and PBI Telechelic Oligomers.

Target M_n (g mol^{-1})	BPS Oligomer		PBI Oligomer	
	M_n (g mol^{-1})[a]	IV (dL g^{-1})[b]	M_n (g mol^{-1})[a]	IV (dL g^{-1})[b]
5,000	5,400	0.22	5,400	0.58
10,000	9,800	0.38	11,700	1.23
15,000	14,700	0.55	16,100	1.64

[a] Determined by ^{1}H NMR end group analyses.

[b] In NMP at 25 ºC.

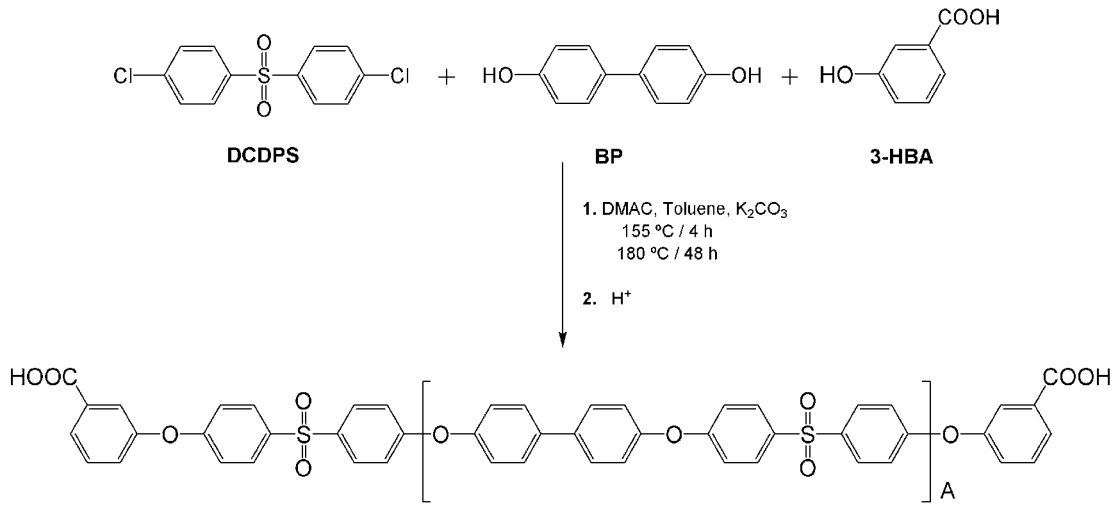

Figure 5. 1. Synthesis of a Benzoic Acid-terminated Poly(arylene ether sulfone) Oligomer.

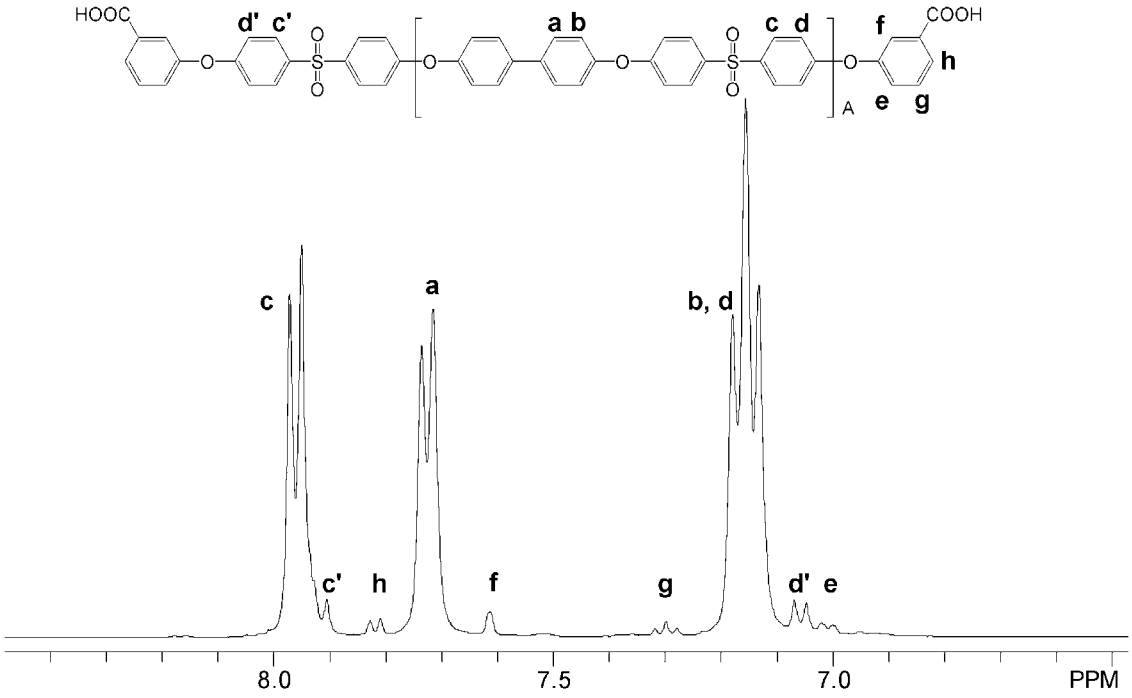

Figure 5. 2. ^{1}H NMR Spectrum of a Benzoic Acid-terminated Poly(arylene ether sulfone) Oligomer.

o-Diamino-terminated polybenzimidazole oligomers (PBI) with the same molecular weight of BPS oligomers were synthesized via step-growth polymerization in polyphosphoric acid (Fig. 5.3). The molecular weight and diamine end group functionality of the oligomers were controlled by offsetting monomer stoichiometry. The number-average molecular weight of each PBI oligomer was determined from the ^{1}H NMR spectrum. The peaks ranging from 6.5 to 7.0 ppm and from 12.8 to 13.5 were assigned to the protons on the o-diamino benzene moieties and the amine protons on benzimidazole moieties, respectively (Fig. 5.4). By comparing the integrals, number-average molecular weights were determined and are summarized in Table 5.1.

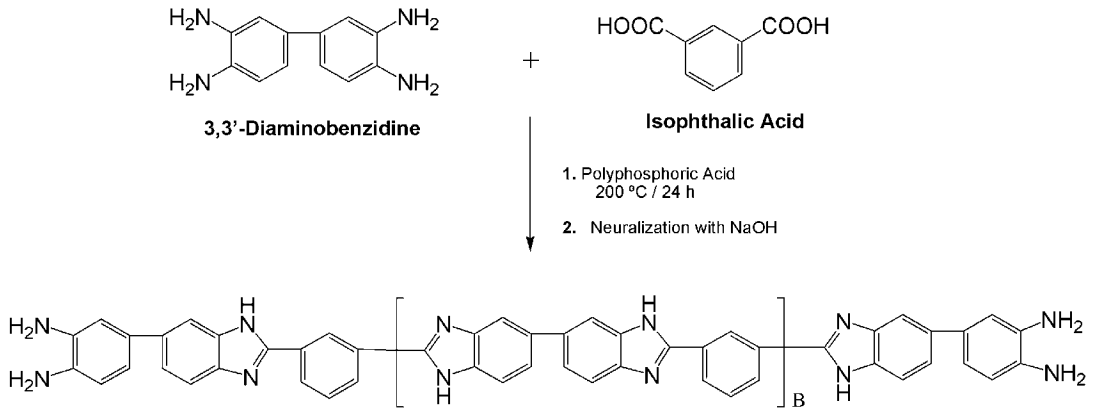

Figure 5. 3. Synthesis of a *o*-Diamino-terminated Polybenzimidazole Oligomer.

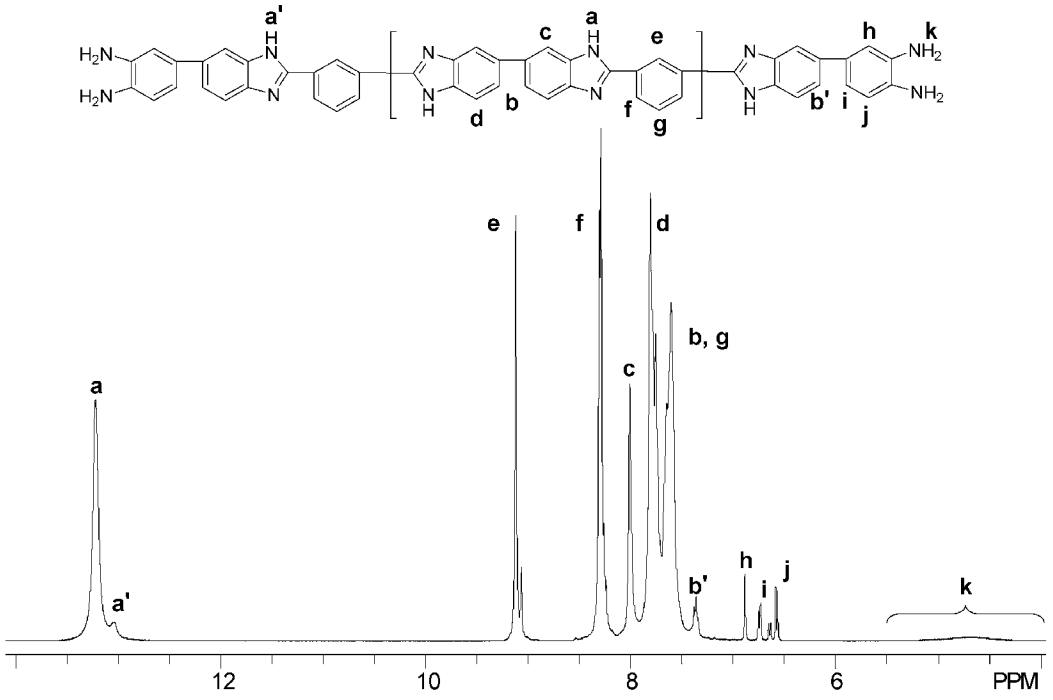

Figure 5. 4. ^{1}H NMR Spectrum of a Diamine-terminated Polyimide Hydrophobic Oligomer.

Intrinsic viscosities of both BPS and PBI oligomers were measured in NMP by using a Ubbelohde viscometer. As expected, increased viscosities were observed with increasing molecular weight. In addition, when the viscosities of the oligomers were plotted with the determined number-average molecular weights in a log-log scale, a linear relationship was observed for both BPS and PBI oligomers which confirmed the successful control of molecular weight for both block series (Fig. 5.5, 5.6).

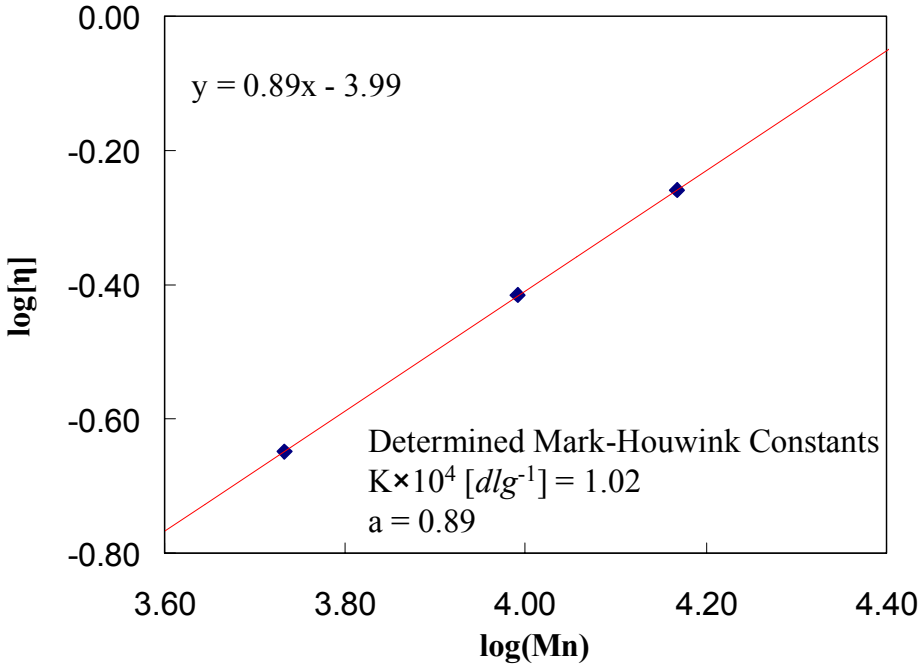

Figure 5. 5. Double Logarithmic Plot of [η] versus M_n of Poly(arylene ether sulfone) Oligomers. Intrinsic Viscosity was Measured in NMP at 25 ºC.

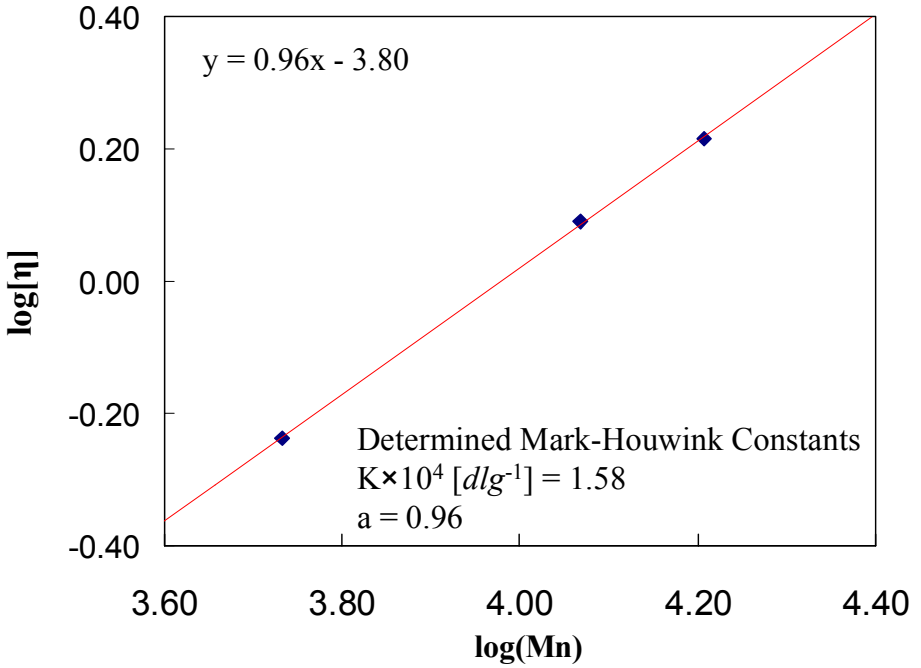

Figure 5. 6. Double Logarithmic Plot of [η] versus M_n of Polybenzimidazole Oligomers. Intrinsic Viscosity was Measured in NMP at 25 ºC.

5.4.2. Synthesis of BPS-PBI Multiblock Copolymers

The multiblock copolymers were synthesized by a coupling reaction between BPS and PBI oligomers of equal block length in NMP. The coupling reaction was achieved by forming benzimidazole moieties between benzoic acid and o-diamino end groups on the BPS and PBI oligomers, respectively (Fig. 5.7). For the coupling reaction, polyphosphoric acid was initially considered as a reaction solvent. However, poor solubility of BPS oligomers made the coupling reaction impossible in polyphosphoric acid. For this reason, the coupling reactions of BPS and PBI oligomers were performed in NMP, which dissolved both BPS and PBI oligomers. Since high molecular weight multiblock copolymers can be readily synthesized from several oligomers of sufficient length, NMP served as a good solvent to conduct the coupling reaction. The ^{1}H NMR spectrum of the BPS-PBI copolymer showed the disappearance of the end group peaks of both BPS and PBI oligomers, which confirmed that the block copolymerization was successful (Fig. 5.8). In addition, ^{13}C NMR experiments also showed the disappearance of the carbonyl carbon peak from the BPS oligomer after the coupling reaction.

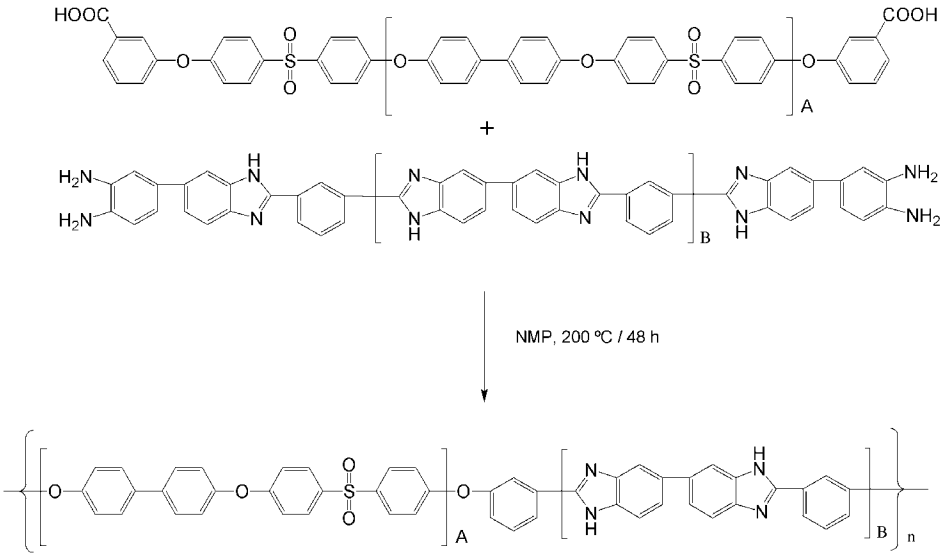

Figure 5. 7. Synthesis of a Poly(arylene ether sulfone)-*b*-polybenzimidazole (BPS-PBI) Copolymer.

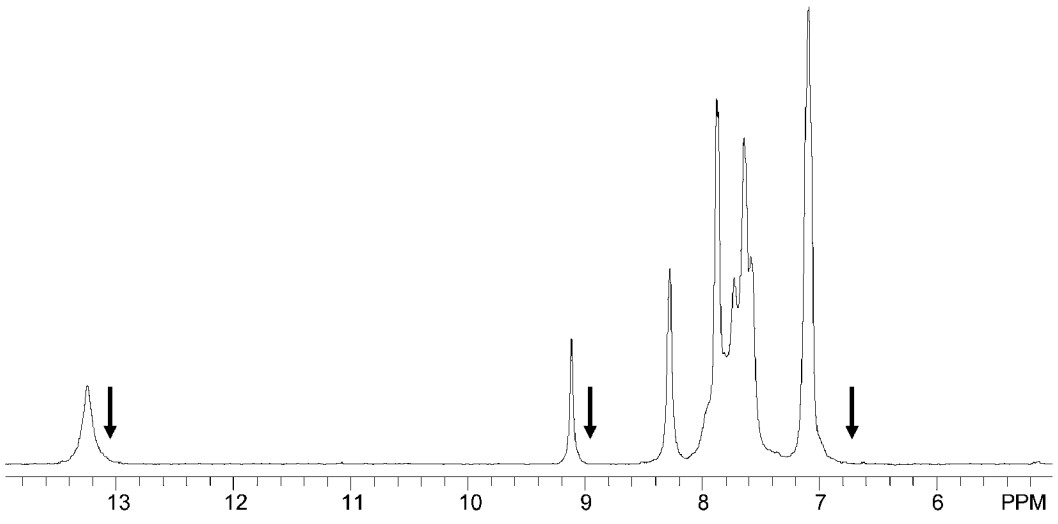

Figure 5. 8. ^{1}H NMR Spectrum of a BPS-PBI Multiblock Copolymer. Black Arrows Represent the Disappearance of the Diamine End Groups on the PBI Blocks after the Coupling Reaction with Benzoic Acid-terminated BPS Blocks.

5.4.3. Characterization of the BPSH-PBI Multiblock Copolymers

The chemical composition of the copolymers was calculated by comparing the peak integrations from each oligomer on ^{1}H NMR spectra. The determined chemical compositions of PBI in the copolymer varied from 45 to 47% , which were slightly lower than the feed value (e.g., 50%). The intrinsic viscosities of the copolymers ranged from 0.78 to 1.91 dL/g. (Table 5.2) All copolymers produced tough, ductile membranes when solvent cast from DMAc. DMA analysis showed that with increasing block length, the two glass transition peaks attributed to the separate BPS and PBI regimes became increasingly distinct (Fig. 5.9). While the glass transition of 360-375 ^{o}C for PBI remained constant, the glass transition for BPS shifted from 276 ^{o}C to 240 ^{o}C. This implies a lower level of a mixed-regime phase as higher block lengths allowed a greater degree of phase separation. The upper Tg from the E' drop seems a bit low, which may be a segment Mn issue, but the tan delta loss seems to be about where one would have expected.

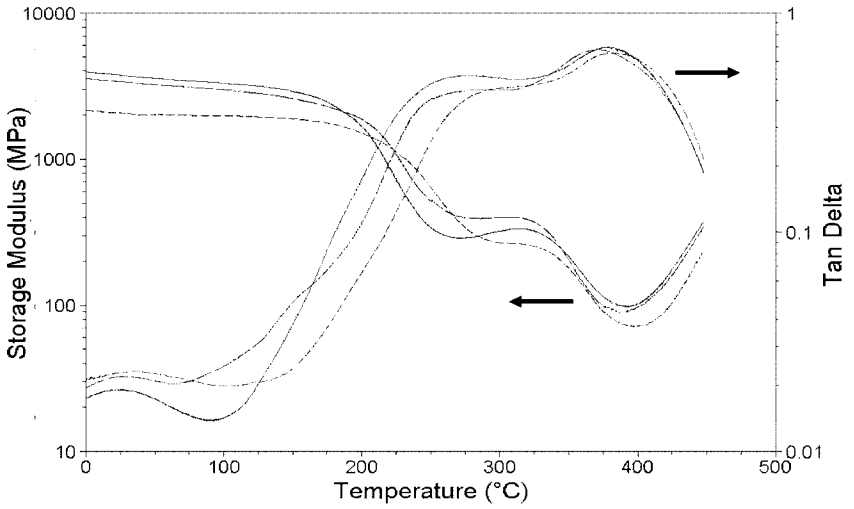

Figure 5. 9. Storage Modulus and Tan Delta Curves for BPS-PBI Copolymers. Short Dash Line, Long Dash Line, and Solid Line Represent BPS5-PBI5, BPS10-PBI10, and BPS15-PBI15, Respectively.

Table 5. 2. Characterization of BPS x –PBI y [a] Copolymers.

Copolymers	Copolymer Composition[b] (BPS/PBI) (%)	IV (dL g^{-1})[c]	T_g (°C)[d]	
			1st	2nd
BPS 5 – PBI 5	54 / 46	0.78	276	360
BPS 10 – PBI 10	53 / 47	1.00	250	375
BPS 15 – PBI 15	55 / 45	1.91	240	375

[a] Acronym for copolymers (BPS x – PBI y) :

x = molecular weight of the poly(arylene ether sulfone) block (BPS) in units of kg/mol

y = molecular weight of the polybenzimidazole block (PBI) in units of kg/mol

[b] Determined by ^{1}H NMR

[c] In NMP at 25 ºC

[d] Measured by DMA; E' Modulus drop

5.4.4. Water Uptake, H_3PO_4 Doping Level, and Swelling Ratio

The copolymers were soluble in DMAc without any insoluble residue and produced transparent and ductile membranes. A series of acid doped copolymer

membranes were prepared using various concentrations of H_3PO_4 solution. First, to determine the time required to saturate the copolymer membranes in different concentrations of H_3PO_4 solution, the membranes were immersed in 3, 9, and 14.6 M H_3PO_4 solutions and their weight gains were measured as a function of time. Figure 5.10 shows the weight increase behavior of BPS10-PBI10 with different acid concentrations. As can be seen from the figure, a higher concentration of doping solution reduces the time to saturate the film with H_3PO_4. With the 3 M H_3PO_4 solution, at least 24 h was necessary to saturate the membrane while only 6 h was adequate for the 14.6 M H_3PO_4 solution. Based on the results, further doping experiments were performed for 72 h to obtain the maximum acid doping level.

To determine the doping level and water uptake, a series of BPS-PBI copolymers with different block lengths was immersed in different concentrations of H_3PO_4 solution. After 72 h of immersion in the acid solutions, their weight increases were measured and plotted as a function of the doping concentration (Fig. 5.11). As expected, larger weight gains were observed for higher concentrations of doping solutions. However, no significant variation of weight increase was observed with changes of block lengths.

The weight increases of acid doped membranes can be attributed both to imbibed H_3PO_4 and water. To evaluate the contribution of each factor in the weight increase, the acid doped membranes were dried in a vacuum oven at 110 °C for 24 h. The drying process selectively removed water out of the membrane without the condensation of H_3PO_4 in the membranes. The weight loss after the drying was interpreted as the water uptake of the sample while remaining weight increase was considered as the weight of H_3PO_4 by the doping process. Fiqure 12 shows the contribution of the water uptake and

the acid doping for the weight increases. Interestingly, as the concentration of acid doping solution increased, the water uptake of the copolymers remained similar values while the weight increases by acid were significant. This behavior is well matched with the earlier study which was performed by Bjerum et.al.[15]

The doping levels of the membranes were also determined (Fig. 5.13). The doping levels increased linearly with increasing solution concentration up to 12 M. However, when the concentration was higher than 12 M, the doping level increased more rapidly and reached 12 for the 14.6 M acid concentration. It is noteworthy that the doped copolymer membranes showed limited swelling ratios even at high doping levels. For H_3PO_4 doped conventional PBI homopolymer membranes, it has been generally accepted that the doping level 5 is the highest value for practical applications without any observed deterioration of mechanical strength and ionic conductivity.[15] However, when BPS-PBI and PBI homopolymer membranes were immersed in 14.6 M H_3PO_4 solution for 72 h, the BPS-PBI membranes with high doping levels (e.g., 9.65-12.02) showed less than 4% in-plane and 60% through-plane swelling ratios while PBI homopolymer exhibited 22% and 105% swelling ratios, respectively. (Table 5.3). This result is not surprising if we consider that the acid contents of the doped multiblock copolymer membranes (e.g., 59-63 wt.%) are lower than that of the homopolymer PBI(78 wt.%). To compare the swelling behaviors of the two systems with similar acid contents, a homopolymer PBI membrane with 60.9% acid content was also fabricated by immersion in 12 M H_3PO_4 solution. Although the acid content of the homopolymer PBI membrane was reduced to 60.9% to match the acid contents of multiblock copolymers, the PBI homopolymer membrane still showed much a higher swelling ratio than those of multiblock copolymers.

A possible explanation of the low swelling ratios of the multiblock copolymers might be the selective doping of the acid in the multiblock copolymer membranes. Since poly(arylene ether sulfone) BPS segments do not absorb phosphoric acid, the doped phosphoric acid mainly exists in the PBI segments while the poly(arylene ether sulfone) segments maintain physical integrity and reduced the swelling ratios even with high doping levels. Hence, the low swelling ratios and minor softening of the acid doped multiblock copolymer membranes suggest that higher doping levels (e.g., > 6) could be utilized to further enhance the ionic conductivities without any significant deterioration of the mechanical strength. Detailed mechanical properties of BPS15-PBI15 with different doping levels are summarized in Table 5.4.

Table 5. 3. Swelling Ratios of BPS –PBI and PBI Homopolymer Membranes Doped with H_3PO_4 Solution for 72 h.

Copolymers	Length (%)	Thickness (%)	Volume (%)	Acid Conc. for Doping (M)	Acid in Sample (wt.%)
PBI[a]	22.7	105.5	209	14.6	78.8
PBI[a]	9.5	95.5	134	12.0	60.9
BPS 5 – PBI 5	2.7	60.0	69	14.6	63.5
BPS 10 – PBI 10	2.7	42.9	51	14.6	59.2
BPS 15 – PBI 15	1.7	56.3	62	14.6	62.6

[a] Intrinsic viscosity in NMP at 25 °C was 2.35 dL/g

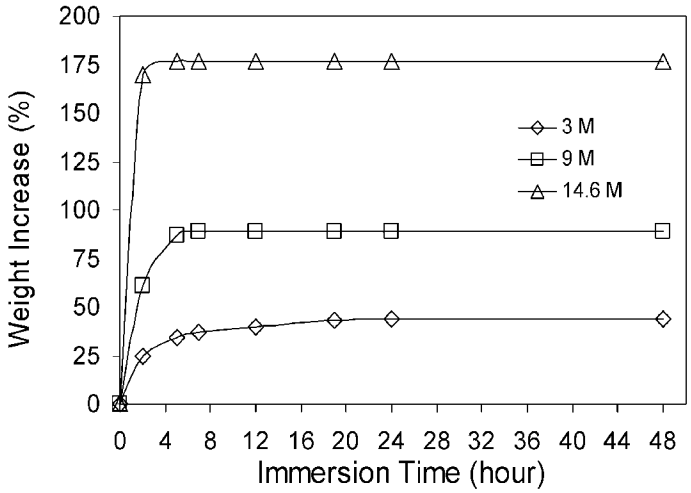

Figure 5. 10. Weight Gains of BPS10-PBI10 as a Function of Immersion Time with Different Acid Concentrations.

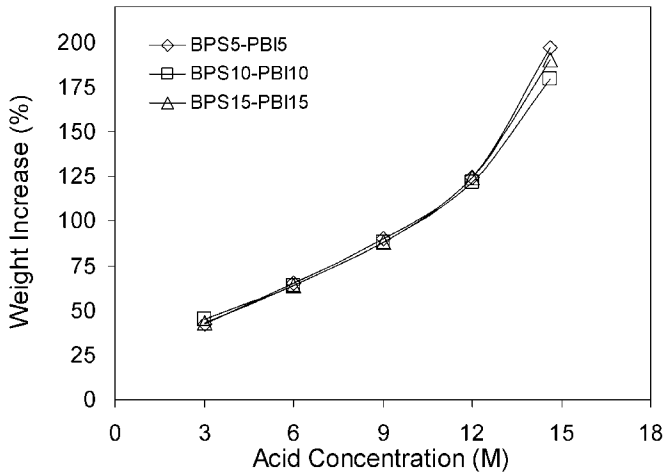

Figure 5. 11. Weight Increases of BPS-PBI Membranes as a Function of the Acid Concentration with Different Block Lengths.

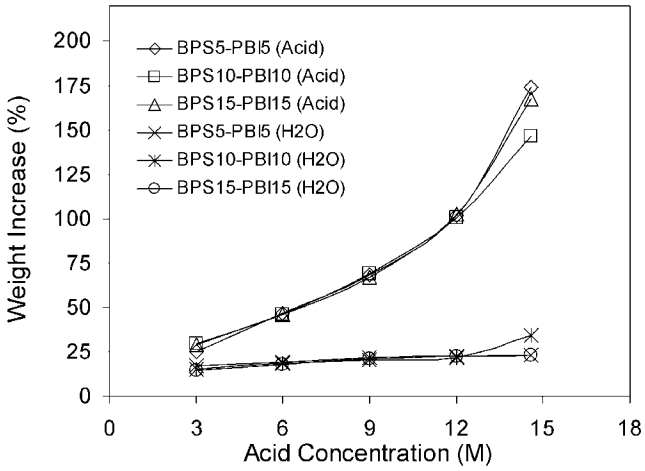

Figure 5. 12. Contribution of Phosphoric and Water to the Weight Increases of BPS-PBI Membranes as a Function of the Acid Concentration with Different Block Lengths.

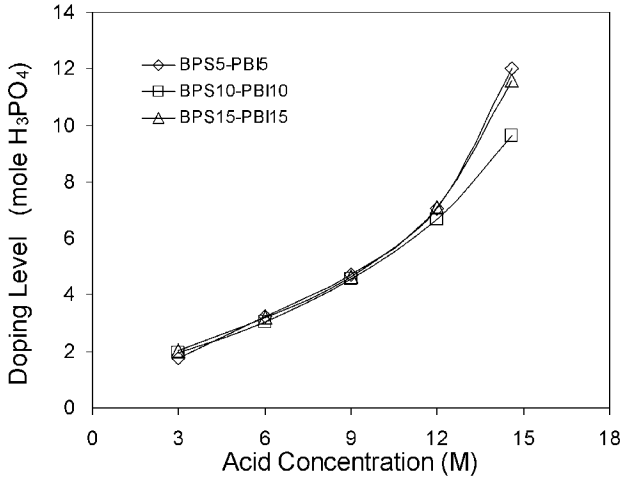

Figure 5. 13. Phosphoric Acid Doping Level of BPS-PBI Membranes as a Function of the Acid Concentration with Different Block Lengths.

Table 5. 4. Mechanical Properties of BPS15 –PBI15 with Different Doping Levels.

Doping Level	Acid in Sample (wt.%)	Modulus (MPa)	Stress at Break (MPa)	Elongation at Break (%)
0	0	2880 ± 100	73 ± 3	10 ± 2
4.6	40.0	860 ± 60	46 ± 5	149 ± 12
11.5	62.6	440 ± 80	31 ± 6	205 ± 16

5.4.5. Influence of Temperature and Doping Levels of Phosphoric Acid on Ionic Conductivity

The ionic conductivities of the BPS-PBI copolymers were determined as a function of temperature without any external humidification supply. The temperature range was 100 to 200 °C. Figure 5.14 represents the temperature vs. conductivity plot for BPS5-PBI5 doped with different concentrations of phosphoric acid (e.g., 3, 9, 12, and 14.6 M). A similar study was conducted for the BPS10-PBI10 and BPS15-PBI15 samples as shown in Figures 5.15 and 5.16. The numbers within the brackets in the legends refer to the doping levels of the samples.

In all cases, the ionic conductivities increased with increasing temperature and doping levels. However, the conductivities of the copolymers doped at higher concentrations (e.g., 12 and 14.6 M) increased more rapidly with temperature than in samples doped with lower concentrations (e.g., 3 and 9 M). For the membranes doped with lower acid concentrations (3 and 9 M), the doping levels ranged from 4 to 5. As the theoretical number of "bound" phosphoric acid units is 4, ionic conduction at this doping level can occur only through proton hopping between the N-H site and the phosphate anion.[23] However when the membranes were doped with higher acid concentrations (12

and 14.6 M), the doping levels were between 6-12 and the presence of "free" phosphoric acid or the quickly diffusing $H_2PO_4^-$ anions increases the ionic conductivity significantly.

Ionic conductivity measured as a function of temperature also showed an increasing trend for all samples. However, a change in slope was observed above 150 ^oC, which may be attributed to a change in the conduction mechanism. It is known that "fused" phosphoric acid can be formed from the "free" phosphoric acid at high temperatures and so the slope change may indicate a transition from a hopping mechanism to a vehicle mechanism involving bodily diffusion of protons as proposed by Hayamizu et al.[23] The activation energy for ionic transport was determined for all samples over the temperature range of 100 ^oC to 150 ^oC. The activation energy calculated showed a strong dependence on doping level as shown in Figure 5.17. A significant drop in activation energy from 60 to 20 kJ/mol was observed for the BPS15-PBI15 sample as the doping level was increased from 2 to 6. A similar trend was also seen in the BPS5-PBI5 and BPS10-PBI10 samples. This sharp decrease can be attributed to the involvement of the free phosphoric acid or the phosphate anion in the transport process. A further increase in phosphoric acid content resulted in a nominal decrease in the activation energy value.

Among the copolymers, the highest conductivity at 200 °C was 47 mS/cm from BPS15-BPS15 with a doping level of 11.5. This value is relatively low when compared to the current record conductivity of 250 mS/cm at 200 °C which was acquired with the phosphoric acid doped PBI membrane via the sol-gel process.[19] However, considering doping level of the sol-gel processed membrane is extraordinarily high (e.g., 20-40), the ionic conductivity of 47 mS/cm with the doping level of 11.5 is reasonable.

It is worthwhile to compare ionic conductivities of the multiblock copolymer system and conventional PBI system with similar acid contents instead of doping levels. Since the PBI compositions of the multiblock copolymers are around half of the system, at the same doping level, the acid contents in the multiblock copolymers will be much lower than those of homopolymer PBI. For example, the weight based acid content in the BPS15-PBI15 (PBI composition 45%) with a doping level of 11.5 will be the same as that of conventional PBI system with a 5.18 doping level. Previously, Litt et. al., reported ionic conductivity of the conventional phosphoric acid doped PBI system with 5.01 doping level. The ionic conductivities ranged from 25 to 40 mS/cm with 5-10% relative humidity (RH) at 190 °C.[16]

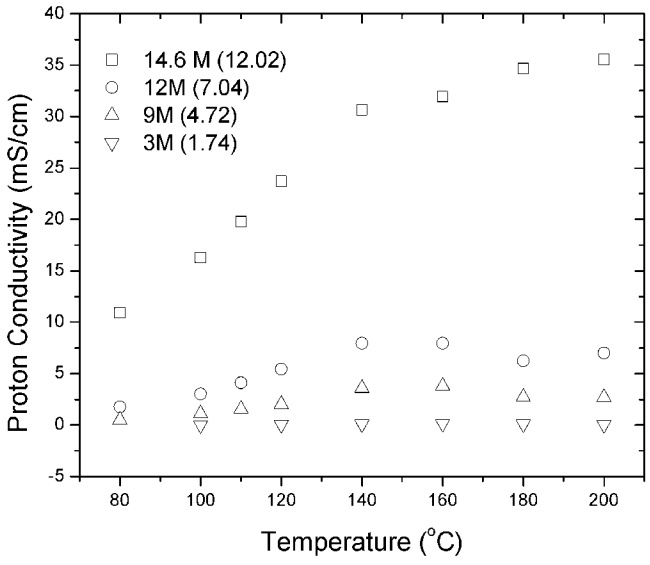

Figure 5. 14. Influence of Temperature on Ionic Conductivity for BPS5-PBI5 Samples at Varying Phosphoric Acid Doping Levels.

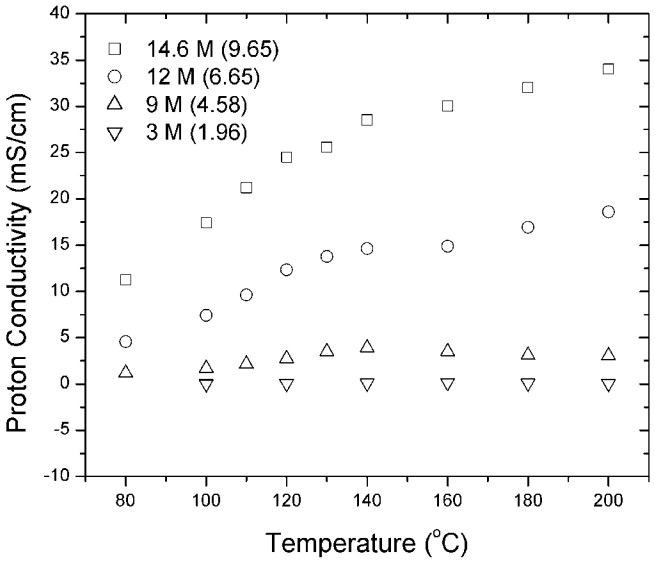

Figure 5. 15. Influence of Temperature on Ionic Conductivity for BPS10-PBI10 Samples at Varying Phosphoric Acid Doping Levels.

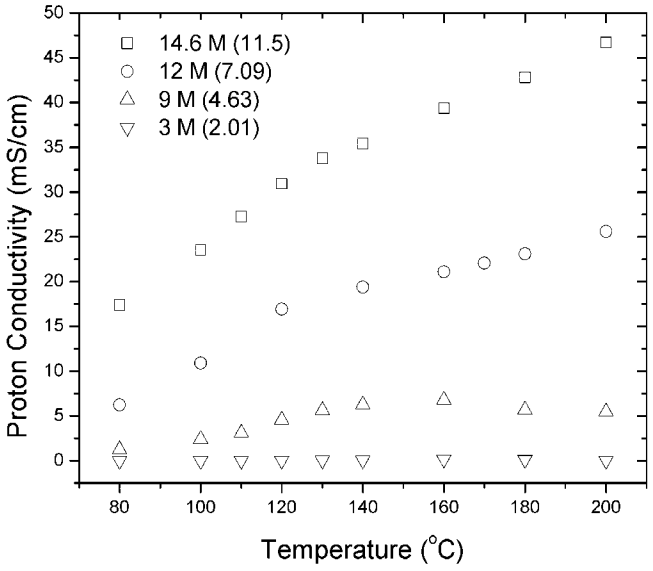

Figure 5. 16. Influence of Temperature on Ionic Conductivity for BPS15-PBI15 Samples at Varying Phosphoric Acid Doping Levels.

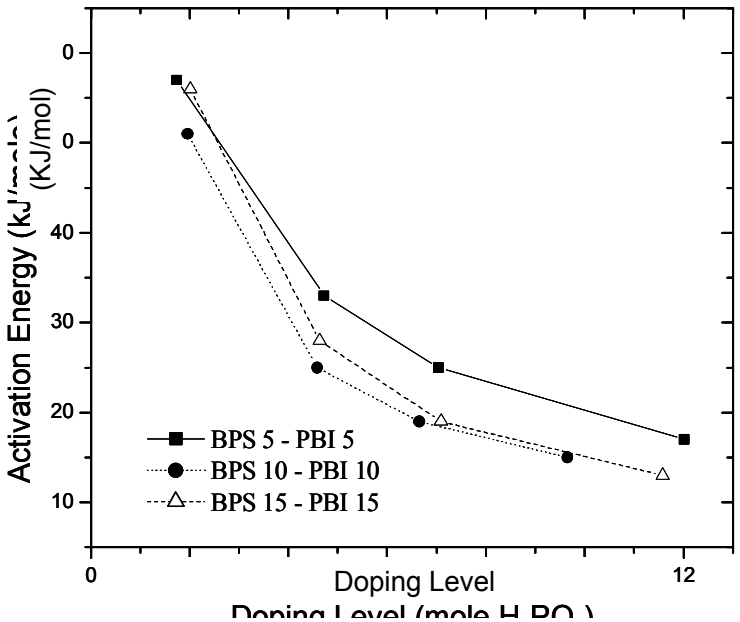

Figure 5. 17. Influence of Phosphoric Acid Content on Activation Energy.

5.4.6. Influence of the Microstructure of the Multiblocks on Ion Transport.

Over the last few years, our group has been investigating the influence of morphology on proton transport of sulfonic acid containing multiblock copolymers as a function of relative humidity (RH). The proton conductivity under partially hydrated conditions was found to increase with increasing block length or with the extent of phase separation.[36] In the current investigation with the selectively doped BPS-PBI system, ion conduction was studied as a function of doping level at 140 $^{\circ}$C. The three copolymers with varying block lengths were compared as shown in Figure 5.18. Among the copolymers, the conductivities of BPS15-BPS15 and BPS10-BPS10 showed a similar trend with doping level in contrast to the BPS5-PBI5 sample. This suggests a morphological change from the BPS5-BPS5 sample to the BPS10-BPS10 sample. At a given doping level, the ionic conductivity was found to increase with increasing block length. The effect was more pronounced at lower doping levels (6-7). This can be

attributed to the formation of a phase separated morphology with increasing block lengths as indicated by the DMA study. The phase separated morphology resulted in improved connectivity within the PBI units. This is consistent with our earlier findings with the sulfonic acid containing multiblock copolymers. The increased connectivity with block length is expected to lower the morphological barrier for ion transport with increased ionic conductivity. Thus by synthesizing phase separated multiblock copolymers, improved ionic conductivity can be achieved with lower phosphoric acid doping levels.

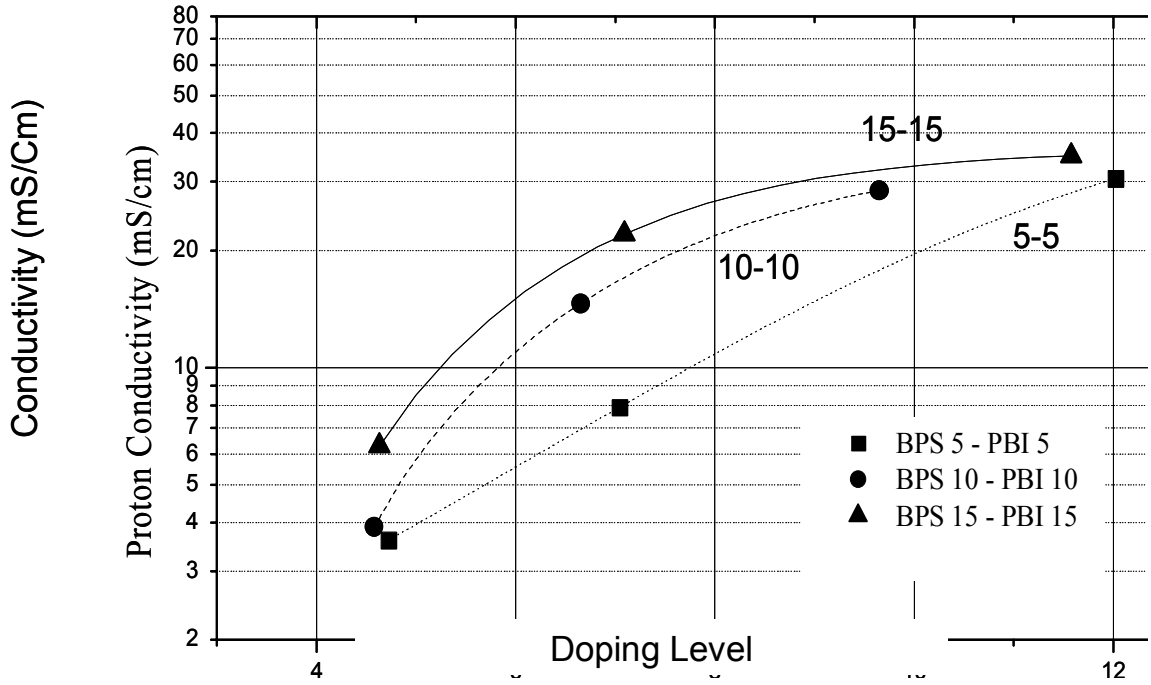

Figure 5. 18. Influence of Block Length on Ion Conduction with Varying Phosphoric Acid Doping Level at 140 °C.

5.4.7. Synthesis and Characterization of BPS-PBI Copolymers with Higher PBI Contents

As shown in the previous sections, the equal block length BPS-PBI multiblock copolymers showed high proton conductivity with excellent mechanical properties. Based on the results, another series of BPS-PBI multiblock copolymer with higher PBI content was synthesized. The main purpose of utilizing higher PBI content multiblock copolymer was to incorporate more H_3PO_4 in the system for higher ionic conductivity. Multiblock copolymers with 33/67 and 40/60 of BPS/PBI composition were synthesized with 10K-10K and 15K-15K block length and their actual compositions determined by ^{1}H NMR are summarized in Table 5.5.

Table 5. 5. Feed Ratio and Determined Composition of Unequal BPS-PBI Copolymers.

Copolymer	Feed Ratio (BPS/PBI)	Determined Composition (BPS/PBI) from ^{1}H NMR
BPS10-PBI10	40/60	42/58
BPS10-PBI10	33/67	35/65
BPS15-PBI15	40/60	42/58

BPS15-PBI15	33/67	34/66

The higher PBI contents were achieved by slightly upsetting the feed ratio of BPS and PBI oligomers for the coupling reaction. Since the oligomers already had relatively high molecular weights, a slightly reduced degree of coupling reaction due to the offset stoichiometry between the BPS and PBI oligomers did not influence the final copolymers' mechanical properties. The prepared copolymers were then doped with a 14.6 M H_3PO_4 solution at 30 ºC for 24 h and their swelling behavior was evaluated (Table 5.6). As expected, multiblock copolymers with higher PBI composition could absorb more acid up to 10% compared to the equal block multiblock copolymers. The increased acid content resulted in higher swelling ratios but the values are much lower than those of PBI homopolymer.

Table 5. 6. Acid Content and Swelling Behavior of BPS-PBI Copolymers.

	Composition (BPS/PBI)	Acid Content in Membrane (wt.%)	Swelling Ratios (in-plane, through-plane)
PBI homopolymer	0/100	79 %	23%, 106%
BPS10-PBI10	53/47	56 %	6%, 65%
BPS10-PBI10	42/58	65 %	12%, 74%
BPS10-PBI10	35/65	66 %	17%, 100%
BPS15-PBI15	52/48	56 %	7%, 51%
BPS15-PBI15	42/58	63 %	10%, 56%
BPS15-PBI15	34/66	66 %	15%, 70%

We investigated the mechanical behavior of block copolymer membranes, both in the undoped and doped form. In Figure 5. 19, these data are presented. The testing was done at 25 ºC at a rate of 5 mm/minute, after being equilibrated at 40% RH. The control copolymers (undoped BPS-PBI) were for the most part tough ductile films with a rather high modulus and some variability in the ultimate elongation. Nevertheless, the films were creasible and ductile. After doping selectively the PBI phase, the modulus has decreased quite a bit, reflecting the plasticization of the PBI phase. However, the tensile strength and the elongation are excellent—approximately three times the strength of Nafion 112, and roughly equivalent elongation at break.

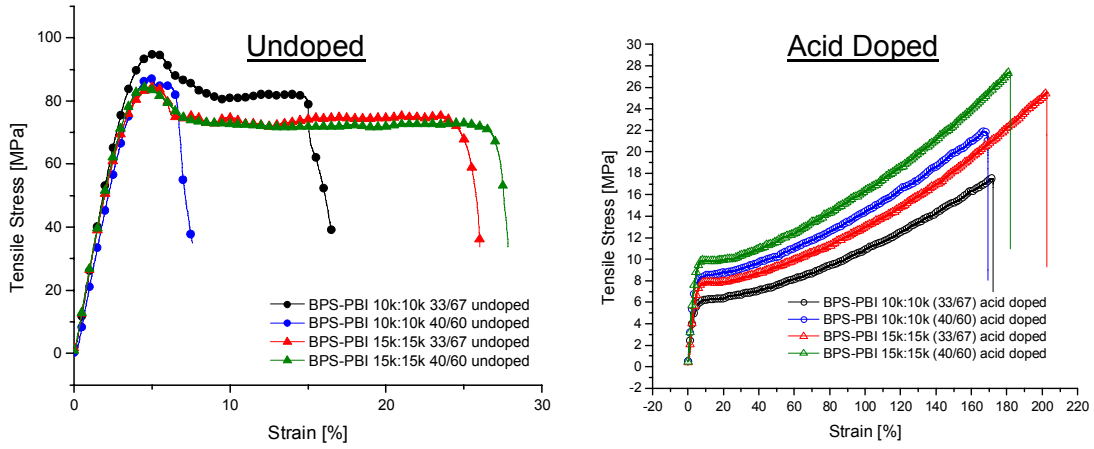

Figure 5. 19. Mechnical Behavior of Undoped and Doped BPS-PBI Multiblock Copolymers.

In Figure 5. 20, there is an increase in the tensile modulus as a function of the concentration of the hydrophobic polysulfone phase in these early experiments. It is not noticed in the updoped system, but particularly for the doped system, and it is believed that this reflects the fact that the polysulfone phase is not plasticized and can provide desirable continuing stiffness.

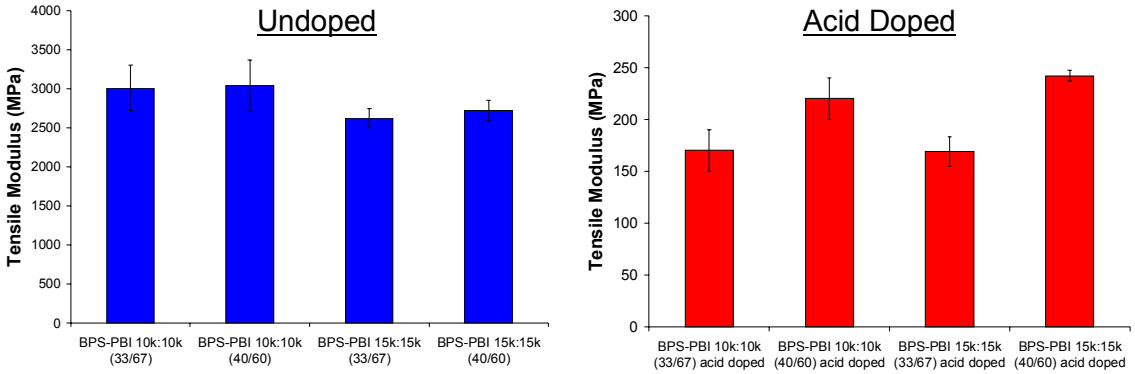

Figure 5. 20. Tensile Modulus of Undoped and Doped BPS-PBI Multiblock Copolymers.

In Figure 5. 21, the tensile strength can also be shown to increase with block and molecular weight and polysulfone content, and it suggests that this will likely reflect a sharper nanophase separation as the blocks become longer.

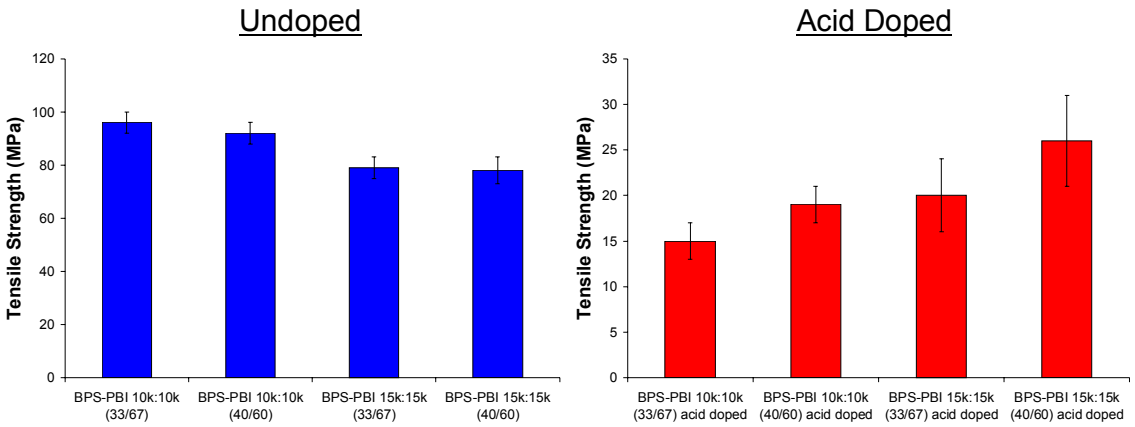

Figure 5. 21. Tensile Strength of Undoped and Doped BPS-PBI Multiblock Copolymers.

Ionic conductivity of BPS-PBI multiblock copolymers was measured as a function of temperature and RH. In Figure 5. 22, the results for the BPS15-PBI15 (BPS/PBI:34/66) block copolymer at 120°C are compared with state-of-the-art Nafion 212 systems.

Conductivities at higher humidities are comparable; however, the conductivity at 50% humidity is significantly improved relative to even the Nafion NRE 212 system.

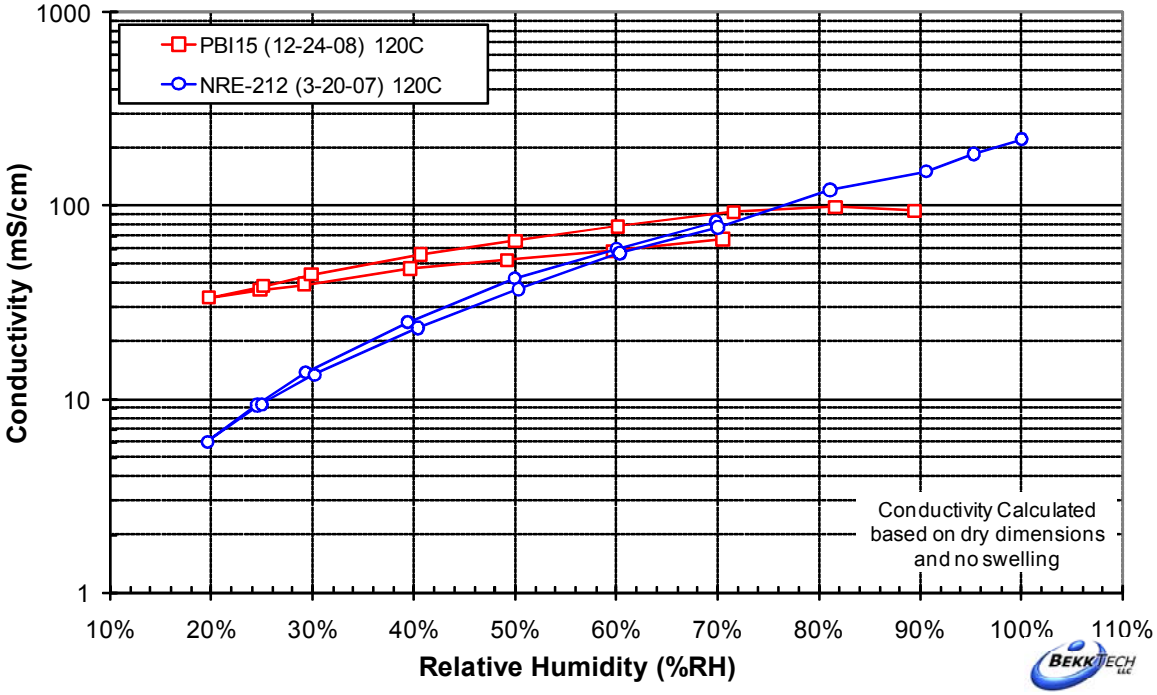

Figure 5. 22. Ionic Conductivity Comparison between Nafion and BPS-PBI at 120 ºC under Partially Hydrated Conditions.

In Figure 5. 23, the ionic conductivities of the BPS15-PBI15 at different temperatures are compared. Clearly, the conductivity increases with increasing temperature and the conductivity improvement at lower RH was more pronounce. It should be noted that the conductivity shown in the figure was measured with increasing RH mode.

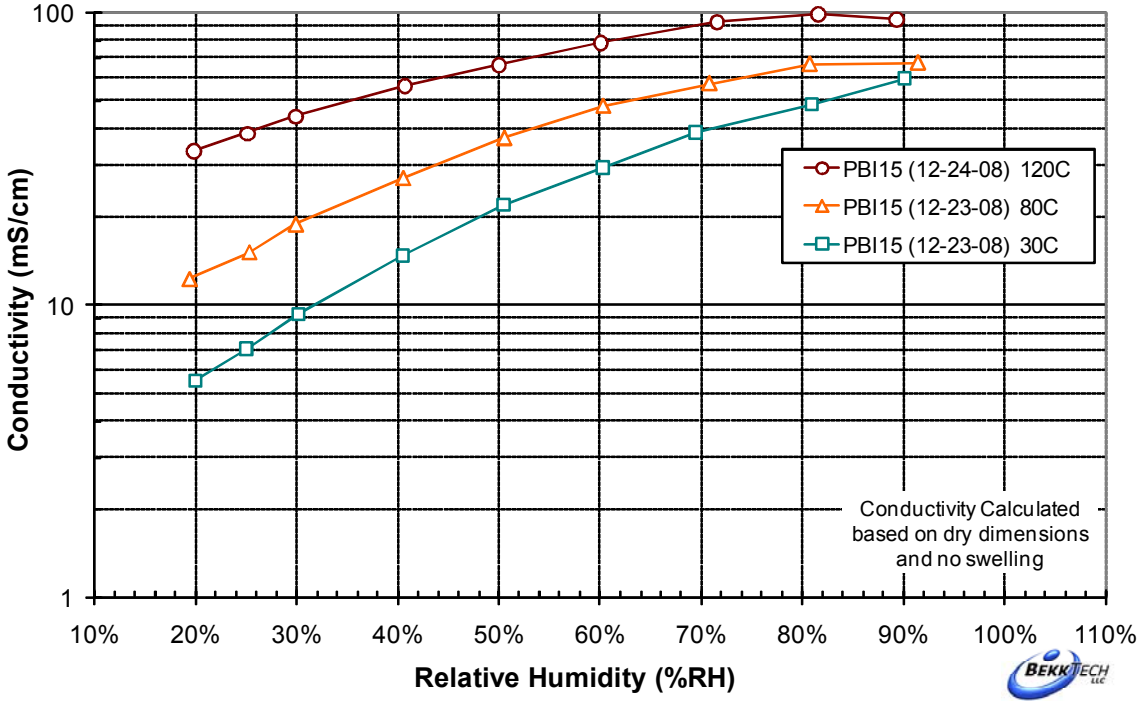

Figure 5. 23. Ionic Conductivity of BPS-PBI Copolymer as a Function of Temperature (Measured with Increasing RH Mode)

In Figure 5. 24, the sequences down and up are compared at 30, 80 and 120°C. As shown in the figure, the conductivities with increasing RH were always higher than those with decreasing RH. The conductivity difference was pronounced at higher temperature. At 80% the 100 mS seems to be about observed; at 60% it's about 80, but at 50% it is still less than 70 in the increasing RH mode.

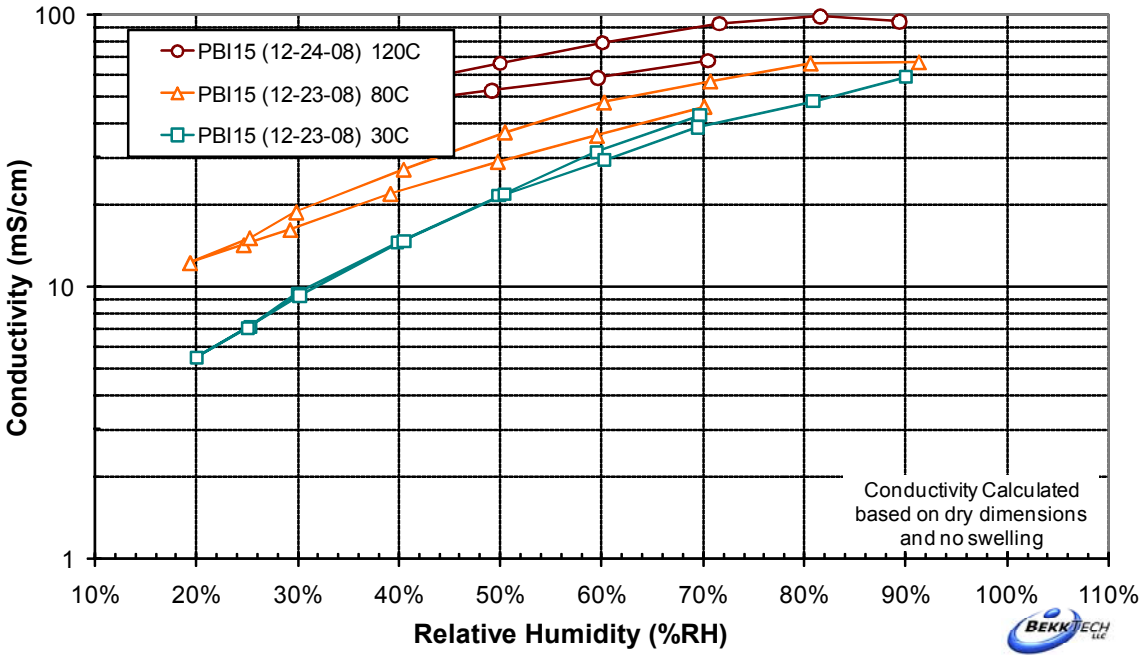

Figure 5. 24. Ionic Conductivity of BPS-PBI Copolymer as a Function of Temperature

In Figure 5. 25, the conductivity of the BPS15-PBI15 block copolymer at 30°C is compared with Nafion 212. Clearly, there is a significant improvement relative the control, but again at 80% humidity the conductivity is approximately 50 or slightly less.

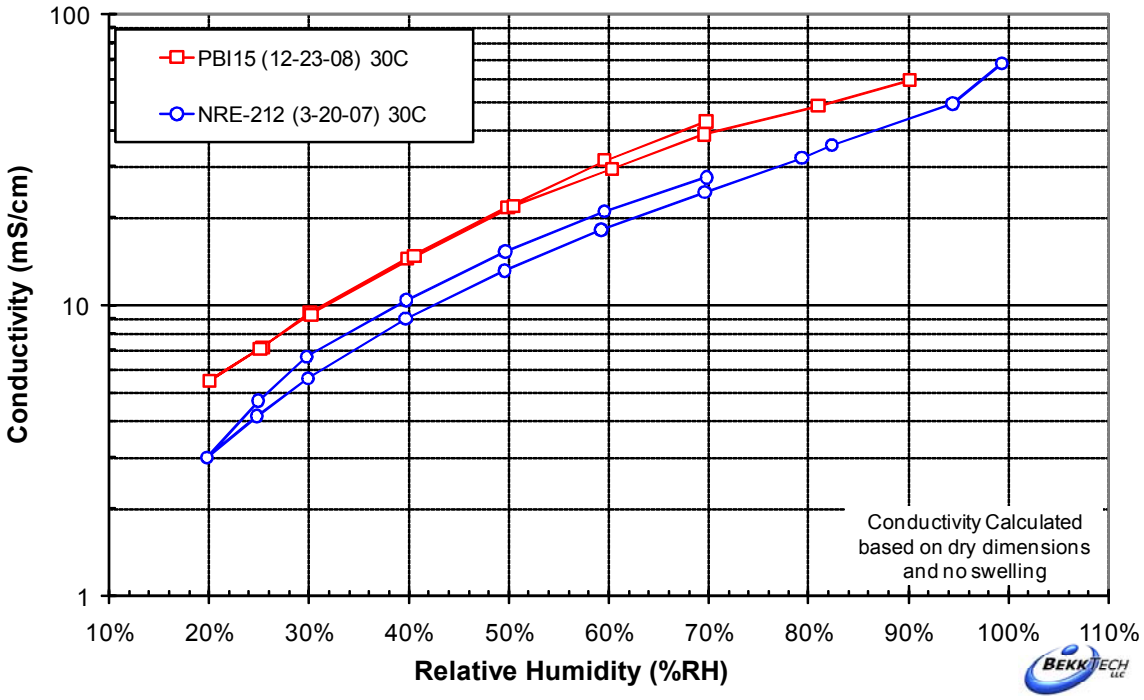

Figure 5. 25. Ionic Conductivity of BPS15-PBI15 Comparison to Nafion at 30 ºC.

In Figure 5. 26, the results for a BPS15-PBI15 multiblock copolymer at 120°C are compared with state-of-the-art Nafion 212 systems. Conductivities at higher humidities are comparable; however, the conductivity at 50% humidity is significantly improved relative to even the Nafion NRE 212 system.

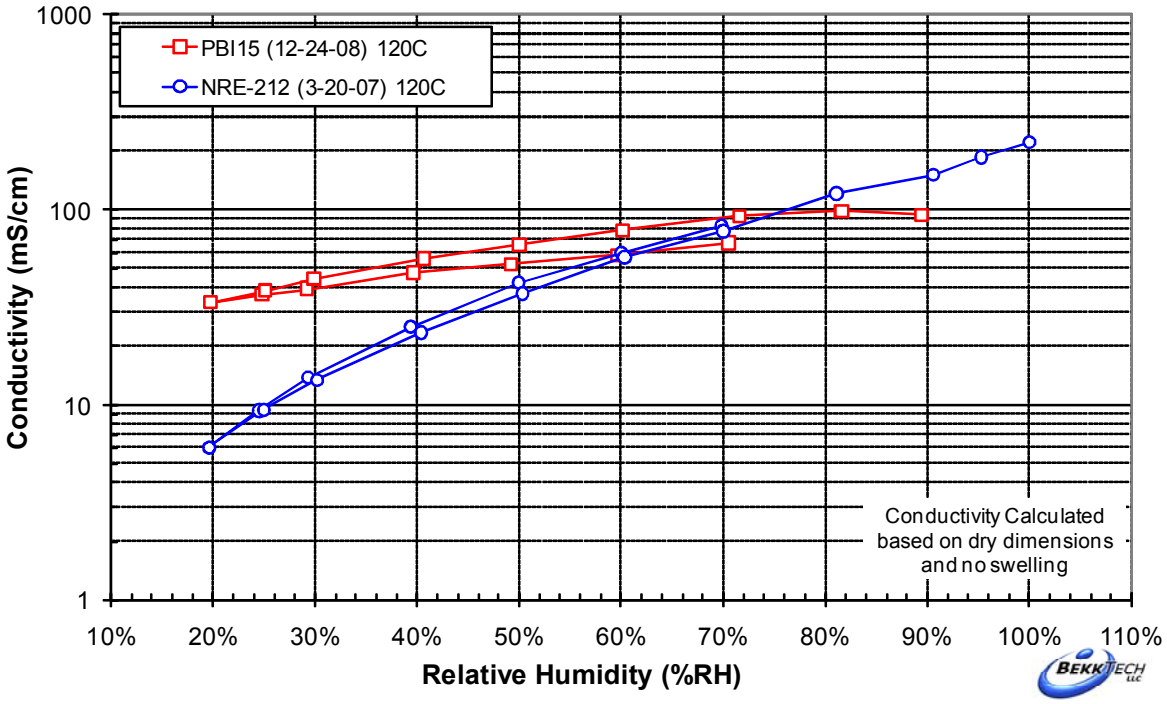

Figure 5. 26. Ionic Conductivity of BPS15-PBI15 Comparison to Nafion at 120 ºC.

5.5. Conclusions

A novel thermally stable multiblock copolymer system was developed and characterized for low humidity high temperature PEM applications. The multiblock copolymers were synthesized via a coupling reaction between telechelic carboxyl functional poly(arylene ether sulfone) and *o*-diamine terminated polybenzimidazole. Transparent and ductile membranes were prepared by solvent casting from DMAc and two distinct T_gs were observed by DMA. The ionic conduction of the membranes was achieved by immersing the membranes in H_3PO_4 solution. A doping level and water uptake study revealed that the doping levels of the membranes strongly depend on the concentration of H_3PO_4 doping solution while the water uptake has a limited influence. The ionic conductivity study revealed that there was a strong dependency on temperature, doping level and more importantly the microstructure of the samples. The ionic conductivity was found to increase significantly after a particular doping level for all the copolymers and was attributed to the appearance of "free" phosphoric acid. At a given doping level, the ionic conductivity was found to increase with increasing block length. The formation of the phase separated morphology with increasing block length was confirmed by DMA analysis. The increased phase separation resulted in better connectivity and improved ion transport.

The authors thank the Department of Energy (DE-FG36-06G016038) for its support of this research.

5.6. References

1. Savadogo, O. Emerging membranes for electrochemical systems: (I) solid polymer electrolyte membranes for fuel cell systems. *Journal of New Materials for Electrochemical Systems* **1998,** 1, (1), 47-66.
2. Kreuer, K. D. On the development of proton conducting polymer membranes for hydrogen and methanol fuel cells. *Journal of Membrane Science* **2001,** 185, (1), 29-39.
3. Banerjee, Shoibal; Curtin, Dennis E. Nafion perfluorinated membranes in fuel cells. *Journal of Fluorine Chemistry* **2004,** 125, (8), 1211-1216.
4. Hamrock, Steven J.; Yandrasits, Michael A. Proton exchange membranes for fuel cell applications. *Polymer Reviews (Philadelphia, PA, United States)* **2006,** 46, (3), 219-244.
5. Kim, Yu Seung; Dong, Limin; Hickner, Michael A.; Glass, Thomas E.; Webb, Vernon; McGrath, James E. State of Water in Disulfonated Poly(arylene ether sulfone) Copolymers and a Perfluorosulfonic Acid Copolymer (Nafion) and Its Effect on Physical and Electrochemical Properties. *Macromolecules* **2003,** 36, (17), 6281-6285.
6. Kreuer, Klaus Dieter; Rabenau, Albrecht; Weppner, Werner. Vehicle mechanism, a new model for interpretation of the conductivity of fast proton conductors. *Angewandte Chemie* **1982,** 94, (3), 224-225.
7. Kim, Yu Seung; Wang, Feng; Hickner, Michael; Zawodzinski, Thomas A.; McGrath, James E. Fabrication and characterization of heteropoly acid (H3PW12O40)/directly polymerized sulfonated poly(arylene ether sulfone) copolymer composite membranes for higher temperature fuel cell applications. *Journal of Membrane Science* **2003,** 212, (1-2), 263-282.
8. Hill, Melinda L.; Kim, Yu Seung; Einsla, Brian R.; McGrath, James E. Zirconium hydrogen phosphate/disulfonated poly(arylene ether sulfone) copolymer composite membranes for proton exchange membrane fuel cells. *Journal of Membrane Science* **2006,** 283, (1+2), 102-108.
9. Costamagna, P.; Yang, C.; Bocarsly, A. B.; Srinivasan, S. Nafion115/zirconium phosphate composite membranes for operation of PEMFCs above 100 DegC. *Electrochimica Acta* **2002,** 47, (7), 1023-1033.
10. Hickner, Michael A.; Ghassemi, Hossein; Kim, Yu Seung; Einsla, Brian R.; McGrath, James E. Alternative Polymer Systems for Proton Exchange Membranes (PEMs). *Chemical Reviews (Washington, DC, United States)* **2004,** 104, (10), 4587-4611.
11. He, Ronghuan; Li, Qingfeng; Xiao, Gang; Bjerrum, Niels J. Proton conductivity of phosphoric acid doped polybenzimidazole and its composites with inorganic proton conductors. *Journal of Membrane Science* **2003,** 226, (1-2), 169-184.
12. Steininger, H.; Schuster, M.; Kreuer, K. D.; Kaltbeitzel, A.; Bingoel, B.; Meyer, W. H.; Schauff, S.; Brunklaus, G.; Maier, J.; Spiess, H. W. Intermediate temperature proton conductors for PEM fuel cells based on phosphonic acid as protogenic group: A progress report. *Physical Chemistry Chemical Physics* **2007,** 9, (15), 1764-1773.

13. Sammes, Nigel; Bove, Roberto; Stahl, Knut. Phosphoric acid fuel cells: fundamentals and applications. *Current Opinion in Solid State & Materials Science* **2005,** 8, (5), 372-378.
14. Kongstein, O. E.; Berning, T.; Borresen, B.; Seland, F.; Tunold, R. Polymer electrolyte fuel cells based on phosphoric acid doped polybenzimidazole (PBI) membranes. *Energy (Oxford, United Kingdom)* **2006,** 32, (4), 418-422.
15. Lobato, Justo; Canizares, Pablo; Rodrigo, Manuel A.; Linares, Jose J. PBI-based polymer electrolyte membranes fuel cells. *Electrochimica Acta* **2007,** 52, (12), 3910-3920.
16. Wainright, J. S.; Wang, J. T.; Weng, D.; Savinell, R. F.; Litt, M. Acid-doped polybenzimidazoles: a new polymer electrolyte. *Journal of the Electrochemical Society* **1995,** 142, (7), L121-L123.
17. Xiao, Lixiang; Zhang, Haifeng; Choe, Eui-Won; Scanlon, Eugene; Ramanathan, L. S.; Benicewicz, Brian C. Synthesis and characterization of pyridine-based polybenzimidazoles as novel fuel cell membrane materials. *Preprints of Symposia - American Chemical Society, Division of Fuel Chemistry* **2003,** 48, (1), 447-448.
18. Li, Qingfeng; He, Ronghuan; Berg, Rolf W.; Hjuler, Hans A.; Bjerrum, Niels J. Water uptake and acid doping of polybenzimidazoles as electrolyte membranes for fuel cells. *Solid State Ionics* **2004,** 168, (1-2), 177-185.
19. Xiao, Lixiang; Zhang, Haifeng; Scanlon, Eugene; Ramanathan, L. S.; Choe, Eui-Won; Rogers, Diana; Apple, Tom; Benicewicz, Brian C. High-Temperature Polybenzimidazole Fuel Cell Membranes via a Sol-Gel Process. *Chemistry of Materials* **2005,** 17, (21), 5328-5333.
20. van Grotthuss, C. J. D. *Ann. Chim.* **1806,** 58, 54.
21. Agmon, Noam. The Grotthuss mechanism. *Chemical Physics Letters* **1995,** 244, (5,6), 456-462.
22. Hughes, Colan E.; Haufe, Stefan; Angerstein, Brigitta; Kalim, Ratna; Maehr, Ulrich; Reiche, Annette; Baldus, Marc. Probing Structure and Dynamics in Poly[2,2'-(m-phenylene)-5,5'-bibenzimidazole] Fuel Cells with Magic-Angle-Spinning NMR. *Journal of Physical Chemistry B* **2004,** 108, (36), 13626-13631.
23. Aihara, Yuichi; Sonai, Atsuo; Hattori, Mineyuki; Hayamizu, Kikuko. Ion Conduction Mechanisms and Thermal Properties of Hydrated and Anhydrous Phosphoric Acids Studied with 1H, 2H, and 31P NMR. *Journal of Physical Chemistry B* **2006,** 110, (49), 24999-25006.
24. Li, Q.; He, R.; Jensen, J. O.; Bjerrum, N. J. PBI-based polymer membranes for high temperature fuel cells - preparation, characterization and fuel cell demonstration. *Fuel Cells (Weinheim, Germany)* **2004,** 4, (3), 147-159.
25. Xu, Hongjie; Chen, Kangcheng; Guo, Xiaoxia; Fang, Jianhua; Yin, Jie. Synthesis and properties of hyperbranched polybenzimidazoles via A2 + B3 approach. *Journal of Polymer Science, Part A: Polymer Chemistry* **2007,** 45, (6), 1150-1158.
26. Li, Qingfeng; Pan, Chao; Jensen, Jens Oluf; Noye, Pernille; Bjerrum, Niels J. Cross-Linked Polybenzimidazole Membranes for Fuel Cells. *Chemistry of Materials* **2007,** 19, (3), 350-352.
27. Staiti, P.; Minutoli, M. Influence of composition and acid treatment on proton conduction of composite polybenzimidazole membranes. *Journal of Power Sources* **2001,** 94, (1), 9-13.

28. Harrison, W. L.; Hickner, M. A.; Kim, Y. S.; McGrath, J. E. Poly(arylene ether sulfone) copolymers and related systems from disulfonated monomer building blocks: synthesis, characterization, and performance - a topical review. *Fuel Cells (Weinheim, Germany)* **2005,** 5, (2), 201-212.
29. Kim, Yu Seung; Hickner, Michael A.; Dong, Limin; Pivovar, Bryan S.; McGrath, James E. Sulfonated poly(arylene ether sulfone) copolymer proton exchange membranes: composition and morphology effects on the methanol permeability. *Journal of Membrane Science* **2004,** 243, (1-2), 317-326.
30. Lee, Hae-Seung; Badami, Anand S.; Roy, Abhishek; McGrath, James E. Segmented Sulfonated Poly(arylene ether sulfone)-b-Polyimide Copolymers for Proton Exchange Membrane Fuel Cells. I. Copolymer Synthesis and Fundamental Properties. *Journal of Polymer Science, Part A: Polymer Chemistry* **2007,** 45, (21), 4879-4890.
31. Wang, Hang; Badami, Anand S.; Roy, Abhishek; McGrath, James E. Multiblock copolymers of poly(2,5-benzophenone) and disulfonated poly(arylene ether sulfone) for proton-exchange membranes. I. Synthesis and characterization. *Journal of Polymer Science, Part A: Polymer Chemistry* **2006,** 45, (2), 284-294.
32. Lee, Hae-Seung; Roy, Abhishek; Badami, Anand S.; McGrath, James E. Synthesis of multiblock copolymers based on sulfonated segmented hydrophilic-hydrophobic blocks for proton exchange membranes. *PMSE Preprints* **2006,** 95, 210-211.
33. Ghassemi, Hossein; Ndip, Grace; McGrath, James E. New multiblock copolymers of sulfonated poly(4'-phenyl-2,5-benzophenone) and poly(arylene ether sulfone) for proton exchange membranes. II. *Polymer* **2004,** 45, (17), 5855-5862.
34. Lee, Hae-Seung; Roy, Abhishek; Lane, Ozma; Dunn, Stuart; McGrath, James E. Hydrophilic-hydrophobic multiblock copolymers based on poly(arylene ether sulfone) via low-temperature coupling reactions for proton exchange membrane fuel cells. *Polymer* **2008,** 49, (3), 715-723.
35. Cooper, Kevin L. *Virginia Polytechnic Institute and State University, Dissertation* **1991**.
36. Roy, Abhishek; Hickner, Michael A.; Yu, Xiang; Li, Yanxiang; Glass, Thomas E.; McGrath, James E. Influence of chemical composition and sequence length on the transport properties of proton exchange membranes. *Journal of Polymer Science, Part B: Polymer Physics* **2006,** 44, (16), 2226-2239.

CHAPTER 6

Synthesis and Characterization of Multiblock Copolymers Based on Hydrophilic Disulfonated Poly(arylene ether sulfone) and Hydrophobic Partially Fluorinated Poly(arylene ether ketone) for Fuel Cell Applications

Hae-Seung Lee, Abhishek Roy, Ozma Lane and James E. McGrath*

Macromolecules and Interfaces Institute,

Macromolecular Science and Engineering,

Virginia Polytechnic Institute and State University, Blacksburg, VA 24061

*Correspondence to: James E. McGrath

(Email: jmcgrath@vt.edu, Phone: 540-231-5976, Fax: 540-231-8517)

6.1. Abstract

Novel sulfonated fluorinated multiblock copolymers were synthesized and characterized for proton exchange membrane (PEM) fuel cell applications. The multiblock copolymers were synthesized via a coupling reaction between fully disulfonated poly(arylene ether sulfone) (BPSH100) with phenoxide end-groups and hexafluorobenzene (HFB) end-capped partially fluorinated poly(arylene ether ketone) (6FK) as hydrophilic and hydrophobic blocks, respectively. The coupling reactions between the hydrophilic and hydrophobic oligomers were conducted at relatively low temperatures to prevent a possible trans-etherification, which can randomize the hydrophilic-hydrophobic sequences. Tough ductile membranes were prepared by solution casting and their membrane properties were evaluated. With similar ion exchange capacities (IECs), proton conductivities and water uptake values were strongly influenced by the hydrophilic and hydrophobic block lengths. Conductivity and water uptake increased with increasing block length by developing nanophase separated morphologies. Atomic force microscopy (AFM) experiments revealed that the connectivity of the hydrophilic segments was enhanced by increasing the block length. The systematic synthesis and characterization of the copolymers are reported.

Keywords: Multiblock copolymers; Sulfonated poly(arylene ether sulfone); Proton exchange membrane

6.2. Introduction

Proton exchange membrane (PEM) materials have typically consisted of perfluorinated sulfonic acid containing ionomers (PFSAs), which can be synthesized from a copolymerization of tetrafluoroethylene (TFE) and a perfluorinated vinyl ether comonomer with a sulfonyl fluoride moiety in its side chain.[1] Due to their Teflon-like backbone, these membranes demonstrate good chemical stability and mechanical strength along with high proton conductivity.[2] Although PFSAs have performed well at moderate operation temperatures, their mechanical and electrochemical properties severely deteriorate at higher temperatures (>80 °C), which unfortunately can be essential for many practical applications.[3, 4] Another drawback of these materials is high fuel permeability especially in direct methanol fuel cell (DMFC) applications.

A significant effort has been devoted to the study of sulfonated aromatic copolymers as alternatives to PFSAs. Aromatic backbone-based PEMs have several favorable characteristics over PFSAs including excellent thermal and oxidative stability, high acid and hydrolytic resistance, and lower production costs.[5-7] The most frequently utilized aromatic high temperature copolymers for PEM applications are poly(arylene ether sulfone)s,[8, 9] poly(arylene ether ketone)s,[10, 11] and poly(phenylene)s.[12, 13] Although PEM performance can be significantly improved by utilizing these high performance materials, there are still a number of drawbacks that must be addressed. One of the main challenges is enhancing low proton conductivity under partially hydrated conditions. It has been widely accepted that many of the aromatic backbone-based PEMs form narrower and less well-connected ion channels in comparison to PFSAs under low relative humidity (RH) conditions.[14]

In order to overcome low proton conductivity, the use of PEMs based on hydrophilic-hydrophobic multiblock copolymers has recently been proposed due to their ability to form nanophase separated morphologies.[15-18] PEMs based on hydrophilic-hydrophobic sequenced multiblock copolymers can form well-connected hydrophilic ionic channels, which can facilitate proton transport under low humidity conditions. In addition, well-connected nonionic hydrophobic domains can provide dimensional stability. In the case of DMFCs, their hydrophobic domain may also serve as a barrier against methanol permeability.

The McGrath group has been developing various types of hydrophilic-hydrophobic multiblock copolymers based on disulfonated poly(arylene ether sulfone)s.[16, 18-21] These multiblock copolymers have displayed significantly enhanced transport properties and improved performance, but their synthesis is more difficult than random copolymer. Specifically, careful oligomer preparation with proper end-group chemistry is essential for a successful coupling reaction. To address these issues, we have recently developed a convenient methodology to synthesize multiblock copolymer systems. This method utilizes highly reactive perfluorinated small molecules such as decafluorobiphenyl (DFBP) and hexafluorobenzene (HFB) as the linkage groups for the hydrophilic and hydrophobic oligomers.[18] The use of highly reactive DFBP or HFB facilitates the coupling reactions at low temperatures and prevents a possible trans-etherification, which can randomize the hydrophilic-hydrophobic sequences.

This study, therefore, addresses the synthesis and characterization of novel multiblock copolymers based on fully disulfonated poly(arylene ether sulfone) (BPSH100) and partially fluorinated poly(arylene ether ketone) (6FK) as the hydrophilic

and hydrophobic block, respectively. The fluorination of the hydrophobic segment is expected to promote nanophase separation with the hydrophilic segment, resulting in improved proton transport properties. The coupling reaction between the hydrophilic and hydrophobic blocks was achieved using HFB as the linkage group under mild reaction conditions (e.g. <110 °C). Using the synthetic procedures described below, ten multiblock copolymers with different IECs and block lengths were developed. Various membrane parameters, such as proton conductivity (under fully and partially hydrated conditions), water uptake, swelling behavior, and morphology will be described with respect to their impact on PEM performance.

6.3. Experimental

6.3.1. Materials

4,4'-Biphenol (BP) and 4,4'-dichlorodiphenyl sulfone (DCDPS) were provided by Eastman Chemical Company and Solvay Advanced Polymers, respectively, and were dried *in vacuo* at 110 °C for 24 h prior to use. The disulfonated monomer, 3,3'-disulfonated-4,4'-dichlorodiphenyl sulfone (SDCDPS), was synthesized and purified as reported earlier.[22] The purity of SDCDPS was determined via UV-Vis spectroscopy measurements.[23] 4,4'-Hexafluoroisopropylidenediphenol (6F-BPA) (Ciba) and 4,4'-difluorobenzophenone (Aldrich) were recrystallized from toluene and ethanol, respectively, and dried *in vacuo* prior to use. N,N-dimethylacetamide (DMAc) was received from Aldrich and vacuum distilled before use. Potassium carbonate (K_2CO_3), hexafluorobenzene (HFB), 2-propanol (IPA), acetone, and toluene were purchased from Aldrich and used without further purification.

6.3.2. Synthesis of Hydrophilic and Hydrophobic Oligomers with Phenoxide Telechelic Functionality

Fully disulfonated poly(arylene ether sulfone) hydrophilic oligomers (BPS100) and partially fluorinated poly(arylene ether ketone) hydrophobic oligomers (6FK) were synthesized with different number-average molecular weights ($\overline{M_n}$). The oligomers were designed to be terminated with phenoxide end-groups by stoichiometrically off-setting the feed ratios of the monomers. A sample synthesis of 5,000 g/mol BPS100 hydrophilic oligomer is as follows: 8.9720 g (48.2 mmol) of BP, 21.0280 g (42.8 mmol) of SDCDPS and 7.9911 g (57.8 mmol) of K_2CO_3 were charged to a three-necked 250-mL flask

equipped with a condenser, a Dean Stark trap, a nitrogen inlet, and a mechanical stirrer. Then distilled DMAc (120 mL) and toluene (60 mL) were added to the flask and the reaction was heated at 145 °C with stirring. The solution was allowed to reflux at 145 °C while the toluene azeotropically removed the moisture in the system. After 4 h, the toluene was removed from the reaction by stripping off the Dean Stark trap and the reaction temperature was slowly increased to 180 ºC. The reaction was kept at this temperature with nitrogen purging for another 96 h. The reaction solution was cooled to room temperature and filtered to remove salts. The oligomer was coagulated in IPA by pouring the filtered solution. The oligomer was vacuum dried at 110 °C for 24 h. A sample synthesis of 5,000 g/mol 6FK hydrophobic oligomer is as follows: 11.0665 g (50.7 mmol) of 4,4'-difluorobenzophenone, 18.9335 g (56.3 mmol) and 9.3392 g (67.6 mmol) of potassium carbonate were reacted in DMAc at 180 ºC for 36 h. The detailed synthesis and purification procedures for the hydrophobic oligomers are similar to the BPS100 hydrophilic block synthesis.

6.3.3. End-capping of the Hydrophobic Oligomers with Hexafluorobenzene (HFB)

End-capping of the phenoxide terminated 6FK oligomers with HFB was conducted via a nucleophilic aromatic substitution reaction. A typical end-capping reaction of 5,000 g/mol 6FK oligomer is as follows: 5.0000 g (1.0 mmol) of 6FK oligomer and 0.5528 g (4.0 mmol) of potassium carbonate were charged to a three-necked 100-mL flask equipped with a condenser, a Dean Stark trap, a nitrogen inlet, and a mechanical stirrer. Distilled DMAc (50 mL) and cyclohexane (15 mL) were added to the flask. The solution was allowed to reflux at 100 °C to azeotropically remove the

moisture in the system. After 4 h, the cyclohexane was removed from the system. The reaction temperature was lowered to 80 °C and the nitrogen purge was stopped. Then 1.1163 g (6.0 mmol) of HFB was added and the reaction was allowed to proceed for 12 h. The solution was then cooled and filtered. The filtered solution was coagulated in methanol and filtered. The reacted oligomer was dried at 110 °C *in vacuo* for 24 h.

6.3.4. Synthesis of Multiblock Copolymers

The multiblock copolymers were synthesized by coupling HFB end-capped 6FK hydrophobic oligomers and phenoxide terminated BPS100 hydrophilic oligomers. A typical coupling reaction was conducted as follows: 5.0000 g (1.0 mmol) of BPS100 ($\overline{M_n}$ = 5,000 g/mol), 0.5528 g (4.0 mmol) of potassium carbonate, 100 mL of DMAc, and 30 mL of cyclohexane were added to a three-necked 250 mL flask equipped with a condenser, a Dean Stark trap, a nitrogen inlet, and a mechanical stirrer. The reaction mixture was heated at 100 ºC for 4 h to dehydrate the system with refluxing cyclohexane. After removing the cyclohexane, 5.0000 g (1.0 mmol) of vacuum dried HFB end-capped 6FK hydrophobic oligomer ($\overline{M_n}$ = 5,000 g/mol) was added. The coupling reaction was conducted at 105~110 ºC for 24 h. The reaction solution was filtered and precipitated in IPA. The copolymer was purified in a Soxhlet extractor with methanol for 24 h and with chloroform for another 24 h to remove the unreacted hydrophilic and hydrophobic oligomers, respectively. The copolymer was dried at 120 °C *in vacuo* for 24 h.

6.3.5. Characterization

The chemical structures of the oligomers and copolymers were confirmed by ^{1}H NMR analyses on a Varian INOVA 400 MHz spectrometer with DMSO-d_6. In addition, ^{1}H NMR spectroscopy was utilized for end-group analyses of the oligomers to determine their $\overline{M_n}$. Intrinsic viscosities were determined in NMP containing 0.05 M LiBr at 25 ºC using an Ubbelohde viscometer. The ion exchange capacity (IEC) values were determined by titration using a 0.01 M NaOH solution.

6.3.6. Film Casting and Membrane Acidification.

Initial membranes were cast in their salt form by solution casting. The salt form copolymers were dissolved in DMAc (7% w/v) and filtered with syringe filters (0.45 μm Teflon®). The filtered solutions were then cast onto clean glass substrates. The films were dried under an IR ramp at 60 ºC for 1 day, followed by drying *in vacuo* at 110 ºC for 24 h. The acid form membranes were obtained by boiling in 0.5 M sulfuric acid aqueous solution for 2 h, followed by boiling in deionized water for 2 h. The membranes were kept in deionized water at room temperature for 24 h for further characterization.

6.3.7. Determination of Proton Conductivity and Water Uptake.

Fully and partially hydrated proton conductivities were evaluated in a water bath and a humidity-temperature controlled chamber, respectively. The conductivity of the membrane was determined from the geometry of the cell and resistance of the film, which was obtained at the frequency that produced the minimum imaginary response. A Solartron (1252A +1287) impedance/gain-phase analyzer over the frequency range of 10

Hz - 1 MHz was used for the measurements. The membrane water uptake was determined by the weight difference between dry and wet membranes. The vacuum dried membranes were weighed (W_{dry}), and then immersed in deionized water at room temperature for 24 h. The wet membrane was blotted dry and immediately weighed again (W_{wet}). The water uptake of the membranes was calculated according to the following equation.

$$Water\,Uptake\ (\%) = \frac{W_{wet} - W_{dry}}{W_{dry}} \times 100$$

The hydration number (λ), which can be defined as the number of water molecules absorbed per sulfonic acid unit, was determined from the water uptake and the ion content of the dry membrane, according to the following equation.

$$\lambda = \frac{(W_{wet} - W_{dry}) / MW_{H_2O}}{IEC \times W_{dry}} \times 1000$$

where MW_{H2O} is the molecular weight of water (18.01 g/mol).

6.3.8. Atomic Force Microscopy (AFM)

Tapping mode AFM was performed using a Veeco Multimode Atomic Force Microscope. Samples were equilibrated at 30% relative humidity (RH) at room temperature for at least 24 h and sealed before imaging.

6.3.9. Determination of Swelling Ratio

The swelling ratios of the membranes were explored both in-plane and through-plane. The ratios were determined from the dimensional changes from wet to dry state. Membranes were stored in water for 24 h and wet dimensions were measured. The dried dimensions were obtained by drying the wet membrane at 80 ^{o}C in a convection oven for 2 h.

6.4. Results and Discussion

6.4.1. Controlled Molecular Weight Hydrophilic and Hydrophobic Oligomer Synthesis

Hydrophilic and hydrophobic telechelic oligomers with controlled molecular weight were synthesized via step-growth polymerization (Fig. 6.1 and 6.2). The hydrophilic oligomers were fully disulfonated poly(arylene ether sulfone)s (BPS100) and the hydrophobic oligomers were partially fluorinated poly(arylene ether ketone)s (6FK). Controlling the molecular weight and end-group functionality of the oligomers was achieved by offsetting the stoichiometry of the monomers. Because phenoxide terminated hydrophilic and hydrophobic blocks were desired, a calculated excess amount of BP and 6F-BPA was used for the hydrophilic and hydrophobic block synthesis, respectively. Different molecular weight oligomers were prepared ranging from 3 to 20 kg/mol. Determining the molecular weight of the oligomers was conducted by comparing the integrals of the end-groups and the other main peaks on ^{1}H NMR spectra. For the BPS100 hydrophilic block, the phenoxide end-group peaks were located at 6.80 , 7.40, 7.05 and 6.80 ppm (Fig. 6.3). These correspond to the protons on the BP moieties, which bear the phenoxide moieties. Conversely, the peaks at 7.1 and 7.65 were assigned to the protons on the BP moieties, which bear ether linkages with SDCDPS. The number-average molecular weights of oligomers were determined by calculating the ratios of the end group BP and the main chain BP. Using a similar calculation, the number-average molecular weights of the hydrophobic oligomers were determined. On the ^{1}H NMP spectrum of 6FK oligomer (Fig. 6.4), the two small peaks at 6.73 and 7.03 ppm were assigned to the terminal 6F-BPA moieties, while 6F-BPA moieties in the middle of the chain were assigned to the peaks at 7.20 and 7.48 ppm. The target and actual molecular

weights of the oligomers are summarized in Table 6.1, along with their determined intrinsic viscosities. When a log-log plot between intrinsic viscosity and number-average molecular weight was generated, it showed a linear relationship, thereby confirming that the molecular weight for both the hydrophilic and hydrophobic block series was successfully controlled (Fig. 6.5).

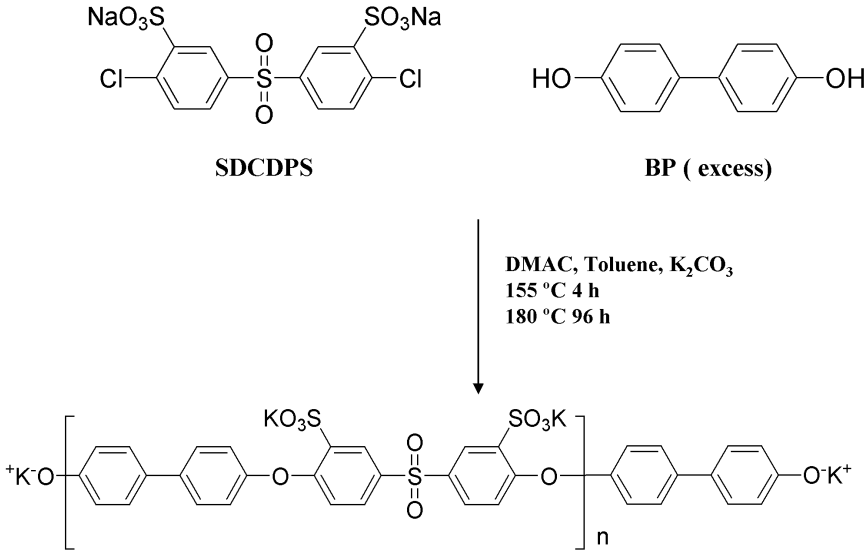

Figure 6. 1. Synthesis of a Phenoxide Terminated, Fully Disulfonated Poly(arylene ether sulfone) (BPS100) Hydrophilic Oligomer.

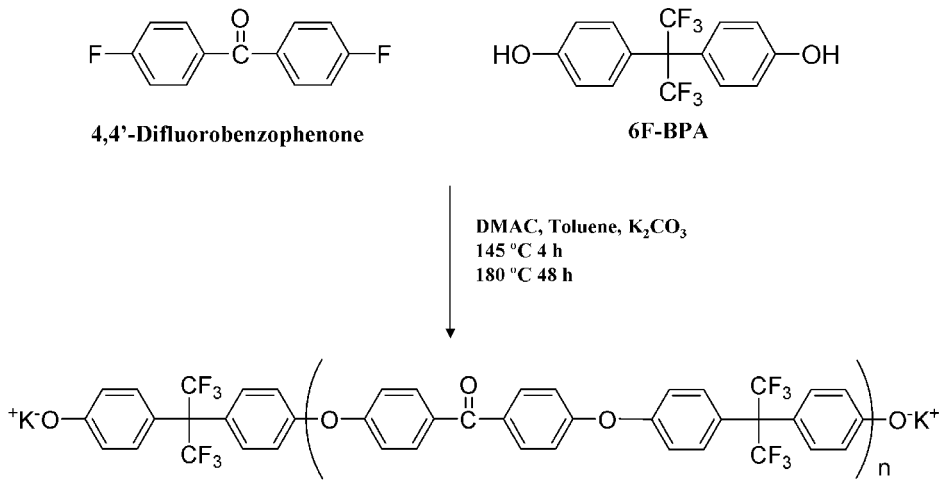

Figure 6. 2. Synthesis of a Partially Fluorinated Poly(arylene ether ketone) (6FK) Hydrophobic Oligomer with Phenoxide Telechelic Functionality.

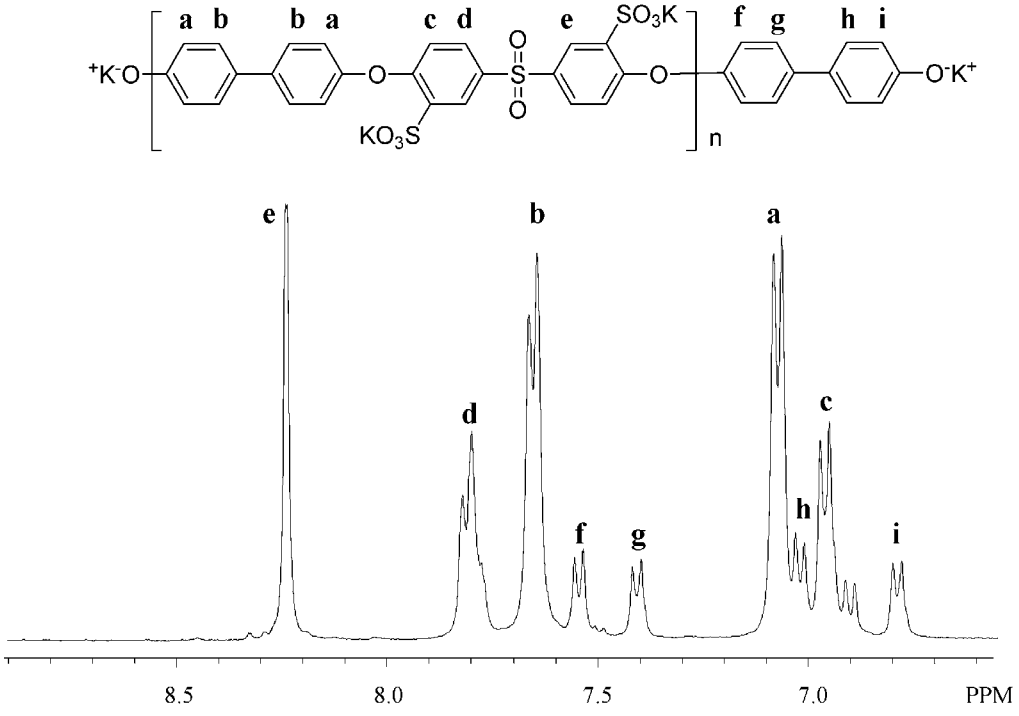

Figure 6. 3. ^{1}H NMR Spectrum of Phenoxide Terminated BPS100 Hydrophilic Oligomer.

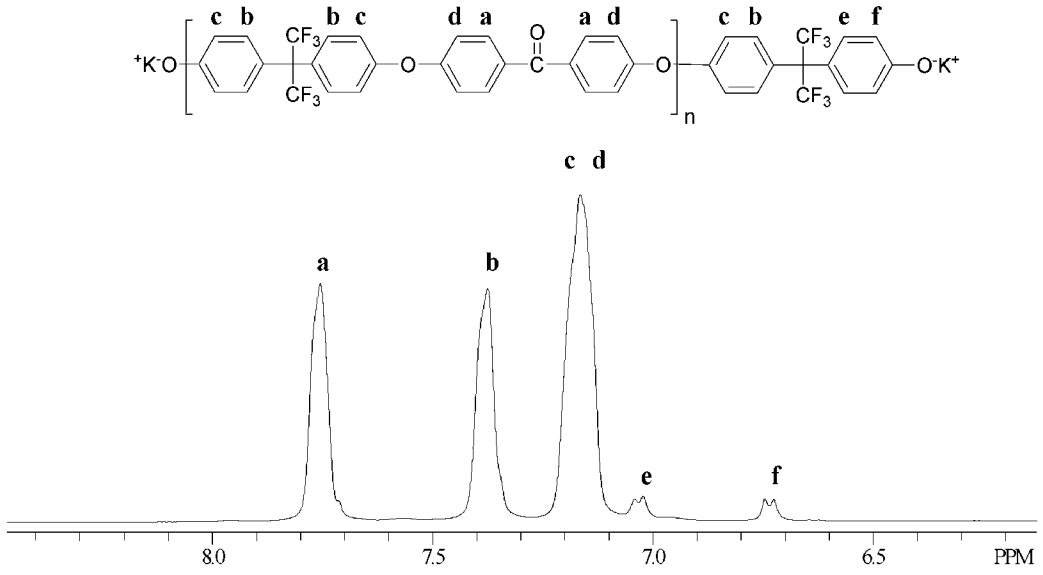

Figure 6. 4. ^{1}H NMR Spectrum of Phenoxide Terminated 6FK Hydrophobic Oligomer.

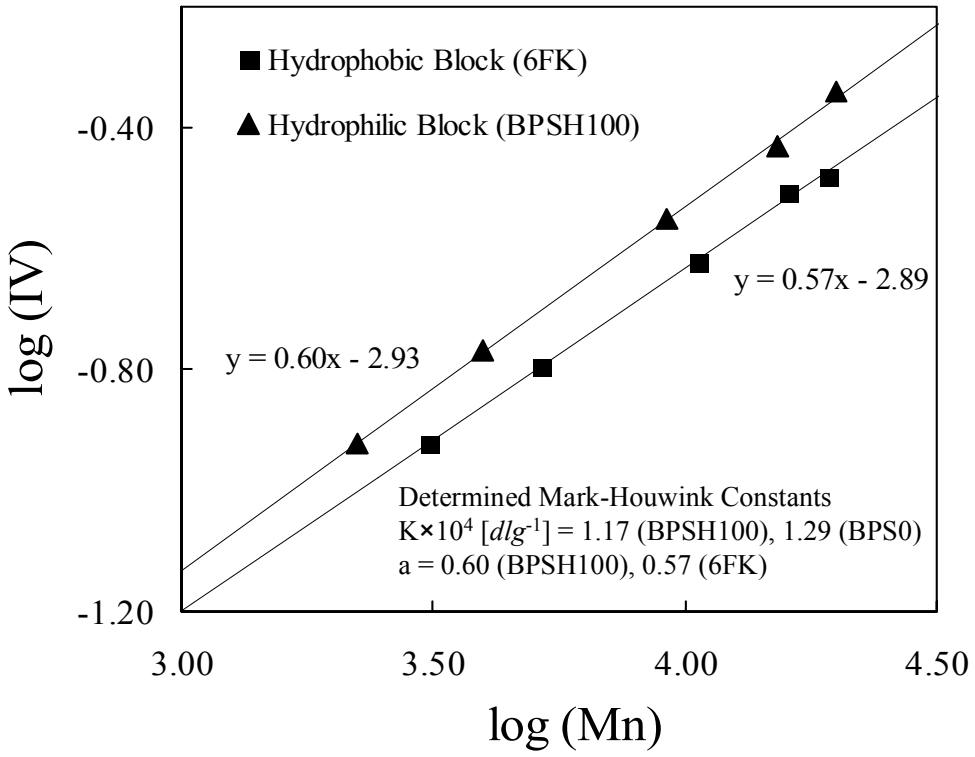

Figure 6. 5. Double Logarithmic Plot of [η] versus M_n of Hydrophilic (BPS100) and Hydrophobic (6FK) Oligomers. Intrinsic Viscosity was Measured in NMP with 0.05 M LiBr at 25 ºC.

Table 6. 1. Characterization of Hydrophilic and Hydrophobic Telechelic Oligomers.

Target M_n **(g mol^{-1})**	**Hydrophilic Blocks**		**Hydrophobic Blocks**	
	M_n (g mol^{-1})[a]	**IV (dL g^{-1})[b]**	**M_n (g mol^{-1})[a]**	**IV (dL g^{-1})[b]**
3,000	3,200	0.12	3,100	0.12
5,000	4,800	0.17	5,200	0.16
10,000	9,200	0.28	10,600	0.24
15,000	15,300	0.37	15,900	0.31
20,000	20,000	0.46	19,200	0.33

[a] Determined by ^{1}H NMR.

[b] In NMP with 0.05 M LiBr at 25 ºC.

6.4.2. End-capping of the Hydrophobic Oligomers

Phenoxide terminated 6FK hydrophobic oligomers were end-capped with hexafluorobenzene (HFB) to facilitate a coupling reaction with the phenoxide terminated BPS100 hydrophilic blocks (Fig. 6.6). Due to the high volatility of HFB, the reaction was conducted around the boiling point of HFB without a nitrogen purge to achieve both high reaction kinetic and minimal loss of HFB. The highly reactive nature of HFB allowed the completion of the reaction at low temperature, which was confirmed by ^{1}H NMR spectra (Fig. 6.7). As seen from the NMR spectrum of the end-capped oligomer, the phenoxide end-group peaks completely disappeared at 6.73 and 7.03. New peaks were found at 7.23 and 7.33, which can be assigned to the protons on 6F-BPA moieties connected with HFB. Because HFB is not a unifunctional but rather a multifunctional molecule, it was possible that the HFB was acting as a chain-extender between the hydrophobic oligomers via inter-oligomer coupling to form high molecular weight polymers. To eliminate this possibility, excess amounts of HFB toward the phenoxide end-groups were used. Since the equivalent amount of HFB needed to end-cap a single 6FK oligomer is 2, the theoretical molar ratio between HFB and 6FK oligomer is 2:1. However, in order to avoid an inter-oligomer coupling reaction, the actual molar ratio used was 6:1. Once the end-capping reaction had completed, we determined the intrinsic viscosities of the end-capped oligomers and compared them to their original values (Table 6.2). Although minor incremental increases were observed with the end-capped oligomers, this was likely due to the chain length extension by the HFB, rather than inter-oligomer coupling.

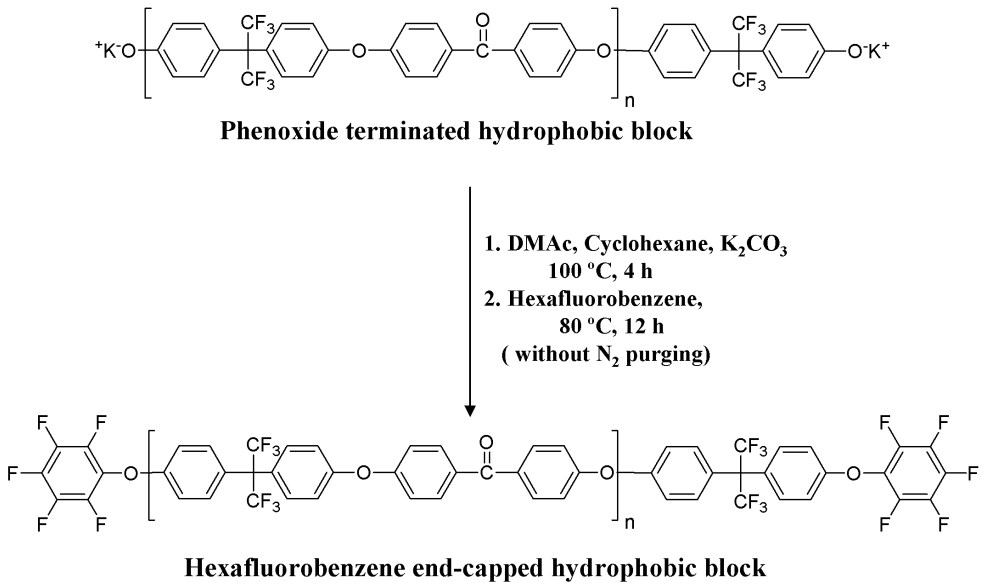

Figure 6. 6. End-capping of a Phenoxide Terminated 6FK Hydrophobic Oligomer with HFB.

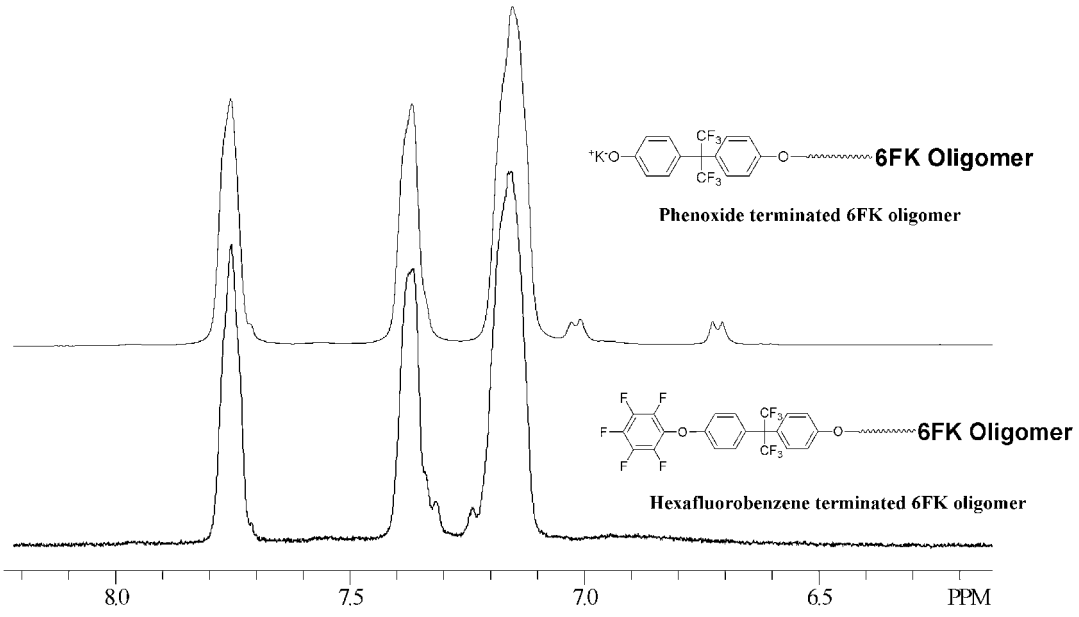

Figure 6. 7. [1]H NMR Spectra of 6FK and HFB End-capped 6FK Hydrophobic Oligomers.

Table 6. 2. Intrinsic Viscosities of 6FK Hydrophobic Blocks Before and After End-capping.

M_n[a] (g mol^{-1})	Initial IV (dL g^{-1})[b]	IV after end-capping (dL g^{-1})[b]
5,200	0.16	0.17
10,600	0.24	0.28
15,900	0.31	0.36
19,200	0.33	0.34

[a] Determined by ^{1}H NMR.
[b] In NMP with 0.05 M LiBr at 25 ºC.

6.4.3. Synthesis of BPSH-6FK Multiblock Copolymers

Multiblock copolymers with various block lengths were synthesized by coupling the phenoxide terminated BPS100 and the HFB end-capped 6FK oligomers (Fig. 6.8). Hereafter, an acronym for the multiblock copolymer—namely BPSHx-6FKy—will be used, where the BPSH and 6FK imply the hydrophilic and hydrophobic oligomers while the x and y denote the number-average molecular weights of the reacted oligomers in Kg/mol unit. The coupling reaction was conducted at 105 ºC, which was low enough to prevent possible trans-etherification. Since low temperature boiling HFB was already attached to the 6FK hydrophobic oligomers, it was not necessary to conduct the coupling reaction at 80 ºC. The completion of the coupling reaction was confirmed by comparing the ^{1}H NMR spectra of the oligomers with that of the copolymers. As shown on the ^{1}H NMR spectrum of the copolymer, the phenoxide end group peaks on the BPS100 oligomers at 6.80, 7.40, 7.05 and 6.80 ppm completely disappeared. This means that all

the phenoxide end-groups reacted with the HFB on the 6FK hydrophobic oligomers to form multiblock copolymers (Fig. 6.9).

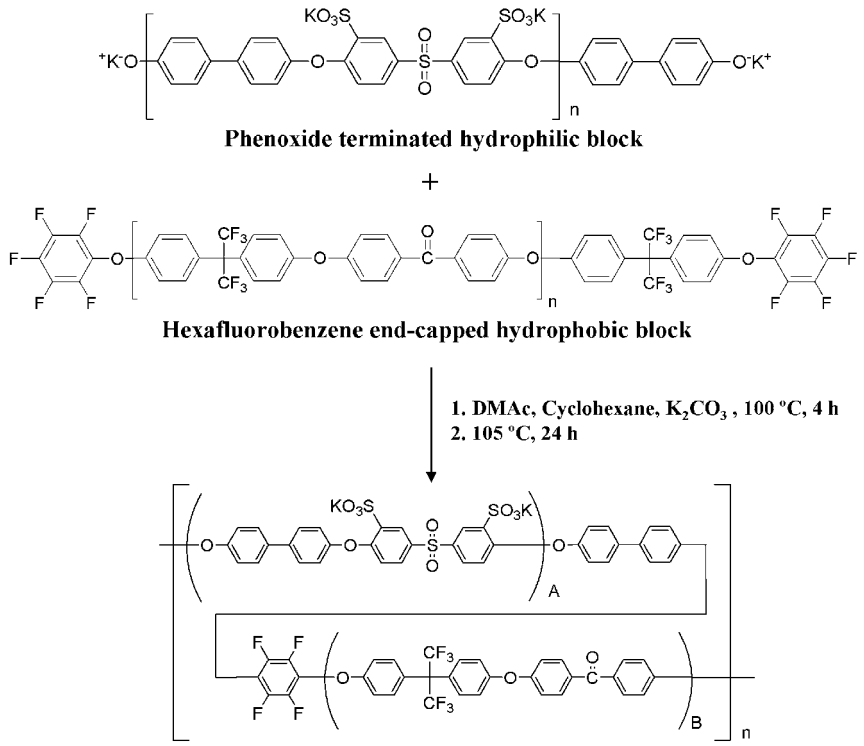

Figure 6. 8. Synthesis of Segmented Sulfonated Multiblock Copolymers (BPSH-6FK) with HFB Linkage Group.

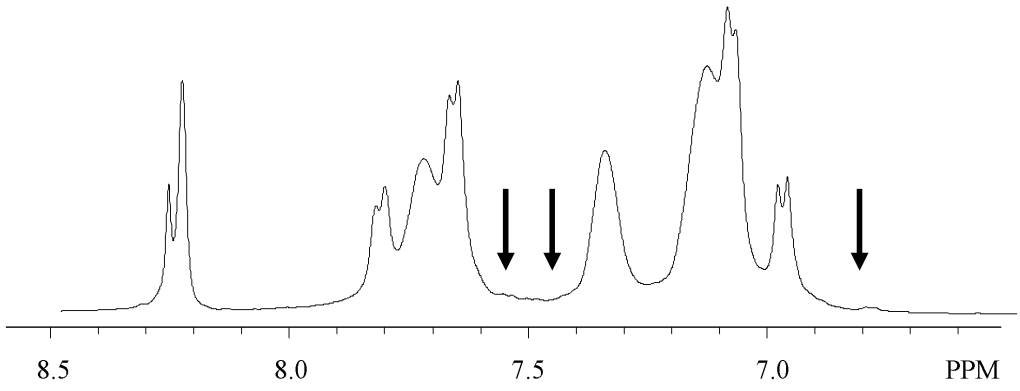

Figure 6. 9. [1]H NMR Spectrum of BPSH3-6FK3. Black Arrows Indicate the Disappearance of the End groups on the Hydrophilic Blocks after the Coupling Reaction with Fluorine-terminated Hydrophobic Blocks.

6.4.4. Characterization of Membrane Properties of BPSH-BPS Multiblock Copolymers

Ten BPSH-6FK multiblock copolymers with different block lengths were systematically synthesized and their fundamental membrane properties were evaluated, which are summarized in Table 6.3, along with values for the control PEM materials, Nafion 112 and BPSH35. The multiblock copolymers were categorized into three subgroups according to their IEC values. The low IEC copolymers displayed longer hydrophobic block lengths compared to the hydrophilic blocks, with IEC values ranging from 1.01-1.33 meq/g. The medium IEC copolymers displayed equal hydrophilic and hydrophobic block lengths, with IEC values of around 1.5 meq/g. And the copolymers with high IEC values displayed longer hydrophilic block lengths compared to the hydrophobic blocks. In each subgroup, different block length copolymers with similar IEC values were prepared to evaluate the effect of hydrophobic-hydrophobic block length on membrane properties.

Table 6. 3. Properties of BPSH–BPS Multiblock Copolymers in the Sulfonic Acid Form.

Copolymers	Calculated IEC (meq g^{-1})	Experimental IEC (meq g^{-1})[a]	Intrinsic Viscosity (dL g^{-1})[b]	Water Uptake (%)	Conductivity (S cm^{-1})[c]	Hydration Number (λ)
Nafion 112	-	0.90	-	25	0.090	15.0
BPSH 35	1.53	1.50	0.70	36	0.070	13.3
BPSH 5 – 6FK 10	1.03	1.01	0.62	23	0.04	13
BPSH 10 – 6FK 15	1.21	1.32	0.80	20	0.07	8
BPSH 15 – 6FK 20	1.47	1.33	0.65	45	0.10	19
BPSH 3 – 6FK 3	1.68	1.51	0.78	31	0.08	12
BPSH 5 – 6FK 5	1.59	1.53	0.62	69	0.10	25
BPSH 10 – 6FK 10	1.54	1.48	0.88	81	0.11	30
BPSH 15 – 6FK 15	1.62	1.34	0.70	100	0.12	41
BPSH 10 – 6FK 5	2.11	1.86	0.94	300	0.06	90
BPSH 15 – 6FK 10	1.96	1.70	0.60	170	0.08	55
BPSH 20 – 6FK 15	1.84	1.70	0.72	178	0.09	58

[a] Determined by titration with NaOH.
[b] In NMP with 0.05 M LiBr at 25 ºC.
[c] Measured in deionized water at 30 ºC.

The IEC values for all the copolymers were determined by titration and subsequently compared with their theoretical values. The similar IEC vs. theoretical values confirmed the successful coupling reaction between the hydrophilic and hydrophobic oligomers. The intrinsic viscosity of the copolymers ranged from 0.6 to 0.94 dL/g, which was sufficiently high to obtain tough ductile membranes. As expected, the water uptake results for the multiblock copolymers were strongly dependent on their IEC

values, which is associated with increased ionic moieties in the system. In addition to the impact of IEC, the water uptake behavior of the multiblock copolymers was also strongly influenced by hydrophilic and hydrophobic block lengths. Specifically, the water uptake values for the multiblock copolymers with similar IECs increased with increasing block length. For example, the BPSH3-6FK3, BPSH5-6FK5, and BPSH10-6FK10 copolymers displayed very similar IEC values of around 1.5 meq/g. If water uptake is exclusively dependent on IEC, then the water uptake values for these copolymers should have been very similar. However, the results showed that water uptake was strongly influenced by the hydrophilic and hydrophobic block lengths, which increased from 31% for the BPSH3- 6FK3, to 81% for the BPSH10- 6FK10. It should be noted that while the BPSH15- 6FK15 displayed somewhat lower IEC (1.34 meq/g) than other equal length block copolymers, its water uptake was even higher than that of the BPSH10-6FK10.

A similar trend was observed with respect to proton conductivity measurements for the equal block length multiblock copolymers. The lowest conductivity measurement was 0.08 S/Cm for the shortest block length copolymer (BPSH3-6FK3), and then increased with increasing block length. The longest block length copolymer (BPSH 15-6FK 15) displayed the highest conductivity of 0.12 S/Cm. Based on the results, it is proposed that the observed increases in both water uptake and conductivity were influenced by morphological changes in the multiblock copolymer. Because the ionic compositions were similar, any change in properties with increasing block length would inevitably result from the expected increase in phase separation between the hydrophobic and hydrophilic phases in these multiblock copolymers.

Figure 6.10 shows the relationship between temperature and the proton conductivity of the fully hydrated multiblock copolymers. As clearly demonstrated, proton conductivity increased with increasing temperature, reaching 185 mS/Cm at 80 ºC for the BPSH10-6FK10. Moreover, the conductivity-temperature slope for each of the copolymers is similar, implying that the copolymers have a similar conduction mechanism. Compared with Nafion 112, the multiblock copolymers displayed a slightly lower temperature dependence on proton conductivity.

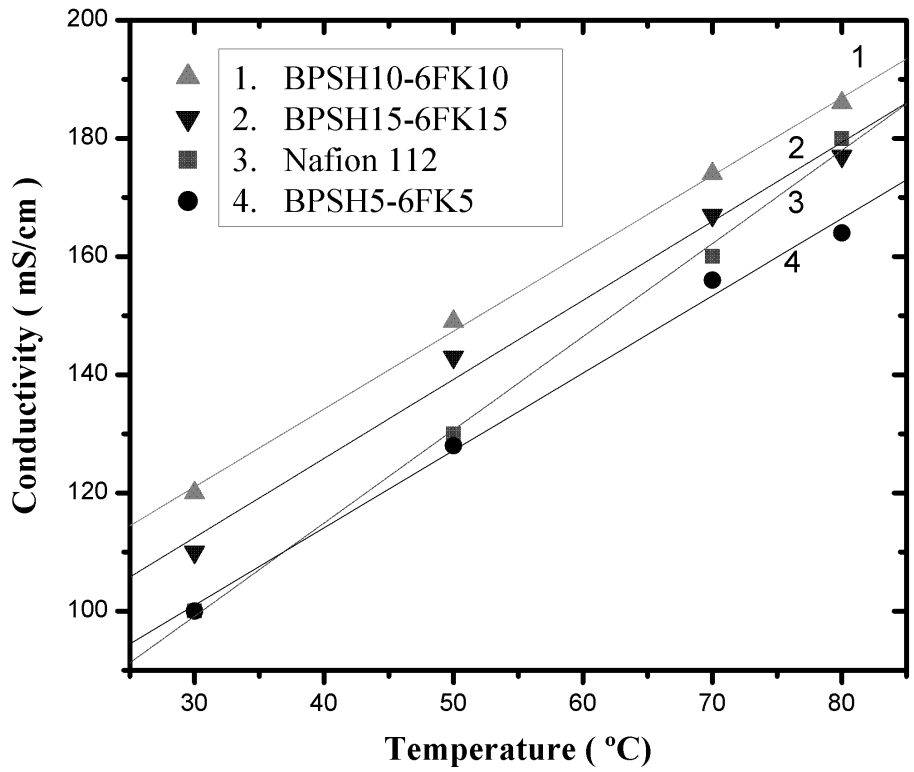

Figure 6. 10. Proton Conductivities of BPSH-6FK and Nafion112 in Terms of Temperature

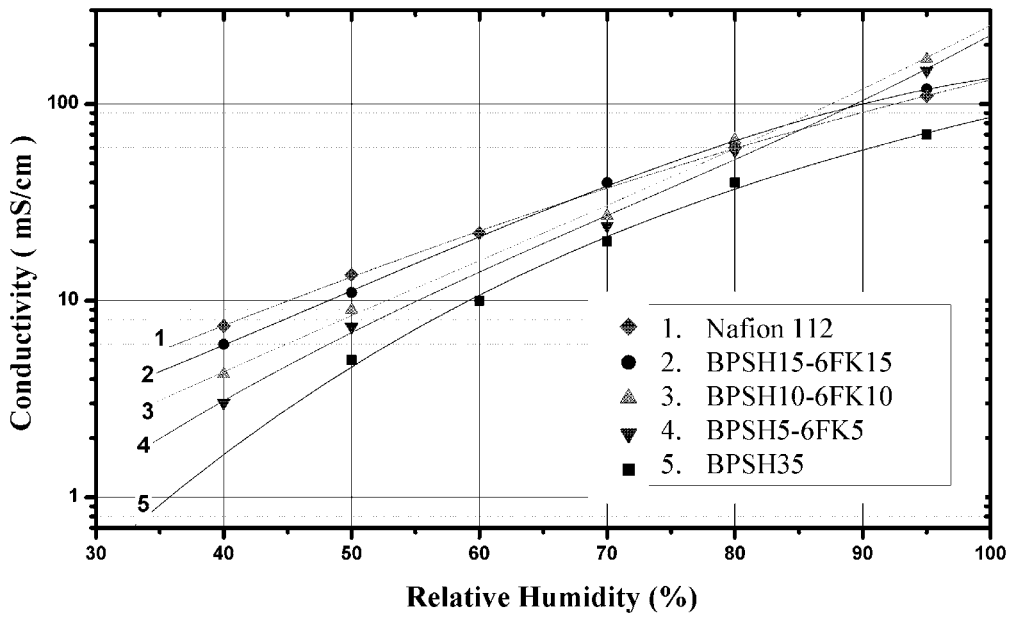

Figure 6. 11. Proton Conductivities of BPSH-6FK and Nafion112 under Partially Hydrated Conditions at 80 ºC

Proton conductivity as a function of relative humidity (RH) at 80 ºC was studied (Fig. 6.11). As shown in the figure, the proton conductivity of the BPSH35 random copolymer dropped rapidly at lower RH values. Although BPSH35 demonstrated acceptable proton conductivity under fully hydrated conditions on account of sufficient water content, its proton conductivity under partially hydrated conditions decreased significantly due to the scattered hydrophilic domains in the random copolymer. In short, the absence of the hydrophilic domain connectivity and insufficient water content in the membrane was unable to maintain high proton conduction under partially hydrated conditions.

Conversely, the performance of the multiblock copolymers under partially hydrated conditions was superior to the random copolymer, and also improved with increasing block lengths. For example, the conductivity of the BPSH15–6FK15 under

partially hydrated conditions was comparable to that of Nafion 112. This performance improvement seems to be related to the formation of well-connected hydrophilic channels at higher block lengths. By forming continuous hydrophilic channels in the membranes, proton transport behavior can be significantly enhanced, especially under partially hydrated conditions.

Figure 6.12 shows AFM phase images of the BPSH-6FK multiblock copolymers with different block lengths. The bright and dark regions in the images correspond to hard hydrophobic and soft hydrophilic segments, respectively. Although no distinct phase-separation was observed for the BPSH5-6FK5 system (Figure 6.12 (a)), enhancements in connectivity of hydrophilic domain were found in longer block lengths multiblock systems (Figure 6.12 (b), (c)). Thus, by utilizing the well-connected hydrophilic regime for proton conduction, improved proton conductivity under partially hydrated conditions was achieved.

Another phenomenon that can be related to morphological changes in the copolymer is swelling ratio. Table 6.4 shows the swelling ratios of the BPSH-6FK multiblock copolymers in comparison with the BPSH35 and Nafion controls. The x,y represent the in-plane swelling and z represents the through-plane swelling ratios. All the multiblock copolymers showed anisotropic swelling behaviors, while the BPSH 35 random copolymer and Nafion (NRE211) exhibited isotropic behaviors. Although the in-plane swelling ratios of the multiblock copolymers were very similar with no significant dependency on block length, the through-plane swelling ratios were strongly influenced by block length. Specifically, the swelling ratios increased from 15% to 66% with increasing block length from 5 Kg/mol to 15 Kg/mol. The increase in water uptake and

through-plane swelling with increasing block length suggests the formation of ordered hydrophilic domains within the membranes. In addition, the lower in-plane swelling ratios for the higher block length copolymers could be beneficial for reducing mechanical fatigue during swelling-deswelling cycling operation under low RH conditions.

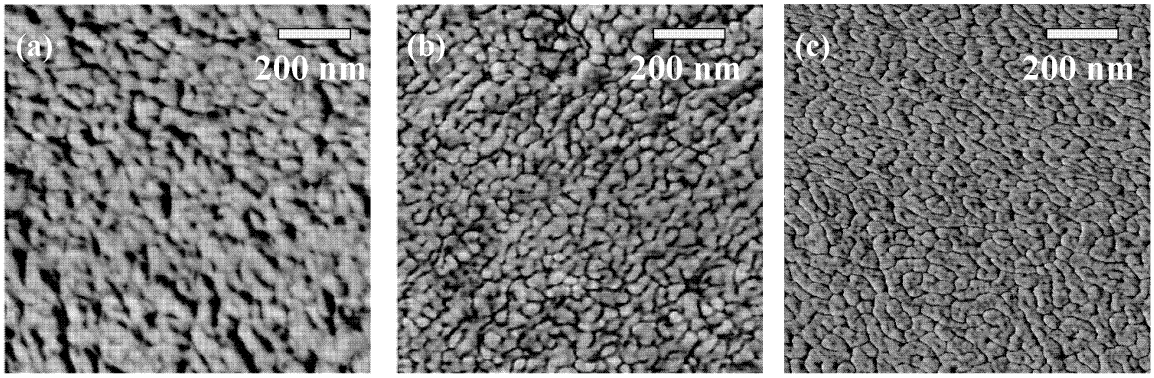

Figure 6. 12. AFM Phase Images of BPSH-6FK Multiblock Copolymers. (a) BPSH3-6FK3, (b) BPSH10-6FK10, and (c) BPSH10-6FK15.

Table 6. 4. Swelling Behavior of BPSH–6FK Multiblock Copolymers.

Copolymers	X direction[a] (%)	Y direction[a] (%)	Z direction[b] (%)	Volume (%)
Nafion 211	15	16	18	57
BPSH 35	15	16	16	55
BPSH 3 – 6FK 3	9	9	15	37
BPSH 5 – 6FK 5	12	15	26	62
BPSH 10 – 6FK 10	10	10	37	66
BPSH 15 – 6FK 15	7	9	66	94

[a] In-plane (length) swelling ratio
[b] Through-plane (thickness) swelling ratio

6.5. Conclusions

Multiblock copolymers with hydrophilic-hydrophobic sequences were developed as potential materials for proton exchange membranes. For systematic synthesis of the multiblock copolymers, various block lengths fully disulfonated poly(arylene ether sulfone) and partially fluorinated poly(arylene ether ketone) were prepared as hydrophilic and hydrophobic oligomers, respectively, and coupled to produce the multiblock copolymers. To minimize a possible sequence randomization during the coupling reaction, the highly reactive perfluorinated small molecule, hexaflurobenzene (HFB), was utilized as a linkage group. Due to its high reactivity, the coupling reaction could be performed at 105 ºC. The copolymers produced tough ductile membranes via DMAc solution casting. Resulting proton conductivity and water uptake measurements revealed that changes in hydrophilic and hydrophobic block length influenced membrane properties at similar IEC values by forming nanophase separated morphologies. The multiblock copolymer membranes showed highly anisotropic swelling behavior in comparison to the random copolymers, which were isotropic.

Aknowledgements

The authors thank the Department of Energy (DE-FG36-06G016038) for its support of this research.

6.6. References

1. Banerjee, Shoibal; Curtin, Dennis E. Nafion perfluorinated membranes in fuel cells. *Journal of Fluorine Chemistry* **2004,** 125, (8), 1211-1216.
2. Mauritz, Kenneth A.; Moore, Robert B. State of understanding of Nafion. *Chemical Reviews (Washington, DC, United States)* **2004,** 104, (10), 4535-4585.
3. Kim, Yu Seung; Dong, Limin; Hickner, Michael A.; Glass, Thomas E.; Webb, Vernon; McGrath, James E. State of Water in Disulfonated Poly(arylene ether sulfone) Copolymers and a Perfluorosulfonic Acid Copolymer (Nafion) and Its Effect on Physical and Electrochemical Properties. *Macromolecules* **2003,** 36, (17), 6281-6285.
4. Savadogo, O. Emerging membranes for electrochemical systems Part II. High temperature composite membranes for polymer electrolyte fuel cell (PEFC) applications. *Journal of Power Sources* **2004,** 127, (1-2), 135-161.
5. Rusanov, Alexandre L.; Likhatchev, Dmitri; Kostoglodov, Petr V.; Mullen, Klaus; Klapper, Markus. Proton-exchanging electrolyte membranes based on aromatic condensation polymers. *Advances in Polymer Science* **2005,** 179, (Inorganic Polymeric Nanocomposites and Membranes), 83-134.
6. Hamrock, Steven J.; Yandrasits, Michael A. Proton exchange membranes for fuel cell applications. *Polymer Reviews (Philadelphia, PA, United States)* **2006,** 46, (3), 219-244.
7. Hickner, Michael A.; Ghassemi, Hossein; Kim, Yu Seung; Einsla, Brian R.; McGrath, James E. Alternative Polymer Systems for Proton Exchange Membranes (PEMs). *Chemical Reviews (Washington, DC, United States)* **2004,** 104, (10), 4587-4611.
8. Wang, Feng; Ji, Qing; Harrison, William; Mecham, Jeff; McGrath, James E.; Formato, R.; Kovar, R. Synthesis of sulfonated poly(arylene ether sulfone)s via direct polymerization. *Book of Abstracts, 219th ACS National Meeting, San Francisco, CA, March 26-30, 2000* **2000**, POLY-151.
9. Wang, Feng; Hickner, Michael; Kim, Yu Seung; Zawodzinski, Thomas A.; McGrath, James E. Direct polymerization of sulfonated poly(arylene ether sulfone) random (statistical) copolymers: candidates for new proton exchange membranes. *Journal of Membrane Science* **2002,** 197, (1-2), 231-242.
10. Sangeetha, Dharmalingam. Sulphonated poly(ether ether ketone) proton exchange membranes for fuel cell applications. *International Journal of Polymeric Materials* **2007,** 56, (5), 535-548.
11. Li, Xianfeng; Zhao, Chengji; Lu, Hui; Wang, Zhe; Na, Hui. Direct synthesis of sulfonated poly(ether ether ketone ketone)s (SPEEKKs) proton exchange membranes for fuel cell application. *Polymer* **2005,** 46, (15), 5820-5827.
12. Nakabayashi, Kazuhiro; Matsumoto, Kazuya; Shibasaki, Yuji; Ueda, Mitsuru. Synthesis and properties of sulfonated poly(2,5-diphenethoxy-p-phenylene). *Polymer* **2007,** 48, (20), 5878-5883.
13. Wu, Shuqing; Qiu, Zhiming; Zhang, Suobo; Yang, Xiurong; Yang, Fan; Li, Zhiying. The direct synthesis of wholly aromatic poly(p-phenylene)s bearing

sulfo benzoyl side groups as proton exchange membranes. *Polymer* **2006,** 47, (20), 6993-7000.

14. Kreuer, K. D. On the development of proton conducting polymer membranes for hydrogen and methanol fuel cells. *Journal of Membrane Science* **2001,** 185, (1), 29-39.
15. Lee, Hae-Seung; Roy, Abhishek; Badami, Anand S.; McGrath, James E. Synthesis and characterization of sulfonated poly(arylene ether) polyimide multiblock copolymers for proton exchange membranes. *Macromolecular Research* **2007,** 15, (2), 160-166.
16. Lee, Hae-Seung; Badami, Anand S.; Roy, Abhishek; McGrath, James E. Segmented Sulfonated Poly(arylene ether sulfone)-b-Polyimide Copolymers for Proton Exchange Membrane Fuel Cells. I. Copolymer Synthesis and Fundamental Properties. *Journal of Polymer Science, Part A: Polymer Chemistry* **2007,** 45, (21), 4879-4890.
17. Roy, Abhishek; Lee, Hae-Seung; McGrath, James E. Hydrophilic-hydrophobic multiblock copolymers based on poly(arylene ether sulfone)s as novel proton exchange membranes - Part B. *Polymer* **2008,** 49, (23), 5037-5044.
18. Lee, Hae-Seung; Roy, Abhishek; Lane, Ozma; Dunn, Stuart; McGrath, James E. Hydrophilic-hydrophobic multiblock copolymers based on poly(arylene ether sulfone) via low-temperature coupling reactions for proton exchange membrane fuel cells. *Polymer* **2008,** 49, (3), 715-723.
19. Wang, Hang; Badami, Anand S.; Roy, Abhishek; McGrath, James E. Multiblock copolymers of poly(2,5-benzophenone) and disulfonated poly(arylene ether sulfone) for proton-exchange membranes. I. Synthesis and characterization. *Journal of Polymer Science, Part A: Polymer Chemistry* **2006,** 45, (2), 284-294.
20. Yu, Xiang; Roy, Abhishek; Dunn, Stuart; Yang, Juan; McGrath, James E. Synthesis and characterization of sulfonated-fluorinated, hydrophilic-hydrophobic multiblock copolymers for proton exchange membranes. *Macromolecular Symposia* **2006,** 245/246, (World Polymer Congress--MACRO 2006), 439-449.
21. Li, Yanxiang; Roy, Abhishek; Badami, Anand S.; Hill, Melinda; Yang, Juan; Dunn, Stuart; McGrath, James E. Synthesis and characterization of partially fluorinated hydrophobic-hydrophilic multiblock copolymers containing sulfonate groups for proton exchange membrane. *Journal of Power Sources* **2007,** 172, (1), 30-38.
22. Sankir, M.; Bhanu, V. A.; Harrison, W. L.; Ghassemi, H.; Wiles, K. B.; Glass, T. E.; Brink, A. E.; Brink, M. H.; McGrath, J. E. Synthesis and characterization of 3,3'-disulfonated-4,4'-dichlorodiphenyl sulfone (SDCDPS) monomer for proton exchange membranes (PEM) in fuel cell applications. *Journal of Applied Polymer Science* **2006,** 100, (6), 4595-4602.
23. Li, Yanxiang; VanHouten, Rachael A.; Brink, Andrew E.; McGrath, James E. Purity characterization of 3,3'-disulfonated-4,4'-dichlorodiphenyl sulfone (SDCDPS) monomer by UV-vis spectroscopy. *Polymer* **2008,** 49, (13-14), 3014-3019.

CHAPTER 7

Development of Multiblock Copolymers with Novel Hydroquinone-Based Hydrophilic Blocks for Proton Exchange Membrane (PEM) Applications

Hae-Seung Lee, Ozma Lane, and James E. McGrath*

Macromolecules and Interfaces Institute,

Macromolecular Science and Engineering,

Virginia Polytechnic Institute and State University, Blacksburg, VA 24061

*Correspondence to: James E. McGrath

(Email: jmcgrath@vt.edu, Phone: 540-231-5976, Fax: 540-231-8517)

7.1. Abstract

Hydrophilic-hydrophobic sequenced multiblock copolymers were synthesized and evaluated for use as proton exchange membranes (PEMs). The multiblock copolymers were prepared by a coupling reaction between fully disulfonated hydroquinone based hydrophilic oligomers (HQS100) and unsulfonated poly(arylene ether sulfone) hydrophobic oligomers (BPS0). The hydroquinone-based hydrophilic oligomers possess several advantages over previously utilized biphenol-based hydrophilic oligomers (BPS100), including higher hydrophilicity, enhanced nano-phase separation with hydrophobic segments, and lower cost. To maintain the hydrophilic-hydrophobic sequences in the system, the coupling reactions were conducted at low temperature (e.g., 105 °C) to avoid ether-ether exchange reactions. The coupling reaction was solvent sensitive due to a low reactivity of the hydroquinone-phenoxide end-group on the HQS100. All copolymers produced tough ductile films when cast from an NMP or DMF solution. Fundamental membrane parameters including water uptake, proton conductivity, and swelling ratio were investigated along with morphology characterizations by atomic force microscopy (AFM).

Keywords: Multiblock copolymers; Sulfonated poly(arylene ether sulfone); Proton exchange membranes

7.2. Introduction

Over the last decade, a substantial body of research has been devoted to developing novel proton exchange membranes (PEMs) which can replace the state-of-the-art Nafion®. Among a variety of candidates, wholly aromatic high temperature polymers have been considered to be the most promising materials.[1-3] The major advantages for utilizing high temperature polymers for fuel cell applications include their excellent thermal and oxidative stability, as well as the fact that they are economical and easy to produce. The most extensively studied materials are the so-called BPSH-type materials, which are statistical random copolymers based on disulfonated poly(arylene ether sulfone)s.[4-6] BPSH-type copolymer systems utilize 3,3'-disulfonated-4,4'-dichlorodiphenylsulfone (SDCDPS) as the key monomer, which can facilitate precise control over the degree of sulfonation, and excellent stability of the sulfonic acid moieties.[2,7] Although PEMs based on BPSH-type materials display improved properties over Nafion® under fully hydrated conditions with respect to conductivity, durability, and fuel cross-over, their proton conductivities under partially hydrated conditions have remained somewhat disappointing. This could be due to the fact that the proton conduction channels in sulfonated hydrocarbon-based materials are narrower than those of Nafion-type materials, which accounts for the significant reduction in conductivity under low humidity conditions.[8,9] A number of strategies have been used to address this problem, including (1) the partial fluorination of the aromatic polymer backbone to form a sharp phase separation,[10,11] (2) the incorporation of bulky pendent groups to increase free-volume,[12, 13] (3) the addition of hydrophilic nano-particles to help retain water,[14] and (4) the addition of heteropolyacid (HPA).[15] Although each of these approaches was

somewhat beneficial in increasing proton conductivity under low RH conditions, none of these methods could overcome important fundamental limitations.

Recently, PEMs based on hydrophilic-hydrophobic sequenced multiblock copolymers have been considered as strong candidates for overcoming limited proton conduction under partially hydrated conditions.[16-21] These multiblock copolymers utilize fully disulfonated biphenol-based poly(arylene ether sulfone) as the hydrophilic block (BPSH100), with various engineering materials used as the hydrophobic block. These multiblock copolymer-based PEMs exhibit nano-phase separated morphologies and well-connected ionic hydrophilic phases. As such, they can facilitate high proton conductivity even under low relative humidity conditions, while the well-connected hydrophobic phase can provide dimensional stability.[16,22,23] A number of extensive structure-property studies revealed that property enhancements can be strongly influenced by the length of the hydrophilic and hydrophobic blocks. Generally, proton conductivity and water uptake increase with increasing hydrophilic and hydrophobic block length by forming long-range co-continuous lamellae morphologies.[16,22,24] Even though the multiblock copolymers based on BPSH100 hydrophilic block were comparable or superior to Nafion with respect to proton conductivity under low humidity conditions, we were unable to achieve even higher conductivity by solely increasing IEC values.[22] Increasing the volume fraction of hydrophilic segments in a system in order to improve IEC values produces a decrease in the hydrophobic segment volume fraction, resulting in poor mechanical properties and excess swelling behavior. In other words, a balancing act is hard to achieve for maintaining both high IEC and advantageous mechanical properties.

A possible solution to this dilemma is utilizing a more hydrophilic (e.g., higher IEC) block for the multiblock copolymer system. When a higher IEC hydrophilic oligomer is used to obtain an IEC multiblock copolymer, the amount of the higher IEC hydrophilic block should be less than that of lower IEC hydrophilic block to obtain the target IEC. Using the same logic, if the feed ratio of the hydrophilic and hydrophobic blocks is fixed, a higher IEC hydrophilic block system will incorporate more sulfonic acid moieties in the multiblock copolymers. As a result, one can increase the IEC values of the multiblock copolymers without scarifying the volume fraction of hydrophobic segments, which plays an important role in producing desirable mechanical properties. In addition, higher IEC hydrophilic blocks can lead a sharper phase separation in the copolymer membrane due to the increased hydrophilic-hydrophobic contrast.

This chapter, therefore, describes the synthesis and characterization of a novel multiblock copolymer system with hydroquinone-based hydrophilic oligomers. The fully disulfonated hydroquinone based poly(arylene ether sulfone) hydrophilic oligomer (HQSH100) has an IEC of 3.89 meq/g, which is approximately 20% higher than that of BPSH100. A series of multiblock copolymers with HQSH100 hydrophilic blocks was synthesized, and their fundamental membrane properties and morphology will be described.

7.3. Experimental

7.3.1. Materials

Monomer grade 4,4'-dichlorodiphenylsulfone (DCDPS), 4,4'-biphenol(BP) were provided by Solvay Advanced Polymers and Eastman Chemical, respectively, and were dried *in vacuo* at 110 °C prior to use. Hydroquinone (HQ) was purchased from Aldrich and was purified by sublimation under reduced pressure. The sulfonated comonomer 3,3'-disulfonated-4,4'-dichlorodiphenylsulfone (SDCDPS) was synthesized and purified according to previously reported procedures.[7] The purity of SDCDPS was determined by UV-Vis spectroscopy.[25] Hexafluorobenzene (HFB) and potassium carbonate were purchased from Aldrich and used without further purification. N-methyl-2-pyrrolidone (MNP), dimethyl sulfoxide (DMSO), N,N-dimetheylacetamide (DMAc), and toluene were received from Aldrich and were distilled at reduced pressure before use.

7.3.2. Synthesis of Hydroquione-based Hydrophilic Oligomers (HQS100) with Phenoxide Telechelic Functionality

HQ-based fully disulfonated hydrophilic blocks of different molecular weights were synthesized via step growth polymerization. A sample oligomer synthesis with molecular weight of 3,000 g/mol is as follows: 66.6 mmol of HQ (7.3351 g), 56.3 mmol of SDCDPS (27.6649 g) and 79.9 mmol of potassium carbonate (20 mol% excess) were dissolved in 140 ml of distilled NMP and 70ml of toluene in a 3-necked flask equipped with a condenser, a Dean Stark trap, nitrogen inlet and mechanical stirrer. The reaction mixture was heated at 150ºC for 4 hours with refluxing toluene to dehydrate the system. The reaction temperature was then slowly increased to 185 ºC to remove the toluene and

allowed to react for 48 hours. The reaction solution was cooled to room temperature and filtered to remove salts. For high molecular weight oligomers, dilution with NMP was necessary to ease the filtration. The oligomer was coagulated in acetone followed by filtration and drying *in vacuo* at 110 ºC for 24 h.

7.3.3. Synthesis of Phenoxide Terminated Poly(arylene ether sulfone) Hydrophobic Oligomers (BPS0) and Their End-capping with Hexafluorobenzene (HFB)

BP based unsulfonated hydrophobic blocks of different molecular weights were synthesized via step growth polymerization. A sample oligomer synthesis with molecular weight of 5,000 g/mol is as follows: 66.5 mmol of BP(13.0210 g), 61.4 mmol of DCDPS (12.0210 g) and 79.8 mmol of potassium carbonate (20 mol% excess) were dissolved in 120 ml of distilled DMAc and 60ml of toluene in a 3-necked flask equipped with a condenser, a Dean Stark trap, nitrogen inlet and mechanical stirrer. The reaction mixture was heated at 150ºC for 4 hours with refluxing toluene to dehydrate the system. The reaction temperature was slowly increased to 175 ºC to remove the toluene and allowed to react for 48 hours. The dried oligomer was obtained according to procedures used for HQS100 synthesis.

The isolated BPS0 oligomers were then end-capped with HFB via a nucleophilic aromatic substitution reaction. A sample end-capping reaction of the 5,000 g/mol oligomer is as follows: 5.0000 g (1.0 mmol) of BPS0 oligomer and 0.5528 g (4.0 mmol) of potassium carbonate were charged to a 3-necked 100-mL flask equipped with a condenser, a Dean Stark trap, a nitrogen inlet, and a mechanical stirrer. Distilled DMAc (50 mL) and cyclohexane (15 mL) were added to the flask. The solution was allowed to

reflux at 100 °C to azeotropically remove the water in the system. After 4 h, the cyclohexane was removed from the system by distillation. The reaction temperature was decreased to 80 °C and the nitrogen purge was stopped to avoid the possible loss of low-temp boiling HFB (b.p.=80 °C). Afterwards, 1.1163 g (6.0 mmol) of HFB was added and the reaction was allowed to proceed for 12 h.

7.3.4. Synthesis of Hydrophilic-hydrophobic Multiblock Copolymers (HQSH-BPS)

Multiblock copolymers with various lengths of hydrophilic and hydrophobic blocks were synthesized. A sample coupling reaction is as follows: Into a 100mL 3-necked flask equipped with a mechanical stirrer, nitrogen inlet and a Dean-Stark trap, 3.0000 g of hydrophilic oligomer (Mn = 3,000 g/mol 1.0 mmol), 0.5528 g of K_2CO_3 (4.0 mmol), 20 mL of cyclohexane and 40 mL of DMSO were added and dehydrated at 100 °C for 4 h. The cyclohexane was then removed by distillation and 5.0000 g of hydrophobic oligomer (Mn = 5,000 g/mol 0.1 mmol) was added. The coupling reaction was conducted at 105 °C for 24 h. The obtained brown polymer solution was coagulated in isopropyl alcohol. The resulting polymer was filtered and dried in a vacuum oven at temperatures up to 110 ºC.

7.3.5. Characterization

The chemical structures of the oligomers and copolymers were confirmed by ^{1}H NMR analyses on a Varian INOVA 400 MHz spectrometer with DMSO-d_6. In addition, ^{1}H NMR spectroscopy was utilized for end-group analyses of the oligomers to determine their $\overline{M_n}$. Intrinsic viscosities were determined in NMP containing 0.05 M LiBr at 25 ºC

using an Ubbelohde viscometer. Ion exchange capacity (IEC) values were determined by titration with a 0.01 M NaOH solution.

7.3.6. Film Casting and Membrane Acidification

The starting membranes were cast in their salt form by solution casting. The salt form copolymers were dissolved in NMP or DMF (7% w/v) and filtered with syringe filters (0.45 μm Teflon®). The filtered solutions were then cast onto clean glass substrates. The films were dried under an IR ramp at 60 ºC for 1 day and followed by drying *in vacuo* at 110 ºC for 24 h. The acid- form membranes were obtained by boiling in a 0.5 M sulfuric acid aqueous solution for 2 h, followed by boiling in deionized water for 2 h. The membranes were kept in deionized water at room temperature for 24 h for further characterization.

7.3.7. Determination of Proton Conductivity and Water Uptake

Both fully and partially hydrated proton conductivities were evaluated in a water bath and a humidity-temperature controllable chamber, respectively. The conductivity of the membrane was determined from the geometry of the cell and resistance of the film, which was taken at a frequency that produced the minimum imaginary response. A Solartron (1252A +1287) impedance/gain-phase analyzer over the frequency range of 10 Hz - 1 MHz was used for the measurements. The membrane water uptake was determined by the weight difference between dry and wet membranes. The vacuum dried membranes were weighed (W_{dry}), and then immersed in deionized water at room temperature for 24 h. The wet membrane was blotted dry and immediately weighed

again (W_{wet}). The water uptake of the membranes was calculated according to the following equation.

$$Water\,Uptake\ (\%) = \frac{W_{wet} - W_{dry}}{W_{dry}} \times 100$$

7.3.8. Atomic Force Microscopy (AFM)

Tapping mode AFM was performed using a Veeco Multimode Atomic Force Microscope. Samples were equilibrated at 30% relative humidity (RH) at room temperature for at least 24 h and sealed before imaging.

7.4. Results and Discussion

7.4.1. Synthesis of Controlled Molecular Weight Hydrophilic Blocks (HQS100)

Different number-average molecular weight hydrophilic oligomers were synthesized via the step growth polymerization of SDCDPS and HQ (Figure 7.1). It was possible to precisely control molecular weight and end-group functionality via a stoichiometric imbalance of the monomers. All oligomers were designed to be terminated with phenoxide end-groups by using an excess amount of HQ. The target molecular weights for hydrophilic blocks ranged from 3,000 to 15,000 g/mol. Earlier, the synthesis was attempted in DMAc at 175 ºC for 96 h. However, the poor solubility of HQS100 in DMAc resulted in premature precipitation within just a few hours. As a result, it was impossible to control both molecular weight and end-group functionality. It has been suggested that the insolubility of the oligomers may stem from the formation of crystallites from the HQ moieties on the main chain backbone.[26] To maintain homogeneous conditions during synthesis, DMSO was also used as the reaction solvent. Although it provided both good solubility and rapid reaction kinetics (i.e., the reaction can be completed in 48 h at 180 ºC), the resulting product was not pure enough to be used for the coupling reaction due to unidentified side reactions. On the one hand, although undesirable side reactions could be avoided when the reactions were conducted at very low temperatures (e.g., 135 ºC), the reaction time was significantly prolonged (e.g., ~200 h). On the other hand, when we conducted the reaction in NMP at 195 ºC for 48 h, we were able to avoid any side reactions. Thus, the latter reaction conditions for preparing the HQS100 oligomers were used in this research.[27] End-group analyses of selected peaks via ^{1}H NMR spectra were used to determine the number-average molecular weight

of the oligomers (Figure 7.2). On the NMR spectrum of the HQS100, two small peaks, **e** and **f,** at 6.75 and 6.83 ppm, respectively, were assigned to the protons on the HQ moieties, located at the end of the chain. Calculating the integration ratios between one of these peaks and one of the other main peaks (**a**, **b**, **c**, and **d**) was used to determine the number-average molecular weight of the oligomers. Table 7.1 lists the characterization data for the HQS100 hydrophilic telechelic oligomers used in this study.

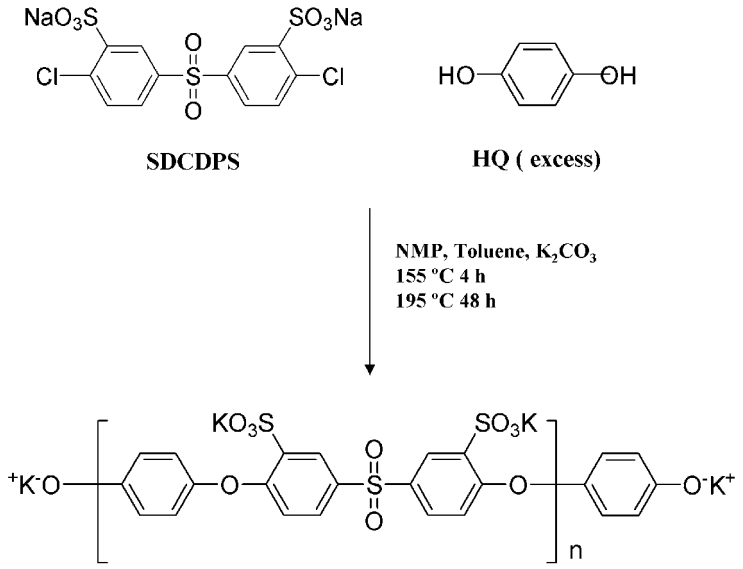

Figure 7. 1. Synthesis of a Phenoxide-terminated Fully Disulfonated Poly(arylene ether sulfone) Hydrophilic Oligomer Based on Hydroquinone (HQS100)

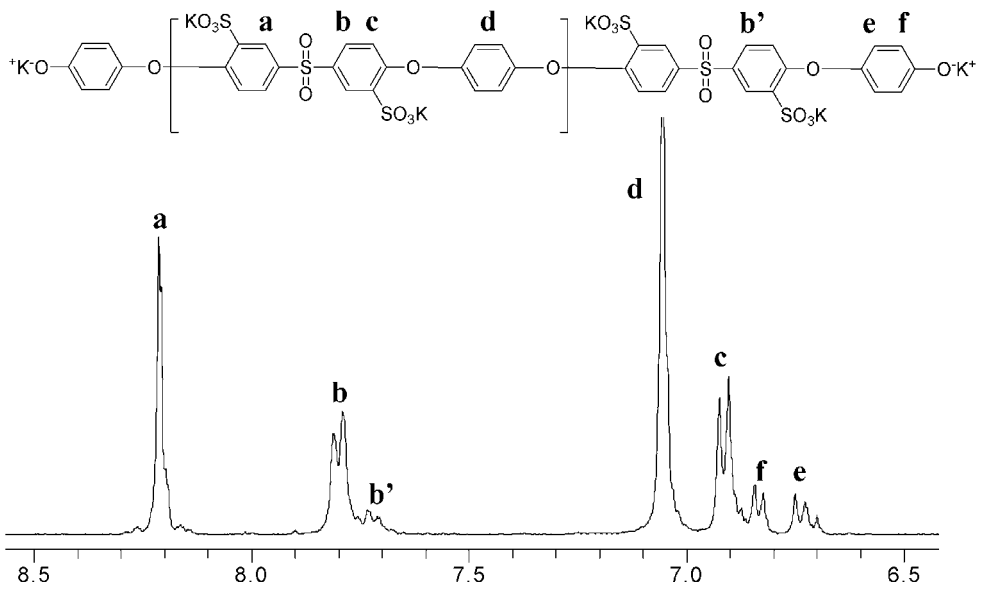

Figure 7. 2. [1]H NMR Spectrum of HQS100 with a Molecular Weight of 3,000 g/mol

Table 7. 1. Characterization of HQS100 Hydrophilic Telechelic Oligomers.

Target M_n (g mol^{-1})	M_n (g mol^{-1})[a]	IV (dL g^{-1})[b]
3,000	3,200	0.12
5,000	4,700	0.14
6,000	5,500	0.16
9,000	9,100	0.22
10,000	10,700	0.23
12,000	12,900	0.24
15,000	14,800	0.29

[a] Determined by [1]H NMR.

[b] In NMP with 0.05 M LiBr at 25 ºC.

7.4.2. Synthesis of Controlled Molecular Weight Hydrophobic Blocks (BPS0) and Their End-capping with Hexafluorobenzene (HFB)

Unsulfonated poly(arylene ether sulfone) oligomers based on biphenol (BPS0) with varying molecular weights were synthesized as hydrophobic blocks (Figure 7.3). Control of molecular weight and end-group functionality was achieved by upsetting the feed ratios of the monomers. ^{1}H NMR spectroscopy of the BPS0 hydrophobic oligomers showed that the oligomers possessed phenoxide end-group functionality as intended, and we were able to determine number-average molecular weight via end-group analyses (Figure 7.4). Molecular weight and intrinsic viscosity data for the BPS0 are summarized in Table 7.2. When log-log plots were made between number average molecular weight and intrinsic viscosity, linear relationships for both the hydrophilic and hydrophobic oligomers were identified (Figure 7.5).

The synthesized hydrophilic and hydrophobic oligomers possessed the same phenoxide end-groups, making them unsuitable for the coupling reaction needed to produce multiblock copolymers since they are not reactive with each other (i.e., both end-groups are nucleophiles). Thus, it was necessary to modify the end-group functionality of either hydrophilic or hydrophobic block to facilitate the coupling reaction. For this research, we chose to modify the BPS0 hydrophilic blocks, which were end-capped with hexafluorobenzene (HFB) (Figure 7.6). In so doing, a conversion of the nucleophilic BPS0 oligomers into elecrophilic, fluorine-terminated BPS0 oligomers was possible, which would facilitate a coupling reaction with the HQS100 oligomers. As shown in Figure 7.7, the end-group peaks for the terminal BP moieties completely disappeared and a new peak appeared at 7.65 ppm. This peak corresponds to the same protons on the terminal BP moieties but were attached to HFB. Although NMR spectra comparisons

before and after end-capping reaction confirmed that all the phenoxide end-groups had reacted with HFB, the formation of high molecular weight BPS0 oligomers via an inter-oligomer coupling reaction was still possible due to the multifunctionality of the HFB. To prevent this from occurring, a large excess of HFB was used. Specifically, the molar ratio between the BPS0 and HFB was 1:6. In addition, intrinsic viscosity studies of the BPS0 oligomers before and after end-capping showed that there was little, if any, inter-oligomer coupling, as evidenced by the less than 0.02 dL/g increase with the end-capped oligomers. This implies that the end-capping reaction was successful without any significant inter-oligomer coupling, and that high molecular weight BPS0 oligomers had formed.

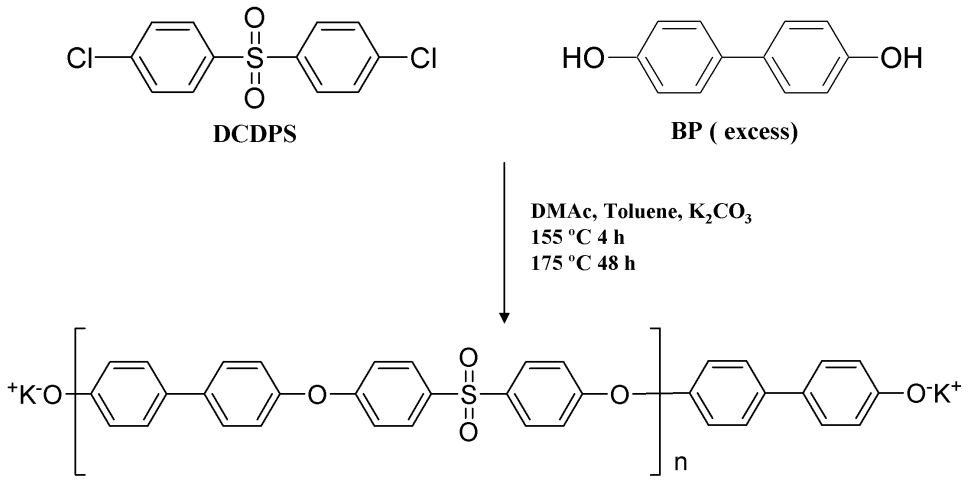

Figure 7. 3. Synthesis of a Phenoxide-terminated Unsulfonated Poly(arylene ether sulfone) Hydrophobic Oligomer Based on Bipheol (BPS0)

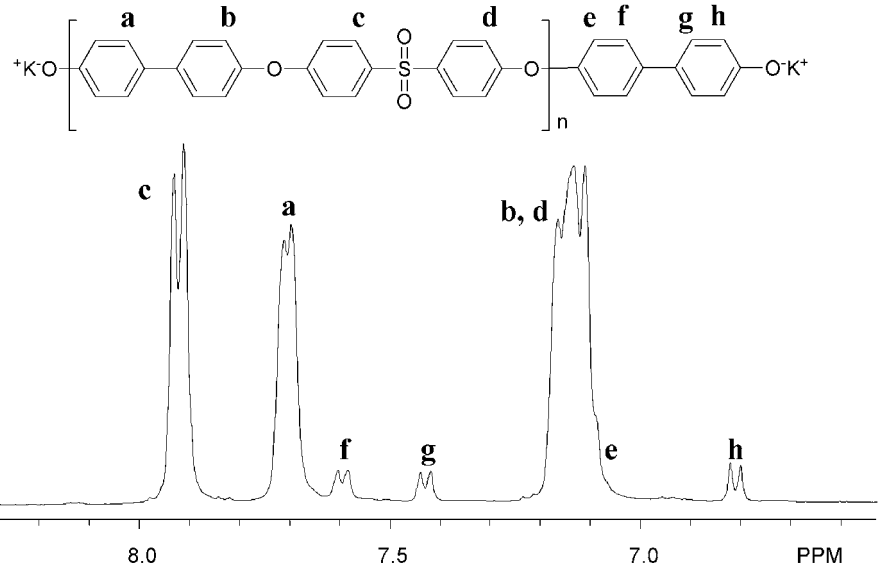

Figure 7. 4. ^{1}H NMR Spectrum of BPS0 with a Molecular Weight of 3,000 g/mol

Table 7. 2. Characterization of BPS0 Hydrophobic Telechelic Oligomers.

Target M_n (g mol^{-1})	M_n (g mol^{-1})[a]	IV (dL g^{-1})[b]
3,000	3,200	0.19
5,000	5,200	0.26
10,000	10,400	0.35
15,000	14,700	0.46
20,000	20,800	0.51
25,000	24,400	0.54

[a] Determined by ^{1}H NMR.

[b] In NMP with 0.05 M LiBr at 25ºC.

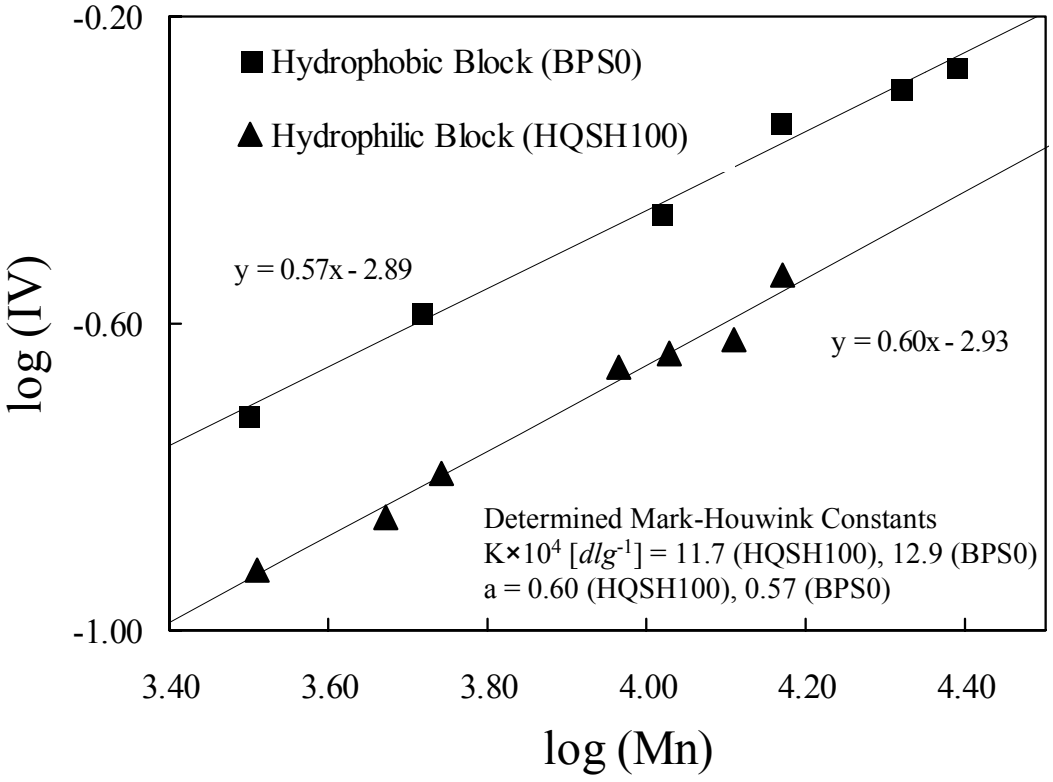

Figure 7. 5. Double Logarithmic Plot of [η] versus M_n of Hydrophilic (HQS100) and Hydrophobic (BPS0) Oligomers. Intrinsic Viscosity was Measured in NMP with 0.05 M LiBr at 25 ºC.

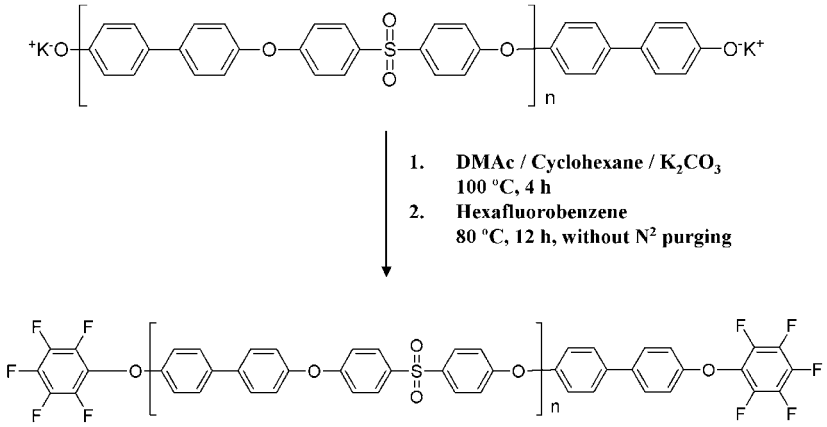

Figure 7. 6. End-capping of the Phenoxide Terminated Hydrophobic Oligomer (BPS0) with HFB. This Procedure Transforms the Nucleophilic Telechelic Oligomer into an Electrophilic Telechelic Oligomer.

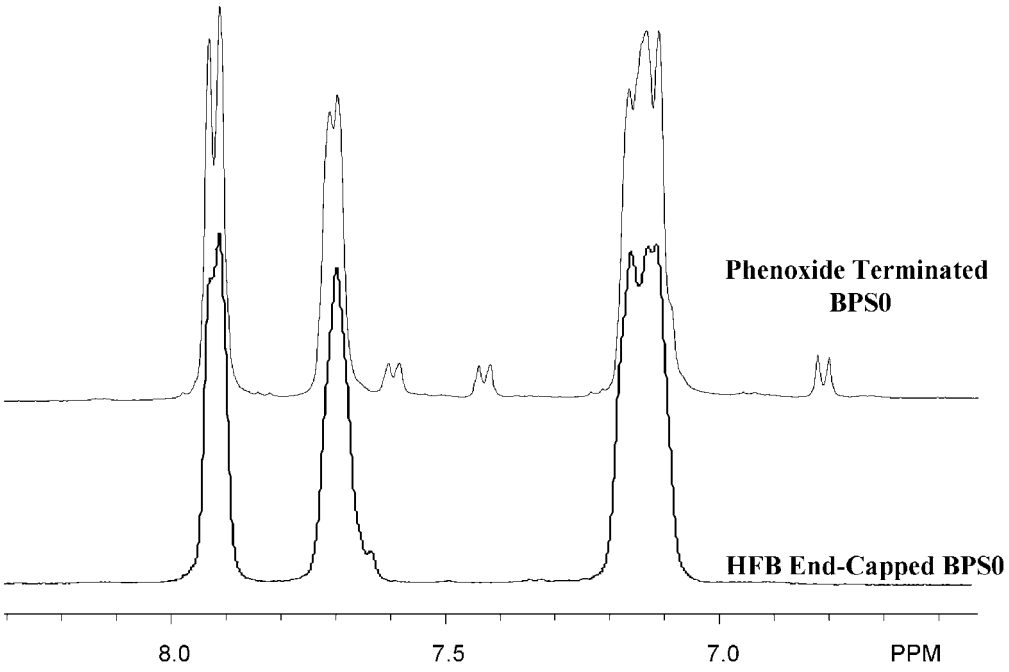

Figure 7. 7. BPS0 Hydrophobic Oligomer ^{1}H NMR Spectra Comparison Before and After the End-capping Reaction with HFB.

7.4.3. Synthesis of Multiblock Copolymers by a Coupling Reaction of Hydrophilic and Hydrophobic Oligomers

Multiblock copolymers of varying hydrophilic and hydrophobic block length were synthesized via a coupling reaction (Figure 7.8). This reaction is a simple nucleophilic aromatic substitution reaction between the phenoxide and the fluorine end groups on the HQS100 and the BPS0 oligomers, respectively. Although expected to be fairly straightforward, this coupling reaction turned out to be solvent sensitive. Specifically, when the coupling reactions were conducted in NMP, the resulting intrinsic viscosity and IEC values for the multiblock copolymers were always lower than expected. Similar problems were observed with either DMAc or DMF. However, the low reactivity between the hydrophilic and hydrophobic oligomers was significantly enhanced when DMSO was used. As shown on the ^{1}H NMR spectrum in Figure 7.9, the end-group peaks associated with the hydrophilic oligomer disappeared, confirming that the coupling reaction was successful. One possible explanation for the solvent sensitivity of the coupling reaction is that the reactivity of the phenoxide group on the HQ moieties could have been influenced by the polarity of the solvents. In other words, DMSO might have solvated the potassium ion more effectively than the other solvents with a higher dielectric constant, thereby increasing the reactivity of the phenoxide anion toward the fluorine electrophile of the BPS0 oligomers. Although the use of DMSO helped to avoid solvent sensitivity, another problem was encountered—namely the poor solubility of the BPS0 oligomers in DMSO, which became even more apparent when high molecular weight BPS0 oligomers were used (e.g., > 10,000 g/mol). This difficulty was addressed by reducing the oligomer concentration during the coupling reaction to 3-4 (w/v) %. All

multiblock copolymers used in this study were synthesized through a coupling reaction in DMSO.

Another strategy to overcome a low degree of coupling was also studied. Since poor reactivity seems to stem from the low reactivity of the HQ phenoxide moieties, we tried to avoid using HQ-phenoxide end-group on the hydrophilic oligomer for the coupling reaction. First, end-capping of the phenoxide terminated HQS100 oligomers with HFB in DMSO was conducted. Since DMSO facilitates both good solubility and high reactivity, end-capping the HQS100 oligomers was successful with no complications. The HFB end-capped HQS100 can then typically be reacted with phenoxide terminated BPS0 oligomers in NMP or DMAc. In this case, the nucleophile is the BP phenoxide moiety which is strong enough to attack the fluorine end-groups on the HQS100 in either NMP or DMAc. By adopting this strategy, the coupling reaction can be successfully conducted without reducing oligomer concentrations. As mentioned earlier, the main reason for employing highly reactive HFB for the coupling reaction is to prevent hydrophilic-hydrophobic sequence randomization via transetherification by reducing the coupling reaction temperature. To confirm that the synthesized multiblock copolymers maintained the sequences, their ^{13}C NMR spectra were compared with that of a random copolymer that had been synthesized from the same monomers (Figure 7.10). As expected, the multiblock copolymer showed sharp singlet or doublet peaks while the random copolymer exhibited complicated mutiplet peaks, thereby confirming that the multiblock copolymer possessed well-defined sequences in the system.

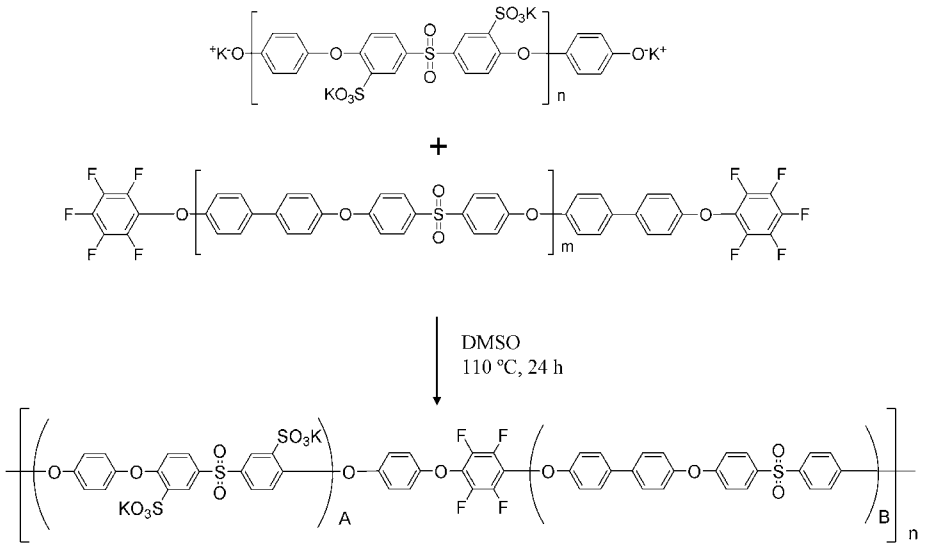

Figure 7. 8. Synthesis of Segmented Sulfonated Multiblock Copolymers via a Coupling Reaction.

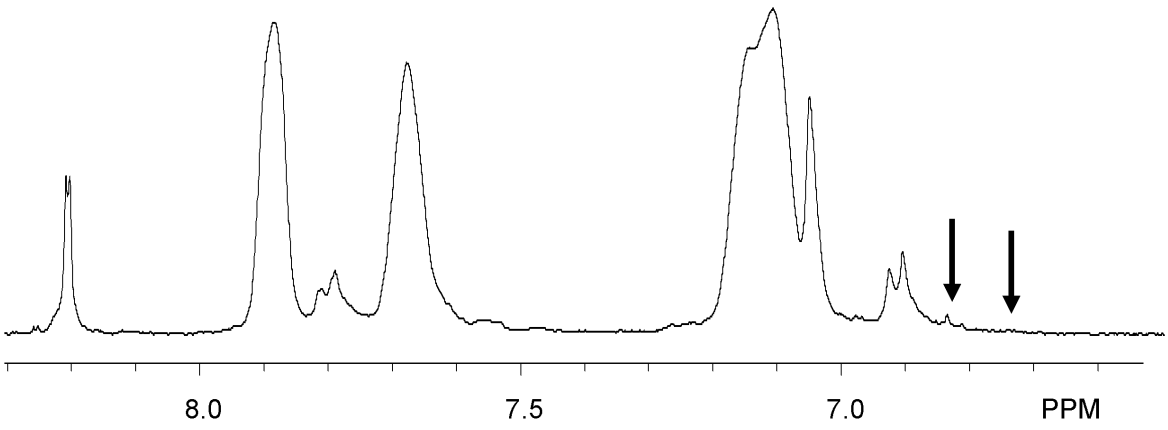

Figure 7. 9. ^{1}H NMR Spectrum of HQSH3-BPS5. Black Arrows Indicate the Disappearance of the End-groups on the Hydrophilic Blocks after the Coupling Reaction with Fluorine-terminated Hydrophobic Blocks.

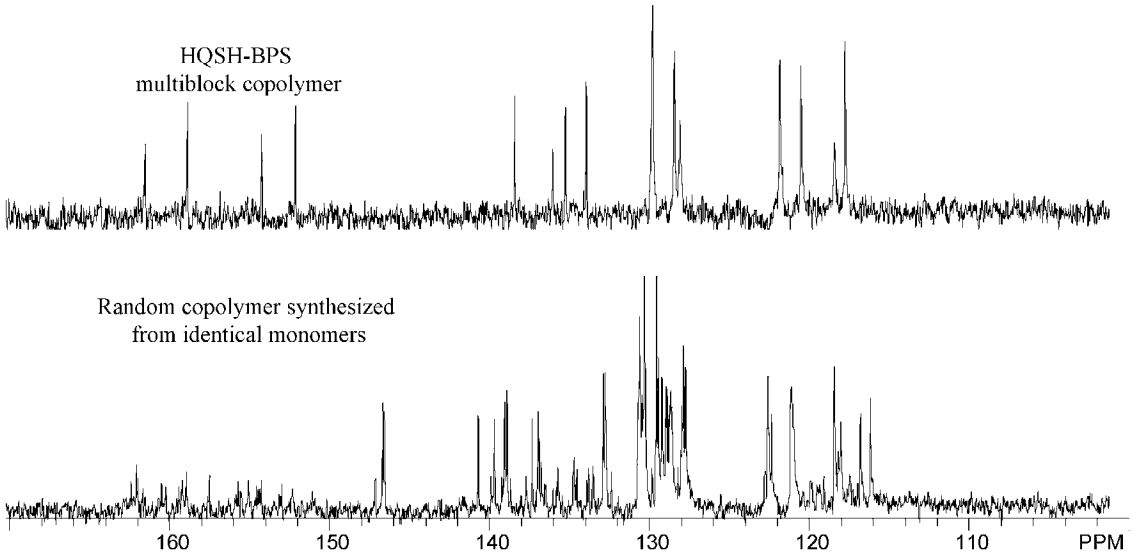

Figure 7. 10. ^{13}C NMR Spectra Comparison of HQSH3-BPS5 Multiblock Copolymer and a Random Copolymer Synthesized from the Identical Monomers.

7.4.4. Characterization of Membrane Properties of HQSH-BPS Multiblock Copolymers

A series of multiblock copolymers with varying hydrophilic and hydrophobic block lengths was synthesized, and subsequently examined to determine their potential fuel cell applications. Their fundamental membrane properties are summarized in Table 7.3. The copolymers are categorized into three groups. The first group includes Nafion 112 and BPSH35, which were used as controls. The second and third groups include the multiblock copolymers with different block lengths. Although varying length of hydrophilic and hydrophobic oligomers were used for the multiblock copolymer synthesis, target IEC values were set to approximately 1.4 and 1.9 meq/g for the second and the third group, respectively. To obtain the target IEC value of 1.4 meq/g for the

second group, the composition ratio between hydrophilic and hydrophobic blocks was set to 3:5. For the third group, a composition ratio of 1:1 was used to attain the target IEC of 1.9. All polymerization feed ratios were calculated based on a 1:1 molar ratio between hydrophilic and hydrophobic oligomers to attain high molecular weight. The acronym developed for these multiblock copolymers is HQSHx-BPSy, where the HQSH and BPS refer to the use of HQSH100 and BPS0 oligomers, while x and y denote the molecular weight in Kg/mol unit of the oligomers, respectively.

All multiblock copolymers displayed high intrinsic viscosities ranging from 0.51 to 0.99 dL/g, and could form tough, ductile membranes from solvent casing. IEC values, which were determined by titration, were close to target values, indicating a high degree of coupling. It should be noted that original design of this study involved the preparation of 1.4 meq/g multiblock copolymers in order to compare their properties with a similar IEC random copolymer (e.g., BPSH35). A prediction was made that the HQSH-BPS multiblock copolymer with a sequenced architecture would outperform the BPSH35 random copolymer. The results, however, were unexpected. The multiblock copolymers displayed much lower water uptake and proton conductivity, with IEC values ranging from 1.2 to 1.4 meq/g, water uptake of 20%, and a proton conductivity of 0.04 S/Cm. These results were significantly lower compared with those of random copolymers with similar IEC values. We were able to explain these results using subsequent AFM characterization.

Figure 7.11 (a) shows an AFM phase image of the HQSH12-BPS20. The bright and dark regions in the images correspond to hard hydrophobic and soft hydrophilic segments, respectively. As shown in the picture, the dark hydrophilic segments are

completely isolated by the hydrophobic segments. This type of morphology would suggest low water uptake and proton conductivity. After additional AFM studies, it turned out that all the copolymers with target IEC values of 1.4 meq/g possessed similarly isolated hydrophilic segments. This unexpected morphology can be explained as follows. Although the multiblock copolymers have adequate sulfonic acid moieties to achieve a high proton conductivity, their hydrophilic segment volume fractions were not sufficient to form well-connected channels. This observation suggests one critical consideration for designing hydrophilic-hydrophobic multiblock copolymers. In developing high proton conductive PEMs from hydrophilic-hydrophobic multiblock copolymers, the volume fraction of the hydrophilic segments should be considered as well as IEC values.

For this reason, in order to increase proton conductivity, the hydrophilic fraction was increased to induce the formation of well-connected hydrophilic regions. Thus, the third group of multiblock copolymers was designed with higher hydrophilic volume fractions by coupling equal block length hydrophilic and hydrophobic oligomers. The resulting multiblock copolymers showed significantly enhanced proton conductivities ranging from 0.13 to 0.21 S/Cm. Water uptake values also significantly increased up to 183% with the HQSH5-BPS5 system. This significant improvement can be ascribed to the formation of well-connected hydrophilic regions, which was confirmed by AFM (Figure 7.11 (b)). As evidenced in this image, the HQSH10-BPS10 displays high connectivity in the hydrophilic segment of the membrane. Thus, by utilizing the well-connected hydrophilic regime for proton conduction, enhanced proton conductivity was realized.

Table 7. 3. Properties of HQSH–BPS Multiblock Copolymers in the Sulfonic Acid Form.

Copolymers	Calculated IEC (meq g^{-1})	Experimental IEC (meq g^{-1})[a]	Intrinsic Viscosity (dL g^{-1})[b]	Water Uptake (%)	Conductivity (S cm^{-1})[c]
Nafion 112	-	0.90	-	25	0.090
BPSH 35	1.53	1.50	0.70	36	0.070
HQSH 3 – BPS 5	1.44	1.32	0.56	27	0.04
HQSH 6 – BPS 10	1.31	1.21	0.60	18	0.03
HQSH 9 – BPS 15	1.45	1.20	0.68	13	0.03
HQSH 12 – BPS 20	1.45	1.37	0.68	17	0.04
HQSH 3 – BPS 3	1.89	1.79	0.52	112	0.13
HQSH 5 – BPS 5	1.79	1.88	0.51	183	0.17
HQSH 10 – BPS 10	1.91	1.78	0.98	156	0.21
HQSH 15 – BPS 15	1.90	1.67	0.99	145	0.16

[a] Determined by titration with NaOH.
[b] In NMP with 0.05 M LiBr at 25 ºC.
[c] Measured in deionized water at 30 ºC.

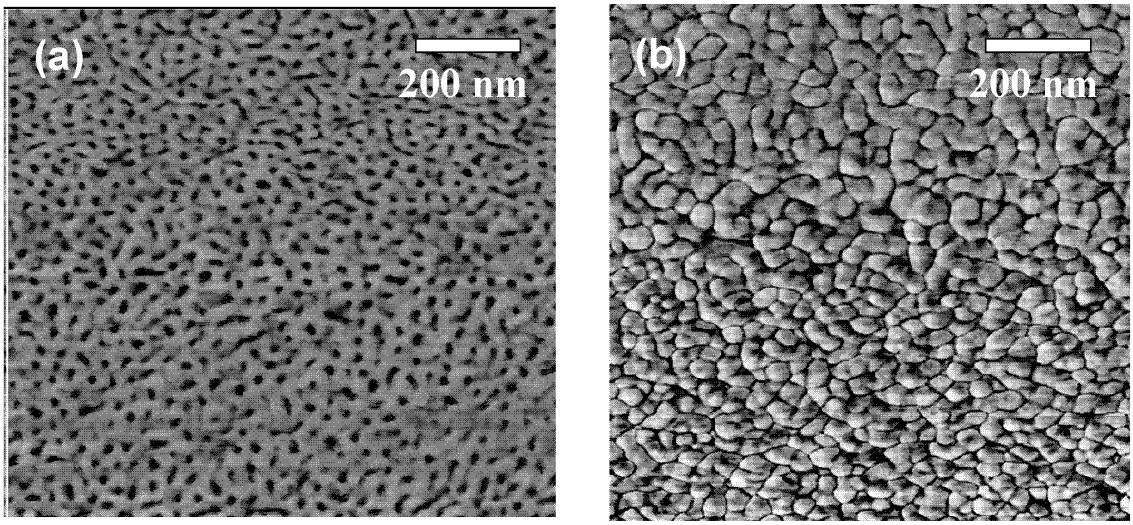

Figure 7. 11. AFM Phase Images of HQSH-BPS Multiblock Copolymers. (a) HQSH12-BPS20, and (b) HQSH10-BPS10.

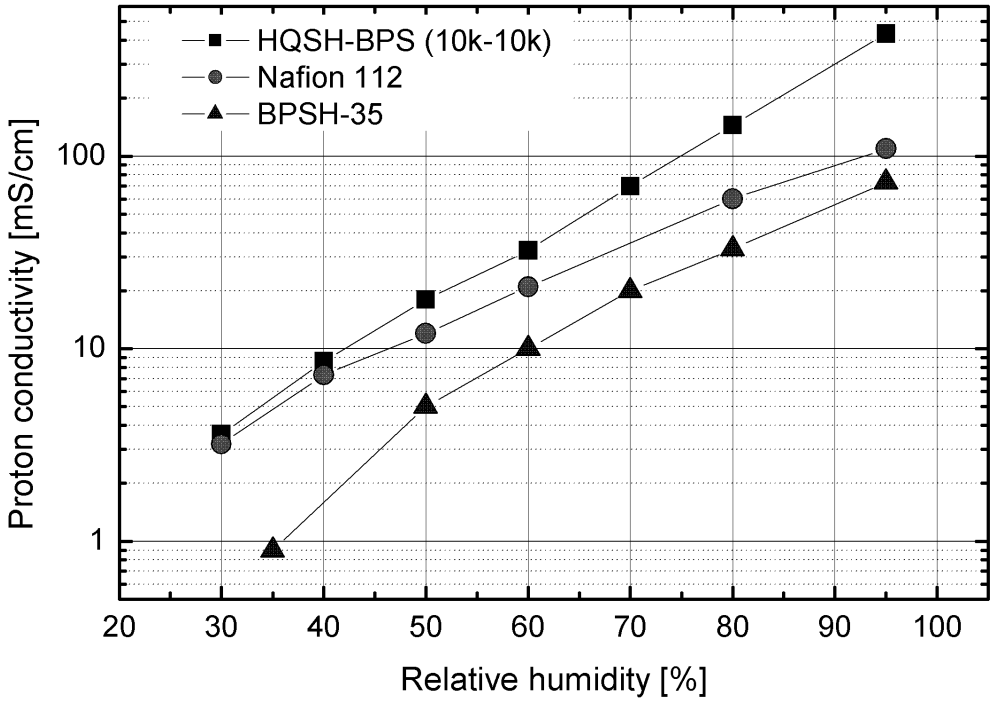

Figure 7. 12. Proton Conductivities of HQSH10-BPS10, BPSH35, and Nafion112 under Partially Hydrated Conditions at 80 ºC.

To evaluate ion transport property of the multiblock copolymer under partially hydrated conditions, conductivity of the HQSH10-BPS10 was measured as a function of relative humidity (RH) and compared with BPSH35 and Nafion 112 (Fig. 12). The measurement was conducted at 80 ºC. As shown in the figure, the proton conductivity of the BPSH35 random copolymer dropped rapidly at lower RH values due to the scattered hydrophilic domains in the system. Nafion 112 showed better performance than BPSH35 under low RH range but its enhancement under high RH range was limited. Conversely, the HQSH10-BPS10 showed significantly enhanced conductivity over entire RH range than those of BPSH35 and Nafion112. The enhancement is due to the well-connected hydrophilic segments in the multiblock copolymer system which was shown in Figure 7. 11 (b).

7.5. Conclusions

Segmented sulfonated multiblock copolymers with varying block lengths were synthesized via a coupling reaction between phenoxide terminated hydrophilic oligomers (HQS100) and HFB end-capped hydrophobic oligomers (BPS0). The coupling reaction was conducted under mild reaction conditions (< 110°C) to prevent an ether-ether exchange reaction, which could result in randomized hydrophilic-hydrophobic sequences. The coupling reactions were solvent sensitive due to the low reactivity of the phenoxide groups on hydroquinone moieties. All the copolymers produced tough, ductile membranes when cast from NMP or DMF.

Several fundamental membrane parameters were investigated, including water uptake and proton conductivity. Characterization studies revealed that the volume fraction of the hydrophilic segments was critical for forming continuous hydrophilic channels, as well as improving IEC values. Using HQSH-BPS multiblock copolymers with high IEC values, we were able to achieve high proton conductivity up to 0.21 S/Cm at 30 ºC in liquid water via the formation of a nano-phase separated morphology. The results confirm that the multiblock copolymers described herein are potential candidates for use as PEM materials.

Acknowledgements

The authors thank the Department of Energy (DE-FG36-06G016038) for its support of this research.

7.6. References

1. Hickner, M. A.; Ghassemi, H.; Kim, Y. S.; Einsla, B. R.; McGrath, J. E., Alternative Polymer Systems for Proton Exchange Membranes (PEMs). *Chemical Reviews (Washington, DC, United States)* **2004,** 104, (10), 4587-4611.
2. Harrison, W. L.; Hickner, M. A.; Kim, Y. S.; McGrath, J. E., Poly(arylene ether sulfone) copolymers and related systems from disulfonated monomer building blocks: synthesis, characterization, and performance - a topical review. *Fuel Cells (Weinheim, Germany)* **2005,** 5, (2), 201-212.
3. Rusanov, A. L.; Likhatchev, D.; Kostoglodov, P. V.; Mullen, K.; Klapper, M., Proton-exchanging electrolyte membranes based on aromatic condensation polymers. *Advances in Polymer Science* **2005,** 179, (Inorganic Polymeric Nanocomposites and Membranes), 83-134.
4. Wang, F.; Hickner, M.; Ji, Q.; Harrison, W.; Mecham, J.; Zawodzinski, T. A.; McGrath, J. E., Synthesis of highly sulfonated poly(arylene ether sulfone) random (statistical) copolymers via direct polymerization. *Macromolecular Symposia* **2001,** 175, (Polymerization Processes and Polymer Materials II), 387-395.
5. Wang, F.; Hickner, M.; Kim, Y. S.; Zawodzinski, T. A.; McGrath, J. E., Direct polymerization of sulfonated poly(arylene ether sulfone) random (statistical) copolymers: candidates for new proton exchange membranes. *Journal of Membrane Science* **2002,** 197, (1-2), 231-242.
6. Wang, F.; Ji, Q.; Harrison, W.; Mecham, J.; McGrath, J. E.; Formato, R.; Kovar, R., Synthesis of sulfonated poly(arylene ether sulfone)s via direct polymerization. *Book of Abstracts, 219th ACS National Meeting, San Francisco, CA, March 26-30, 2000* **2000**, POLY-151.
7. Sankir, M.; Bhanu, V. A.; Harrison, W. L.; Ghassemi, H.; Wiles, K. B.; Glass, T. E.; Brink, A. E.; Brink, M. H.; McGrath, J. E., Synthesis and characterization of 3,3'-disulfonated-4,4'-dichlorodiphenyl sulfone (SDCDPS) monomer for proton exchange membranes (PEM) in fuel cell applications. *Journal of Applied Polymer Science* **2006,** 100, (6), 4595-4602.
8. Kreuer, K. D., On the development of proton conducting polymer membranes for hydrogen and methanol fuel cells. *Journal of Membrane Science* **2001,** 185, (1), 29-39.
9. Hamrock, S. J.; Yandrasits, M. A., Proton exchange membranes for fuel cell applications. *Polymer Reviews (Philadelphia, PA, United States)* **2006,** 46, (3), 219-244.
10. Sankir, M.; Kim, Y. S.; Pivovar, B. S.; McGrath, J. E., Proton exchange membrane for DMFC and H2/air fuel cells: Synthesis and characterization of partially fluorinated disulfonated poly(arylene ether benzonitrile) copolymers. *Journal of Membrane Science* **2007,** 299, (1+2), 8-18.

11. Li, Y.; Yang, J.; Roy, A.; Einsla, B.; Wang, F.; McGrath, J. E., Partially fluorinated disulfonated poly (arylene ether sulfone) copolymers with controlled molecular weights and their applications to proton exchange membrane fuel cells. *Preprints of Symposia - American Chemical Society, Division of Fuel Chemistry* **2005,** 50, (2), 573-574.

12. Miyatake, K.; Hay, A. S., Synthesis and properties of poly(arylene ether)s bearing sulfonic acid groups on pendant phenyl rings. *Journal of Polymer Science, Part A: Polymer Chemistry* **2001,** 39, (19), 3211-3217.

13. Tian, S. H.; Shu, D.; Wang, S. J.; Xiao, M.; Meng, Y. Z., Poly(arylene ether)s with sulfonic acid groups on the backbone and pendant for proton exchange membranes used in PEMFC applications. *Fuel Cells (Weinheim, Germany)* **2007,** 7, (3), 232-237.

14. Sacca, A.; Pedicini, R.; Carbone, A.; Gatto, I.; Passalacqua, E., Comparative investigation on nano-sized SiO2 as a filler for proton exchange membranes (PEM) fuel cells. *ECS Transactions* **2007,** 11, (1, Part 1, Proton Exchange Membrane Fuel Cells 7, Part 1), 357-366.

15. Hill, M.; Einsla, B.; McGrath, J. E.; Kim, Y. S., Synthesis and characterization of sulfonated poly(arylene ether sulfone)/zirconium phenylphosphonate composite membranes for proton exchange membrane fuel cell applications. *Abstracts of Papers, 228th ACS National Meeting, Philadelphia, PA, United States, August 22-26, 2004* **2004**, FUEL-050.

16. Lee, H.-S.; Badami, A. S.; Roy, A.; McGrath, J. E., Segmented Sulfonated Poly(arylene ether sulfone)-b-Polyimide Copolymers for Proton Exchange Membrane Fuel Cells. I. Copolymer Synthesis and Fundamental Properties. *Journal of Polymer Science, Part A: Polymer Chemistry* **2007,** 45, (21), 4879-4890.

17. Lee, H.-S.; Roy, A.; Badami, A. S.; McGrath, J. E., Synthesis and characterization of sulfonated poly(arylene ether) polyimide multiblock copolymers for proton exchange membranes. *Macromolecular Research* **2007,** 15, (2), 160-166.

18. Lee, H.-S.; Roy, A.; Lane, O.; Dunn, S.; McGrath, J. E., Hydrophilic-hydrophobic multiblock copolymers based on poly(arylene ether sulfone) via low-temperature coupling reactions for proton exchange membrane fuel cells. *Polymer* **2008,** 49, (3), 715-723.

19. Li, Y.; Roy, A.; Badami, A. S.; Hill, M.; Yang, J.; Dunn, S.; McGrath, J. E., Synthesis and characterization of partially fluorinated hydrophobic-hydrophilic multiblock copolymers containing sulfonate groups for proton exchange membrane. *Journal of Power Sources* **2007,** 172, (1), 30-38.

20. Yu, X.; Roy, A.; Dunn, S.; Yang, J.; McGrath, J. E., Synthesis and characterization of sulfonated-fluorinated, hydrophilic-hydrophobic multiblock copolymers for proton exchange membranes. *Macromolecular Symposia* **2006,** 245/246, (World Polymer Congress--MACRO 2006), 439-449.

21. Wang, H.; Badami, A. S.; Roy, A.; McGrath, J. E., Multiblock copolymers of poly(2,5-benzophenone) and disulfonated poly(arylene ether sulfone) for proton-

exchange membranes. I. Synthesis and characterization. *Journal of Polymer Science, Part A: Polymer Chemistry* **2006,** 45, (2), 284-294.

22. Roy, A.; Lee, H.-S.; McGrath, J. E., Hydrophilic-hydrophobic multiblock copolymers based on poly(arylene ether sulfone)s as novel proton exchange membranes - Part B. *Polymer* **2008,** 49, (23), 5037-5044.
23. Badami, A. S.; Roy, A.; Lee, H.-S.; Li, Y.; McGrath, J. E., Morphological investigations of disulfonated poly(arylene ether sulfone)-b-naphthalene dianhydride-based polyimide multiblock copolymers as potential high temperature proton exchange membranes. *Journal of Membrane Science* **2009,** 328, (1+2), 156-164.
24. Roy, A.; Hickner, M. A.; Yu, X.; Li, Y.; Glass, T. E.; McGrath, J. E., Influence of chemical composition and sequence length on the transport properties of proton exchange membranes. *Journal of Polymer Science, Part B: Polymer Physics* **2006,** 44, (16), 2226-2239.
25. Li, Y.; VanHouten, R. A.; Brink, A. E.; McGrath, J. E., Purity characterization of 3,3'-disulfonated-4,4'-dichlorodiphenyl sulfone (SDCDPS) monomer by UV-vis spectroscopy. *Polymer* **2008,** 49, (13-14), 3014-3019.
26. Yu, X. Synthesis and Characterization of Hydrophilic-Hydrophobic Disulfonated Poly(Arylene Ether Sulfone)-Decafluoro Biphenyl Based Poly(Arylene Ether) Multiblock Copolymers for Proton Exchange Membranes (PEMs). Dissertation, Virginia Polytechnic Institute and State University, 2007.
27. Hedrick, J. L.; Mohanty, D. K.; Johnson, B. C.; Viswanathan, R.; Hinkley, J. A.; McGrath, J. E., Radiation resistant amorphous-all aromatic polyarylene ether sulfones: synthesis, characterization, and mechanical properties. *Journal of Polymer Science, Part A: Polymer Chemistry* **1986,** 24, (2), 287-300.

CHAPTER 8

Overall Conclusions

Beginning in 2001 when the McGrath Group first developed disulfonated poly(arylene ether sulfone)-based proton exchange membranes (BPSH), these materials have attracted worldwide interest. Under fully hydrated conditions, these BPSH systems have a number of advantages over the state-of-the-art perfluorinated sulfonic acid membrane material, Nafion®, including reduced cost, and excellent thermal and oxidative stability. In the nearly 10 years since those initial efforts, McGrath et al. have been conducting research on hydrocarbon-based proton exchange membrane materials—most recently on hydrophilic-hydrophobic multiblock copolymer systems that will address some of the drawbacks of the BPSH-type materials. For example, BPSH suffers from low proton conduction under partially hydrated conditions due to the scattered distribution of its sulfonic acid moieties. Therefore, a hypothesis was made that by using hydrophilic-hydrophobic sequenced multiblock copolymers to form co-continuous lamellae morphologies, it might be possible to overcome some of these morphological barriers. To validate this theory, a variety of hydrophilic-hydrophobic multiblock copolymers with different chemical components was synthesized and characterized.

The first investigated multiblock copolymer was a segmented sulfonated poly(arylene ether sulfone)-*b*-polyimide, which was synthesized via an imidization coupling reaction using an amine-terminated sulfonated poly(arylene ether sulfone) as the hydrophilic block, and an anhydride-terminated polyimide as the hydrophobic block. Transparent and ductile membranes were prepared from NMP by solvent casting. The proton conductivity and water uptake values for this multiblock copolymer were shown

to be strongly influenced by IEC values, as well as by the block length of the hydrophilic and hydrophobic units. Morphological characterization by tapping-mode AFM showed clear nanophase separation of hydrophilic and hydrophobic domains. As a result of their nanophase separated morphologies, these copolymers displayed significantly enhanced proton conduction under partially hydrated conditions, with conductivities comparable to Nafion.

Based on these results, an evaluation of a true sequence effect by comparing BPSH random copolymers and multiblock copolymers with similar chemical compositions was attempted. The multiblock copolymers were synthesized via a coupling reaction of sulfonated and unsulfonated poly(arylene ether sulfone) oligomers utilizing highly reactive DFBP and HFB as the linkage groups, which were expected to lower the coupling reaction temperatures. Specifically, mild reaction conditions prevent possible ether-ether interchange, which can randomize the hydrophilic-hydrophobic sequences. The multiblock copolymers displayed ordered sequences as confirmed by ^{13}C NMR. Transparent ductile membranes were prepared from NMP by solvent casting. Subsequent studies confirmed that the proton conductivity and water uptake value of the multiblock copolymer membrane systems were influenced by block length—even at similar IEC values. As block length increased, proton conductivity and water uptake also increased. The proton conductivities of these multiblock copolymers were comparable or even higher than those of the BPSH random copolymers with similar IECs, which supports the existence of well connected hydrophilic domains in the system. Few other systems have been developed using these concepts, our property measurement results

have confirmed that proton transport phenomena can be significantly enhanced by incorporating hydrophilic-hydrophobic sequences in multiblock copolymer systems.

In addition to the sulfonic acid containing proton exchange membrane systems, inorganic acid imbibed basic polymer materials were also studied using the sequenced multiblock copolymer concept for possible application as high temperature and low humidity fuel cell materials. The multiblock copolymers were synthesized via a coupling reaction between telechelic carboxyl functional poly(arylene ether sulfone) and *o*-diamine terminated polybenzimidazole. Transparent ductile membranes were prepared by solvent casting from DMAc, and two distinct T_gs were observed via DMA. Ionic conduction was achieved by immersing the membranes in a H_3PO_4 solution. Subsequent ionic conductivity studies revealed a strong dependency on temperature, doping level and, most importantly, the microstructure of the samples. Specifically, ionic conductivity increased significantly after a particular doping level for all the copolymers, which was attributed to the appearance of "free" phosphoric acid. Moreover, at a given doping level, ionic conductivity increased with increasing block length. The formation of the phase separated morphology with increasing block length was confirmed by DMA analysis. The increased phase separation resulted in better connectivity and improved ion transport.

As a result of this thorough investigation of hydrophilic-hydrophobic multiblock copolymers for fuel cell applications, it was determined that the copolymer systems described herein exhibited both high proton transport and robust mechanical properties. Therefore, these multiblock copolymers appear to be promising next generation materials for high temperature proton exchange membrane applications.